Acta Universitatis Szegediensis

Acta Biologica Szegediensis

Volume 58, Number 1, 2014

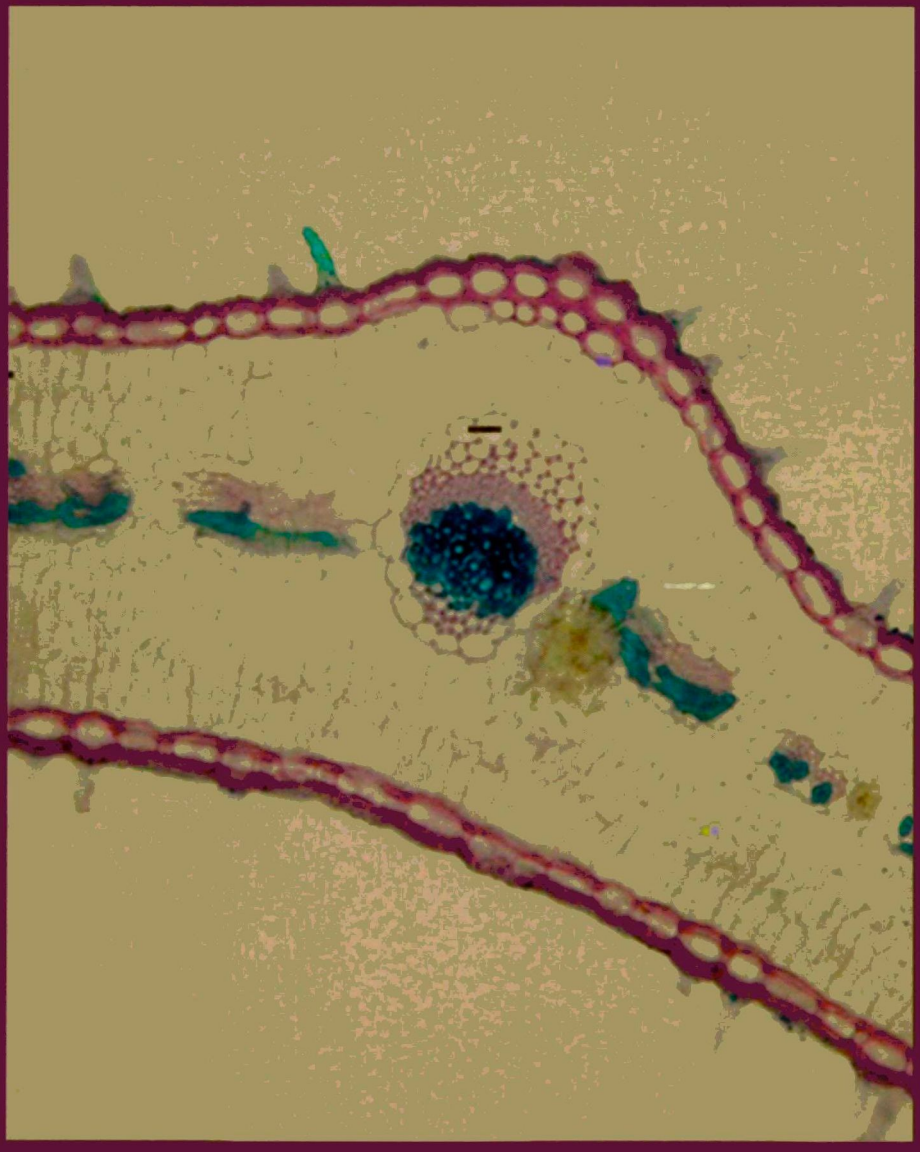

University of Szeged, Szeged, Hungary

Acta Biologica Szegediensis

Acta Biologica Szegediensis (ISSN 1588-385X print form; ISSN 1588-4082 online form) is an international peer-reviewed, open access journal published by the University of Szeged yearly, in two issues per volume.

Acta Biologica Szegediensis publishes novel findings in various fields of biology with special focus on innovative research in modern experimental life sciences. The journal publishes experimental and theoretical papers, reviews, short communications and descriptions of new methods. Letters to the editor and conference proceedings may also be published, subject to the approval of the Editor-in-Chief.

Acta Biologica Szegediensis provides peer review by expert researchers, fast publication times, no page charge and free online accessibility. Table of contents and all issues of the journal are available at http://www2.sci.u-szeged.hu/ABS.

Acta Biologica Szegediensis is indexed in BIOSIS Database, EMBASE, Excerpta Medica, Elsevier BIOBASE (Current Awareness in Biological Sciences), Scopus, SCImago and Zoological Record.

Subscriptions

All subscriptions relate to the calendar year and must be pre-paid. The annual subscription rate is currently 100 USD and includes air mail delivery and handling.

Editor-in-Chief: Csaba Vágvölgyi
Department of Microbiology, Faculty of Science and Informatics
University of Szeged, Közép fasor 52., H-6726 Szeged, Hungary
Phone: 36 (62) 544-822, fax: 36 (62) 544-823
E-mail: csaba@bio.u-szeged.hu

Technical Editor: Tamás Mikola
Acta Biologica Szegediensis, Editorial Office
Közép fasor 52., H-6726 Szeged, Hungary
Phone: 36 (62) 544-822, fax: 36 (62) 544-823
E-mail: abs@bio.u-szeged.hu

ACTA BIOLOGICA SZEGEDIENSIS VOLUME 58(1), 2014

Table of Contents

Articles

Edit Ludmerszki, Ilona Rácz, Szabolcs Rudnóy
S-methylmethionine alters gene expression of candidate genes in *Maize dwarf mosaic virus* infected and drought stressed maize plants 1

Youhua Chen
Ecogeography of haplotype composition of *Sagittaria trifolia* L. (Alismataceae): environment, space, vicariance and selective sweeps 7

Ádám Solti, Gergana Mihailova, Éva Sárvári, Katya Georgieva
Antioxidative defence mechanisms contributes to desiccation tolerance in *Haberlea rhodopensis* population naturally exposed to high irradiation 11

M. Keshavarzi, M. Mahdavinejad, M. Sheidai, A. Gholipour
Anatomical study of some *Silene* L. species of *Lasiostemones* Boiss. section in Iran 15

Attila Ördög, Dóra Bernula, Barnabás Wodala
The effect of xanthan gum as an elicitor on guard cell function and photosynthesis in *Vicia faba* 21

Neda Atzazadeh, Maryam Keshavarzi, Masoud Sheidai, Abbas Gholipour
Morphological and karyotype diversity in populations of four *Silene* species (Caryophyllaceae) 27

Namphung Klomklung, Samantha C. Karunarathna, Kevin D. Hyde, Ekachai Chukeatirote
Optimal conditions of mycelial growth of three wild edible mushrooms from northern Thailand 39

Lilla Szalóki-Dorkó, Fleur Légrádi, László Abrankó, Mónika Stéger-Máté
Effects of food processing technology on valuable compounds in elderberry (*Sambucus nigra* L.) varieties 45

Torda Varga, Zsolt Merényi, Zoltán Bratek, Ádám Solti
Mycorrhizal colonization by *Tuber aestivum* has a negative effect on the vitality of oak and hazel seedlings 49

Tünde Takács, Anna Füzy, Kálmán Rajkai, Imre Cseresnyés
Investigation of arbuscular mycorrhizal status and functionality by electrical impedance and capacitance measurement 55

Elvira Nacsa-Farkas, Eliza Kerekes, Erika Beáta Kerekes, Judit Krisch, Popescu Roxana, Daliborca Cristina Vlad, Pauliuc Ivan, Csaba Vágvölgyi
Antifungal effect of selected European herbs against *Candida albicans* and emerging pathogenic non-albicans *Candida* species 61

Tünde Kupi, Tamás Deák, György D. Bisztray, Ernő Szegedi
Detection of self-complementary inverted repeats by single forward primer driven PCR 65

C. Tsompos, C. Panoulis, K Toutouzas, G. Zografos, A. Papalois
The effect of the antioxidant drug U-74389G on endometrial edema during ischemia reperfusion injury in rats 69

Dissertation summaries 73

On the cover: Leaf cross section structure in *Silene tenella* (see Keshavarzi et al. in this issue).

Volume 58(1):1-5, 2014
Acta Biologica Szegediensis
http://www.sci.u-szeged.hu/ABS

ARTICLE

S-methylmethionine alters gene expression of candidate genes in *Maize dwarf mosaic virus* infected and drought stressed maize plants

Edit Ludmerszki*, Ilona Rácz, Szabolcs Rudnóy

Department of Plant Physiology and Plant Molecular Biology, Eötvös Loránd University, Budapest, Hungary

ABSTRACT In the present work we investigated the potential beneficial effects of the exogenous application of S-methylmethionine (*SMM*) that plays an important role in the plants' sulphur metabolism and contributes to the production of certain defence compounds. The possible beneficial effects were challenged against *Maize dwarf mosaic virus* infection and drought stress. We studied the expression changes of *GF14-6* and *SAMS* during viral infection and *DREB2A* and *DBP2* during drought stress. The product of *GF14-6* recognise the viral coat protein and contributes to RNA-silencing, while the product of *SAMS* plays a central role in the plant sulphur metabolism and contributes to the production of several defence compounds. The products of *DREB2A* and *DBP2* contribute to better plant defence against drought stress and increase the efficiency of water uptake. According to our results, SMM pretreatment has a considerable change on the investigated genes' expression. It significantly decreases the gene expression of *GF14-6*, while infection results in a higher expression level. On the other hand, a more prolonged and long lasting increase is measured in *SAMS* expression as a result to SMM pretreatment followed by infection. *SMM* lessens the gene expression of *DREB2A*, while no changes were observed in *DBP2* compared to drought stressed plants.
Acta Biol Szeged 58(1):1-5 (2014)

KEY WORDS

drought
gene expression
maize
Maize dwarf mosaic virus
S-methylmethionine

Maize (*Zea mays* L.) is one of the most widely cultivated crops worldwide. Apart from being a well-known food and feed plant, it also plays an important role in industry as well, therefore, a great emphasis is put on its research in order to maintain health and crop production.

Maize dwarf mosaic virus (MDMV) is one of the most important pathogens of cultivated sweet corn varieties. The infection usually causes crop losses of 10-45% (Oertel et al. 1997). MDMV preferentially colonizes members of the Poaceae family (such as *Z. mays*) and spreads via aphid, pollen and seed transmission (Tóbiás et al. 2007; Gell et al. 2010; Stewart et al. 2012). Though the precise molecular details of maize response reactions are largely unknown the enhanced expression of *S-adenosylmethionine synthase* (*SAMS*, GenBank: BT054969) and *GF14-6* (MaizeGDB: BG836057.1) (Uzarowska et al. 2009) are considered as typical answers in maize varieties. *SAMS* is important in the synthesis of S-adenosylmethionine, which molecule is important in cellular methylation processes and contributes to the synthesis of plant defence hormones and compounds (Mudd and Datko 1990). *GF14-6* is a member of the 14-3-3 protein family, and is capable of recognising parts of the viral coat protein therefore it has an important regulatory role during plant defence (Konagaya et al. 2004).

As sessile organisms, plants are constantly challenged by a wide range of abiotic stresses as well, from which drought can be mentioned. Drought affects more than 10% of land crops, resulting in more than 50% of crop loss worldwide (Lata and Prasad 2011). In the last decades severe droughts were experienced in the Carpathian basin, mainly due to global climate change, therefore it is becoming a crucial problem in agriculture. During drought stress the upregulation of *DREB2A* (MaizeGDB: AB218833) and *Zea mays DRE-binding protein 2* (*DBP2*, MaizeGDB: FJ805750) genes can be observed, which represent the two main molecular pathways activated during drought. *DREB2A* is present in an abscisic acid independent pathway (Sakuma et al. 2006), while on the other hand *DBP2* takes place in an abscisic acid dependent route and directly binds to DNA and exerts its effects (Zhang et al. 2011). Both of these genes are important in plant defence and are responsible for a more efficient water uptake and drought stress tolerance.

The use of biologically active compounds could be a feasible way of improving tolerance to certain abiotic and biotic stress factors. S-methylmethionine [SMM, $(CH_3)_2$-S-$(CH_2)_2$-CH(NH_2)-COOH], which occurs naturally in the plant kingdom as a non-proteinogenic, sulfur-containing amino

Accepted Aug 25, 2014
*Corresponding author. E-mail: ludmerszki.edit@gmail.com

Table 1. A list of primers used in the investigation, including the reference genes (*Z. mays actin - ZA, maize membrane protein PB1A10.07c* - MEP) and the genes of interest (*GF14-6, SAMS, DREB2A* and *DBP2*).

Gene	Forward primer sequence (5' to 3')	Reverse primer sequence (5' to 3')	qRT-PCR efficiency E
ZA	CGCTAGTGGGCGAACAACT	CGCATGAGGAAGTGTGTATCC	1.983
MEP	TTCCTCATGTTCTTCGTGCC	CAGTTCTCATTCCATCCGTG	1.994
GF14-6	AGAGCAATGTCCTGGGCAG	CAAGATGAAGGGTGATTACTAC	1.992
SAMS	CATTGAGCAGCAGTCCCCT	GGTCTCGTCAGTCGCATAC	1.987
DREB2A	GTGCTGTGGTGCATGGT	CGTAGGCCCATCTCGTGATC	1.991
DBP2	GCCCGATGGCATTTTAGACG	AACCAGGAGATTAGCACGCA	1.989

acid, could be used to enhance resistance. In plants, SMM is synthesized from methionine and can also be regenerated in the SMM-cycle (Mudd and Datko 1990). Similarly as S-adenosylmethionine, SMM is involved in the methylation processes taking place in the cytoplasm, and is an important compound in the transport and storage of sulphur (Bourgis et al. 1999). SMM contributes to improved plant resistance, as it is a direct precursor of the osmoprotectant sulfopropionates involved in defence mechanisms, while also influencing the biosynthesis of plant regulatory and defence compounds such as polyamines and ethylene (Ko et al. 2004).

The aim of this work was to reveal the gene expression changes following viral infection or drought stress both coupled with SMM treatment, by which means the protective effects of SMM can be demonstrated. The changes of *GF14-6*, *SAMS*, *DREB2A* and *DBP2* are evaluated here, whose products are all important in plant defence.

Materials and Methods

Plant growth conditions

Zea mays L. var. *rugosa Jubilee* (sweet corn) plants were grown on Hoagland solution of ¼ strength (containing 80 µM Fe(III)-EDTA as iron form) in growth chamber SANYO MLR-350 HT, with a 14/10 h light/dark period and a light intensity of 300 µmol photon m^{-2} s^{-1}, a day/night temperature of 25/22 °C and 70% relative humidity. To study the effects of SMM, 11-d-old plants were placed in Hoagland solution of ¼ strength containing 2 mg l^{-1} SMM for 24 h. MDMV infection was carried out on the 12th and 14th days of the treatment. The first and second leaves of the plants were inoculated mechanically with Dallas-A strain MDMV particles. Leaves from infected plants developing macroscopic symptoms were homogenized in Sörensen phosphate buffer (pH 7.2, 0.06 M, 0.3 mg dm^{-3}) and were used for inoculation. Carborundum was added as an abrasive. Gene expression changes of the investigated genes were measured 1, 2 and 3 weeks after the infections. To demonstrate drought stress on the 12th day of the treatment PEG-6000 was added to the Hoagland solution of ¼ strength (in 15% of concentration), and plants were grown on that medium for a 1-week period. The real-time PCR measurements were carried out during this 1-week period on the 1st, 3rd and 7th days.

Gene expression changes

qRT-PCR measurements were carried out using the Power SYBR® Green PCR Master Mix (Life Technologies, Foster, CA, USA). The experiments were run on an ABI StepOnePlus Real-Time PCR System (Life Technologies, Foster, CA, USA). The primer efficiencies were evaluated by applying a standard curve, generated from five points of a tenfold dilution series. The slope of the standard curve was fitted into the following equation: $E = 10^{-1/slope}$, where E stands for the efficiency of the given primer pair. The results are indicated in Table 1. The relative changes in gene expression were quantified according to the modified ΔΔCt method of Pfaffl (2001), where E (efficiency) values are taken into account.

Statistical analysis

The results were evaluated using analysis of variance (ANOVA) with SPSS® statistical software (version 20, IBM®) followed by Duncan's multiple range test (DMRT) to test for significant differences between means at $P \leq 0.05$ (Duncan 1955). DMRT considers the pairwise Student's t test comparisons of different datasets. In DMRT letters of the alphabet show the significant differences, where letter 'a' indicates the greatest significantly different average value of a data group, 'b' stands for the second greatest, and so on. Mixed letters (such as 'ab') indicate that these data groups do not differ significantly from 'a' or 'b' values. Three biological and three technical repeats were performed for each experiment.

Results and Discussion

In the present work, the stress responses of maize plants infected with MDMV and exposed to drought stress were studied, and compared to the data of SMM-treated plants and untreated controls. The spread of MDMV was monitored over a three-week period after virus inoculation, while the effects of drought stress for one week.

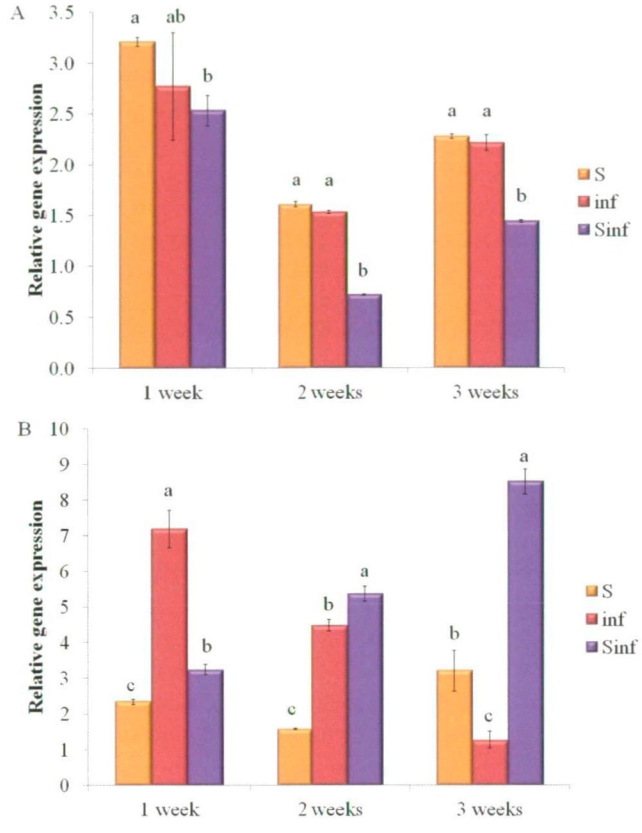

Figure 1. Changes in the relative gene expressions of *GF14-6* (A) and *SAMS* (B) of SMM-treated and MDMV-infected *Z. mays* leaves, shown in relate to control, meaning that the values of the control are equivalent to 1 unit of relative gene expression in all cases. Abbreviations: S - SMM-treated, inf - MDMV-infected, Sinf - SMM-pretreated followed by MDMV infection, *GF14-6 - G-box factor 14-6, SAMS - S-adenosylmethionine synthase*. Letters indicate significant differences at $P \leq 0.05$ according to DMRT. Letter 'a' indicates the greatest significantly different average value of a data group, 'b' stands for the second greatest, and so on. Mixed letters (such as 'ab') indicate that these data groups do not differ significantly from 'a' or 'b' values. Error bars represent standard deviations, n=9.

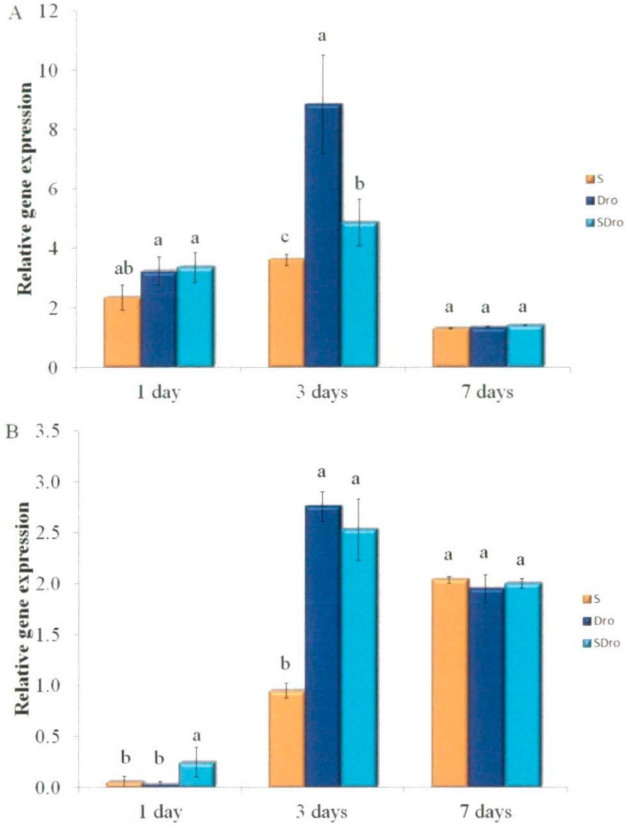

Figure 2. Changes in the relative gene expressions of *DREB2A* (A) and *DBP2* (B) of SMM-treated and drought-stressed *Z. mays* leaves, shown in relate to control, meaning that the values of the control are equivalent to 1 unit of relative gene expression in all cases. Abbreviations: S - SMM-treated, Dro - drought-stressed, SDro - SMM-pre-treated followed by drought stress. Letters indicate significant differences at $P \leq 0.05$ according to DMRT. Letter 'a' indicates the greatest significantly different average value of a data group, 'b' stands for the second greatest, and so on. Mixed letters (such as 'ab') indicate that these data groups do not differ significantly from 'a' or 'b' values. Error bars represent standard deviations, n=9.

In infected plants the mechanical effects of the rubbing (without virus particles), referred to as negative control were investigated previously. According to our results, in a short term period (1-3 days after the mechanical rubbing) stress response was detected, but only in the mechanically rubbed 1st and 2nd leaves. One week after the infections the harmful effects diminished, and when gene expression measurements were conducted from the younger leaves of negative control (4th to 6th leaves), the average values did not differ significantly from control plants.

During the course of MDMV infection significant changes occur in the plant metabolism, therefore in gene regulation as well. The gene expression levels of *GF14*-6 changed in a similar manner in all treated groups, since the 2.5-3-fold increase in the 1st week was followed by a decrease in the 2nd week and a subsequent elevation in the 3rd week (Figure 1A). The decrease was the most expressed in infected plants that were SMM-pretreated as well, whose *GF14-6* expression values decreased under the control level in the *2nd* week, and were always exceeded by the two other groups, indicating a weaker stress response. Based on Konagaya et al. (2004), 14-3-3 proteins can recognize parts of the coat protein of *Tobacco mosaic virus*, contributing to RNA silencing. We assume that in the case of MDMV infection a similar mechanism may take place. Therefore, we propose that the gene product of *GF14-6* regulates MDMV coat protein recognition and RNA-silencing. Hence the fall in the expression in SMM-pretreated and afterwards infected plants could be related to improved plant defense as a result of SMM pretreatment

MDMV infection caused a 7-fold rise in expression of

SAMS one week after the treatment (Figure 1B), though a continuous fall-off was found in the gene activity, approaching control level in the 3rd week. By contrast, in SMM-pretreated and subsequently infected plants the gene expression increased in a moderate rate with a continuous elevation, reaching a more than 8-fold enhancement (compared to control) in the 3rd week, indicating a less rapid but even long-lasting response to the MDMV infection. In only SMM-treated plants the expression of *SAMS* changed about 1.5-3-fold. These results suggest that this gene product play an important role during MDMV infection, probably by up-regulating the formation of S-adenosylmethionine involved in numerous methylation processes, and therefore enhancing the SMM-cycle, further contributing to the production of defence compounds. SMM pre-treatment remarkably changed this profile. A more prolonged increase was observed compared to only infected plants, ensuring a constant long-lasting expression of this versatile enzyme involved in many aspects of gene transcription, cell housekeeping and secondary metabolite production. SMM treatment in uninfected plants slightly increased the expression of *SAMS*, presumably due to the contribution to the methionine and SMM-cycles.

Osmotic stress triggers either abscisic acid-dependent or abscisic acid-independent molecular pathways, resulting in an advanced plant defence. *DREB2A* is located in the abscisic acid-independent pathway in an upstream position, whereas *DBP2* is localised in the abscisic acid-dependent pathway and in a more downstream position (Sakuma et al. 2006; Zhang et al. 2011). Therefore a comprehensive picture is acquired with the expression study of these two genes about drought stress signalling. During the investigation 1-d, 3-d and 7-d stressed plants were studied. The gene expression changes of *DREB2A* were most pronounced in 3-d stressed plants (Figure 2A). In drought-stressed plants approximately a 9-fold increase was measured compared to control plants, while when SMM pretreatment was applied prior to drought stress, only a 4.5-fold increase was detected. Even in 1-d stressed plants a considerable increase is observed in the gene expression (around 3-fold increase in drought-stressed plants), due to the protein's upstream regulation. The results show that the product of *DREB2A* plays an important role in osmotic stress, its relatively early appearance support its importance in early plant defence. When SMM was given to drought-stressed plants a slighter increase was observed in the gene expression indicating a moderate activation of the ABA-independent pathway.

Slightly different results were acquired in the case of *DBP2* (Figure 2B). In 1-d stressed plants a significant decrease was found in all treated groups. 3-d stressed plants had a 3-fold increase compared to the control, irrespectively of SMM treatment prior to drought stress. After 7-d all treated groups showed an about 2-fold expression of the control. The data indicate that the abscisic acid-dependent pathway is also active during osmotic stress, but lower levels of gene expression show its less importance in this process. Also, SMM pretreatment resulted in no changes compared to drought stressed plants, indicating that SMM may not play such an important role in this pathway.

The results suggest that the gene products of *GF14-6*, *SAMS*, *DREB2A* and *DBP2* play a crucial role in the mechanisms of plant defence against MDMV infection and drought stress. The natural compound SMM has a beneficial effect on the stress response, resulting in an increase in the defence potential of maize plants during MDMV infection and drought stress. Furthermore we assume that similar results would be achieved while observing other biotic and abiotic stresses as well. These observations are in agreement with our previous findings (Rácz et al. 2008; Ludmerszki et al. 2011).

Acknowledgements

The authors thank Györgyi Balogh and Asztéria Almási for their technical assistance. This research was supported by the European Union and the State of Hungary, co-financed by the European Social Fund in the framework of TÁMOP 4.2.4. A/1-11-1-2012-0001 'National Excellence Program , and by the grant of the Hungarian Scientific Research Fund (OTKA 108834).

References

Bourgis F, Roje S, Nuccio ML, Fisher DB, Tarczynski MC, Li C, Herschbach C, Rennenberg H, Pimenta MJ, Shen TL, Gage DA, Hanson AD (1999) S-methylmethionine plays a major role in phloem sulfur transport and is synthesized by a novel type of methyltransferase. Plant Cell 11:1485-1497.

Duncan DB (1955) Multiple range and multiple F tests. Biometrics 11:1-42.

Gell Gy, Balázs E, Petrik K (2010) Genetic diversity of Hungarian Maize dwarf mosaic virus isolates. Virus Genes 40:277-281.

Ko SH, Eliot AC, Kirsch JF (2004) S-methylmethionine is both a substrate and an inactivator of 1-aminocyclopropane-1-carboxylate synthase. Arch Biochem Biophys 421:85-90.

Konagaya KI, Matsushita Y, Kasahara M, Nyunoya H (2004) Members of 14-3-3 protein isoforms interacting with the resistance gene product N and the elicitor of Tobacco mosaic virus. J Gen Plant Pathol 70:221-231.

Lata C and Prasad M (2011) Role of DREBs in regulation of abiotic stress responses in plants. J Exp Bot 62:4731-4748.

Ludmerszki E, Rudnóy S, Almási A, Szigeti Z, Rácz I (2011) The beneficial effects of S-methyl-methionine in maize in the case of Maize dwarf mosaic virus infection. Acta Biol Szeged 55:109-112.

Mudd SH and Datko AH (1990) The S-methylmethionine cycle in Lemna paucicostata. Plant Physiol 93:623-630.

Oertel U, Schubert J, Fuchs E (1997) Sequence comparison of the 3'-terminal parts of the RNA of four German isolates of sugarcane mosaic potyvirus (SCMV). Arch Virol 142:675-687.

Pfaffl MW (2001) A new mathematical model for relative quantification in real-time RT-PCR. Nucleic Acids Res 29:e45.

Rácz I, Páldi E, Szalai G, Janda T, Pál M, Lásztity D (2008) S-methylmethionine reduces cell membrane damage in higher plants exposed to low-temperature stress. J Plant Physiol 165:1483-1490.

Sakuma Y, Maruyama K, Qin F, Osakabe Y, Shinozaki K, Yamaguchi-Shinozaki K (2006) Dual function of an Arabidopsis transcription factor

DREB2A in water-stress-responsive and heat-stress-responsive gene expression. PNAS 49:18822-18827.

Stewart LR, Bouchard R, Redinbaugh MG, Meulia T (2012) Complete sequence and development of a full-length infectious clone of an Ohio isolate of Maize dwarf mosaic virus (MDMV). Virus Res 165:219-224.

Tóbiás I, Bakardjieva N, Palkovics L (2007) Comparison of Hungarian and Bulgarian isolates of maize dwarf mosaic virus. Cereal Res Commun 35:1643-1651.

Uzarowska A, Dionisio G, Sarholz B, Piepho HP, Xu M, Ingvardsen CR, Wenzel G, Lübberstedt T (2009) Validation of candidate genes putatively associated with resistance to SCMV and MDMV in maize (Zea mays L.) by expression profiling. BMC Plant Biol 9:15.

Zhang X, Zhen J, Li Z, Kang D, Yang Y, Kong J, Hua J (2011) Expression profile of early responsive genes under salt stress in upland cotton (Gossypium hirsutum L.). Plant Mol Biol Rep 29:626-637.

Volume 58(1):7-10, 2014
Acta Biologica Szegediensis
http://www.sci.u-szeged.hu/ABS

ARTICLE

Ecogeography of haplotype composition of *Sagittaria trifolia* L. (Alismataceae): environment, space, vicariance and selective sweeps

Youhua Chen

Department of Renewable Resources, University of Alberta, Edmonton, Canada

ABSTRACT In the present report, the relative influence of environment and space was evaluated for explaining the variation of haplotype composition of 42 populations of *Sagittaria trifolia* L. (Alismataceae) in China. The results showed that, neither environment nor space could explain current haplotype composition patterns of *S. trifolia*, and most variation in haplotype composition could not be explained. Vicariance was recognized to explain the pattern that most haplotypes (25 out of 27 ones) were rare, being found in only one or two populations of *S. trifolia* in China. Finally, an emerging selective sweep from increasing human activity and habitat destruction explained the dominance patterns of haplotypes 5 and 8 among populations of *S. trifolia*.

Acta Biol Szeged 58(1):7-10 (2014)

KEY WORDS

environmental filtering,
genetic drift,
population genetic structure,
vicariance,
variation partitioning

Environmental filtering and dispersal limitation are known to influence the phylogeographic patterns of many species (Kelly et al. 2006; Viruel et al. 2012). Phylogeographic and population genetic structure of some herb species in the genus *Sagittaria* (family Alismataceae) have been quantified in recent studies in China (Chen et al. 2008; Tan et al. 2008; Liu et al. 2010). However, the role of environment and dispersal in generating the observed genetic structure has not been assessed thus far.

Among these species whose population genetic structure has been recently characterized is *S. trifolia*, a perennial herb that is widely distributed in Eurasian areas (Chen et al. 2008). This species is an ideal candidate to investigate the influence of historical contingency and contemporary environment on its distribution (Chen et al. 2008). In the present study, the effects of environment and space on haplotype composition and distribution of the species range was examined.

S. trifolia can disperse by several mechanisms including water and animals, especially bees and other insects (Cook 1990; Chen et al. 2008). The wide distribution of this species in Eurasia could be a result of its long-distance dispersal ability. I thus predicted that the variation in haplotype composition among different populations of *S. trifolia* in China would be closely related to the geographic distance between populations (field locations). The wide distributional range of *S. trifolia* over the territory of China, however, also includes many distinct climatic domains (Chen et al. 2006; Qin et al. 2006). The influence of environmental filtering (or environmental gradients) should thus also be critical in determining the haplotype composition pattern of *S. trifolia*. Given that both dispersal limitation and environmental filtering might function simultaneously in determining the geographic distribution of *S. trifolia*, I sought to quantify the relative importance of both mechanisms. I utilized a variation partitioning technique to quantitatively assess the relative contribution of space and environment on the population genetic structure of *S. trifolia* in China in terms of haplotype composition.

Accepted June 11, 2014
*Corresponding author. E-mail: haydi@126.com

Materials and Methods

Distribution and haplotype information

Forty-two *S. trifolia* populations were considered in the present study that covered a wide range of the territory of China, representing almost all the natural distributional ranges for the species (Chen et al. 2008). Details on the field locations have been recorded in a previous study (Chen et al. 2008). In general, there are 11 northeast populations, 2 northwest populations, 1 north population, 5 east populations, 6 central populations, 3 south populations and 14 southwest populations (Chen et al. 2008). Figure 1 presented the geographic distribution of these populations over the territory of China. Haplotype information for the 42 *S. trifolia* populations was determined by using and comparing the atpB-rbcL noncoding intergenic spacer region of Chloroplast DNA of the 108 individuals over different populations (Chen et al. 2008). In total, 27 haplotypes were identified constituting a 42×27 population-haplotype matrix for analysis (Table 1).

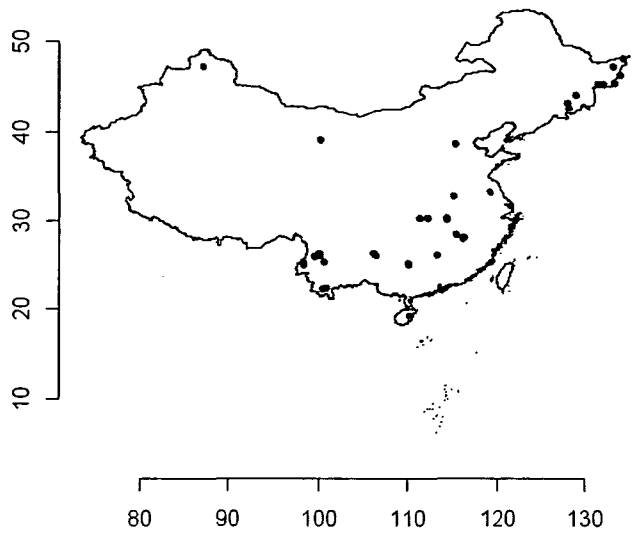

Figure 1. Forty-two sampling locations for species *S. trifolia* across territory of China as presented in Fig. 1 of the previous study (Chen et al. 2008).

Spatial and environmental variables

Latitude and longitude were the two most important spatial variables used to quantify the strength of dispersal in structuring haplotype composition of *S. trifolia* populations. However, because the raw spatial variables may not have been accurate in characterizing the structure of spatial autocorrelation within the haplotype data, I performed a transformation using principal coordinates of neighboring matrices (PCNM) (Dray et al. 2006; Legendre et al. 2009).

Environmental data characterizing the field locations were gathered from the IPCC (http:// www.ipcc-data.org/) and Hydro 1k (http://gcmd.nasa.gov/records/GCMD_HYDRO1k.html) databases. Fifteen variables were considered including diurnal temperature range, ground frost frequency, precipitation, solar radiation, temperature (minimum, mean and maximum), vapor pressure, wet day frequency, elevation, wetness index, aspect, slope, flow direction and flow accumulation. To avoid potential collinearity among the environmental variables in the variation partitioning, I performed a principal component analysis and extracted the first five principal axes as the representative of important environmental gradients influencing population genetic structure of *S. trifolia*.

Variation partitioning technique

Variation partition has been widely applied in community ecology (Borcard et al. 1992; Legendre and Legendre 1998; Meot et al. 1998; Legendre 2007; Legendre et al. 2009). This technique can elucidate the relative contribution of different groups of explanatory variables on the variation in species composition (*i.e.*, beta diversity). The larger the proportion of variation explained by a group of explanatory variables is, the higher influence it has on the species composition.

A simplified version for the variation partitioning method was presented here (Borcard et al. 1992; Legendre and Legendre 1998; Chen 2013; Goncalves-Souza et al. 2014): Suppose that we have the covariate matrices E and S for environmental and spatial variables respectively (each column represents one factor). G is the combined matrix by merging both E and S. Y is the response matrix (here is the presence-absence matrix for the hyplotypes of *S. trifolia*). Then, I

Table 1. Geographic locations of 42 *S. trifolia* populations in China and associated haplotype presence/absence patterns from the previous study (Chen et al. 2008). Codes: 0: absence; 1: presence.

Population ID	Longitude (E)	Latitude (N)	Haplotype composition
JL-1	128.13	43.19	00000001000000000001000000000
JL-2	128.15	43.23	00001001000000000000000000000
JL-3	128.28	42.57	00001000000000000000000000000
HLJ-1	131.51	45.3	00000000000000000000001000100
HLJ-2	132.16	45.27	00000001000000000000000000000
HLJ-3	132.16	45.27	00000000000000000000010100000
HLJ-4	129.11	44.06	00101001000000000000000000000
HLJ-5	134.01	46.44	00001001000000000000000000000
HLJ-6	134.24	48.2	00001000000000000000000000000
HLJ-7	133.18	47.25	00001010000000000000000000000
HLJ-8	133.35	45.47	00000000000010100000010000
XJ-1	87.19	47.37	00000000000000000000000000001
GS-1	100.27	39.03	00000001000000000000000000000
HEB-1	115.56	38.54	00000001000000000000000000000
YN-1	100.11	26.14	00101001000000000000000000000
YN-2	100.1	26.36	00000001000000000000000000000
YN-3	98.33	25.43	00000001000000000001000000000
YN-4	100.15	26.34	00001001000000000000000000000
YN-5	100.56	22.4	00011000000000000000000000000
YN-6	98.33	25.07	00001001000001000000000000000
YN-7	101.01	22.45	11000000000000000000000000010
YN-8	99.56	26.06	00001001000000000000000000000
YN-9	100.6	25.42	00001000000000000000000000000
YN-10	100.1	26.36	00001001000000000000000000000
GZH-1	106.4	26.24	10001000000000000000000000000
GZH-2	106.2	26.25	00000001000000000000000000000
GZH-3	106.27	26.29	00001001000000000000000000000
GZH-4	106.16	26.25	00001001000000000000000000000
HUB-1	114.37	30.24	00001001000000000000000000000
HUB-2	114.41	30.2	00001001000000000000000000000
HUB-3	111.35	30.28	00001001000000000000000000000
HUB-4	112.22	30.31	00001000000100000000000000000
HUN-1	113.4	26.16	00001001000000000000000000000
HEN-1	115.24	32.7	00001000010000000000000000000
JS-1	119.29	33.24	00000000000000011000000000000
JS-2	119.29	33.19	00000001001000000000000000000
JX-1	116.37	28.14	00001000000000000000000001000
JX-2	115.51	28.45	00001000000000000000000000000
JX-3	116.31	28.05	00000001000000000000000000000
HAIN-1	110.34	19.21	00001100100000000000000000000
GX-1	110.18	25.23	00001000000000000000000000000
GX-2	110.16	25.05	00001001000000000000000000000

perform redundancy analysis (or multivariate regression analysis) on the covariate matrices to the response matrix as: $Y_E = E(E^TE)^{-1}EY$; $Y_S = S(S^TS)^{-1}SY$; $Y_G = G(G^TG)^{-1}GY$. Defining the variation operator as $COV(X) = \frac{1}{n}Trace((X-\bar{X})^T(X-\bar{X}))$. Then, the variation explained solely by the environmental covariates E is given by $COV(Y_G) - COV(Y_S)$; the variation explained solely by the spatial covariates S is given by $COV(Y_G) - COV(Y_E)$; and the variation jointly explained by both environmental and spatial covariates is given by $COV(Y_S) + COV(Y_E) - COV(Y_G)$. At last, the unexplained variation is $COV(Y) - COV(Y_G)$.

Variance partitioning was applied at the population level for *S. trifolia*. I used composition (or distribution) of the 27 haplotypes over the 42 *S. trifolia* populations and evaluated the relative influence of environmental and spatial descriptors on influencing the haplotype composition among populations. The program "vegan" (Oksanen et al. 2012) in the R environment (R Development Core Team 2013) was used to perform variation partitioning with the function "varpart". The multivariate method, canonical correspondence analysis (CCA) (ter Braak 1986), was implemented when performing variation partitioning.

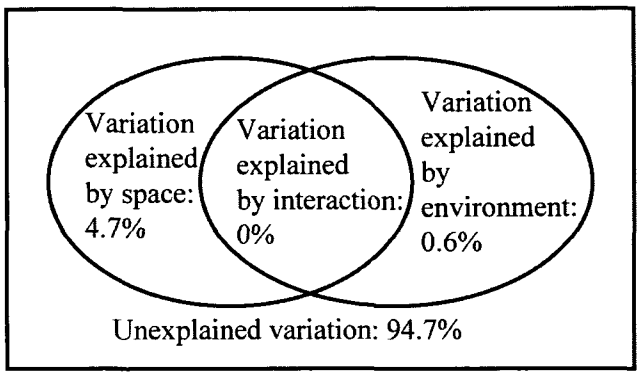

Figure 2. Result of variation partitioning explaining haplotype composition of *S. trifolia* populations in China. The term "interaction" inside the intersection of the two ellipses indicates the interaction of space and environment.

Results

Interestingly, neither space nor environment could strongly explain the haplotype composition of *S. trifolia* populations (Fig. 2). Space explained only 4.7% of total variation, while environment explained essentially none (0.6%) of the total variation of the haplotype composition of *S. trifolia* populations. The interaction between space and environment also did not explain any (0%) of the variation in haplotype composition. Most variation (94.7%) in haplotype composition could not be explained using the selected variables.

Given the fact that there are too much variation unexplained based on the results, the possible explanations on the relative importance of spatial and environmental filtering on structuring haplotype distribution of *S. trifolia* distributed over China are challenging. However, because the composition of haplotypes among the natural populations of *S. trifolia* presented interesting patterns (*i.e.*, some haplotypes dominate across different populations) (Chen et al. 2008), some discussions and conclusions still can be drew as in the discussion section.

Discussion

Spatial and environmental effects did not play a substantial role in influencing the population genetic structure of *S. trifolia* in China in terms of haplotype composition. Thus, my hypothesis that space and environment structure haplotype composition of *S. trifolia* populations was not supported.

My results suggest that haplotype divergence of *S. trifolia* may not be related to environmental filtering and may be only slightly related to spatial limitation. However, it should be acknowledged that the present study suffers certain limitations that affect this interpretation. Firstly, the 47 populations of *S. trifolia* included in the study were all within the territory of China. We might have found evidence of environmental filtering or space if populations in Russia or Europe were also included (Chen et al. 2008). Secondly, haplotype information examined in this study derived from only one DNA marker (a noncoding region of chloroplast +DNA), which may be not sufficient to reflect the true haplotype condition of the species over different populations. The combination of haplotype information from different microsatellite loci (Hosid et al. 2010; Viruel et al. 2012) is necessary to systematically and holistically reveal the haplotype composition of the species and uncover the emerging roles of environment and space on influencing haplotype diversity and composition of the species.

A different mechanism that may be more important than space and environment in determining the haplotype composition of *S. trifolia* populations is vicariance (*i.e.*, geographic isolation) (Estep et al. 2005; Viruel et al. 2012). There is indication in the data that vicariance could be an important driver of *S. trifolia* composition in that most haplotypes were rare, being found in only one or two of the 42 populations examined. Indeed, out of a total 27 haplotypes found in the samples, 23 haplotypes were found in just a single population and 2 haplotypes were present in just 2 populations (Table 1). This high divergence of haplotypes between populations could be a result of dispersal barriers, habitat discreteness or isolated areas (Kelly et al. 2006). A high vicariance level among populations leads to higher divergence when comparing different populations (Estep et al. 2005; Kelly et al. 2006; Viruel et al. 2012). It is noted, however, that limited sampling may also explain why the occurrence of haplotypes was so rare between populations.

Interestingly, it was observed that haplotypes 5 and 8 were highly predominant among the different populations. It is possible that recent dispersal, genetic drift or a selective sweep

(Depaulis et al. 1999; Depaulis et al. 2000; Messer and Neher 2012) is emerging among isolated populations, leading to the increasing dominance of haplotypes 5 and 8 in China. Mutations in specific nucleotide sites for haplotypes 5 and 8 may provide a survival advantage and increased fitness. A selective sweep resulting in the dominance of haplotypes 5 and 8 might be also driven by human activity and habitat destruction, as high-speed economic development and environmental change in China (Chen et al. 2006; Qin et al. 2006) have increased arthropogenic impacts on the native habitats of *Sagittaria* (Chen et al. 2008; Tan et al. 2008; Liu et al. 2010).

In conclusion, to better elucidate haplotype composition of *S. trifolia*, more field sampling and DNA sequencing are advised. As discussed above, the haplotype information should be as comprehensive as possible if ones want to better quantify the relative influence of neutrality and niche mechanisms in structuring the spatial distribution patterns of *S. trifolia* haplotypes.

Acknowledgements

I thank Gennifer Meldrum for her great help on improving the language aspect of the work. I appreciate an anonymous reviewer for providing constructive comments on helping improve an earlier version of the work. The study is supported by China Scholarship Council.

References

Borcard D, Legendre P, Drapeau P (1992) Partialling out the Spatial Component of Ecological Variation. Ecology 73:1045.

Ter Braak CJF (1986) Canonical correspondence analysis: a new eigenvector technique for multivariate direct gradient analysis. Ecology 67:1167-1179.

Chen J, Liu F, Wang Q, Motley T (2008) Phylogeography of a marsh herb *Sagittaria trifolia* (Alismataceae) in China inferred from cpNA atpB-rbcL intergenic spacers. Mol Phylogenet Evol 48:168-175.

Chen Y (2013) A comparison of synonymous codon usage bias patterns in DNA and RNA viruus genomes: quantifying the relative importance of mutational pressure and natural selection. Biomed Res Int 2013:406342.

Chen Y, Ding Y, She Z, et al. (2006) Assessment of climate and environment changes in China (II): Impacts, adaptation and mitigation of climate and environment changes. Adv Clim Chang Res 2:6-12.

Cook C (1990) Aquatic plant book. SPB Academic Publishing, The Hague, The Netherlands.

Depaulis F, Brazier L, Mousset S, Turbe A, Veuille M (2000) Selective sweep near the In(2L)t inversion breakpoint in an African population of *Drosophila melanogaster.* Genet Res 76:149-158.

Depaulis F, Brazier L, Vuille M (1999) Selective sweeps at the *Drosophila melanogaster* suppressor of hairless locus and its association with the In(2L)t inversion polymorphism. Genetics 152:1017-1024.

Dray S, Legendre P, Peres-Neto PR (2006) Spatial modelling: a comprehensive framework for principal coordinate analysis of neighbour matrices (PCNM). Ecol Modell 196:483-493.

Estep MC, Connell MU, Henson RN, Murell ZE, Small RL (2005) Testing a vicariance model to explain haplotype distribution in the psammophilic scorpion *Paruroctonus utahensis*. Southwest Nat 50:150-157.

Goncalves-Souza T, Diniz-Filho J, Romero G (2014) Disentangling the phylogenetic and ecological components of spider phenotypic variation. PLoS One 9:e89314.

Hosid E, Yusim E, Grishkan I, Frenkel ZM, Wasswer SP, Nevo E, Korol A (2010) Microsatellite diversity in natural populations of ascomycetous fungus, *Emericella nidulans*, from different climatic-edaphic conditions in Israel. Isr J Ecol Evol 56:119-134.

Kelly D, Maclsaac H, Heath D (2006) Vicariance and dispersal effects on phylogeographic structure and speciation in a widespread estuarine invertebrate. Evolution (N Y) 60:257-267.

Legendre P (2007) Studying beta diversity: ecological variation partitioning by multiple regression and canonical analysis. J Plant Ecol 1:3-8.

Legendre P, Legendre L (1998) Numerical ecology. Elsevier Science BV, Amsterdam

Legendre P, Mi X, Ren H, Ma K, Yu M, Sun I-F, He F (2009) Partitioning beta diversity in a subtropical broad-leaved forest of China. Ecology 90:663-674.

Liu F, Zhao S-Y, Li W, Chen J-M, Wang Q-F (2010) Population genetic structure and phylogeographic patterns in Chinese endemic species *Sagittaria lichuanensis*, inferred from cpDNAatpB-rbcL intergenic spacers. Botany 88:886-892.

Meot A, Legendre P, Borcard D (1998) Partialling out the spatial component of ecological variation: questions and propositions in the linear modelling framework. Environ Ecol Stat 5:1-27.

Messer P, Neher R (2012) Estimating the strength of selective sweeps from deep population diversity data. Genetics 191:593-605.

Oksanen J, Blanchet G, Kindt R, et al. (2012) vegan: Community Ecology Package. R package version 2.0-4.

Qin D, Ding Y, Su J, et al. (2006) Assessment of climate and environment changes in China (I): Climate and environment changes in China and their projections. Adv Clim Chang Res 2:1-5.

R Development Core Team (2013) R: A Language and Environment for Statistical Computing, Vienna, Austria. ISBN 3-900051-07-0, URL http://www.R-project.org.

Tan B, Liu K, Yue X-L,Liu F, Chen J-M, Wang Q-F (2008) Chloroplast DNA variation and phylogeographic patterns in the Chinese endemic marsh herb *Sagittaria potamogetifolia*. Aquat Bot 89:372-378.

Viruel J, Catalan P, Segarra-Moragues J (2012) Disrupted phylogeographical microsatellite and chloroplast DNA patterns indicate a vicariance rather than long-distance dispersal origin for the disjunct distribution of the Chilean endemic *Dioscorea biloba* (Dioscoreaceae) around the Atacama Desert. J Biogeogr 39:1073-1085.

Volume 58(1):11-14, 2014
Acta Biologica Szegediensis
http://www.sci.u-szeged.hu/ABS

ARTICLE

Antioxidative defence mechanisms contributes to desiccation tolerance in *Haberlea rhodopensis* population naturally exposed to high irradiation

Ádám Solti[1]*, Gergana Mihailova[2], Éva Sárvári[1], Katya Georgieva[2]

[1]Department of Plant Physiology and Molecular Plant Biology, Eötvös University, Budapest, Hungary, [2]Institute of Plant Physiology and Genetics, Bulgarian Academy of Sciences, Sofia, Bulgaria

ABSTRACT Drought induced stress is one of the most important among the environmental challenges. *Haberlea rhodopensis*, a chlorophyll-retaining resurrection plant, can survive desiccation to air-dry stage in its usual low irradiance habitat ("shade" plants). Nevertheless, in the past years, some populations living under high irradiance ("sun" plants) have been also discovered with the same ability to survive dehydration. In order to clarify the adaptation mechanisms to a high irradiation habitat, superoxide dismutase (SOD) activity determined by activity staining on polyacrylamide gels and malondialdehyde (MDA) content of sun and shade plants collected from high and low irradiance environment, respectively, were studied. Desiccation induced a significantly higher induction in SOD activity and thus a smaller increase in the MDA content in sun compared to shade plants. The MDA content and SOD activity was restored in both sun and shade plants after six-day rehydration. Nevertheless, the SOD activity remained higher in rehydrated sun leaves compared to the well-hydrated initial stage. The early enhancement of SOD activity in dehydrating sun plants contributes to the higher stress tolerance of these populations.

Acta Biol Szeged 58(1):11-14 (2014)

KEY WORDS

drought
Haberlea rhodopensis
malondialdehyde
resurrection plant
superoxide dismutase

Environmental challenges deeply influence plant productivity. However, plants evolved mechanisms in order to tolerate various stresses including drought. One of the most amazing set of tolerance mechanisms is evolved by the resurrection higher plants which have a unique ability to survive dehydration to the air-dry state. *Haberlea rhodopensis* Friv. (Gesneriaceae) is a Balkan endemism that belongs to the homoiochlorophyllous (chlorophyll-retaining) resurrection type (Tuba et al. 1998). Most of the *H. rhodopensis* populations grow in deep shadow under natural conditions, and they are very sensitive to high irradiation especially during desiccation (Georgieva and Maslenkova 2006). In fact, desiccation at 350 μmol m^{-2} s^{-1} irradiance induced irreversible damages in the photosynthetic apparatus, and thus mature leaves were not able to recover during rehydration (Georgieva et al. 2008). Nevertheless, recent studies revealed a high ecological plasticity of *H. rhodopensis* in natural habitats (Daskalova et al. 2011). In spite of the majority of *H. rhodopensis* prefers deeply shaded light environment, several populations inhabit rock surfaces exposed to high light irradiance, drought, high and low temperatures. Previous results showed that the membrane integrity of sun plants is protected (Georgieva et al. 2012). They were shown to have a higher ability to dissipate absorbed excitation energy by an antennae-based non-photochemical quenching route, thus have a reduced photosystem II inactivation during desiccation in contrast to shade plants (Solti et al. 2014). It is also known that resurrection plants use antioxidative defence systems to cope with desiccation (Farrant 2000; Dinakar et al. 2012). For a better understanding of the adaptation of sun plant to the high-light habitat, the oxidative damage and antioxidative defence was compared in *H. rhodopensis* sun and shade plants.

Accepted July 30, 2014
*Corresponding author. E-mail: adam.solti@ttk.elte.hu

Materials and Methods

Plant material

Experiments were conducted on *Haberlea rhodopensis* Friv. plants growing in Rhodope Mountains, South-West Bulgaria, Orehovo region (N41°52.231; E024°36.171). Plants of various hydration stages were collected on slopes exposed to full sunlight (1500-1700 μmol m^{-2} s^{-1} average summer photosynthetically active radiation [PAR], leaf-level temperature of 30-37 °C and relative air humidity of about 15-30%; 'sun' plants). Sun plants were compared to understory plants growing in shaded habitats (25 μmol m^{-2} s^{-1} average summer PAR, leaf-level temperature of 21-25 °C and a relative humidity of 40-45%; 'shade' plants). Light intensity was measured at the surface of the collected plants by QSPAR Quantum Sensor (Hansatech Ltd., United Kingdom). Leaf temperature and

Table 1. Superoxide dismutase (SOD) activity (expressed in total pixel density of activity stained gel lanes mg^{-1} total soluble protein) in leaves of shade and sun adapted *Haberlea rhodopensis* plants under desiccation and rehydration. 90% RWC - well-hydrated control; 50% RWC – mild dehydration; 8% RWC - desiccated; R1 - rehydration for one day; R6 - rehydration for six days. Error bars represent SD values. One-way ANOVAs with Tukey-Kramer *post-hoc* tests were performed to analyse statistical differences (P<0.05).

Stages	Shade plants	Sun plants
	pixel density mg^{-1} protein	
90% RWC	190.9±45.8 ^{a}	197.4±32.9 ^{a}
50% RWC	220.9±11.8 ^{a}	382.4±40.1 ^{bc}
8% RWC	266.5±50.6 ^{ab}	423.9±6.4 ^{c}
R1	240.6±4.5 ^{a}	307.1±37.9 ^{bc}
R6	211.7±36.3 ^{a}	301.5±8.2 ^{b}

Table 2. Malondialdehyde (MDA) content of shade and sun adapted *Haberlea rhodopensis* leaves under desiccation and rehydration. 90% RWC - well-hydrated control; 50% RWC – mild dehydration; 8% RWC - desiccated; R1 - rehydration for one day; R6 - rehydration for six days. Error bars represent SD values. One-way ANOVAs with Tukey-Kramer *post-hoc* tests were performed to analyse statistical differences (P<0.05).

Stages	Shade plants	Sun plants
	mmol MDA g^{-1} D.W.	
90% RWC	0.110±0.020 ^{a}	0.155±0.027 ^{ab}
50% RWC	0.128±0.047 ^{ab}	0.151±0.051 ^{ab}
8% RWC	0.287±0.030 ^{c}	0.200±0.030 ^{b}
R1	0.167±0.070 ^{ab}	0.135±0.025 ^{ab}
R6	0.108±0.017 ^{a}	0.105±0.032 ^{a}

relative humidity values were detected by a Pocket Profi-Termohygrometer (TFA, Germany). Leaves of plants with approximately 90%, 50% and 8% relative water content (RWC) were collected. Rehydration experiments were performed under laboratory conditions and samples were taken after one day (50-60% RWC – R1) and six days rehydration (90-95% RWC – R6). The RWC of *H. rhodopensis* leaves was determined gravimetrically by weighing them before and after oven drying at 80°C to a constant mass and expressed as the percentage of water content in dehydrated tissue compared to water-saturated tissues, using the equation: RWC (%) = (fresh weight – dry weight) 100/(saturated weight – dry weight). Saturated weight was measured on leaf discs maintained 16 h at 4°C in the dark floating on water.

Superoxide dismutase enzyme assay

The activity of superoxide dismutase (SOD, EC 1.15.1.1) was measured according Giannopolitis and Ries (1977) with some modifications. 100 mg leaf samples were homogenized on ice in 1 ml isolating buffer (50 mM Na-K-phosphate buffer [pH 7.0], 1.0 mM ethylenediaminetetraacetic acid (EDTA), 0.1% (w/v) Triton X-100, 2 mM polyvinylpyrrolidone and 50 mM Na-ascorbate) and centrifuged at 15000 × g for 15 min, and the supernatants were collected as crude extract. Samples were solubilised mildly (5 mM Tris-HCl [pH 6.8], 0.01% SDS, 10% glycerol and 0.001% bromophenol blue). Soluble proteins were separated by native PAGE using 10-18% gradient acrylamide gels by Laemmli (1970) containing only 0.01% SDS. Gels were stained for SOD activity in 50 mM Na-K-phosphate buffer [pH 7.8], 0.1 mM EDTA, 13 mM methionine, 60 µM riboflavin, 2.25 mM Nitro Blue Tetrazolium. Activity stained gels were evaluated by densitometry using the Phoretix software (Phoretix International, Newcastle upon Tyne, UK).

To determine the protein content of samples, solubilised proteins were run on 10-18% acrylamide gradient gels containing 0.1% SDS (Laemmli 1970). Protein content was calculated by comparing the total density of the Coomassie-stained protein lanes to that of the lane of the protein standard of known protein content.

Determination of MDA content

Malondialdehyde content was determined as described by Esterbauer and Cheeseman (1990). 250 mg leaf material was homogenized at 4 °C in 3 ml of 0.1% TCA, and centrifuged at 10000 × g for 15 min. To the supernatant, 0.5 ml of 0.1 M Tris-HCl (pH 7.6) and 1 ml of 15% (m/v) trichloracetic acid; 0.375% (m/v) thiobarbituric acid; 0.25 M HCl reaction mixture were added. This solution was boiled in water bath for 15 min, centrifuged at 2000 × g for 5 min, and the absorbance was read at 532 nm (ε = 155 mM^{-1} cm^{-1}) for the determination of MDA.

Statistical analysis

Measurements were repeated in six independent replications, the similarity of the samples were analysed using one-way ANOVA with Tukey-Kramer *post-hoc* test ($p<0.05$) analysed by InStat v. 3.00 software (GraphPad Software, Inc.).

Results

In well-hydrated (90% RWC) leaves, a notable SOD activity was measured which showed no significant differences between the samples, regardless of the habitat of plants (Table 1). At the same time, the changes in SOD activity under desiccation and rehydration showed habitat dependence. Desiccation induced an increase in SOD activity in both the sun and shade leaves. Though the highest SOD activity was measured in fully desiccated leaves (8% RWC) in both populations, the SOD activity of sun leaves was more enhanced compared to shade leaves. Similarly, rehydration caused a decrease in the total activity in both type of leaves but the total SOD activity remained significantly higher compared to that of the initial,

well-hydrated stage in sun leaves, while relaxed to the control value in shade leaves.

The MDA content showed no differences in well-hydrated stage, whereas changed differently during desiccation and rehydration in shade and sun leaves (Table 2). Moderate dehydration had negligible effect on the MDA content of either shade or sun leaves, which only increased drastically in desiccated shade leaves. In sun leaves, no significant increase of MDA content was measured even in desiccated stage. In the rehydration phase, the MDA content decreased tendentiously in shade and also somewhat in sun leaves, thus it reached the typical value of well-hydrated plants after 6-days rehydration. Nevertheless, in sun plants, the MDA content was somewhat higher in the well-hydrated than in rehydrated stage.

Discussion

Reactive oxygen species (ROS) are common by-products in aerobic organisms. Environmental stresses such as drought increases the ROS level in cells, particularly in chloroplasts (Cruz de Carvalho 2008). The photosynthetic apparatus have a high sensitivity against oxidative damage that primarily causes inactivation of photosystem II. To protect cells against the damaging effects of ROS and maintain the redox equilibrium, antioxidative defence systems, including the SOD enzymes, have evolved (Asada 2006). In chloroplasts, SOD isoforms are responsible for the elimination of superoxide anion radicals which are among the most dangerous ROS.

Antioxidative defence systems were shown to be involved in the protection of resurrection plants during desiccation (Farrant 2000; Dinakar et al. 2012). We also confirmed their role in desiccation tolerance of *H. rhodopensis* sun and shade populations: increased SOD activity during desiccation was accompanied by only moderate elevation of MDA content in both shade and sun leaves. Desiccation increased the SOD activity, which correlated with the total antioxidative defence of the plant in many plant species (e.g. *Pisum*, Moran et al. 1994; *Glycyrrhiza*, Pan et al. 2006).

Desiccation-induced oxidative stress was significantly higher in shade than in sun leaves of *H. rhodopensis*. The lower MDA accumulation together with the higher SOD activity in sun leaves indicates that ROS eliminating mechanisms are more enhanced in sun than in shade leaves. Earlier studies on SOD activity under desiccation and rehydration of flowering and post-flowering *H. rhodopensis* plants (Yahubyan et al. 2009) found that mild desiccation decreases, whereas strong desiccation increases the SOD activity in shade *H. rhodopensis* leaves. They found a significantly higher SOD activity in well-hydrated flowering, compared to post-flowering plants. In plants of similar origin (Bachkovo region) to that studied in the paper of Yahubyan et al. (2009), Georgieva et al. (2012) found a decreased MDA content under desiccation, whereas a stable level in a population originated from Sitovo region, grown under higher irradiance. Concerning our results, the sun populations of Orehovo region also showed a significantly higher elevation in SOD activity under desiccation than the shade ones collected from a close locality. In agreement, sun plants were shown to cope with less photoinhibition during desiccation compared to shade ones (Solti et al. 2014). As one of the reasons for photoinhibition is the ROS accumulation, the enhanced SOD activity and the consequently decreased oxidative stress (MDA content) of desiccating sun *H. rhodopensis* plants contribute to the maintenance of photosynthetic activity under mild desiccation and prevent the stronger damage under total dehydration. The SOD activity in rehydrated sun leaves remained significantly higher compared to the initial well-hydrated stage, which may also contribute to the adaptation to the unfavourable conditions in their natural habitat.

Acknowledgements

This work was supported by the travel exchange agreements of the Bulgarian and Hungarian Academy of Sciences [No. SNK-47/2013]. We thank Zsuzsa Ostorics for technical assistance. This work was presented on the 11th Congress of the Hungarian Society of Plant Biology, 27-29 August, 2014, Szeged, Hungary.

References

Alscher RG, Erturk N, Heath LS (2002) Role of superoxide dismutases (SODs) in controlling oxidative stress in plants. J Exp Bot 53:1331-1341.

Asada K (2006) Production and scavenging of reactive oxygen species in chloroplasts and their functions. Plant Physiol 141:391-396.

Cruz de Carvalho MH (2008) Drought stress and reactive oxygen species: Production, scavenging and signalling. Plant Signal Behav 3:156-165.

Daskalova E, Dontcheva S, Yahoubian G, Minkov I, Toneva V (2011) A strategy for conservation and investigation of the protected resurrection plant *Haberlea rhodopensis* Friv. BioRisk 6:41-60.

Dinakar C, Djilianov D, Bartels D (2012) Photosynthesis in desiccation tolerant plants: Energy metabolism and antioxidative stress defence. Plant Sci 182:29-41.

Esterbauer H, Cheeseman KH (1990) Determination of aldehydic lipid peroxidation products: malonaldehyde and 4-hydroxynonenal. Methods Enzymol 186:407-421.

Farrant JM (2009) A comparison of mechanisms of desiccation tolerance among three angiosperm resurrection plant species. Plant Ecol 151:29-39.

Georgieva K, Maslenkova L (2006) Thermostability and photostability of photosystem II of the resurrection plant *Haberlea rhodopensis* studied by chlorophyll fluorescence. Z Naturforsch 61C:234-40

Georgieva K, Lenk S, Buschmann C (2008) Responses of the resurrection plant *Haberlea rhodopensis* to high irradiance. Photosynthetica 46:208-15.

Georgieva K, Doncheva S, Mihailova G, Petkova S (2012) Response of sun- and shade-adapted plants of *Haberlea rhodopensis* to desiccation. Plant Growth Regul 67:121-32.

Giannopolitis CN, Ries SK (1977) Superoxide dismutases I.: Occurrence in higher plants. Plant Physiol 59:309-314.

Laemmli UK (1970) Cleavage of structural proteins during assembly of the head of bacteriophage T4. Nature 227:680-685.

Moran JF, Becana M, Iturbe-Ormaetxe I, Frechilla S, Klucas RV, Aparicio-Tejo P (1994) Drought induces oxidative stress in pea plants. Planta

194:346-352.

Pan Y, Wu LJ, Yu ZL (2006) Effect of salt and drought stress on antioxidant enzymes activities and SOD isoenzymes of liquorice (*Glycyrrhiza uralensis* Fisch). Plant Growth Regul 49:157-165.

Solti Á, Lenk S, Mihailova G, Mayer P, Barócsi A, Georgieva K (2014) Effects of habitat light conditions on the excitation quenching pathways in desiccating *Haberlea rhodopensis* leaves: an Intelligent FluoroSensor study. J Photochem Photobiol 130B:217-25.

Tuba Z, Proctor MCF, Csintalan Z (1998) Ecophysiological responses of homoiochlorophyllous and poikilochlorophyllous desiccation tolerant plants: a comparison and an ecological perspective. Plant Growth Regul 24:211-7.

Yahubyan G, Gozmanova M, Denev I, Toneva V, Minkov I (2009) Prompt response of superoxide dismutase and peroxidase to dehydration and rehydration of the resurrection plant *Haberlea rhodopensis*. Plant Growth Regul 57:49-56.

Volume 58(1):15-19, 2014
Acta Biologica Szegediensis
http://www.sci.u-szeged.hu/ABS

ARTICLE

Anatomical study of some *Silene* L. species of *Lasiostemones* Boiss. section in Iran

M. Keshavarzi[1]*, M. Mahdavinejad[1], M. Sheidai[2], A. Gholipour[3]

[1]Biology Department, Alzahra University, Tehran, Iran, [2]Faculty of Biological Sciences, Shahid Beheshti University, Tehran, Iran, [3]Biology Department, Payamenour University Sari Branch, Mazandaran, Iran

ABSTRACT *Silene* (Caryophyllaceae) composed of 110 species in Iran from which 35 species are endemic. *Lasiostemones* section is one of *Silene* sections with 10 species in Iran. In present study leaf and stem anatomical structure were considered for the first time. In order to study the anatomical variations of stem and leaf, 36 populations of 7 species of *Silene* (*Lasiostemones* section) were collected from different habitats of Iran. In leaf anatomy vascular bundle shape, shape of dorsal surface of mid vein, cortex diameter, hair presence in dorsal and ventral surface of leaf, mid rib diameter, cuticle upper and lower thickness, fiber presence in mid rib, stomata cell shape, stomata index and hair frequency show significant differences among studied species. In stem anatomy features as shape of cross section, hair type, cortex and xylem and phloem diameter were of diagnostic value in species separation. **Acta Biol Szeged 58(1):15-19 (2014)**

KEY WORDS

Silene
Lasiostemones
Caryophyllaceae
stem and leaf anatomy

The genus *Silene* L. (Caryophyllaceae) based on *Flora Iranica* is composed of 110 species in Iran, form which 35 species are endemic (Melzheimer 1980). One of *Silene* sections is *Lasiostemones* Boiss with 10 species in Iran (Melzheimer 1980). This section is distinguished from other sections by perennial form of life, raceme inflorescences, white flowers, short, obconical to cylindrical and hairy calyx and nerves of calyx producing reticulate, scabrous filaments (Melzheimer 1980).

Relationships of *Silene* species have been discussed mainly by morphological data sets. There are no extensive anatomical studies in this section. Chalk and Metcalfe (1950) provide general anatomical features of carnation family. Kilic (2009) studied stem and leaf anatomical structure of 8 species of Silene in Turkey. Fathi et al. (2010) studied stem anatomy of 10 species of *Silene* of four sections. Jafari et al. (2008) studied epidermis features of *Silene* as diagnostic ones in taxonomic studies. Yildiz and Minareci (2008) specified *S. urvillei* for its glandular hairs and stomata in leaf both surface.

Evaluation the anatomical structure of leaves of some *Silene* species in Pakistan showed a considerable variation in anatomical structure and the importance of shape and size of epidermal cells, hairs and crystals in species separation (Sahreen et al. 2010).

Diacytic stomata type is a diagnostic feature in Caryophyllaceae family. In *Silene* the main stomata type is diacytic but there are also anisocytic and anomocytic. In present study leaf and stem anatomical features of some *Silene* (*Lasiostemones* section) species have been studied for the first time in order to find valuable characters for taxonomic purposes.

Accepted May 11, 2014
*Corresponding author. E-mail: Keshavarzm@alzahra.ac.ir

Materials and Methods

In order to study the leaf and stem anatomical features, 36 populations of 7 *Silene* species of *Lasiostemones* section were collected from different parts of Iran (Table 1). Ten individuals from each species have been studied. Form each individual, 3 leaves were sampled form the uppermost internode. Handmade sections were done for basal leaves and lower parts of stems. Double coloration by methyl green and Congo red was used. Dorsal epidermis was prepared for study by tissue removal method. A camera bearing Olympus DP12 microscope was used in this research. Altogether, 21 qualitative and quantitative anatomical features were measured and evaluated (Table 2).

For stomata index, the number of stomata and epidermal cells present in a leaf unit area were calculated using a micrometer. The following formula was used:

$$\text{Stomatal Index (\%)} = \frac{\text{Stomatal density x 100}}{\text{Stomatal density + epidemal cell density}}$$

Vouchers are deposited at Herbarium of Shahid Beheshti University (HSBU) and Herbarium of Payamenour University – Sari Branch (PNUSH).

In order to detect significant differences in the studied characters among the various studied species, an analysis of variance (ANOVA) was performed. To reveal the species relationships, we have used cluster analysis and principal

Table 1. Population details of studied *Silene* species (♦ leaf, ■ epidermis and ● stem anatomical studies).

Taxon	Studies	Population details
S. claviformis Litv.	♦■	Kerman, Chatroud, Gholipour, 86070 PNUSH
S. longipetala vent.	♦	Chaharmahal and Bakhtiari, Gholipour, 8500251 HSBU
S. longipetala	♦■	Western Azerbaijan, Naghadeh, Oshnaviyeh, Gholipour, 8500250 HSBU
S. marschallii C.A.Mey.	♦	Lorestan, Borojerd, Gholipour, 87018 PNUSH
S. marschallii	♦	Isfahan, Khonsar, Golestan Kuh, Gholipour, 8500245 HSBU
S. marschallii	♦	Tehran, Firouz Kuh Road, Gholipour, 8500236 HSBU
S. marschallii	♦●	Zanjan, Anguran Mount., Gholipour,86095 PNUSH
S. marschallii	♦	Markazi, Arak, Gholipour, 87024 PNUSH
S. marschallii	♦	Western Azerbaijan, Ashk Island, Gholipour,--
S. marschallii	♦	Mazandaran, Chalous to Kandovan, Gholipour, --
S. marschallii	♦	Tehran, Firouzkouh, Gholipour, 8686PNUSH
S. marschallii	♦	Mazandaran, Damavand Peak, Gholipour, 8500243HSBU
S. marschallii	♦	Mazandaraan, Tonekabon, Chagoul, Gholipour, 86140PNUSH
S. marschallii	♦	Tehran, Touchal Highlands, Gholipour, --
S. marschallii		Zanjan, Zanjan, Gholipour, 86026PNUSH
S. marschallii	♦	Eastern Azerbaijan, Tabriz, Khoy, Gholipour, 87040PNUSH
S. marschallii		Semnan, Khonar Fields, Gholipour, -
S. marschallii	♦■	Eastern Azerbaijan. Tabriz to Kaleybar, Gholipour, 8500249SBU
S. parrowiana Boiss. & Hausskn. ex Boiss.	♦■	Kermanshah, Bisotun, Pero, Gholipour, 86102 PNUSH
S. propinqua Schischk.	♦	Kurdistan, Divandare to Sanandaj, Gholipour, 86097 PNUSH
S. propinqua	♦	Western Azerbaijan, Uromiyeh, Khalil Kuh, Gholipour, 87053 PNUSH
S. propinqua	♦■●	Western Azerbaijan, Uromiyeh, Khoy, Gholipour, 87097 PNUSH
S. ruprechtii Schischkin	♦■●	Eastern Azerbaijan, Tabriz, Ahar, Gholipour, 85012 PNUSH
S. tenella A.Huet ex Schenk	♦	Tehran, Firouzkuh, Gholipour, 86087 PNUSH
S. tenella	♦	Eastern Azerbaijan, Sahand Mount, Gholipour, 87030 PNUSH
S. tenella	♦	Western Azerbaijan, Uromiyeh, Khalil Kuh, Gholipour, 87055 PNUSH
S. tenella	♦	Western Azerbaijan, Ziveh, Gholipour, 900862 PNUSH
S. tenella	♦	Ardebil, Gholipour, 86111 PNUSH
S. tenella	♦	Firouzkouh, Gadouk defile, Gholipour, 86087 PNUSH
S. tenella	♦	Guilan, Gholipour, 86138 PNUSH
S. tenella	♦	Ardebil, Neor Lake, Gholipour, 8500228HSBU
S. tenella	♦	Mazandaran, Nour, Gholipour,--
S. tenella	♦	Ardebil, Sabalan, Gholipour, 86110 PNUSH
S. tenella	♦	Mazandaran, Damavand Mount, Gholipour, 86080 PNUSH
S. tenella	♦	Mazandaran, Balade, Gholipour, 900558 PNUSH
S. tenella	■	Tehran, Firouzkuh, Gadouk defile, Gholipour, 8500230HSBU

component analysis (PCA) (Ingrouille 1986). For multivariate analysis, the mean of the quantitative characters was used, while qualitative characters were coded as binary/multi-state characters. Standardized variables were used for multivariate statistical analysis. Average taxonomic distances and squared Euclidean distances were applied as dissimilarity coefficient in the cluster analysis of anatomical data. In order to determine the most variable characters among the studied species, factor analysis based on principal components analysis was performed. SPSS ver. 19 software was used for statistical analysis.

Results

Analysis of variance showed that nerve number for all studied species is constant and observed variation in quantitative features as cuticle thickness at adaxial and abaxial surface and average vascular bundle diameter are not significant. Observed variation in other studied characters are significant and can be used as diagnostic features (Table 3). Post hoc tests used for qualitative features revealed that form of central vein, hair on the ventral and dorsal surface, collenchymas presence at central vein, form of dorsal surface of the mid rib and fiber condition in the central vessel are of significance.

Leaf cross section

For leaf anatomical observations 34 populations of seven *Silene* species were studied. In all studied species mid rib shape is ellipsoid, orbicular or triangular, with one vascular bundle. Collenchymas are present under dorsal epidermis and crystals are present in mesophyll. Dorsal surface of mid rib is smooth, round, dome-shaped or acute. All studied species has oxalate crystals in mesophyll. In leaf cross section of *S. claviformis* mid rib dorsal surface is smooth and vascular bundle is rounded with sclerenchymas fiber (Fig. 1.c). *S.*

Table 2. Qualitative and quantitative anatomical features used in present research.

State of Character	Character	
Presence/ absence	Calcium oxalate	
Round/ elliptic/ triangular	Mid rib shape	
Presence/ absence	Hair at leaf dorsal surface	Qualitative characters
Presence/ absence	Hair at leaf ventral surface	
Presence/ absence	Collenchyma at mid rib	
Round/ smooth/angled/ pointed	Dorsal shape of mid rib	
Presence/ absence	Fiber at mid rib vascular bundle	
Rectangular/ jigsaw puzzle shaped/ oblong	Epidermal cell shape	
Smooth/ undulate	Epidermal cell wall shape	
Quantitative characters		
Cortex thickness	Number of hairs per leaf area	Epidermal cells length
Vascular bundle number	Stomata index	Epidermal cells width
Width at middle of leaf blade	Stomata width	Stomata length
Leaf adaxial cuticle thickness	Leaf abaxial cuticle thickness	Average vascular bundle diameter

Table 3. The quantitative data of the epidermis in different *Silene* species.

Species	Stomata Length (µm)	Stomata width (µm)	Epidermis length (µm)	Epidermis width (µm)	Hair no.	Stomata index
S. claviformis	33.43	26.13	82.05	48.31	4.00	.37
S. longipetala	49.33	37.72	52.12	43.73	11.00	.33
S. marschallii	33.06	20.30	94.50	15.92	23.00	.15
S. tenella	30.75	26.06	37.54	57.75	17.00	.21
S. ruprechti	31.20	21.84	36.53	41.06	.00	.42
S. propinqua	32.25	25.00	67.77	51.21	10.00	.37
S. parowiana	31.80	20.40	36.40	42.30	2.00	.15

ruprechtii and *S. parrowiana* are similar in leaf anatomical features. Both species show angled mid rib, rounded vascular bundle, bilateral phloem without sclerenchymatous fibers (Fig. 1b & d).

In *S. longipetala* leaf cross section, mid rib is rounded and the central vascular bundle is ellipsoid, with bilateral phloem and sclerenchymatous fibers (Fig. 1 h). In *S. propinqua* mid rib is rounded to angled, main vascular bundle is rounded, sclerenchymatous fiber is not present, phloem is bilateral. Hairs are thicker than other studied species (Fig. 1 g). Populations of *S. marschallii* and *S. tenella* show great intra-specific variations in leaf cross sections features as mid rib and vascular bundle shape and phloem condition (Fig. 1 a, e & f).

Leaf epidermis

Epidermal cells in all studied taxa are rectangular except in *S. pa*rrowiana and *S. ruprechtii. S. marschallii* has elongated rectangular epidermal cells. Cell walls are smooth except in *S. parrowiana* and *S. ruprechtii* that undulated cell walls have been observed. Main stomata type in *Silene* is diacytic but in *S. parrowiana* and *S. propinqua* there are also anisocytic type (Fig. 2 a - g)

Stem cross section

Four species are studied for their stem cross sections. In *S. marschallii* and *S. tenella* stem general shape is round, in *S. ruprechtii* ellipsoid and in *S. propinqua* quadrangular. Among studied species, *S. propinqua* has long single celled and multicellular hairs on stem, *S. ruprechtii* has no hairs and two other species have small single-celled hairs. Presence of continuous sclerenchyma in cortex and oxalate crystals in pith parenchymas are common features in studied species (Fig. 3).

Discussion

In order to clarify the species relationships cluster analysis by WARD method was done. In phenogram two main clusters are observed. In first main cluster *S. parowiana* and *S. ruprechtii* are grouped while in second cluster there are two sub-clusters. *S .longipetala* has a separate and isolate position. Four species are grouped in two subsets. *S. marschallii* and *S. tenella* in one set and *S. claviformis* and *S. propinqua* in another one show more similarities (Fig. 4). Cluster analysis and PCA ordination of the studied species of *Silene*, based on both quantitative and qualitative anatomical characters, have produced similar results (Fig. 5).

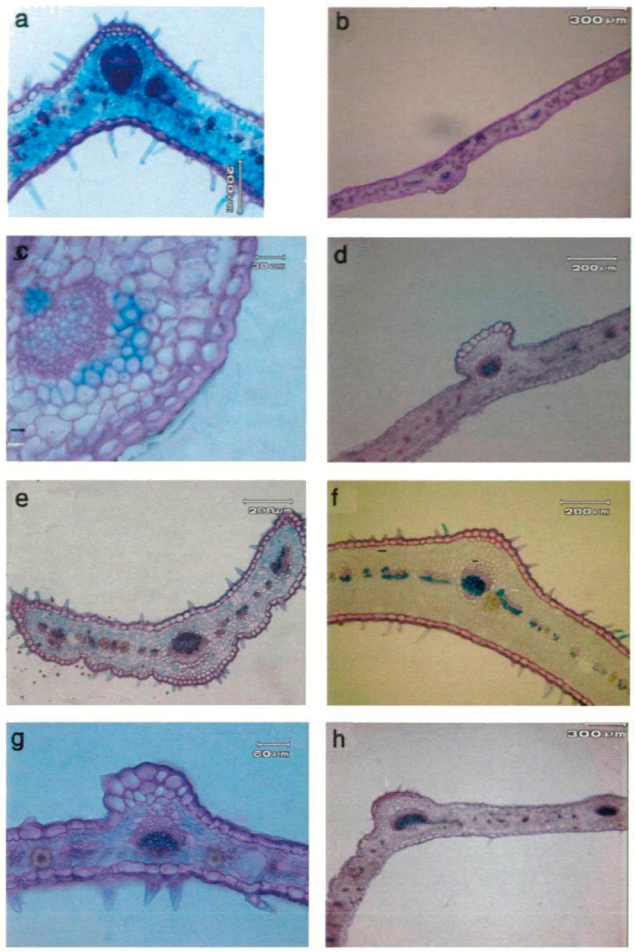

Figure 1. Leaf cross section structure in different studied *Silene* species. a: *S. marschallii*, b: *S. parrowiana*, c: *S. claviformis*, d: *S. ruprechtii*, e & f: *S. tenella*, g: *S. propinqua*, h: *S. longipetala*.

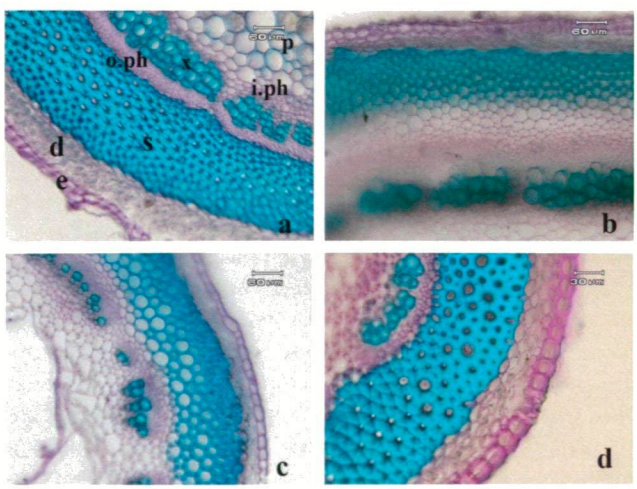

Figure 3. Stem cross sections in studied *Silene* species. a: *S. marschallii*, b: *S. tenella*, c: *S. ruprechtii*, d: *S. propinqua*. (e: epidermis, d: cortex, s: sclerenchyma, o.ph: outer phloem, i.ph: inner phloem, x: xylem, p: pith parenchyma).

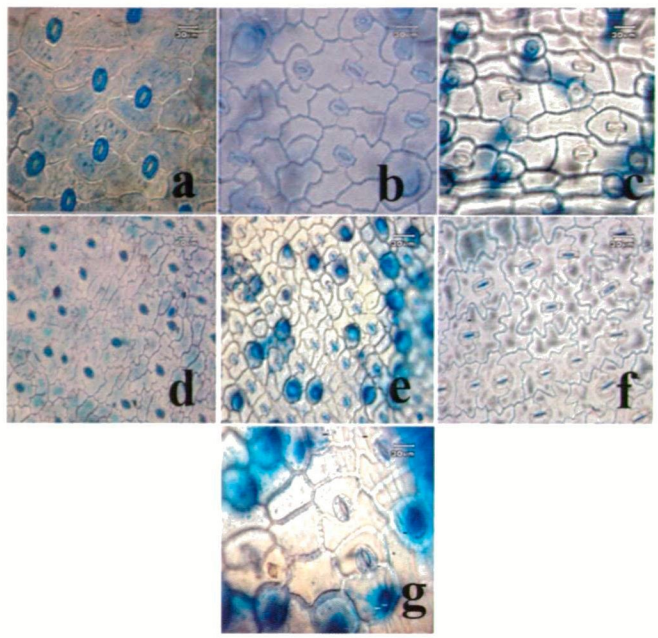

Figure 2. Leaf epidermis in studied *Silene* species. a: *S. claviformis*, b: *S. longipetala*, c: *S. marschallii*, d: *S. ruprechtii*, e: *S. tenella*, f: *S. parrowiana*, g: *S. propinqua*.

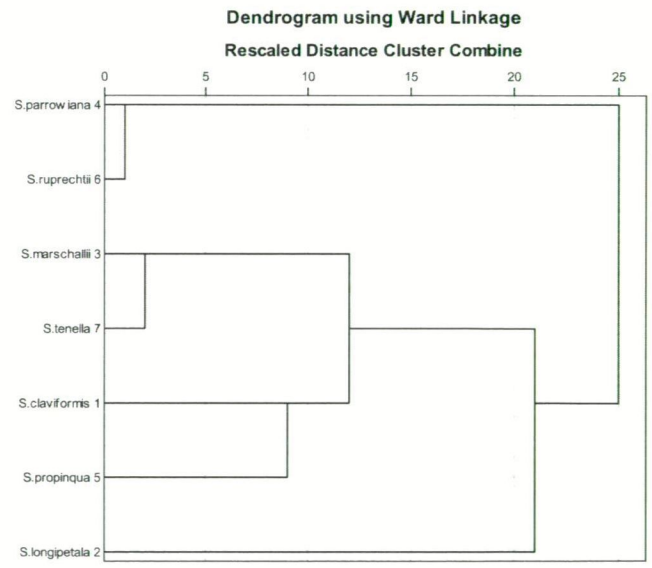

Figure 4. Cluster analysis by WARD method for studied species by leaf anatomical data.

It is the first leaf anatomical study of *Lasiostemones* species. Selected features of leaf anatomy appeared to be of taxonomic importance and could clearly separate the species. In leaf cross section a close relationship is found between *S. ruprechtii* and *S. parrowiana*. These species are morphologi-

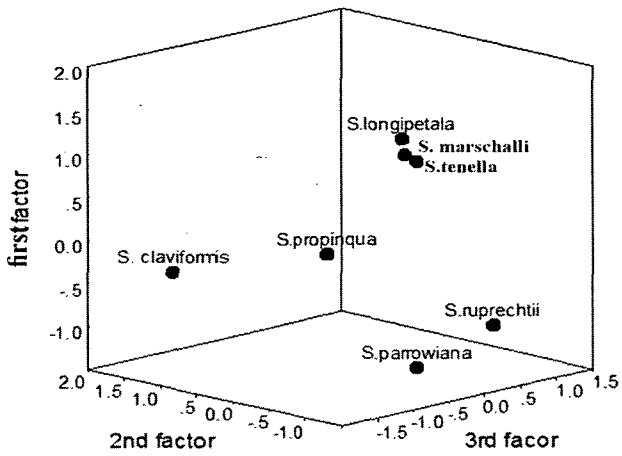

Figure 5. PCA scatter diagram by leaf anatomical features for studied species.

cally similar too. There are similarities between *S.marschallii* and *S. tenella* and *S. claviformis* and *S. propinqua* in the other hand. Most diagnostic features are mid rib shape, vascular bundle diameter, fiber presence in central vascular bundle and phloem position. Other diagnostic features like hair types, epidermal hairs and cuticle and cortex diameter are in concordant with previous studies (Jafari et al. 2008; Kilic 2009).

Studying epidermis shows its diagnostic importance and in concordant with Chalk and Metcalfe (1950) results. Sahreen et al. (2010) emphasized on diagnostic importance of epidermal features for 12 species of *Silene*. Epidermis in *S. clavformis* and *S. propinqua* show similarities. There are also similarities between *S. ruprechtii* and *S. parrowiana* which is in concordant with our leaf anatomical results. An identification key based on leaf dorsal epidermis is presented:

1a- Epidermal cells irregular	2
b- Epidermal cells regular	3
2a- Epidermis without hair	*S. ruprechtii*
b- Epidermis hairy	*S. parrowiana*
3a- Epidermal cell shape elongated rectangle	*S. marschallii*
b- Epidermal cell shape not elongated	4
4a- Stomata type diacytic	5
b- Stomata type diacytic and anisocytic	*S. propinqua*
5a- Few hairs in epidermis surface	*S. claviformis*
b- Frequent hairs in epidermis surface	6
6a- Epidermis cell length 30-40 micrometer	*S. tenella*
b- Epidermis cell length 45-60 micrometer	*S. longipetala*

Stem anatomical study of some *Lasiostemones* species in present study show some diagnostic features which are of taxonomic importance. These findings are in concordant with some previously published results (Jafari et al. 2008; Kilic 2009; Fathi et al. 2010). In all studied taxa there was a continuous cylinder of sclerenchymas fiber in cortex as was pointed by Fathi et al (2010). *S. marschallii* and *S. tenella* show similarities in their stem anatomy too.

References

Fathi Z, Jafari A, Zokai M (2010) Comparative study of stem structure and wood analysis in different species of *Silene* L. genus (Mashhad and Country side). J Plant Sci Res 5(2):28-35 [Persian].

Ingrouille MJ (1986) The construction of cluster webs in numerical taxonomic investigation. Taxon 35:541-545.

Jafari A, Zokai M, Fathi Z (2008) A biosystematical investigation on *Silene* L. species in North-East of Iran. Asian J Plant Sci 7(4):394-398.

Kilic S (2009) Anatomical and pollen characters in the genus *Silene* L. (Caryophyllaceae) from Turkey. Bot Res J 2(2-4):34-44.

Melzheimer V (1988) *Silene* (Caryophyllaceae). In Flora Iranica. Rechinger KH, Person K, Wendelbo P (Eds). Akad Druck-U. Verlagsanstalt. Graz, Austria, pp. 163:341-509.

Metcalfe CR, Chalk L (1950) Anatomy of the Dicotyledons. Oxford at the Clarendon Press, UK, 1:147-152.

Sahreen S, Khan MA, Khan MR, Khan RA (2010) Leaf epidermal anatomy of the genus *Silene* (Caryophyllaceae) from Pakistan. Biol Divers Conserv 3(1):93-102.

Yildiz K, Minareci E (2008) Morphological, anatomical, palynological and cytological investigation on *Silene urvillei* Schott. (Caryophyllaceae). J Appl Biol Sci 2(2):41-47.

Volume 58(1):21-26, 2014
Acta Biologica Szegediensis
http://www.sci.u-szeged.hu/ABS

ARTICLE

The effect of xanthan gum as an elicitor on guard cell function and photosynthesis in *Vicia faba*

Attila Ördög*, Dóra Bernula, Barnabás Wodala

Department of Plant Biology, University of Szeged, Szeged, Hungary

ABSTRACT Many plant species respond to pathogen attacks by closing stomata in a process called basal resistance. Pathogen-associated molecular patterns (PAMPs) are recognized by pattern recognition receptors (PRRs). This interaction can lead to the activation of different signaling cascades, which can lead to stomatal closure. The immune-active behavior of the bacterial elicitor xanthan gum has been demonstrated in barley where a xanthan treatment lead to the accumulation of the enzyme ß-1,3 glucanase. However, its short-term physiological effects have not been investigated yet. In this study we investigated the effect of xanthan gum on the guard cell function. Xanthan gum applied at dawn can induce stomatal closure, reduce stomatal conductance and the rate of CO_2 assimilation, and it can also reduce PSII photochemistry in guard cells.

Acta Biol Szeged 58(1):21-26 (2014)

KEY WORDS

xanthan gum
biotic stress
guard cell
photosynthesis

Stomata are formed by guard cells – two specialized cells in the epidermis, which are morphologically and functionally different from general epidermal cells. Guard cells are multisensory hydraulic valves responsible for regulating the aperture of stomata (Franks and Farqhuar 2007) in order to control gas exchange between the inside of the leaf and the environment and also to control transpirational water loss (Lawson 2009). In addition, stomata are responsible for leaf cooling, metabolite fluxes, long distance signaling and they also serve as the first line of defence against pathogens. As natural openings, stomata are ideal points of entry for pathogenic microorganisms. Guard cells recognize and respond to the presence of microbes by perception of PAMPs, such as xantan gum (Nicaise et al. 2009). The first response is the induction of immediate stomatal closure or the inhibition of the stomatal opening (Rong et al. 2010). In wheat, it has been shown that a pre-treatment with 0.5 mg ml^{-1} xanthan gum (48 h before inoculation) provides protection against an infection by *Bipolaris bicolor*, *Bipolaris sorokiniana*, and *Drechslera tritici-repentis* (Bach et al. 2003). The efficiency of the xanthan gum treatment was attributed to biochemical changes, such as an increase in the concentration of proteins and the enzyme ß-1,3-glucanase, and a decrease in phenol concentration. Castro and Bach (2004) obtained similar results in the induction of local and systemic resistance using xanthan gum as an elicitor in barley plants, with protection levels over 90%, and attributed the efficiency to the increased synthesis and accumulation of the enzyme ß-1,3 glucanase. However, the short-term physiological effects of xanthan gum have not been investigated yet.

Accepted Aug 11, 2014
*Corresponding author. E-mail: aordog@bio.u-szeged.hu

In the present work, we explore the short-term effects of xanthan gum on guard cell function. We examine whether it affects stomatal opening and closure in the model plant *Vicia faba*. We also study whether the action of xanthan involves a reduction in the photosynthetic activity of mesophyll and guard cells. Fluorescent probes were used to determine the levels and cellular localization of signaling components H_2O_2 and NO following the xanthan gum treatment.

Materials and Methods

Plant material and experimental solutions

All experiments, except leaf photosynthetic measurements, were carried out on abaxial epidermal strips peeled from the third to fourth completely unfolded leaves of 2-3 week-old broad bean (*Vicia faba* L. cv. Mirna) plants. Plant were grown hydroponically in a solution containing: 2 mM $Ca(NO_3)_2$, 1 mM $MgSO_4$, 0.5 mM KCl, 0.5 mM KH_2PO_4, 0.5 mM Na_2HPO_4, 0.001 mM $MnSO_4$, 0.005 mM $ZnSO_4$, 0.0001 mM $(NH_4)_6Mo_7O_{24}$, 0.01 mM H_3BO_4 and 0.02 mM Fe(III)-EDTA, pH 6 in a controlled environmental chamber (Fitoclima S 600 PLH, Aralab, Portugal) under 12h light (6:00 am – 18:00 pm) and 12h dark (18:00 pm – 6:00 am) cycles at 25 °C (day) and 20 °C (night).

Xanthan gum (Sigma-Aldrich, Budapest, Hungary) was dissolved in the experimental solution (10 mM MES, 100 µM $CaCl_2$, 10 mM KCl, pH 6.15 with TRIS) to a final concentration of 1 mg ml^{-1}. The experimental solution without xanthan gum was used as control in all experiments.

Stomatal aperture measurements

The width of stomatal apertures was measured in digital

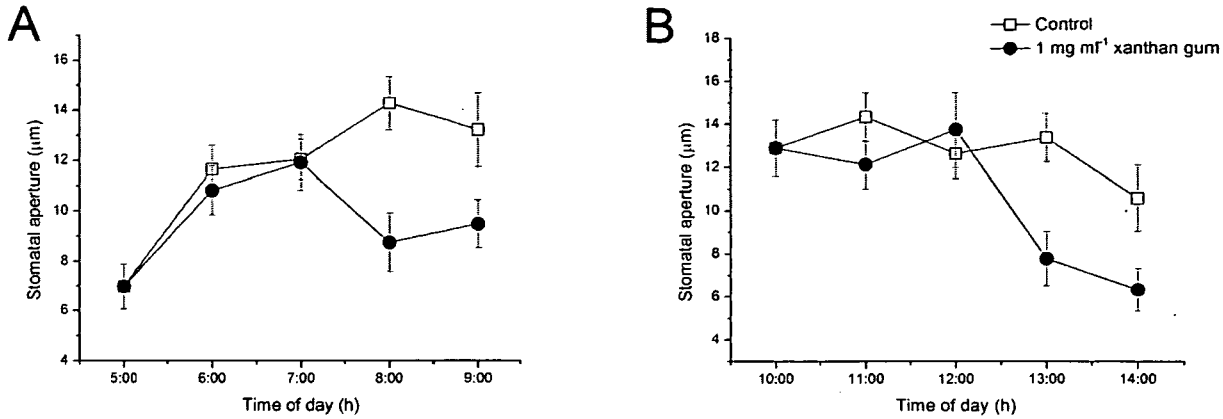

Figure 1. Stomatal aperture sizes of control and 1 mg ml^{-1} xanthan gum treated *Vicia faba* leaves in the course of a day. Treatments were applied 60 min before the start of illumination at 5:00 am (A) and by day at 10:00 am (B). The data presented are the average values (± SE) of 3 independent experiments, each yielding the average of at least 90 aperture widths.

images taken from freshly peeled epidermal strips using the Image-Pro Plus 5.1 image analyzer software. The experiments were repeated on three different days, each yielding the average of at least 90 aperture widths. The data presented are the average values (± SE) of these results.

Epidermal strip bioassay

Experiments in this study were carried out using epidermal strips, which eliminated the influence of mesophyll cells on stomatal function. Prior to each experiment, the abaxial epidermis was peeled carefully from the third to fourth completely unfolded leaf submerged in the experimental solution. The strips contained only small regions contaminated with mesophyll cells – mainly around the major veins – and these regions were excised with a razor blade. The strips were transferred and washed for 5 minutes in the hypoosmotic control solution in order to remove any remaining mesophyll cell debris and mesophyll chloroplasts by severe osmotic shock.

Cell viability tests carried out following the preparation of epidermal strips showed that guard cells remained intact after floating in the incubating medium. Microscopy PAM measurements confirmed that this treatment did not influence the chlorophyll fluorescence parameters in guard cells. In addition, no correlation was found in the photosynthetic performance of epidermal strips and the age of the plant (2 to 3 weeks), or the position of the leaf (third or fourth) they were collected from (Ördög et al. 2013).

Photosynthesis measurements

Chlorophyll a fluorescence measurements

Chlorophyll a fluorescence of 4-5 stomata from a mesophyll-free abaxial epidermis patch was monitored with a MYCROSCOPY-PAM chlorophyll fluorometer (Heinz Walz GmbH, Germany) mounted on an inverted epifluorescence microscope (Zeiss Axiovert 40, Zeiss GmbH, Germany). Light intensities were measured with a Micro Quantum Sensor (MC-MQS, Heinz Walz GmbH, Germany).

Rapid light-response curves were obtained using a light-curve protocol, consisting of 8 consecutive 30-s steps with increasing actinic light intensity. Due to the short time of each step, the photosynthetic activity of guard cells did not achieve steady state at any of the light intensities. At the end of each step the steady state fluorescence was measured, which was followed by a 0.8 s width saturation pulse to obtain the maximal fluorescence yield of the light-adapted sample. Prior to the light response curve the stomata were dark-adapted and the minimum as well as the maximum fluorescence in the dark-adapted state were recorded. Based on these fluorescence values the following fluorescence parameters were calculated: maximum quantum efficiency of dark-adapted PS II (F_v/F_m according to Butler 1978), maximum quantum efficiency of light-adapted PSII photochemistry (F_v'/F_m'), the coefficient of photochemical fluorescence quenching (qL according to Kramer et al. 2004), the apparent relative linear electron transport rate (ETR) and the Stern-Volmer type non-photochemical quenching (NPQ according to Bilger and Björkman 1990).

Determination of assimilation rate and stomatal conductance

Photosynthetic activity of broad bean leaves were assayed by measuring assimilation and stomatal conductance using an LI-6400 Portable Photosynthesis and Fluorescence System (LI-COR Environmental, Lincoln, Nebraska, USA) equipped with a 6400-40 leaf chamber fluorometer (LI-COR Environmental). Measurements were carried out at room temperature, ambient CO_2 concentration and humidity values using a fixed chamber illumination of 150 µmol m^{-2} s^{-1} provided by the in-

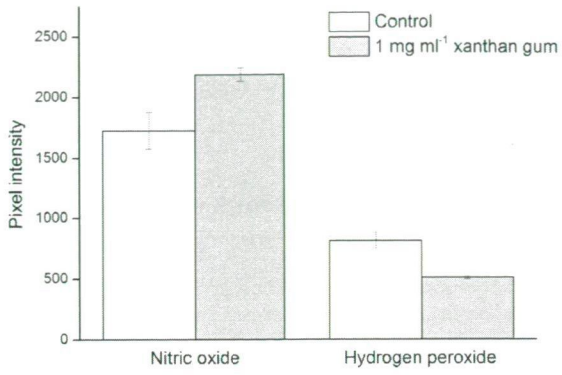

Figure 2. Average fluorescence intensities of specific DAF-FM (NO) and AR (H_2O_2) fluorophores in *Vicia faba* guard cells after 3 hours of treatment with experimental solution or 1 mg ml^{-1} xanthan gum. The data presented are the average values (± SE) of 3 independent experiments, each yielding the average of at least 20 stomata.

ternal light source of the leaf chamber fluorometer. Stomatal conductance (g_s, mol H_2O m^{-2} s^{-1}) and assimilation rate (P_n, µmol CO_2 m^{-2} s^{-1}) values of each leaves were collected in every five minutes over 4 hours (Poór et al. 2011).

Localization of fluorescent probes using confocal microscopy

Localization of the fluorescent probes in the abaxial epidermis of intact leaves was visualized using confocal laser scanning microscope (Olympus FV1000 LSM, Olympus Life Science Europa GmbH, Hamburg, Germany). H_2O_2 was detected by a specific probe 10-acetyl-3,7-dihydroxyphenoxazine (Amplex Red, Molecular Probes Invitrogen, Carlsbad, CA). NO was localized by the frequently used cell-permeable 4-amino-5-methylamino-2 ,7-difluorofluorescein diacetate (DAF-FM DA, Sigma-Aldrich, Budapest, Hungary) .

Results and Discussion

Stomatal opening and closure requires diverse signalization pathways and transporters (Pandey et al. 2007). As xanthan gum may act differently on the opening and closure of stomata, leaves were treated with xanthan gum at dawn when most stomata were closed and also by day when they were already fully open.

Xanthan gum slightly inhibits stomatal opening at dawn and induces stomatal closure applied by day

In the first experiment the broad bean leaves were sprayed with the experimental solution with or without 1 mg ml^{-1} xanthan gum. After 30 minutes the leaves were illuminated and leaves from control and treated plants were peeled hourly and digital images were taken immediately to determine the actual stomatal aperture sizes. At 5:00 am stomata were almost entirely closed with an average size of 6.97 ± 0.89 µm. After 3 hours of illumination stomatal apertures of control plants reached their maximal value with an average size of 14.26 ± 1.08 µm, while the stomata of treated plants showed a slight decrease in the opening with an average aperture size of 8.73 ± 1.16 µm (Fig. 1A).

When the plants were treated at 10:00 am – when stomata were almost fully opened (12.88 ± 1.31 µm) – the aperture sizes of control plants did not change during the 4 hours of the experiment while the stomata treated with 1 mg m^{-1} xanthan gum showed a significant decrease (7.78 ± 1.25 µm) after 3 hours (Fig. 1B).

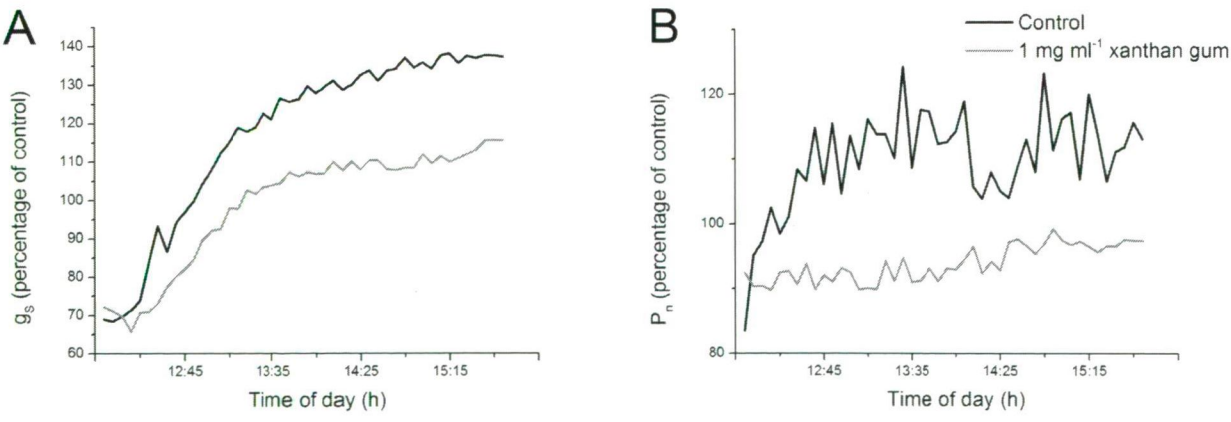

Figure 3. Stomatal conductance (A) and assimilation rate (B) after 1 mg ml^{-1} xanthan treatment. Both parameters are shown as percentage of control, which was measured prior to each treatment. It can clearly be seen that the treated leaves showed decreased stomatal conductance and assimilation rate during the whole experiment. Sampling was made every five minutes. The data presented are the average values of 3 independent experiments.

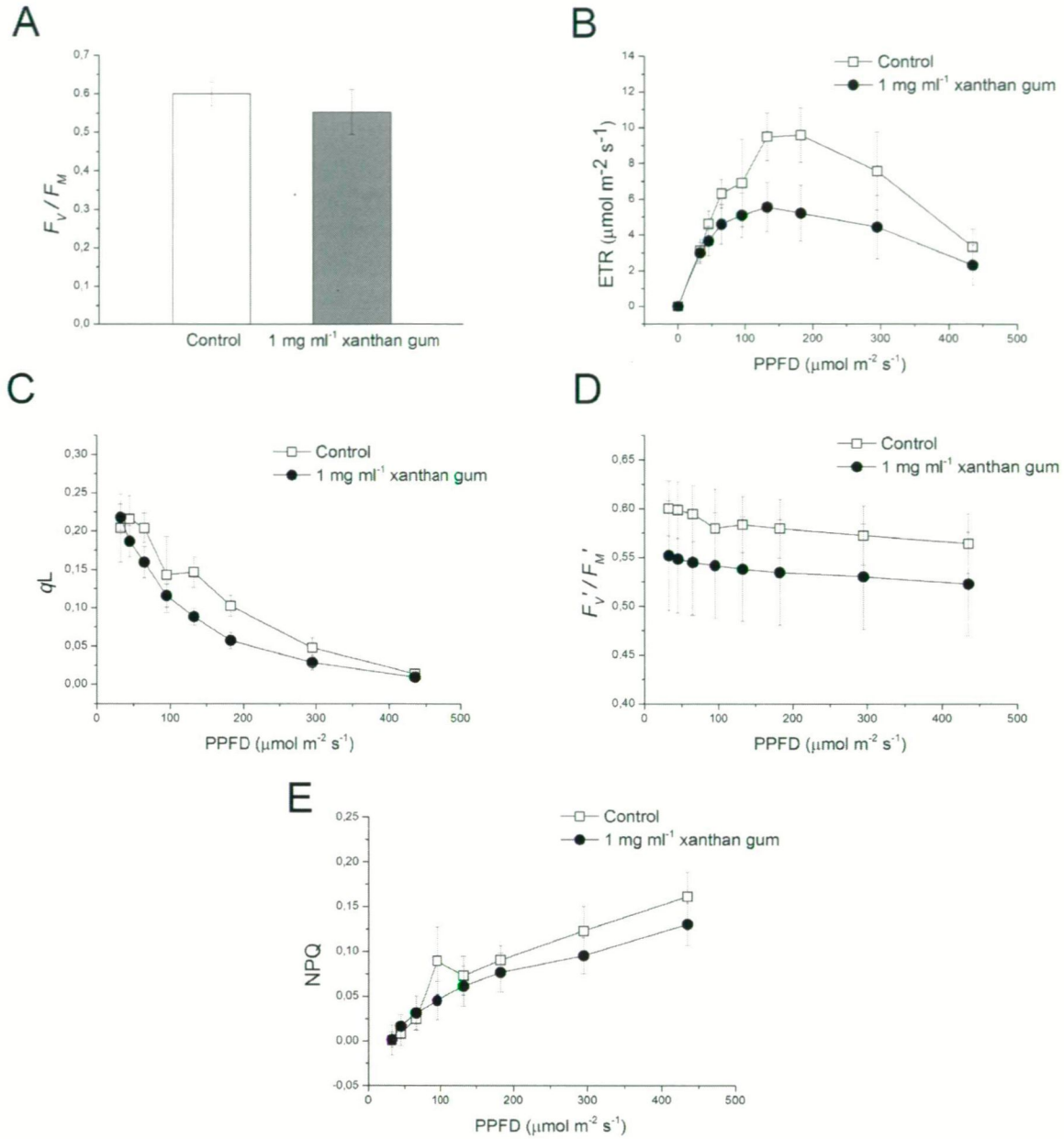

Figure 4. Photosynthetic parameters obtained from rapid light-response curves of dark-adapted abaxial guard cells in control and xanthan gum-treated leaves. Treatments were applied before the light period at 5:00 am and measurements were taken between 7:00 and 9:00 am. The data are displayed as averages (± SE) of 3 independent experiments, each measuring the fluorescence of 4-5 stomata.

These results clearly show that xanthan gum is recognized by guard cells of broad beans and that it requires 3 hours to induce stomatal closure both at dawn and during the daytime, which prompted us to investigate its effects on guard cell signaling and photosynthesis.

Xanthan gum induced NO accumulation but decreased the level of H_2O_2 in the guard cells of *Vicia faba*

Both H_2O_2 and NO are crucial components of the signaling of stomatal movements, especially stomatal closure (Srivastava et al. 2009). In order to investigate the production of H_2O_2 following the xanthan gum treatment, we applied a specific fluorescent sensor AR (Snyrychova et al. 2009). Abaxial epidermal peels from control and xanthan-treated leaves were incubated in experimental solution containing 50 µM AR for 30 min in dark. The peels were washed twice. AR reacts with H_2O_2 producing the highly fluorescent resorufin, whose emission was detected between 585 and 610 nm using 543 nm HeNe laser excitation. We found that the treatment

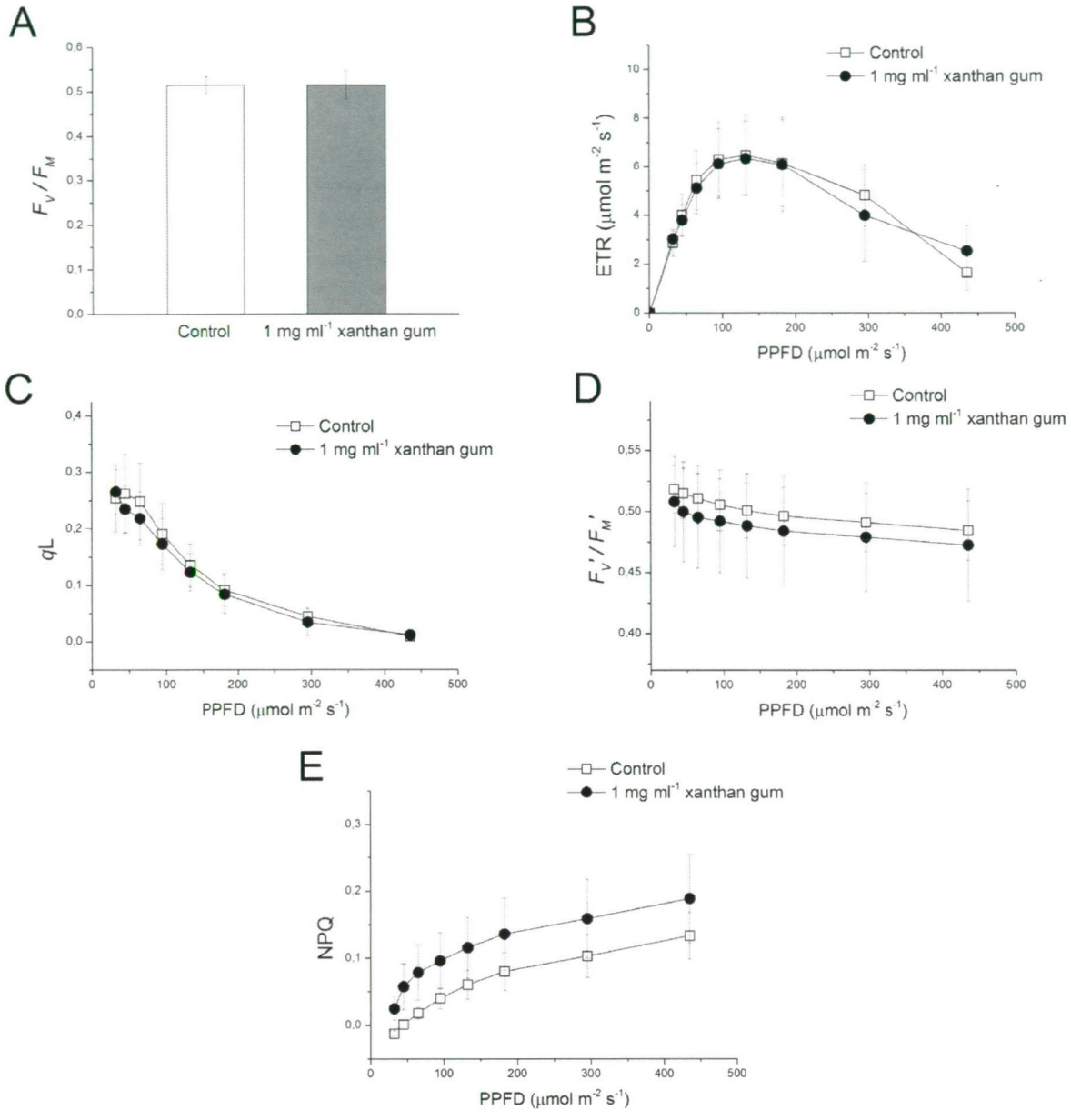

Figure 5. Photosynthetic parameters obtained from rapid light-response curves of abaxial guard cells in control and xanthan gum-treated leaves. Treatments were applied before 10:00 am and measurements were taken between 13:00 and 14:00 am. The data are displayed as averages (± SE) of 3 independent experiments, each measuring the fluorescence of 4-5 stomata.

with xanthan gum decreased the detectable level of resorufin fluorescence compared to control (Fig. 2), which was quite surprising as it is well established that stomatal closure is induced by an increase in the level of H_2O_2 (Desikan et al. 2004).

The level of NO was monitored by the fluorophore DAF-FM DA. In these experiments abaxial epidermal peels from control and 1 mg ml^{-1} xanthan gum treated leaves were incubated in experimental solution containing 10 μM DAF-FM DA for 15 min in dark. We found that xanthan gum only slightly induced the production of NO, which was mainly localized in the chloroplasts (Fig. 2).

Xanthan gum decreased the stomatal conductance and also the CO_2 assimilation

To continue the investigation on the background of xanthan-induced stomatal closure, stomatal conductance and CO_2 assimilation rate of leaves were monitored for 4 hours after the xanthan treatment with a leaf chamber fluorometer.

The xanthan gum treatment led to a decrease in stomatal conductance (Fig 3A). Dropping g_s values result in reduced CO_2 availability inside the leaves, so it is not surprising that xanthan gum treatment led to a moderate, but marked decline in CO_2 assimilation as well (Fig 3B).

Xanthan gum applied at dawn slows down the linear electron flow in guard cells of *Vicia faba*

As xanthan can reduce the rate of CO_2 fixation, we also investigated the photosynthetic activity in guard cells of *Vicia faba*. Since we found a difference in the effect of xanthan gum on stomatal movements at dawn and during the daytime, the photosynthetic measurements were also examined in these periods.

Figure 4 (A–C) shows that xanthan gum applied at dawn (5:00 am, 1 hour before the onset of illumination) slightly decreased the maximal quantum efficiency of dark-adapted PSII (*Fv/Fm*), the coefficient of photochemical fluorescence quenching (*q*L) and the apparent relative linear electron transport rate (ETR), while the values of the maximal quantum efficiency of light-adapted PSII (*Fv'/Fm'*) and the Stern-Volmer type non-photochesmical quenching (NPQ) did not change significantly. These results suggest that the xanthan-induced decrease in photochemistry might result in a lower level of ATP and NADPH in guard cells, which can lead to altered stomatal function.

When leaves were treated at day (10:00 am) there was no difference in the photosynthetic activity of guard cells from control and xanthan-treated leaves (Fig. 5A–E).

Conclusions

Many plant species respond to pathogen attack by closing stomata in a process called basal resistance, or PAMP-triggered immunity (Boller and Felix 2009). PAMPs can be recognized by PRRs, which can lead to the activation of different signaling cascades including the secondary transducer H_2O_2 and NO. We have shown that xanthan gum causes a moderate decrease in the level of H_2O_2 and increases the level of NO after 3 hours of treatment. We have previously shown that NO decreases the photosynthetic activity of guard cells (Ördög et al. 2013) so we decided to investigate whether xanthan gum can also influence the photosynthetic activity of guard cells. Xanthan gum applied at dawn slightly reduces the linear electron flow in the PSII reaction centers, which can lead to a reduced amount of ATP and NADPH, which in turn may prevent stomatal opening and induce stomatal closure.

In summary, our work shows that xanthan gum may influence the plant immune response not only through the accumulation of the enzyme ß-1,3 glucanase, but it can also induce stomatal closure. However, the underlying process of xanthan-induced stomatal closure is still unknown and awaits elucidation.

Acknowledgements

This research was supported by the European Union and the State of Hungary, co-financed by the European Social Fund in the framework of TÁMOP-4.2.4.A/ 2-11/1-2012-0001 'National Excellence Program'.

References

Bach EE, Barros BC, Kimati H (2003) Induced resistance against *Bipolaris bicolor*, *Bipolaris sorokiniana* and *Drechslera tritici-repentis* in wheat leaves by xanthan gum and heat-inactivated conidial suspension. J Phytopatol 151(7-8):411-418.

Bilger W, Björkman O (1990) Role of the xanthophyll cycle in photoprotection elucidated by measurements of light-induced absorbance changes, fluorescence and photosynthesis in leaves of *Hedera canariensis*. Phot Res 25(3):173-185.

Boller T, Felix G (2009) A Renaissance of Elicitors: Perception of microbe-associated molecular patterns and danger signals by pattern-recognition receptors. Annu Rev Plant Biol 60:379-406.

Butler WL (1978) Energy-distribution in photochemical apparatus of photosynthesis. Annu Rev Plant Physiol Plant Mol Biol 29:345-378.

Castro OL, Bach EE (2004) Increased production of beta-1,3 glucanase and proteins in *Bipolaris sorokiniana* pathosystem treated using commercial xanthan gum. Plant Physiol Biochem 42(2):165-169.

Desikan R, Cheung MK, Bright J, Henson D, Hancock JT, Neill SJ (2004) ABA, hydrogen peroxide and nitric oxide signaling in stomatal guard cells. J Exp Bot 55(395):205-212.

Franks P, Farqhuar GD (2007) The mechanical diversity of stomata and its significance in gas-exchange control. Plant Phys 143(1): 78–87.

Kramer DM, Johnson G, Kiirats O, Edwards G E (2004) New fluorescence parameters for the determination of QA redox state and excitation energy fluxes. Phot Res 79(2):209-218.

Lawson T (2009) Guard cell photosynthesis and stomatal function. New Phytol 181(1):13-34.

Nicaise V, Roux M, Zipfel C (2009) Recent advances in PAMP-triggered immunity against bacteria: Pattern recognition receptors watch over and raise the alarm. Plant Phys 150(4): 1638-1647.

Ördög A, Wodala B, Rózsavölgyi T, Tari I, Horváth F (2013) Regulation of guard cell photosynthetic electron transport by nitric oxide. J Exp Bot 64(5):1357-1366.

Pandey S, Zhang W, Assmann SM (2007) Roles of ion channels and transporters in guard cell signal transduction FEBS Letters 581(12):2325-2336.

Poór P, Gémes K, Horváth F, Szepesi Á, Simon ML, Tari I (2011) Salicylic acid treatment via the rooting medium interferes with stomatal response, CO_2 fixation rate and carbohydrate metabolism in tomato, and decreases harmful effects of subsequent salt stress. Plant Biol 13(1):105-114.

Rong W, Feng F, Zhou JM, He CZ (2010) Effector-triggered innate immunity contributes *Arabidopsis* resistance to *Xanthomonas campestris*. Mol Plant Pathol 11(6):783-793.

Snyrychova I, Ayaydin F, Hideg E (2009) Detecting hydrogen peroxide in leaves *in vivo* - a comparison of methods. Phys Plantarum 135(1):1-18.

Srivastava N, Gonugunta VK, Puli MR, Raghavendra AS (2009) Nitric oxide production occurs downstream of reactive oxygen species in guard cells during stomatal closure induced by chitosan in abaxial epidermis of *Pisum sativum*. Planta 229(4):757-765.

Volume 58(1):27-37, 2014
Acta Biologica Szegediensis
http://www.sci.u-szeged.hu/ABS

ARTICLE

Morphological and karyotype diversity in populations of four *Silene* species (Caryophyllaceae)

Neda Atzazadeh[1], Maryam Keshavarzi[1]*, Masoud Sheidai[2], Abbas Gholipour[3]

[1]Biology Department, Alzahra University, Vanak, Tehran, Iran, [2]Faculty of Biological Sciences, Shahid Beheshti University, Evin, Tehran, Iran, [3]Biology Department, Payamenour University, Sari Branch

ABSTRACT Karyotype and morphometric studies were performed on 14 and 24 Iranian populations of 4 *Silene* (Caryophyllaceae, Sect. *Auriculatae*) species. Phenetic study of 24 populations of *S. commelinifolia*, *S. eremicana*, *S. lucida* and *S. nurensis* from different locations of Iran revealed that a lot of morphological characters as basal and caulinal leaf shape, width and length, capsule shape and condition in calyx, epipetalus stamens to alternate ones, alar pedicel length, lateral pedicel length, epipetalus filament length to claw length and calyx gap length are of taxonomic importance. *S. nurensis* possessed a chromosome number 2n=2x=24, *S. lucida* and *S. eremicana* possessed a chromosome number 2n=4x=48, while *S. commelinifolia* var. *commelinifolia* and *S. commelinifolia* var. *ovatifolia* populations were diploid and tetraploid. The chromosomes were mainly metacentric or sub-metacentric and their size varied from 1.21 μm in *S. nurensis* to 3.96 μm in *S. commelinifolia*. The total size of the chromosomes differed significantly in short and long arm size, indicating the role of quantitative genomic changes in the *Silene* species diversification. The *Silene* species were placed in 1A and 1B classes of Stebbins karyotype symmetry. Presence of B chromosome is recorded for the first time for *S. commelinifolia*. Clustering and ordination methods showed karyotype distinctness in the investigated species.
Acta Biol Szeged 58(1):27-37 (2014)

KEY WORDS

Silene
karyotype
morphometry

The genus *Silene* L. (Caryophyllaceae) is a large genus with worldwide distribution, containing about 700 species. These species are mainly hermaphrodite, although a few species are dioecious or gynodioecious (Bari 1973; Greuter 1995). *Silene* species are mostly distributed throughout the northern hemisphere, Europe, Asia and northern parts of Africa (Greuter 1995) and are annual, biennial, or perennial herbs. Diploid species, which are more frequent have $2n$=18, 20 and 24. Triploid to hexaploid and even higher polyploidy levels, e.g. $2n$=*c*. 96, 120 and 192, are known in the genus (Swank 1932; Bari 1973; Oxelman et al. 1997; Heaslip 1951; Bari 1973; Sopova and Sekovski 1982; Zhang 1994). X=9, 10, 12 and 23 are the known basic chromosome numbers in *Silene*.

Available literature about *Silene* cytogenetic studies indicates the importance of such studies in defining the species relationships (Heaslip 1951; Bari 1973; Melzheimer 1978; Markova et al. 2006). But very limited cytological studies have been carried out on the species growing in Iran and only recently some preliminary karyotype and meiotic studies have been reported from the country (Sheidai et al. 2008; Sheidai et al. 2009a, b; Gholipour and Sheidai 2010a, b; Sheidai et al. 2012).

Accepted July 25, 2014
*Corresponding author. E-mail: neshat112000@yahoo.com

About 110 *Silene* species grow in Iran from which about 35 species are endemic with very limited geographical distribution (Melzheimer 1988). Chowdhuri (1957) placed the *Silene* in 44 sections, although recent molecular studies do not support such sectional classifications (Oxelman et al. 1997, 2000; Burleigh and Holtsford 2003). The section *Auriculatae* (Boiss.) Schischkin is the largest section of the genus containing about 35 species, of which 21 species are endemic to Iran (Melzheimer 1988). The members of this section are caespitose alpine elements with large flowers placed at the end of short stems. Their inflorescence is unifloral or dichasial. The calyx is very cylindrical-clavate, pubescent or glandular-pubescent. The petals have a conspicuous auricle at the end of the claw.

Species relationships in genus *Silene* sect *Auriculatae* L. based on RAPD and morphological analysis have been studied in Iran (Sheidai et al. 2010).The inter-population morphological and molecular diversity in three *Silene* species in the sect *Auriculatae* L. have been studied in Iran (Sheidai et al. 2012). Morphological and micro-morphological features in seven *Silene* species and subspecies in the sect *Auriculatae* L. and *Inflatae* have been studied in Iran (Tabaripour et al. 2013). Gholipour and Sheidai (2010c) considered *S. eremicana* and *S. goniocaula* as separate *Silene* species in Iran, despite Melzheimer opinion (1988).

Table 1. Voucher details and selected studies for each case (M: morphometry and C: cytology).

Studies	Locality	Code	Taxon	No.
M, C	West Azerbaijan, Piranshahr to Naghadeh, Gerd Kashaneh, Lik Bin Village, Landi Sheykhan Mountain, 36 41 7.5 N 45 26 27.1 E, 2400 m, 2010/7/2, 890277.	Com14	*S. commelinifolia* var. *ovatifolia*	1
M, C	Tehran, Darakeh Mountain, 1900 m, 2012/6/20, 91287.	Com11	*S. commelinifolia* var. *ovatifolia*	2
M	Tehran, Darakeh Mountain, 35 49 37.3 N 51 22 47.3 E, 1925 m, 2008/6/20, 8768.	Com12	*S. commelinifolia* var. *ovatifolia*	3
M	West Azerbaijan, Urmia, Anhar, Marmisho, 37 29 0.33 N 44 45 0.22 E, 2327 m, 2011/7/19, 900832.	Com10	*S. commelinifolia* var. *ovatifolia*	4
M	West Azerbaijan, Takab, 2008/6/30.	Com13	*S. commelinifolia* var. *ovatifolia*	5
M, C	Mazandaran, Baladeh, Kamarbon, Gosfandsarai-e chai khaksar, 36 14 16.1 N 51 22 17.1E, 2852m, 2011/7/6, 900624.	Com5	*S. commelinifolia* var. *commelinifolia*	6
M	Tehran, Haraz Road, Polor, 35 48 899 N 52 01 643 E, 2405 m, 2007/6/9, 8637.	Com6	*S. commelinifolia* var. *commelinifolia*	7
M,C	West Azerbaijan, Urmia, Anhar, Marmisho, 37 29 03.2 N 44 36 24.7 E, 3007m, 2012/7/2, 91312.	Com7	*S. commelinifolia* var. *commelinifolia*	8
M, C	Hamedan, Alisadr Cave, 2010/6/29.	Com8	*S. commelinifolia* var. *commelinifolia*	9
M, C	Tehran, Touchal, 35 52 572 N, 51 24 131 E, 2700 m, 2008/6/25, 8771.	Com9	*S. commelinifolia* var. *commelinifolia*	10
C	Tehran, Dizin, Gajerah, Velayatroud Village, 36 03 N 51 23 E, 2500 m, 2008/7/15.	Com11	*S. commelinifolia* var. *commelinifolia*	11
C	Lorestan, Azna, Daretakht, Oshtorankuh, 33 20 473 N 49 20 347 E, 2680 m, 2008/8/19.	Com16	*S. commelinifolia* var. *commelinifolia*	12
M, C	Ardabil, Km 30 Ardabil to Kivi, before Neor Lake, 38 00 549 N 48 55 225 E, 2590 m, 2011/7/15, 900701.	Com1	*S.* cf. *commelinifolia*	13
M, C	Ardabil, Neor Lake, 2008/8/19.	Com2	*S.* cf. *commelinifolia*	14
M, C	East Azerbaijan, Sarab, Shalgoon Village, Bozqush Mountain, 37 45 54 N 47 35 31 E, 2650-3000 m, 2012/7/8, 91387.	Com3	*S.* cf. *commelinifolia*	15
M, C	Hamadan, Alvand Mountain, Ganjnameh, 34 43 475 N 48 25 039 E, 2800 m, 2006/6/25, 86105.	Ere	*S. eremicana*	16
M	East Azerbaijan, Sarab, Shalgoon Village, Bozqush Mountain, 37 45 54 N 47 35 31 E, 2650-3000 m, 2012/7/8.	Luc2	*S. lucida*	17
M	Gilan, Kelachay, Rahim Abad, Eshkevarat, Chakol, Boza kuh, 2800-3100 m, 2007/6/29, 86139.	Luc1	*S. lucida*	18
M	East Azerbaijan, Bostan Abad to Miyaneh, km 75, 2006/6/7, 8516.	Luc3	*S. lucida*	19
C	West Azerbaijan Piranshahr to Naghadeh, Km 5, Selve Village, Sepiarez Mountain, 36 50 59.9 N 44 58 24.8 E, 2820 m, 2010/7/1, 890257.	Luc6	*S. lucida*	20
M	West Azerbaijan, Urmia, Silvana, Kuh-e Khalil, 37 22 44.5 N 44 48 3.8 E, 2594 m, 2008/6/4, 8754.	Luc4	*S. lucida*	21
M	West Azerbaijan, Urmia, Silvana, Kuh- e Khalil, 2008/6/4, 87054.	Luc5	*S. lucida*	22
M	Chaharmahal and Bakhtiari, Farsan, Kuhrang, Zardkuh, 32 18 704 N 50 08 574 E, 3300-3400 m, 2008/7/30, 87082.	Nur2	*S. nurensis*	23
M, C	Chaharmahal and Bakhtiari, Farsan, Kuhrang, Zardkuh, 32 18 704 N 50 08 574 E, 3300-3400 m, 2008/7/30, 8782.	Nur1	*S. nurensis*	24
M	Lorestan, Azna, Daretakht, Oshtorankuh, 33 20 473 N 49 20 347 E, 2680 m, 2008/8/19, 87087.	Nur3	*S. nurensis*	25
M	Lorestan, Azna, Daretakht, Oshtorankuh, 33 20 522 N 49 20 427 E, 2535 m, 2008/8/9, 8787.	Nur4	*S. nurensis*	26
M	Kohgiluyeh and Boyer ahmad, Dehdasht, Sarfariab, Joukhaneh, Kuh-e Nir 30 49 30.9 N 50 55 19E, 2980 m, 2011/6/9, 900400.	Nur5	*S. nurensis*	27

Due to Gholipour and Sheidai (2010) biosystematics studies on this section, some species groups were defined. One of this species group is related to *S. commelinifolia.* Based on flora Iranica there are three varieties in this species: *commelinifolia, ovatifolia* and *isophylla.* There are some problems in varieties delimitation. Based on our previous studies there was a probability for misidentifications in this species complex, so there was a necessity for careful population study to define characters range of variation. Recent studies (Sheidai et al. 2012; Gholipour and Sheidai 2010a, b; Sheidai et al. 2009a,

Table 2. Morphological characters and their code.

Code				Character
	x>35	20≤x≤35	x<20	Plant height
	x>55	35≤x≤55	x<35	Basal leaf length
	x>5	2.5≤x≤5	x<2.5	Basal leaf width
		x>0.5	x≤0.5	Length/width Basal
	x>35	20≤x≤35	x< 25	Cauline leaf length
	x>5	2.5≤x≤5	x< 2.5	Cauline leaf width
	x>0.11	0.8≤x≤0.11	x<0.8	Cauline leaf width/length
x>10	5≤x≤10	2≤x≤5	x<2	Alar pedicel length
	x>5	2≤x≤5	x<2	Lateral pedicel length
x>32	21≤x≤32	15≤x≤20	x<15	Calyx length
	x>5	2.5≤x≤5	x<2.5	Calyx tooth length
	x>15	10≤x≤15	x<10	Petal claw length
	x>7	5≤x≤7	x<5	Petal limb length
	x>5	3≤x≤5	x<3	Epipetalus filaments length to claw
		x>1.3	x<1.3	Corona length
	x>10	7≤x≤10	x<7	Capsule length
x>15	11≤x≤15	5≤x≤10	x<5	Antophore length
		x>1.75	x<1.75	Seed length
		x>1.75	x<1.75	Seed width
		x>1.75	x<1.75	Seed width/length
			Caespitose-suffrutescent	Habit
	Linear-lanceolate	Linear	Ob-lanceolate	Basal leaf form
Linear	Lanceolate	Cordate	Ovate	Cauline leaf form
			Present	Cauline leaf indumentums
			Cylindric-clavate	Calyx form
			Compound dichasium	Inflorescence type
			Present	Calyx outside indumentums
		Absent	Present	Calyx inside indumentums
			Parallel	Calyx veins
			Exerted from calyx	Capsule situation to calyx
		Included in calyx	Exerted from calyx	Claw situation to calyx
		Longer than 1/2 limb	Shorter than 1/2 limb	Petal limb division length
		Inconspicuous	Conspicuous	Auricle size
		As long as epipetal	Shorter than epipetal	Alternate filament length
			Absent	Filament indumentum
			Absent	Style indumentum
		Elongate ovate	Oblong- elliptic	Capsule form
			Present	Antophore indumentum

b; Sheidai et al. 2008), showed the polyploidy variations in accessions that could be the main factor in population divergence. So the population divergence of *S. commelinifolia* and related taxa in Iran is considered in the present study.

Materials and Methods

Plant material

Morphological studies were performed on 23 populations of 4 *Silene* species and varieties of the section *Auriculatae*. Karyotype studies were performed in 14 ones (Table 1.). The studied taxa were *Silene commelinifolia* Boiss. var. *commelinifolia*, *S. commelinifolia* Boiss. var. *ovatifolia* Melzh., *S. nurensis* Boiss. & Hausskn, *S. lucida* Chowdhuri and *S.eremicana* Stapf. The vouchers are deposited in the Herbarium of Shahid Beheshti University (HSBU).

Morphological studies

In total, 38 morphological characters (quantitative and qualitative) were studied (Table 2). Analysis of variance test (ANOVA) was performed to show a significant difference in quantitative morphological characters among the species. For multivariate analyses the mean of quantitative characters was used, while qualitative characters were coded as binary/multistate characters. Standardized variables (mean = 0, variance = 1) were used for statistical analyses. The average taxonomic distance and Manhattan distance were used as dissimilarity coefficients independently in cluster analysis of morphological data (Podani 2000). Grouping of the species based on morphology characteristics was performed using different clustering methods, including un-weighted paired group with arithmetic average (UPGMA), as well as

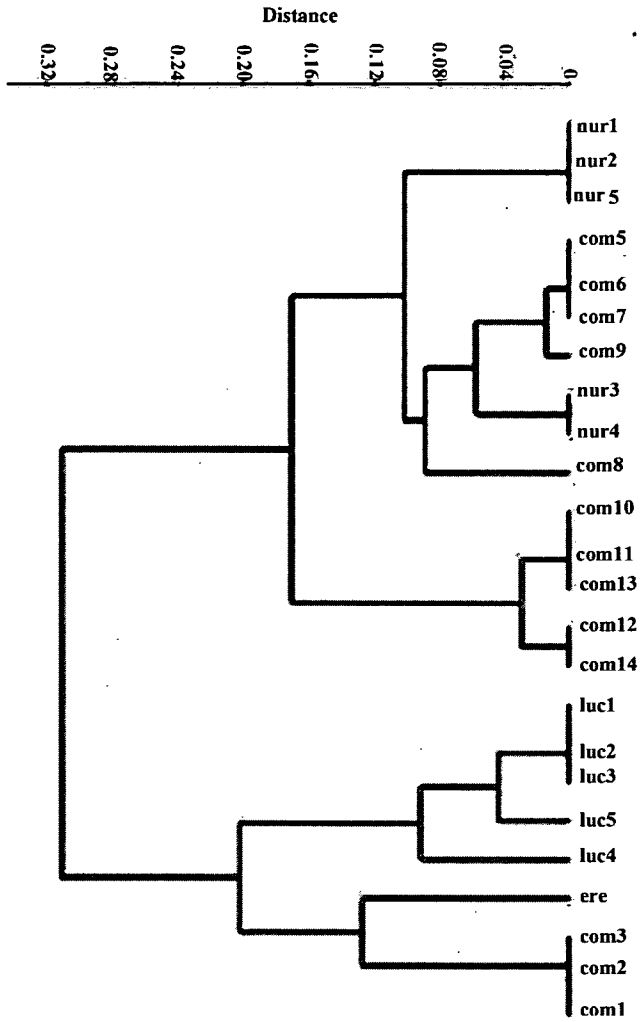

Figure 1. UPGMA dendrogram of studied *Silene* species based on morphological characters. Species code: com5, 6, 7, 8, and 9 = *S. commelinifolia* var. *commelinifolia*; com10, 11, 12, 13 and 14 = *S. commelinifolia* var. *ovatifolia*; com1, 2 and 3 = *S. cf commelinifolia*; nur = *S. nurensis*; luc = *S. lucida* and ere = *S. eremicana*.

principal coordinate analysis (PCO) (Podani 2000). Principal Components Analysis (PCA) and canonical correspondence analysis (CCA) were performed to identify the most variable morphological characters and the plot of the first and second component were used to investigate the species grouping (Podani 2000).

Cytological studies

For karyotype studies freshly grown root tips were collected from the seeds of at least ten randomly selected plants in each species, pretreated with 0.002 mol 8-hydroxyquinolin (1-2 h). Squash technique was used for cytological studies and karyotypic details were studied in at least 5 well prepared metaphase plates as reported earlier (Sheidai and Rashid 2007). The chromosomes were identified according to Levan et al. (1964), karyotype symmetry was determined according to Stebbins (1971). Karyotype parameters as a total form percentage (TF %), coefficient of variation (CV) of the chromosome size as well as A1 indices of Romero- Zarco (1986) were determined (Sheidai and Jalilian 2008).

In order to reveal significant difference, the analysis of variance (ANOVA) followed by the least significant difference test (LSD) was performed on the size of chromosomes, the size of the long arms and the size of the short arms as well as arm ratio among the studied species and populations (Sheidai and Jalilian 2008). Moreover, principal components analysis (PCA) was performed to identify the most variable karyotypic characters. The Karyotypic distinctness of the species studied was checked by using an ordination plot of principal components analysis (PCO) (Sheidai and Jalilian 2008).

Results and Discussion

Morphometry

ANOVA test showed significant differences for almost all quantitative morphological characters studied. UPGMA (Fig. 1) tree, PCA (Fig. 2) and PCO (Fig. 3) plots of morphological characters clearly separated the studied species. However, almost within each species cluster, the populations differed somewhat from each other. PCA analysis of morphological data revealed that three first components comprised about 78% of the total variance (data not shown). In the first component with about 42% of total variance, morphological characters, including basal leaf form, capsule situation to calyx, alternate filament length, basal and cauline leaf length, alar and lateral pedicel length and epipetalus filaments length to claw showed the highest correlation (>0.7). In the second component with about 20% of total variance, basal leaf width, length/width basal and calyx tooth length had the highest correlation (>0.7). In the third component (15% of total variance), cauline leaf form and capsule form had the highest correlation (>0.7).

Based on UPGMA (Fig. 1) dendrogram, PCA (Fig. 2) and PCO (Fig. 3) plot of morphological data, *S. nurensis* populations as Zardkuh and Kuh-e Nir are separated from others by features like plant length, basal leaves length, shape, length and width of caulinar leaves, alar and lateral pedicel length, claw position in calyx, calyx gap length, antophore length and length and width of capsule, although there are some similarities between *S. nurensis* populations and *S. commelinifolia* var. *commelinifolia*.

Populations of Touchal, Mazandaran, Haraz, Marmisho and Alisadr from *S. commelinifolia* var. *commelinifolia* show some differences at varietal level. Populations of *S. commelinifolia* var. *commelinifolia* and *S. commelinifolia* var. *ovatifolia* are grouped in two separate subsets and differed

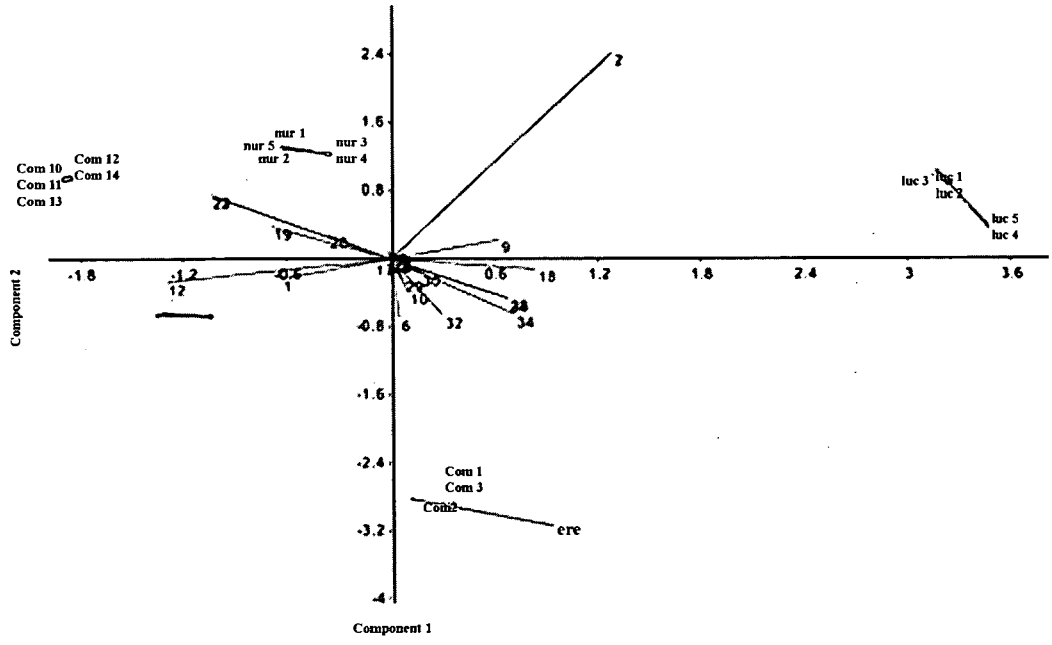

Figure 2. PCA plot of studied *Silene* species based on morphological characters. Species code: com5, 6, 7, 8, and 9 = *S. commelinifolia* var. *commelinifolia*; com10, 11, 12, 13, and 14 = *S. commelinifolia* var. *ovatifolia*; com1, 2, and 3= *S. cf commelinifolia*; nur = *S. nurensis*; luc = *S. lucida* and ere = *S. eremicana*.

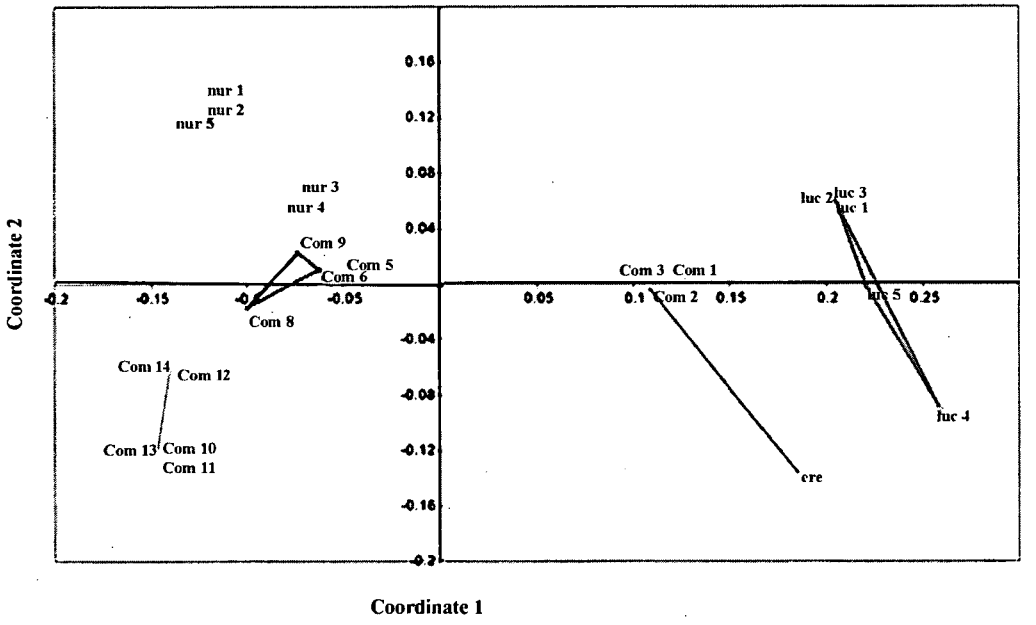

Figure 3. PCO plot of *Silene* species based on morphological characters. Species code: com5,6,7,8,9 = *S. commelinifolia* var. *commelinifolia*, com10,11,12,13,14 = *S. commelinifolia* var. *ovatifolia*, com1,2,3= *S. cf commelinifolia*, nur = *S. nurensis*, luc = *S. lucida* and ere = *S. eremicana*.

in features such as basal leaf width, width to length of basal leaves, shape and width of caulinar leaves, width to length of caulinar leaves, alar and lateral pedicel.

Our morphological observations of Alvand population from *S. eremicana* showed that it is the same plant that is identified as *S. commelinifolia* var. *isophylla*, so as Gholipour and Sheidai (2010c) had suggested it should be considered as synonym for *S. commelinifolia* var. *isophylla*. Kivi, Neor and

Table 3. Karyotype features of the *Silene* species studied.

Kf	St	C.V	A1	X	TF%	L/S	S(μm)	L(μm)	T.L(μm)	2n	Code	Locality	Species
12m	1A	16.00%	0.76	1.99	43.05%	1.83	1.43	2.61	23.91	24	Com7	Marmisho	*S. commelinifolia* var. *commelinifolia*
12m	1A	18.90%	0.83	2.07	45.36%	1.96	1.37	2.69	24.83	24	Com9	Touchal	*S. commelinifoli* var. *commelinifolia*
12m	1B	19.61%	0.81	2.03	44.64%	2.09	1.31	2.74	24.41	24	Com5	Mazan-daran	*S. commelinifoli* var. *commelinifolia*
12m	1A	18.72%	0.76	1.99	43.03%	1.96	1.38	2.70	23.92	24	Com15	Dizin	*S. commelinifoli* var. *commelinifolia*
24m	1B	21.57%	0.78	1.99	43.68%	2.49	1.18	2.94	47.82	48	Com8	Alisadr	*S. commelinifoli* var. *commelinifolia*
24m	1B	19.06%	0.76	2.06	43.14%	2.18	1.34	2.92	49.34	48	Com16	Osh-torankuh	*S. commelinifoli* var. *commelinifolia*
11m+1Sm	1A	15.89%	0.70	1.84	40.94%	1.72	1.35	2.33	22.10	24	Com11	Darakeh	*S. commelinifoli* var. *ovatifolia*
24m	1B	20.50%	0.79	2.73	43.78%	2.39	1.66	3.96	65.63	48	Com2	Neor	*S. cf commelinifolia*
24m	1B	16.49%	0.77	2.21	43.20%	2.05	1.49	3.05	52.96	48	Com1	Kivi	*S. cf commelinifolia*
24m	1B	18.79%	0.74	2.44	42.73%	2.24	1.66	3.71	58.64	48	Com3	Bozqush	*S. cf commelinifolia*
12m	1A	17.22%	0.73	1.74	42.04%	1.89	1.21	2.28	20.93	24	Nur1	Zardkuh	*S. nurensis*
24m	1B	18.08%	0.80	2.05	44.50%	2.13	1.41	2.99	49.31	48	Luc6	Sepiarez	*S. lucida*
-	-	-	-	-	-	-	-	-	-	48	ere	Alvand	*S. eremicana.*
-	-	-	-	-	-	-	-	-	-	48	Com14	Piranshahr	*S. commelinifolia*

Abbreviations: TL = Total chromatin length (μm), L = Size of the longest chromosome pair (μm), S = Size of the shortest chromosome pair (μm), L/S = Ratio of the longest to shortest chromosome, TF = Total form percentage, X = Mean chromatin length (μm), A1 = Romero-Zarco indices, CV = Coefficient of variation, ST = Stebbins' symmetry class, KF = Karyotypic formulae.

Bozqush populations of S. *cf commelinifolia* are grouped with *S. eremicana* due to the similarity in features as shape, width and length of caulinar leaves, length of lateral pedicel, length of calyx gap and capsule shape. Same populations show some similarities in some features as plant size, shape, width and length of basal leaves, calyx length, antophore hair type, petal blade, claw and corona length, alternate to epipetalus stamens and alar pedicel length to *S. commelinifolia.*

Kuh-e Khalil, Gilan, Miyaneh and Bozqush populations of *S. lucida* are grouped in a separate set. These populations show some deviation from the type specimen of *S. lucida* as was described in flora Iranica in plant size, basal and caulinar leaves shape, width and length of basal and caulinar leaves, pedicel length, bract length and width, calyx length, length of calyx gap, length of corona, claw and capsule width and length. These are considered here as *S. cf lucida.*

Cytology

Details of karyotypic analyses in the *Silene* species studied are presented in Table 3 and Fig. 4. In *S. commelinifolia* five studied accessions of Marmisho, Touchal, Mazandaran, Dizin and Darakeh chromosome counts were 2n=2x=24 which is in concordance with previous results (Gholipour and Sheidai 2010a). Six studied accessions of Alisadr, Oshtorankuh, Neor, Kivi, Bozqush and Piranshahr chromosome counts were 2n=4x=48 for the first time. So *S. commelinifolia* showed two ploidy levels. In *S. eremicana* the Alvand population showed 2n=4x=48 which is in agreement with the previous counts (Gholipour and Sheidai 2010a). Sepiarez population of *S. lucida* had chromosome number 2n=4x=48 which is in concordance with the previous result (Gholipour and Sheidai 2010b). *S. nurensis* from Zardkuh population showed 2n=2x=24 chromosome number which is recorded for the first time.

The chromosomes were mostly metacentric (m), but a pair of sub metacentric (sm) chromosome was observed in the Darakeh population of *S. commelinifolia* (Table 3). The size of the longest chromosome varied from 2.28 μm in Zardkuh population of *S. nurensis* to 3.96 μm in Neor population of *S. cf commelinifolia* (Table 3), while the size of shortest chromosomes varied from 1.21 μm in Zardkuh population of *S. nurensis* to 1.66 μm in Neor and Bozqush populations of *S. cf commelinifolia.* The highest haploid total chromatin length as well as mean chromosome length occurred in population of *S. cf commelinifolia* (65.63 and 2.73 μm respectively), while the lowest value of the same occurred in Zardkuh population of *S. nurensis* (20.93 and 1.74 μm, respectively). The highest value of chromosomes size variation (CV= 21.57) occurred in Alisadr population of *S. commelinifolia* while the lowest CV (15.89) occurred in Darakeh population of *S. commelinifolia.*

So in higher CV values, variation in chromosomes sizes is more and karyotype is more asymmetric. Alisadr population has the highest CV values this indicated the highest values

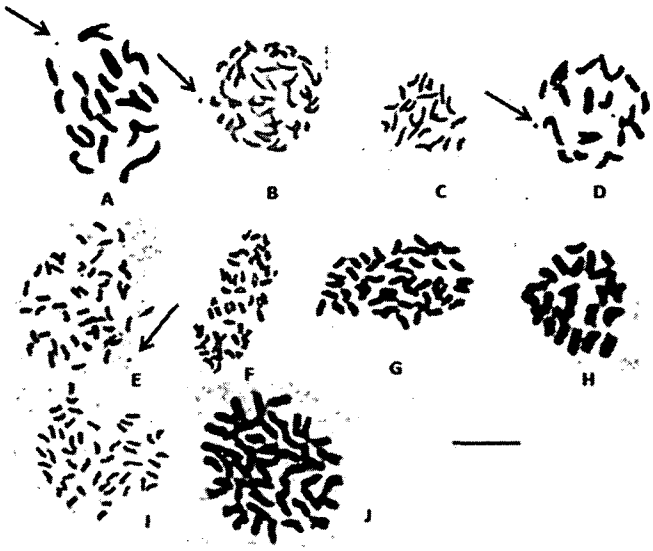

Figure 4. Representative somatic cells. A–C = Somatic metaphase cell in Marmisho, Oshtorankuh and Mazandaran population of *S. commelinifolia* var. *commelinifolia*, respectively. D = Somatic metaphase cell in Darakeh population of *S. commelinifolia* var. *ovatifolia*. E-G = Somatic metaphase cell in Bozqush, Neor and Kivi population of *S. cf commelinifolia*. H = Somatic metaphase cell in Zardkuh population of *S. nurensis*. I = Somatic metaphase cell in Bozqush population of *S. lucida*. J = Somatic metaphase cell in Alvand population of *S. eremicana*. A, B, D and E = arrows show B- chromosomes. Scale bar = 10 μm.

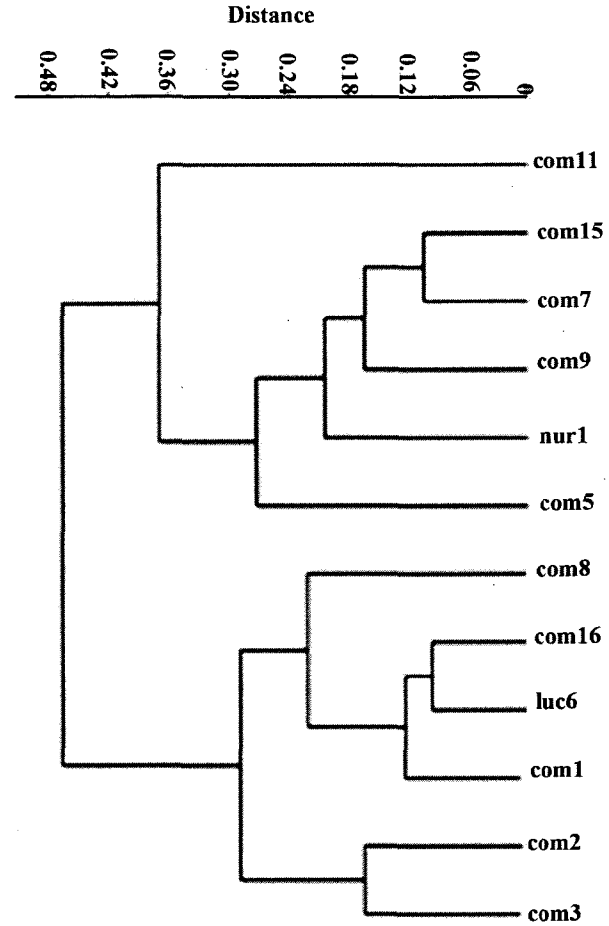

Figure 5. UPGMA clustering of *Silene* species based on karyotype data. Species abbreviations: com5, com 7, com 8, com 9, com 15 and com 16 = *S. commelinifolia* var. *commelinifolia*; com 11 = *S. commelinifolia* var. *ovatifolia*; com 1, com 2 and com 3 = *S. cf commelinifolia*; nur1 = *S. nurensis*, luc6 = *S. lucida*.

in chromosome size variation. The ANOVA and LSD tests revealed a significant difference ($p < 0.05$) for total size of the chromosomes, the size of the short arms and the long arms among the species and populations studied, indicating the role of quantitative genomic changes in the *Silene* species diversification. In PCO diagram (Fig. 7), this population is located far from other populations due to the difference in karyotype features. Total form percentage (TF%) varied from 40.94% in Darakeh to 45.36% in Touchal population of *S. commelinifolia* (Table 3); a higher value of TF% indicates the presence of relatively more symmetrical karyotype. Comparisons of karyotype symmetries based on Stebbins classification (1971) showed that Marmisho, Touchal, Dizin and Darakeh populations of *S. commelinifolia* and Zardkuh population of *S. nurensis* were of A1 class. Mazandaran, Alisadr, Oshtorankuh, Kivi, Neor and Bozqush accessions of *S. commelinifolia* and Sepiarez from *S. lucida* belonged to 1B class which is considered relatively primitive in Stebbins's system. Therefore, it seems that the *Silene* species studied are having symmetrical karyotypes.

Among the species placed in A1 class, Touchal population of *S. commelinifolia* shows a higher value of the A1 index (0.83) of Romero-Zarco index (A1) and, therefore, has a relatively more asymmetrical karyotype. All these results indicate the role of both quantitative and qualitative changes in the genome during the *Silene* species diversification. Lower intra-chromosomal asymmetry index (A1) was observed in Darakeh population (0.7%). The smaller the A1 values the more the frequency of metacentric chromosomes and the more is the symmetry of karyotype.

Different clustering methods, PCA and PCO plot of the *Silene* species based on karyotype data produced similar results (Figs. 5, 6 and 7). In UPGMA dendrogram of karyotype data (Fig. 5) two major clusters were formed; in the first major cluster 2n = 2x = 24 populations and in second one 2n = 4x = 48 populations were located. The first major cluster contains most *S. commelinifolia* populations with Zardkuh population of *S. nurensis* which show similarities and overlaps in morphological features too (Atazadeh 2013). In this sub-cluster, Darakeh population of *S. commelinifolia* var. *ovatifolia* was located far from other populations. Marmisho, Dizin and Touchal populations of *S. commelinifolia* var. *commelinifolia* showed the highest similarities.

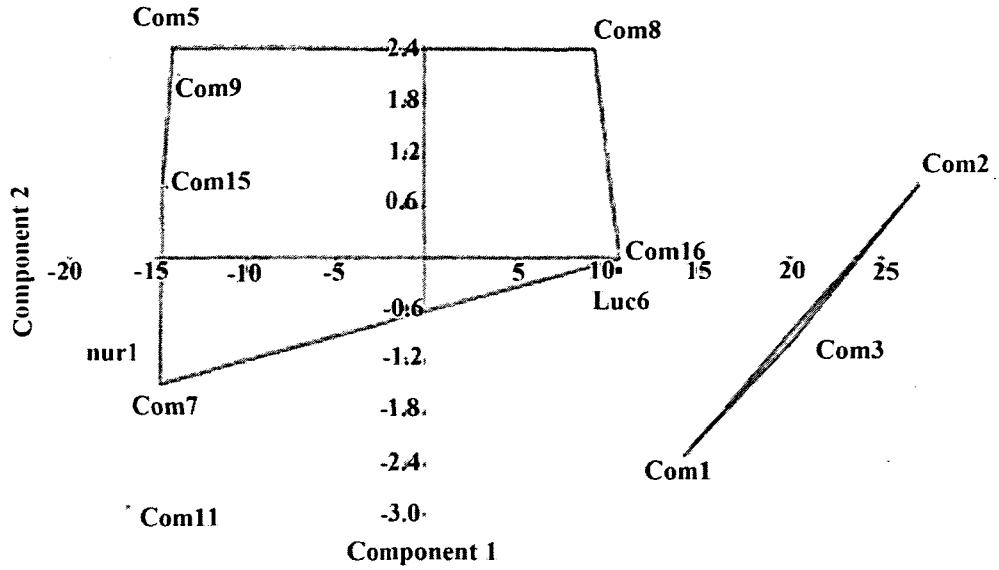

Figure 6. PCA plot of *Silene* species based on karyotype data. Species abbreviations: com 5, com 7, com 8, com 9, com 15 and com 16 = *S. commelinifolia* var. *commelinifolia*; com 11 = *S. commelinifolia* var. *ovatifolia*; com 1, com 2 and 3 = *S. cf commelinifolia*; nur 1 = *S. nurensis*; luc 6 = *S. lucida*.

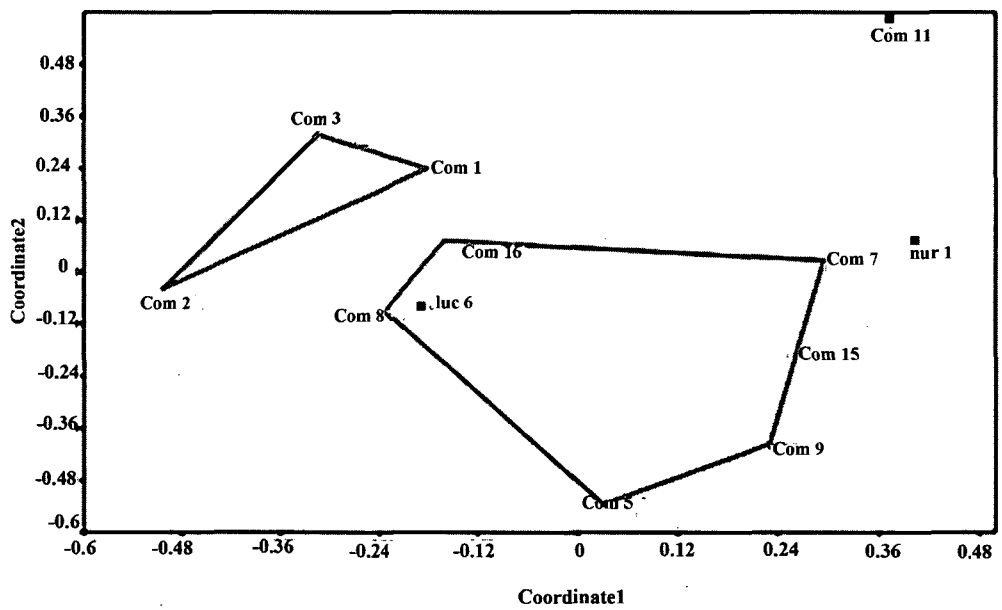

Figure 7. PCO plot of *Silene* species based on karyotype data. Species abbreviations: com 5, com 7, com 8, com 9, com 15 and com 16 = *S. commelinifolia* var. *commelinifolia*; com 11 = *S. commelinifolia* var. *ovatifolia*; com 1, com 2 and 3 = *S. cf commelinifolia*; nur 1 = *S. nurensis*; luc 6 = *S. lucida*.

In the second major cluster, Oshtorankuh and Alisadr of *S. commelinifolia* var. *commelinifolia* and Sepiarez population of *S. lucida* and Neor, Kivi and Bozqush populations of *S.* cf *commelinifolia* show more similarity and are placed together. In this cluster Oshtorankuh and Alisadr populations are more similar to *S. lucida*. Based on PCA (Fig. 6) and PCO (Fig. 7) plots, almost populations of *S. commelinifolia* varieties and *S. nurensis* and *S. lucida* composed a definite group. *S. nurensis* populations and Neor, Kivi and Bozqush population of *S.* cf. *commelinifolia* and *S. commelinifolia* var. *ovatifolia* are

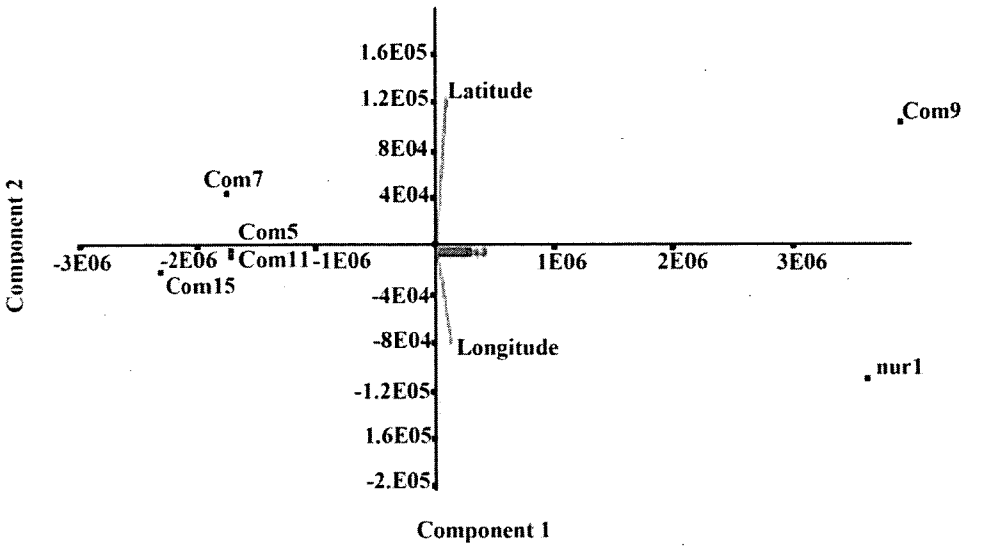

Figure 8. CCA plot of *Silene* species based on longitude and latitude for 2n = 24 populations. Species abbreviations: nur 1 = *S. nurensis*; com 9, com 7, com 15 and com 5 = Touchal, Marmisho, Dizin and Mazandaran populations of *S. commelinifolia* var. *commelinifolia*; com 11 = Darakeh populations of *S. commelinifolia* var. *ovatifolia*.

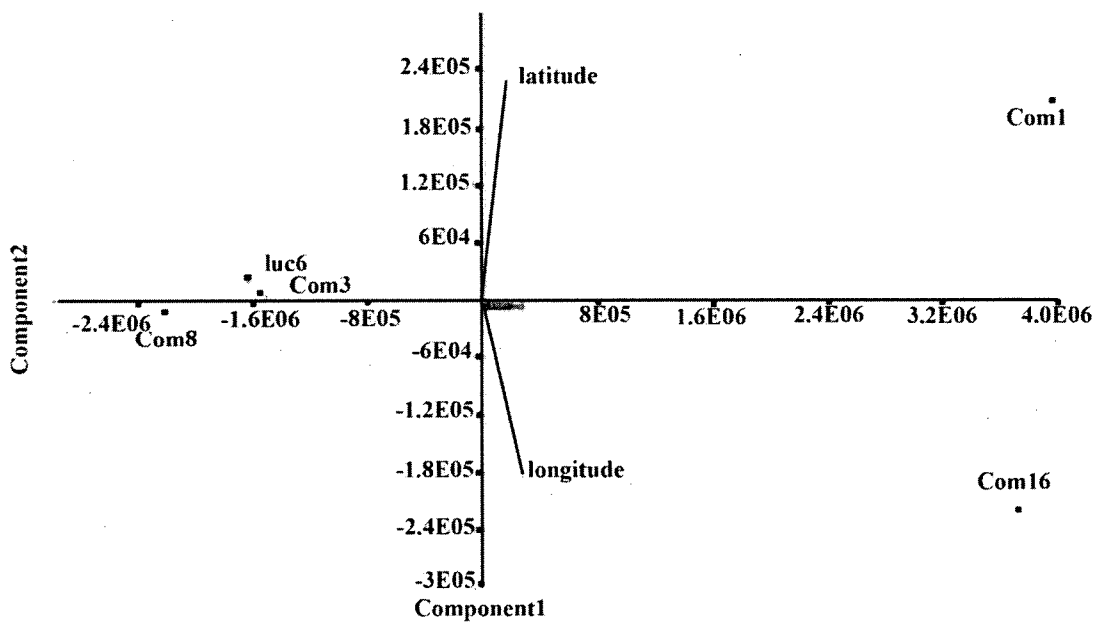

Figure 9. CCA plot of *Silene* species based on longitude and latitude for 2n=48 populations. Species abbreviations: luc 6 = *S. lucida*; com 16 and com 8 = Oshtorankuh, Alisadr populations of *S. commelinifolia* var. *commelinifolia;* com 1 and 3= Kivi, Bozqush populations of *S. cf commelinifolia*.

considered as a separate group. In PCA ordination diagram taxa are clearly separated (Fig. 6).

In populations of *ovatifolia* and *commelinifolia* varieties, two ploidy levels were observed. In *S. commelinifolia* var. *commelinifolia* populations a high karyotypic variation were observed due to two ploidy levels. CCA plot based on latitude and longitude for 2n = 2x = 24 accessions (Fig. 8) it was evident that longitude is efficient in *S. nurensis* separation and latitude in separation of Touchal population of *S. commelinifolia* var. *commelinifolia*. For 2n = 4x = 48 populations, PCA plot (Fig. 9) based on latitude and longitude Oshtorankuh population of *S. commelinifolia* var.

commelinifolia by longitude and Kivi population of *S. cf commelinifolia* by latitude was separated. In the correlation analysis of karyotypic features there was a significant positive correlation between L, S, TL and L/S.

Polyploidy is abundant in most perennial plants which result in adaptation of genomic variation. In *Silene* polyploidy has a great role in speciation and evolution of taxa (Sheidai et al. 2012; Gholipour and Sheidai 2010a, b; Sheidai et al. 2009a, b; Sheidai et al. 2008). Polyploidy is a way for stabilization of equilibrium polymorphism by an increase in heterozygosity. Polyploidy provides gene pool richness and can be used in environmental changes and evolution (Sheidai 2002).

B-chromosomes

Marmisho, Mazandaran, Darakeh, Oshtorankuh, Alisadr and Bozqush populations of *S. commelinifolia* has 0 to 3 B chromosomes (Fig. 4) which are recorded for the first time. B chromosomes are smaller than "A" chromosomes. Such subsidiary chromosomes are found in more than 1300 plant species (Camacho et al. 2000). Evidences showed the adaptive success of organisms with B chromosomes under stress condition. Plants with B chromosomes are more tolerant to dryness and environmental stresses than those lacking such chromosomes (Sheidai 2002).

Conclusion

In morphological results we found some efficient diagnostic features as was mentioned before for studied species and varieties separation. Based on PCA and PCO ordination diagrams of morphological character names of the specimens of Payame Nour University, Sari Branch Herbarium, Alzahra Herbarium and Shahid Beheshti University Herbarium were corrected. The position of Neor, Kivi and Bozqush populations were defined due to results of morphological and karyotype studies and seemed to be a new sub-species of *S. commelinifolia*. Kuh-e Khalil, Gilan, Miyaneh and Bozqush populations here referred to as *S.* cf. *lucida* seemed to be a new species of *Silene* for Iran but not exactly *S. lucida*. PCA & PCO ordination graphs and dendrograms provided by karyotype features indicated the clear separation of species and varieties.

Karyotype analysis of *S. commelinifolia* indicated that there are two ploidy levels in this species as 2n = 2x = 24 (which is in concordance with previous findings of Gholipour and Sheidai 2010a) and 2n = 4x = 48 which is recorded for the first time. B chromosome is recorded for the first time for this species in the world.

As there are two ploidy levels in each variety of *S. commelinifolia* a great morphological variation is also observed in these populations. Polyploidy has a great effect on the phenotype of the organism. Morphological and genomic differences between populations of these two varieties seemed to be more than variety here we propose further phylogenetic and molecular studies to clarify the rank of these taxa.

References

Atazadeh N (2013) Population divergence of *Silene commelinifolia* in Iran. MSc Thesis, University of Alzahra, Iran.

Bari EA (1973) Cytological studies in the genus *Silene* L. New Phytol 72:833-838.

Burleigh JG, Holtsford TP (2003) Molecular systematics of the eastern North American *Silene* (Caryophyllaceae): Evidence from nuclear ITS and chloroplast trnL intron sequences. Rhodora 105:76–90.

Camacho JPM, Sharbel TF, Beukeboom LW (2000) B- chromosome evolution. Phil Trans of the R Soc Lond, B 355:163-178.

Chowdhuri PK (1957) Studies in the genus *Silene*. Notes from the Royal Botanic Garden. Edinburgh 22:221-287.

Gholipour A, Sheidai M (2010c) A taxonomic study of *Silene goniocaula* complex in Iran. Rostaniha 11(1):83-86.

Gholipour A, Sheidai M (2010b) Further contribution to cytotaxonomy of the genus *Silene* L. (Sect. *Auriculatae*, Caryophyllaceae). Acta Biol Szeged 54:111-115.

Gholipour A, Sheidai M (2010a) Karyotype analysis and new chromosome number reports in *Silene* L. species (Sect. *Auriculatae*, Caryophyllaceae). Biologia 65:23-27.

Greuter W (1995) *Silene* (Caryophyllaceae) in Greece: A subgeneric and sectional classification. Taxon 44:543-581.

Heaslip MB (1951) Some cytological aspects in the evolution of certain species of the plant genus *Silene*. Ohio J Sci 51:62-70.

Levan A, Fredga K, Sandberg A (1964) Nomenclature for centromeric position on chromosomes. Hereditas 52:201- 220.

Markova M, Martina L, Zluvova J, Janousek B, Vyskot B (2006) Karyological analysis of an interspecific hybrid between the dioecious *Silene latifolia* and the hermaphroditic *Silene viscose*. Genome 42:373-379.

Melzheimer, V. 1988. Caryophyllaceae in: Flora Iranica, Rechinger, K. H. (ed.), AkademischeDruck-U. Verlagsanstalt, Graz-Austria 163:353-508.

Melzheimer V (1978) Notes on cytology of several species of the genus *Silene* (Caryophyllaceae) from central Greece and from Crete. Pl Syst Evol 130:203-207.

Oxelman B, Lidén M, Berglund D (1997) Chloroplast *rps*16 intron phylogeny of the tribe Sileneae (Caryophyllaceae). Pl Syst Evol 206:411–420.

Podani J (2000) Introduction to the Exploration of Multivariate Data. English translation. Backhuyes Publishers, Leiden, p. 407.

Romero-Zarco C (1986) A new method for estimating karyotype asymmetry. Taxon 35:526 530.

Sheidai M, Jalilian N (2008) Karyological studies of some species and populations of *Lotus* L. in Iran. Acta Bot Croat 67:42-52.

Sheidai M, Rashid S (2007) Cytogenetic study of some *Hordeum* L.species in Iran. Acta Biol Szeged 51:107-112.

Sheidai M (2002) Cytogenetic. Tehran, Adena publisher (in Persian).

Sheidai M, Nikoo M, Gholipour A (2008) Cytogenetic variability and new chromosome number reports in *Silene* L. species (Sect. *Lasiostemones*, Caryophyllaceae). Acta Biol Szeged 52(2):313-319.

Sheidai M, Enayatkhani M, Bahmani F, Gholipour A (2009a) Cytological study in the genus *Silene* (sec. Sclerocalycinae). Cytologia 74:437-442.

Sheidai M, Bahmani F, Enayatkhani M, Gholipour A (2009b) Contribution to cytotaxonomy of *Silene*: Chromosome pairing and unreduced pollen grain formation in sec. *Sclerocalycinae*. Acta Biol Szeged 53: 87-92.

Sheidai M, Gholipour A, Noormohammadi Z (2010) Species relationship in the genus *Silene* L. Section *Auriculatae* (Caryophyllaceae). Based on morphology and RAPD analysis. Acta Biol Szeged 54(1):25-31.

Sheidai M, Eftekharian R, Gholipour A, Noormohammadi Z (2012) Population Diversity and Polyploidy Incidence in 3 *Silene* Species. A Cytologi-

cal Approach. Cytologia 76(4):1-8.
Sopova M, Sekovski Z (1982) Chromosome atlas of some Macedonian angiosperms. III. Godishen Zbornik Bioloshki Fakultet na Univerzitetot Kiril i Metodij 35:145-161.
Stebbins GL (1971) Chromosomal Evolution in Higher Plants. Edward Arnold, London.
Swank GR (1932) The Ethnobotany of the Acoma and Laguna Indians. MA Thesis, University of New Mexico.
Zhang Y-x (1994) Studies on chromosomes of some plants from Guandi Mountain, Shanxi. J. Wuhan Bot Res 12(2):201-206.

Volume 58(1):39-43, 2014
Acta Biologica Szegediensis
http://www.sci.u-szeged.hu/ABS

ARTICLE

Optimal conditions of mycelial growth of three wild edible mushrooms from northern Thailand

Namphung Klomklung[1,2], Samantha C. Karunarathna[1,2], Kevin D. Hyde[1,2], Ekachai Chukeatirote[1,2]*

[1]School of Science, Mae Fah Luang University, Chiang Rai, Thailand; [2]Institute of Excellence in Fungal Research, Mae Fah Luang University, Chiang Rai, Thailand

ABSTRACT In this study, three wild mushrooms namely *Lentinus connatus*, *L. roseus*, and *Pleurotus giganteus* were selected to study if they could be domesticated. Initially, the fruiting bodies of the three mushrooms were collected from forests in northern Thailand and morphologically characterized. In this paper we report the optimal *in vitro* culture conditions of three wild mushrooms. Among seven culture media tested for the optimal mycelial growth of three wild mushrooms, black bean agar, red bean and soy bean agar were the best for the mycelial growth of *L. connatus*, *L. roseus* and *Pleurotus giganteus*, respectively. The mushroom mycelia were able to grow at temperatures ranging from 20-30 °C, with optimal growth temperatures of 30 °C and 25 °C for *Lentinus* and *Pleurotus* species, respectively. The optimum pH range observed for mycelial growth was 5.0 - 7.0. **Acta Biol Szeged 58(1):39-43 (2014)**

KEY WORDS

Lentinus connatus
Lentinus roseus
optimal growth
Pleurotus giganteus
wild mushroom

Generally, mushrooms are regarded as 'functional food' due to their nutritive value and medicinal properties (Barros et al. 2008). Mushrooms are rich in protein and dietary fiber; and they also contain some vitamins and minerals such as vitamin B, vitamin D, potassium and magnesium (Sanmee et al. 2003; Chang and Miles 2004). Several bioactive compounds are also found in mushrooms; for example, eritadenine (known as hypocholesterolemic agent) is found in *Lentinus edodes* (Enman et al. 2007) and bioactive compounds responsible for neurite stimulation can be found in *P. giganteus* (Phan et al. 2012). Glucosylceramide exhibiting antimicrobial activity is present in *Pleurotus citrinopileatus* (Meng et al. 2012). At present, 650-700 mushroom species belonging to 200 genera are known as edible but only about 130 mushroom species can be cultivated (Vargas-Isla and Ishikawa 2008; Mortimer et al. 2012). Many edible mushrooms are wild collected and only available for limited period (*i.e.*, in the raining season), whereas some edible mushrooms are ectomycorrhizal and impossible to domesticate (Sanmee et al. 2003). It is therefore interesting if the new saprobic edible wild mushrooms could be cultivated for commercial purpose as then they would be available all year round.

In 2011, three wild mushrooms namely *Pleurotus giganteus*, *Lentinus roseus*, and *L. connatus*, were collected from Chiang Mai, Thailand (Karunarathna et al. 2010; Karunarathna et al. 2011). The cultivation of *P. giganteus* has recently been reported in China and Malaysia (Phan et al. 2012), whereas cultivation in northern Thailand has been partially successful (Klomklung et al. 2012). In contrast, there are no reports on the cultivation of the two *Lentinus* species (*L. roseus* and *L. connatus*). The discovery of *L. roseus* is quite recent and thus there is not much information except its morphological and phylogenetic data (Karunarathna et al. 2010). *L. connatus* also occurs in the wild and only two reports describe its active compound (connatusin A) exhibiting antimalarial and cytotoxic activities (Rukachaisirikul et al. 2005). Due to limited data of growing *P. giganteus*, *L. roseus*, and *L. connatus* and their potential use as food and medicine, our aim was to further investigate optimal culture conditions for growing these three mushrooms. In this paper, an initial step was performed to determine favorable culture conditions for mycelial growth of *P. giganteus*, *L. connatus* and *L. roseus*.

Accepted July 4, 2014
*Corresponding author. E-mail: ekachai@mfu.ac.th

Materials and Methods

Isolation of mushroom samples

Mushroom samples used in this study are shown in Table 1. For isolating the fungal mycelia, the sterile internal fungal tissues of their fruiting bodies were isolated and placed on potato dextrose agar (PDA). The mycelial culture was then sub-cultured on PDA supplemented with 0.5% yeast extract and incubated at 30 °C until the agar surface was fully covered with the fungal white mycelium.

Effect of culture media

Several raw materials including *Phaseolus vulgaris* (red bean and black bean), *Phaseolus aureus* (mung bean), *Glycine max*

Table 1. Mushroom samples used in this study.

Mushrooms	Isolate No.	Collection site
Pleurotus giganteus	MFLU 10-0154	Chiang Mai
Lentinus connatus	MFLU 08-1389	Chiang Mai
Lentinus roseus	MFLU 08-1376	Chiang Mai

Table 2. Raw materials used for preparation of culture media.

Raw materials	Sources
Red bean (*Phaseolus vulgaris*)	Tesco-Lotus, Chiang Rai
Black bean (*Phaseolus vulgaris*)	Tesco-Lotus, Chiang Rai
Mung bean (*Phaseolus aureus*)	Tesco-Lotus, Chiang Rai
Soy bean (*Glycine max* L.)	Tesco-Lotus, Chiang Rai
Sorghum (*Sorghum bicolor* (L.) Moench)	Chiang Rai local market

L. (soybean), and *Sorghum bicolor* (L.) Moench (sorghum) were used in this study (Table 2). The modified agar media containing such raw materials were prepared as follows: 50 g of each grain were separately soaked in 250 ml distilled water for 12 hours or overnight and boiled for 30 min. These grains were grounded using mortar and pestle, and then filtered through clean cheesecloth. Twenty grams of agar was added to each grain filtrate and the media volume was adjusted to 1 L by adding distilled water. The media were then autoclaved at 15 psi, 121 °C for 15 min; 15 ml of each medium was poured into Petri dishes. Malt extract agar (Difco) and PDA (Criterion) were also used for comparative study of the mycelial growth. Fungal mycelium discs (5 mm in diameter) were used as inocula and transferred onto the center surface of each grain media. After 10 days of incubation at 30 °C, the mycelial growth, density, and growth rate of the three mushrooms were measured.

Effect of pH

To screen an optimal pH for the mycelial growth, a mycelial agar disc (5 mm in diameter) was transferred to soy bean agar, red bean agar and black bean agar for *P. giganteus*, *L. roseus*, and *L. connatus*. The pH of the media was adjusted to a pH range of 5-8 with 1 M NaOH or HCl. The plates were incubated at 30 °C for 12 days. The mycelial growth, density, and growth rate of the three mushrooms were measured.

Effect of temperature

Four different temperatures (20, 25, 30, and 35 °C) were used to find the optimum temperature for mycelial growth of three wild mushrooms. Mycelia discs (5 mm in diameter) were taken from the Petri dishes which were grown under suitable culture media and pH and then placed on the centre of a culture medium plate. Samples were incubated at four different temperatures for 10 days. The mycelial growth, density, and growth rate of the three mushrooms were measured.

Data collection and statistical analysis

A completely randomized design was used in this study. The data obtained for mycelial growth under different conditions were from five replicates. The results were expressed as means and variance. Means were also compared using Duncan's multiple range test by using SPSS-16 program.

Results and Discussion

Effect of culture media

Seven different culture media were used to screen the optimal mycelial growth of three wild mushrooms (Table 3). After 10 days of incubation, *P. giganteus* was able to grow equally well on mung bean agar, black bean agar, red bean agar, sorghum agar, and soy bean agar. On these media, the mushrooms grew best on soy bean agar with the growth rate of 12.59 ± 0.34 mm/day (Table 3). In contrast, *P. giganteus* did not grow well when grown on PDA and MEA. This result, however, was different from the result of Kumla et al. (2013), who reported that the best mycelial growth of *P. giganteus* was observed on PDA.

After one week of incubation, *L. connatus* showed a very good equal growth on mung bean agar, black bean agar, red bean agar, sorghum agar, and soy bean agar (Table 3). The best mycelial growth and density of *L. connatus* was observed on black bean agar with the growth rate of 13.99 ± 0.33 mm/day (Table 3). PDA and MEA also appeared to support its mycelial growth. This result is related to Gbolagade et al. (2006), who reported food materials such as yellow corn agar could support the mycelial growth of *Lentinus subnudus*.

After 8 days of incubation, *L. roseus* grew equally well on mung bean agar, black bean agar, red bean agar, and soy bean agar. The best mycelial growth and density showed on red bean agar with the growth rate of 11.73± 0.25 mm/day (Table 3). The least mycelial growth rate and density were found on MEA. This result is related to Fasola et al. (2007), who reported food grains such as Ife brown beans, wheat, white corn and yellow corn agar could support mycelial growth of *Volvariella speciosa*.

Carbon source, nitrogen source, minerals (such as phosphorus, potassium and magnesium) and vitamins (such as thiamin and biotin) are essential for mycelial growth of fungi (Chang and Miles 2004). Five raw materials were also containing carbon, nitrogen, mineral and vitamin for mycelial growth with different values (Berrios et al. 1999; Mubarak 2005; Habibullah et al. 2007; Rani et al. 2008; Sasanam et al. 2011; Liu et al. 2012). The result showed that the mushrooms could be grown in all the media at 30 °C. Thus, the effect of culture media on mycelial growth varies according to the mushroom species.

Table 3. Effect of culture media on mycelial growth rate (mm/day) of three wild mushrooms. Mycelial density was given in parentheses. Means followed by the same letters are not significantly different by Duncan's multiple range test ($P<0.05$). + very scanty, 2+ scanty, 3+ moderate, 4+ abundant, 5+ very abundant.

Mushrooms	Mung bean agar	Black bean agar	Red bean agar	Sorghum agar
Pleurotus giganteus	10.76 ± 0.25^{b} (+4)	11.96 ± 0.41^{c} (+3)	10.66 ± 0.28^{b} (+2)	12.59 ± 0.38^{d} (+)
Lentinus connatus	13.02 ± 0.27^{e} (+3)	13.99 ± 0.33^{f} (+4)	11.39 ± 0.54^{c} (+4)	12.49 ± 0.28^{d} (+)
Lentinus roseus	10.43 ± 0.25^{d} (+4)	10.89 ± 0.38^{e} (+4)	11.7 3± 0.25^{f} (+5)	7.99 ± 0.16^{b} (+)

Mushrooms	Soy bean agar	MEA	PDA
Pleurotus giganteus	12.59 ± 0.34^{d} (+4)	4.69 ± 0.37^{a} (+4)	4.26 ± 0.34^{a} (+)
Lentinus connatus	10.89 ± 0.22^{b} (+2)	10.26 ± 0.36^{a} (+3)	11.43 ± 0.38^{c} (+4)
Lentinus roseus	10.69 ± 0.39^{de} (+4)	5.93 ± 0.14^{a} (+3)	8.73 ± 0.27^{c} (+5)

MEA = malt extract agar, PDA = potato dextrose agar.

Table 4. Effect of pH on mycelial growth rate (mm/day) of three wild mushrooms. Mycelial density was given in parentheses. Means followed by the same letters are not significantly different by Duncan's multiple range test ($P<0.05$). + very scanty, 2+ scanty, 3+ moderate, 4+ abundant, 5+ very abundant.

Mushrooms	5.0	5.5	6.0	6.5
Pleurotus giganteus	10.20 ± 0.41^{c} (+4)	9.36 ± 0.24^{b} (+4)	9.96 ± 0.24^{c} (+4)	9.63 ± 0.31^{b} (+4)
Lentinus connatus	10.89 ± 0.25^{c} (+4)	12.76 ±0.19^{d} (+4)	10.86 ± 0.24^{c} (+4)	9.76 ±0.34^{b} (+4)
Lentinus roseus	7.13 ± 0.31^{a} (+5)	8.43 ± 0.14^{c} (+5)	7.96 ± 0.24^{b} (+5)	7.93 ±0.36^{b} (+5)

Mushrooms	7.0	7.5	8.0
Pleurotus giganteus	8.22 ± 0.36^{a} (+4)	8.29 ± 0.39^{a} (+4)	8.49 ± 0.33^{a} (+4)
Lentinus connatus	9.76 ± 0.38^{b} (+4)	9.26 ±0.41^{a} (+4)	9.26 ± 0.43^{a} (+4)
Lentinus roseus	8.36 ± 0.29^{c} (+5)	8.09 ± 0.32^{bc} (+5)	6.83 ± 0.23^{a} (+5)

Table 5. Effect of temperature on mycelial growth rate (mm/day) of three wild mushrooms. Mycelial density was given in parentheses. Means followed by the same letters are not significantly different by Duncan's multiple range test ($P<0.05$). + very scanty, 2+ scanty, 3+ moderate, 4+ abundant, 5+ very abundant.

Mushrooms	Temperature (°C)			
	20	25	30	35
Pleurotus giganteus	5.93 ± 0.25^{b} (+3)	9.66 ± 0.23^{d} (+4)	6.33 ± 0.31^{c} (+5)	0.00 ±0.00^{a}
Lentinus connatus	2.69 ± 0.21^{b} (+4)	8.39 ± 0.40^{c} (+4)	10.89 ± 0.19^{d} (+4)	0.00 ± 0.00^{a}
Lentinus roseus	13.25 ± 0.46^{b} (+5)	13.50 ± 0.25^{b} (+4)	14.15 ± 0.28^{c} (+4)	0.00 ± 0.00^{a}

Effect of pH

The effects of pH on mycelial growth of three wild mushrooms are shown in Table 4. The results showed that, these mushrooms grew fairly well in acidic, neutral and alkaline environments (pH 5.0-8.0). The best mycelial growth and density of *P. giganteus* were observed in acidic media of pH 5.0-6.5. This result is related to the result of Kumla et al. (2013), who reported that the optimal pH for the mycelial growth of *P. giganteus* is at pH 7 but it normally grows well at pH range of 4-9.

The best mycelial growth and density of *L. connatus* and *L. roseus* were obtained in slightly acidic to neutral pH ranges from pH 5.0-7.0 (Table 4). These results are related to Gbolagade et al. (2006), who reported that pH range from 4.0-8.0 could support the mycelial growth of *Lentinus subnudus* and the acidic medium (pH 5.0-5.5) is the best for mycelial growth.

The effect of pH is very important when choosing the substrate for mushroom cultivation because the substrate could be a buffer to control the pH (Chang and Quimio 1982).

Generally, calcium carbonate is used in mushroom cultivation to control pH of the medium (Change and Quimio 1982).

Effect of temperature

The results were obtained when three wild mushrooms were under four different temperatures from 20-35 °C (Table 5). The result showed that the three mushrooms were able to grow at a temperature range of 20-30 °C, however, they did not grow at 35 °C. The statistical analysis of *P. giganteus* showed that 25 °C was the best temperature for mycelial growth with the growth rate of 9.66 ± 0.23 mm/day (Table 5). This result is related to Kumla et al. (2013), who reported that the best temperature for mycelial growth of mushrooms is 25 °C.

The best temperature for mycelial growth of *L. connatus* on black bean agar was observed at 30 °C with the growth rate of 10.89 ± 0.19 mm/day (Table 5). *L. roseus* was able to grow well at a temperature range of 20-30 °C. The best mycelial growth and density of *L. roseus* occurred at 30 °C with the growth rate of 14.15± 0.28 mm/day (Table 5). This result is related to Gbolagade et al. (2006) who reported that the most suitable temperature for mycelial growth of *Lentinus subnudus* is 30 °C.

Three wild mushrooms in this study were collected in the tropic region and the results showed that the temperature for mycelial growth of *P. giganteus* was 25 °C and those of the two *Lentinus* were 30°C. Temperature is one of the most important and critical physical factors affecting mycelial growth in mushroom cultivation (Chang and Miles 2004). The optimum temperature is very important for growth, production of metabolic products and sporulation of mushrooms (Chang and Miles 2004). Increasing temperature generally accelerates enzymatic activity but high temperatures can make enzymes inactive which affect the metabolism and growth of mushrooms (Chang and Miles 2004). Several studies have shown that *Pleurotus* and *Lentinus* species could be grown at 25 °C or higher temperatures (45 °C) (Chang and Quimio 1982; Gbolagade et al. 2006; Vargas-Isla and Ishikawa 2008).

Conclusion

In this study, attempts were made to investigate the effect of raw materials (*i.e.*, red bean, black bean, mung bean, soybean, and sorghum), pH, and temperature on the mycelial growth of *P. giganteus*, *L. roseus* and *L. connatus* species. Our results showed that the best mycelial growth can be obtained on black bean agar and red bean agar for *L. connatus* and *L. roseus*, respectively, and both species grew well within a pH range of 5.0-8.0 (optimum 5.5-6.0) and their optimal temperature was 30 °C. The optimal growth of *P. giganteus* was obtained on soybean agar within a pH range of 5.0-6.5 and the optimal temperature of 30 °C. Since almost no researches have been done on growing *L. connatus* and *L. roseus*, these results will be a base for the future domestication research.

Acknowledgement

We are grateful to Thailand Research Fund (BRG 5580009); the National Research Council of Thailand (NRCT/55201020007), and Mae Fah Luang University (MFU 54101020048) for providing financial support for this study.

References

Barros L, Cruz T, Baptista P, Estevinho LM, Ferreira ICFR (2008) Wild and commercial mushrooms as source of nutrients and nutraceuticals. Food Chem Toxicol 46:2742-2747.

Berrios JDJ, Swanson BG, Cheong WA (1999) Physico-chemical characterization of stored black beans (*Phaseolus vulgaris* L.). Food Res Int 32:669-676.

Chang ST, Miles PG (2004) Mushrooms: cultivation, nutritional value, medicinal effect, and environmental impact. 2nd ed., CRC Press, Boca Raton, FL.

Chang ST, Quimio TH (1982) Tropical mushroom: biological nature and cultivation method. The Chinese University Press, Shatin New Town.

Enman J, Rova U, Berglund KA (2007) Quantification of the bioactive compound eritadenine in selected strains of shiitake mushroom (*Lentinus edodes*). J Agr Food Chem 55:1177-1180.

Fasola TR, Gbolagade JS, Fasidi IO (2007) Nutritional requirements of *Volvariella speciosa* (Fr. Ex. Fr.) Sanger, a Nigerian edible mushroom. Food Chem 100:904-908

Gbolagade JS, Fasidi IO, Ajayi EJ, Sobowale AA (2006). Effect of physicchemical factors and semi-synthetic media on vegetative growth of *Lentinus subnudus* (Berk.), an edible mushroom from Nigeria. Food Chem 99:742-747.

Habibullah, Abbas M, Shah HU (2007). Proximate and mineral composition of mung bean. Sarhad J Agr 23:463-466.

Karunarathna SC, Yang ZL, Raspe O, Ko Ko TW, Vellinga EC, Zhao R, Bahkali AH, Chukeatirote E, Degreef J, Callac P, Hyde KD (2011) *Lentinus giganteus* revisited: new collections from Sri Lanka and Thailand. Mycotaxon 118:57-71.

Karunarathna SC, Yang ZL, Zhao R, Vellinga EC, Bahkali AH, Chukeatirote E, Hyde KD (2010) Three new species of *Lentinus* from northern Thailand. Mycol Prog 10:389-398.

Klomklung N, Karunarathna SC, Chukeatirote E, Hyde KD (2012) Domestication of wild strain of *Pleurotus giganteus*. Sydowia 64:39-53.

Kumla J, Suwannarach N, Jaiyasen A, Bussaban B, Lumyong S (2013) Development of an edible wild strain of Thai oyster mushroom for economic mushroom production. Chiang Mai J Sci 40:161-172.

Liu YT, Sun J, Luo ZY, Rao SQ, Su YJ, Xu RR, Yang YJ (2012) Chemical composition of five wild edible mushrooms collected from Southwest China and their antihyperglycemic and antioxidant activity. Food Chem Toxicol 50:1238-1244.

Meng T, Ishikawa H, Shimizu K, Ohga S, Kondo R (2012) A glucosylceramide with antimicrobial activity from the edible mushroom *Pleurotus citrinopileatus*. J Wood Sci 58:81-86.

Mortimer PE, Karunarathna SC, Li Q, Gui H, Yang X, Yang X, He J, Ye L, Guo J, Li H, Sysouphanthong P, Zhou D, Xu J, Hyde KD (2012) Prized edible Asian mushrooms: ecology, conservation and sustainability. Fungal Divers 56:31-47.

Mubarak AE (2005) Nutritional composition and antinutritional factors of mung bean seeds (*Phaseolus aureus*) as affected by some home traditional processes. Food Chem 89:489-495.

Phan C, Wong W, David P, Naidu M, Sabaratnam V (2012) *Pleurotus giganteus* (Berk.) Karunarathna & K.D. Hyde: nutritional value and *in vitro* neurite outgrowth activity in rat pheochromocytoma cells. BMC Complem Altern M 12:102.

Rani V, Grewal RB, Khetarpaul N (2008) Physical characteristics, proximate and mineral composition of some new varieties of soybean (*Glycine max*

L.). Legume Res 31:31-35.
Rukachaisirikul V, Tansakul C, Saithong S, Pakawatchai C, Isaka M, Suvannakad R (2005). Hirsutane sesquiterpenes from the fungus *Lentinus connatus* BCC 8996. J Nat Prod 68:1674-1676.
Sanmee R, Dell B, Lumyong P, Izumori K, Lumyoung S (2003) Nutritive value of popular wild edible mushrooms from northern Thailand. Food Chem 82:527-532.
Sasanam S, Paseephol T, Moongngarm A (2011) Comparison of proximate compositions, resistant starch content, and pasting properties of different colored cowpeas (*Vigna unguiculata*) and red kidney bean (*Phaseolus vulgaris*). World Acad Sci Eng Technol 81:525-529.
Vargas-Isla R, Ishikawa NK (2008) Optimal conditions of *in vitro* mycelial growth of *Lentinus strigosus*, an edible mushroom isolated in Brazilian Amazon. Mycoscience 49:215-219.

Volume 58(1):45-48, 2014
Acta Biologica Szegediensis
http://www.sci.u-szeged.hu/ABS

ARTICLE

Effects of food processing technology on valuable compounds in elderberry (*Sambucus nigra* L.) varieties

Lilla Szalóki-Dorkó[1,2], Fleur Légrádi[1], László Abrankó[3], Mónika Stéger-Máté[1]*

[1]Department of Food Preservation, Faculty of Food Science, Corvinus University of Budapest, Budapest, Hungary,
[2]Department of Applied Chemistry, Faculty of Food Science, Corvinus University of Budapest, Budapest, Hungary,
[3]Institute of Organic Chemistry, Research Centre of Natural Sciences, Hungarian Academy of Sciences, Budapest, Hungary

ABSTRACT Elderberry (*Sambucus nigra* L.) is a potential source of natural food colorants because of its high anthocyanin content. The aim of this work is to reveal which technology step has effect on the valuable components (total anthocyanins, total polyphenols) and on the color parameters in elderberry and in this regard to determine possible differences between elderberry varieties. Based on experiment results concentrate production steps have great effects on the studied parameters in case of two varieties especially in the heating and microfiltration steps but in different ratio. Polyphenolic compounds in 'Samocco' are more stable during the juice production than 'Haschberg'. Color stability test revealed that in case of colored samples 'Samocco' had stronger color intensity in the foods/ models. These differences should be taken into account when selecting a certain variety for industrial utilization.
Acta Biol Szeged 58(1):45-48 (2014)

KEY WORDS

food colorant
technological steps
anthocyanin
polyphenol
color stability

The study of natural colorants is an extensive and active area of investigation since the synthetic colorants have recently been associated with adverse effects in humans. As a result, food producers are trying to replace their synthetic food coloring agents with natural food colorants. There are several permitted pigments in food industry derived from natural sources, which may be used for food coloration. Among them, anthocyanins demonstrate a high potential to be used as natural food colorants due to their attractive orange, red and purple colors and water solubility that allows their incorporation into aqueous food system (Lee and Finn 2007; Del Caro and Piga 2008). Elderberry is a potential source of natural food colorants because of its high amount of anthocyanins and its "easy-to-grow" characteristics. Elderberry pigments are made up of only cyanidin glycosides, from which cyanidin-3-*O*-glucoside and cyanidin-3-*O*-sambubioside are the major ones (Dawidowicz et al. 2006). Apart from them, cyanidin-3-*O*-sambubioside-5-*O*-glucoside and cyanidin-3,5-*O*-diglucoside were detected as minor compounds (Hong and Wrolstad 1990). These natural food colorants are generally used in the form of powder, concentrate or extract during food-industrial processes. Hence, the composition of these products is also influenced by the steps of preparing method (pressing, enzymatic treatment, heat treatment etc.). Most of the studies concern the characterization and analysis of these compounds in raw materials before their processing; however, in our experiments, changes in anthocyanin and polyphenol content and color parameters were investigated during juice production technology at the laboratory circumstances in case of two elderberry varieties.

Accepted July 6, 2014
*Corresponding author. E-mail: monika.stegernemate@uni-corvinus.hu

Materials and Methods

Materials

Elderberry fruit samples were harvested in 2012 from Nagyvenyim in Hungary. After the harvest they were processed within 2 hours. One Austrian variety, Haschberg and one Danish variety, Samocco were investigated in our research. 'Haschberg' is the leading European variety and the only Hungarian state-recognized breed. According to our preliminary maturity investigations, 'Samocco' has higher anthocyanin content than the other Danish elderberries grown in Hungary (Szalóki-Dorkó et al. 2013).

Methanol and hydrochloric acid (VWR International Ltd.) were used for extraction and dilution of the samples. Pectinex BE XXL pectolytic enzyme (Novozyme) was used for the treatment of elderberry fruits. Bentonite and ErbiGel were purchased from Kerttrade Ltd. to clarify the juice.

Methods

Production of elderberry concentrate

Concentrates of elderberries were prepared under laboratory condition according to the industrial practice using the steps presented in Figure 1.

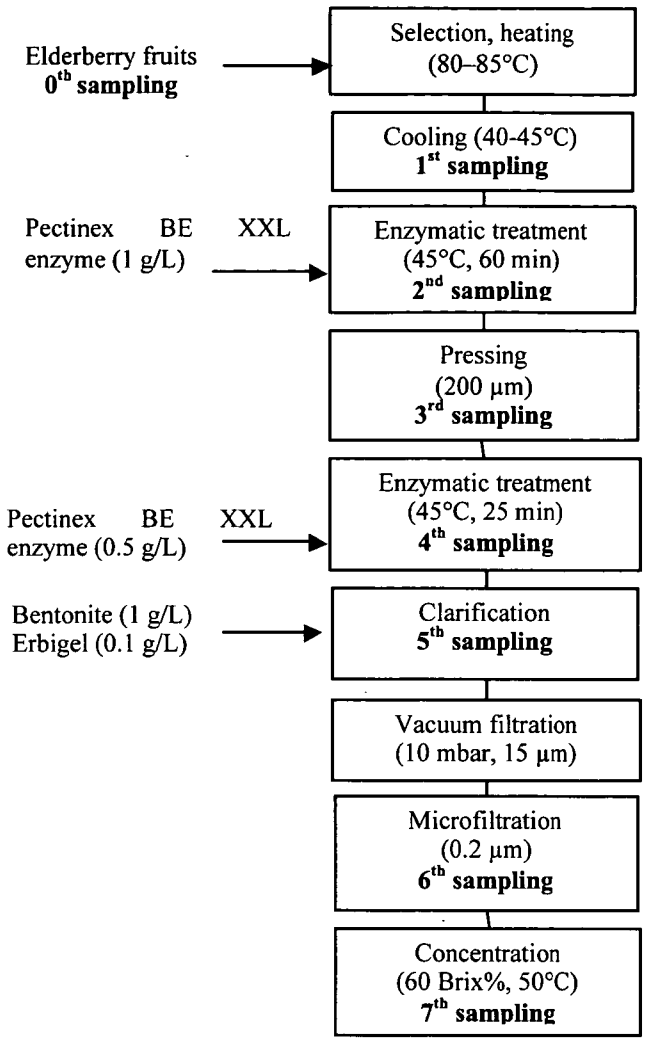

Figure 1. Food technological steps for production of elderberry concentrates.

Sample extraction

After homogenization by commercial food mixer, an amount of 2.5 g sample was weighed into an Falcon-tube and 20 mL of 60.9% aqueous methanol containing 0.1% hydrochloric acid was added. Samples were extracted for 30 min in an ultrasonic bath. After extraction, the treated samples were centrifuged at 4000 rpm for 8 min at room temperature and the supernatant was examined for their total anthocyanin and polyphenol content.

Analytical methods

Total anthocyanin content was determined by the method of Füleki and Francis (1968). The absorbance (A) of samples was measured at 530 nm with U-2000A Hitachi spectrophotometer. The content of total anthocyanins was expressed in mg cyanidin equivalents (CGE) per L of elderberry samples.

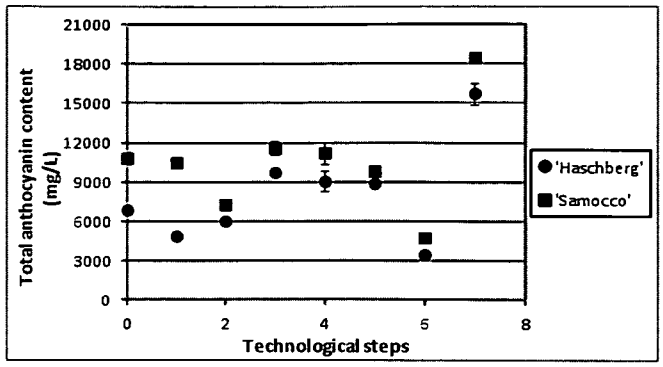

Figure 2. Total anthocyanin content during food technology in two elderberry varieties.

Total anthocyanin (TA) content was calculated by the following equation: TA (mg CGE/L)= A ×15 ×dilution. Color parameters were measured by digital colorimeter (Konica Minolta CR 410) during which L* (lightness factor), a* (red-green value) and b* (blue-yellow value) parameters were recorded. The most informative values of the color ability of elderberries are a* because of its red tone and b* because of its blue tone. Total polyphenol content was determined spectrophotometrically according to the method of Singleton and Rossi (1965) at 765 nm, and was calculated after calibration with gallic acid.

Color stability test

Water, natural yoghurt and jam and juice model samples were used to perform color stability tests. Jam and juice samples were modeled with 60 m/m% and 10 m/m% sugar solutions, respectively. For juice models, sugar solution was supplemented with citric acid to maintain the acidic conditions. After preparation, equal amount of 'Haschberg' and 'Samocco' concentrates were added to the samples and color parameters were measured as described above.

Statistical analysis

T-test was used to analyze the data derived from total anthocyanin and color parameter measurements. Differences were considered statistically significant when $P<0.05$. All measurements were done in three replicates and standard deviations of mean values were also calculated. Statistical analyses were performed using Statistica 9 (StatSoft Inc., Tulsa, USA) software.

Results and Discussion

Concentrate production steps have affected the concentration of total anthocyanin in both elderberry varieties (Fig. 2). The highest pigment content was detected in concentrate form of 'Samocco' (18472 mg CGE/L), and the lowest was in

Table 1. P values between technology steps in total anthocyanin content in case of two elderberry varieties.

Technology steps	P values Haschberg	Samocco
0-1	0.001*	0.339
1-2	0.006*	0.000*
2-3	0.000*	0.000*
3-4	0.233	0.558
4-5	0.736	0.055
5-6	0.000*	0.000*
6-7	0.000*	0.000*

*representing significant differences in anthocyanin content between technology steps (P <0.05)

'Haschberg' (4768 mg CGE/L) after microfiltration step (6th section). There are several technological steps which reduced the total anthocyanin content: cooling after heating (1st step), enzymatic treatment (2nd and 4th steps), clarification (5th step) and filtration (6th step). Thermal degradation of natural pigment in elderberry is a well-known phenomenon (Sadilova et al. 2006). In our study, elderberry varieties had different heat sensitivity since about 4% reduction could be observed by 'Samocco', while about 29% by 'Haschberg'. Clarification and filtration steps bound and kept back anthocyanin compounds during technology presumably which results the reduction of pigment concentration. This result is in contrast with the black carrot juice because bentonite treatment caused 20% increase in monomeric anthocyanin content (Turkyılmaz et al. 2012). Increase in anthocyanin content could be observed during the first enzymatic treatment by the variety of 'Haschberg', which is in contrast to that detected by 'Samocco'. It is probably due to the different pectin composition and anthocyanin profile of varieties. Pigment concentration was increased due to the effect of pressing (3rd step) because the molecules were liberated from the shells of berries. The samples were concentrated by evaporation and in this way the highest pigment content ('Haschberg' 15744 mg CGE/L; 'Samocco' 18472 mg CGE/L) was presented per unit volume. Before processing 'Samocco' contained higher pigment content (10808 mg CGE/L) than 'Haschberg' (6880 mg CGE/L) which is in contrast to the results of Kaack et al. (2008). This difference did not change during the whole experiment. They documented a maturity test in which 'Haschberg' has higher anthocyanin content than 'Samocco' in Denmark. This difference may arise from the different climate and different pomological technology of the two countries. The differences in total anthocyanin content between the two elderberry varieties were not significant (P>0.05) during the whole technology, but during some technological steps, significant differences were observed (Table 1).

The total polyphenol content (Fig. 3) of elderberry varieties did not change equally during the process. The samples reached the maximum values in concentrate form ('Haschberg' 20995 mg/L, 'Samocco' 23764 mg/L) and the minimum value can be found after the microfiltration step ('Haschberg' 1179 mg/L, 'Samocco' 4862 mg/L). Increase in polyphenol content could be detected after the 2nd enzymatic treatment (ca. 7%) and juice clarification (ca. 2.3%) by 'Samocco', while reduction occurred in case of 'Haschberg' (ca. 2% and 11%). Nevertheless, polyphenolic components of 'Samocco' were more stable during pressing, 2nd enzymatic treatment and juice clarification than 'Haschberg', which had reduced polyphenol content after these three technological steps. Filtration (6th step) and evaporation (7th step) sections influenced the polyphenol concentration similarly to that can be observed at anthocyanins.

In color parameter tests, the red-green ratio decreased during the processing. However, after concentration, a slight increase could be observed by the values of 'Haschberg' elderberry variety (Fig. 4). Despite the lower anthocyanin content, 'Haschberg' concentrate showed higher a* value (0.58) than 'Samocco' (0.01); however, this difference is not visible to the naked eye. Anyway, the initial red-green ratio

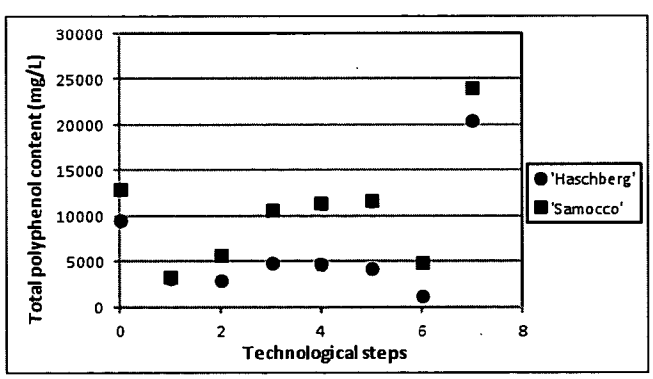

Figure 3. Total polyphenol content during food technology.

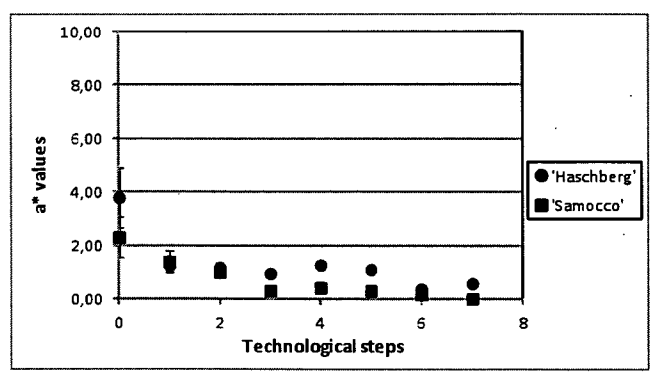

Figure 4. The a* values during food technology in case of two elderberry varieties.

Table 2. Color parameters of samples colored by elderberry concentrates.

Samples	Amount of concentrates (g)	Haschberg			Samocco		
		L*	a*	b*	L*	a*	b*
Water	1	22.40 ± 0.22	11.73 ± 0.53	3.21 ± 0.14	19.60 ± 0.20	6.58 ± 0.38	2.32 ± 0.04
Natural yoghurt	0.5	61.41 ± 0.08	14.88 ± 0.05	0.10 ± 0.03	60.21 ± 0.18	14.86 ± 0.09	0.15 ±0.02
Jam model	1	24.53 ± 1.87	17.67 ± 2.32	8.09 ± 1.45	23.93 ± 2.37	16.32 ± 2.03	6.47 ± 2.30
Juice model	1	24.24 ± 1.03	19.61 ± 1.71	9.15 ± 1.12	23.22 ± 1.62	14.79 ± 1.52	5.60 ±0.86

Average values of three replicates (n=3) ± standard errors are presented.

Table 3. P values between coloring samples in color parameters in case of two elderberry varieties.

Samples	P values		
	L*	a*	b*
Water	0.000	0.000	0.000
Natural yogurt	0.000	0.635	0.000
Jam model	0.669	0.355	0.100
Juice model	0.284	0.001	0.000

had decreased with ca. 85% and ca. 95% by 'Haschberg' and 'Samocco', respectively, during technological processing.

The color stability test revealed that 'Samocco' caused stronger color intensity in the foods/models than 'Haschberg' samples (Table 2). This is presumably due to the instability of anthocyanin compounds because their stability is highly variable depending on their structure and the composition of the food matrix (Wrolstad 2000).'Samocco' concentrate had darker blue color in water and the jam / juice models, namely, 'Haschberg' concentrates had higher L*, a* and b* values in these samples. Except a* value of natural yoghurt and jam model, L* value of jam model and juice model ($P>0.05$), significant differences were observed between samples colored by the two different elderberry concentrates ($P< 0.05$) (Table 3.).

Conclusions

Elderberry fruit is predominantly used for food coloration and varieties with higher anthocyanin content are particularly suitable for commercial applications. Food colorants are usually added as concentrate; however, according to our results, total anthocyanin content, total polyphenol content and color parameters are influenced by the fruit-processing technological steps. 'Samocco', the new Danish elderberry variety had higher pigment concentration and color intensity than the variety of 'Haschberg' during processing steps. Food coloring tests revealed that Danish variety may cause darker blue color in certain foods; this property should be considered in industrial applications.

Acknowledgement

The authors acknowledge the financial help of TÁMOP 4.2.1/B-09/1/KMR-2010-0005 and OTKA-PD 100506 grants.

References

Dawidowicz AL, Wianowska D, Baraniak B (2006) The antioxidant properties of alcoholic extracts from *Sambucus nigra* L. (antioxidant properties of extracts). LWT-Food Sci Technol 39:308-315.

Del Caro A, Piga, A (2008) Polyphenol composition of peel and pulp of two Italian fresh fig fruits cultivars (*Ficus carica* L.). Eur Food Res Technol 226:715-719.

Füleki T, Francis FJ (1968) Quantitative methods for anthocyanins. : 3. Purification of cranberry anthocyanins. J Food Sci 33(3):266-274.

Hong V, Wrolstad RE (1990) Characterization of anthocyanin-containing colorants and fruit juices by HPLC/photodiode array detection. J Agric Food Chem 38:698-708.

Kaack K, Fretté XC, Christensen LP, Landbo AK, Meyer AS (2008) Selection of elderberry (*Sambucus nigra* L.) genotypes best suited for the preparation of juice. Eur Food Res Technol 226:843-855.

Lee J, Finn CE (2007) Anthocyanins and other polyphenolics in American elderberry (*Sambucus canadensis*) and European elderberry (*S. nigra*) cultivars. J Sci Food Agric 87:2665-2675.

Sadilova E, Stintzing FC, Carle R (2006) Thermal degradation of acylated and nonacyalted anthocyanins. J Food Sci 71:C504-C512.

Szalóki-Dorkó L, Stéger-Máté M, Abrankó L (2013) Variety dependent anthocyanin profiles of elderberry cultivars (*Sambucus nigra* L.). Food Science Conference 2013: Book of proceedings, Corvinus University of Budapest, Budapest, Hungary, pp. 226-229.

Singleton VL, Rossi JA (1965) Colorimetry of total phenolics with phosphomolybdic-phosphotungstic acid reagents. Am J Enol Vitic 16:144-158.

Turkyılmaz W, Yemis O, Özkan M (2012) Clarification and pasteurisation effects on monomeric anthocyanins and percent polymeric color of black carrot (*Daucus carota* L.) juice. Food Chem 134:1052-1058.

Wrolstad RE (2000) Anthocyanins. In Lauro GJ, Francis J, eds., Natural Food Colorants. Marcel Dekker. New York, pp. 237-252.

Volume 58(1):49-53, 2014
Acta Biologica Szegediensis
http://www.sci.u-szeged.hu/ABS

ARTICLE

Mycorrhizal colonization by *Tuber aestivum* has a negative effect on the vitality of oak and hazel seedlings

Torda Varga*, Zsolt Merényi, Zoltán Bratek, Ádám Solti

Department of Plant Physiology and Molecular Plant Biology, Eötvös Loránd University, Budapest, Hungary

ABSTRACT Ectomycorrhizal fungi have a great impact on the ecosystem in boreal and temperate regions, and it has commercial, silvicultural and crop importance as well. The summer truffle (*Tuber aestivum*), a common mycorrhizal partner of several trees, is a valuable ectomycorrhizal fungus since its fruit bodies (ascomata) are a popular and expensive product on the global markets. To understand the physiology and ecology of a natural forest or a plantation, the participants and relationships between them should be examined. Hence, the maximal quantum efficiency of photosystem II centers, that is vitality of half a year old oak (*Quercus robur*) and hazel (*Corylus avellana*) seedlings inoculated with summer truffle was measured. The relation between the vitality of the plants and the rate of colonization of the fungus was examined applying single and multiple linear regressions. In the case of the oak seedlings contamination of *Scleroderma* spp. morphotype colonization was observed. Negative relationship between rate of colonization and the vitality was detected in the case of hazel seedling and non-contaminated oak seedlings. Multiple linear regression analysis revealed that there is no effect of truffle and contaminant fungi together, but alone the truffle has a negative impact. Consequently, the *Scleroderma* ectomycorrhiza seemed to have a balancing effect on the negative impact of summer truffle.
Acta Biol Szeged 58(1):49-53 (2014)

KEY WORDS

chlorophyll a fluorescence induction
mycorrhiza
Tuber aestivum
Corylus avellana
Quercus robur

One of the most common interactions between plants and fungi are the mycorrhizal associations. In boreal and temperate forest regions, the ectomycorrhizal (ECM) fungi are the dominant mycorrhizal partners of trees (Smith and Read 2008). Basically, this association is widely accepted as a mutualistic relationship, in which the fungus, due to its very efficient nutrient uptake, provides water and nutrients for the plant partner and receives assimilates from the host (Peterson et al. 2004; Kirk et al. 2008; Smith and Read 2008). Nevertheless, ECM associations are not always truly mutualistic. At different stages in the life cycle of ECM fungi and depending on the environmental conditions, the same fungus can have saprotrophic, mutualistic, endophytic or necrotrophic stages (Nylund et al. 1982; Downes et al. 1992; Sen et al. 1999; Koide et al. 2011; Vaario et al. 2012; see Figure 2. in Hall et al. 2003 and Figure 1. in Brundrett 2004). As the impact of ECM fungi on the ecosystem is evident (Smith and Read 2008), the study of the physiological effects of ECM fungus species on different woody plant species has an emerging importance.

Several studies showed the positive effect of ECM on the vitality of land plants (Bougher et al. 1990; Muhsin and Zwiazek 2002; Corrêa et al. 2006; Danielsen and Polle 2014), where the vitality was indicated on a dry weight (e.g. Bougher et al. 1990), total chlorophyll content (e.g. Vodnik and Gogala 1994; Kraj and Grad 2013) or photosynthetic activity basis (e.g. Corrêa et al. 2006). The photosynthetic apparatus, especially the photosystem II (PSII) is very sensitive to environmental changes. Among others, both of nutrient deficiencies (Lippemeier et al. 2001), salinity stress (Chen et al. 2004), drought stress (Colom and Vazzana 2003) and pathogen attacks (Berger et al. 2007) decrease the maximum quantum efficiency of PSII. The direct reasons for the measureable decrease are the disturbances of the PSII acceptor side (Šetlík et al. 1990) and the inhibition of the Calvin-cycle (Takahashi and Murata 2005). Thus, photosynthetic activity is strongly related with the vitality of plants (Tsimilli-Michael and Strasser 2008; Baker 2008) and it is widely used in stress detection in plant physiology.

Summer truffle (*Tuber aestivum*) was shown to be associated with numerous temperate European and North-American tree species, such as *Quercus* spp., *Fagus sylvatica*, *Corylus avellana* and *Pinus* spp., *Castanea sativa* and *Carya illioinensis* (Chevalier and Frochot 1997; Wedén et al. 2009; Benucci et al. 2012). Host trees have commercial, silvicultural and crop importance, and the summer truffle as well. The summer truffle, in contrast to the Périgord black truffle (*Tuber melanosporum*), has a wide distribution and tolerates a broad range of climatic condition thus it is one of the most popular truffles (Hall et al. 2007; Benucci et al. 2011). In spite of the economic importance of this fungus, its biology

Accepted Sept 2, 2014
*Corresponding author. E-mail: varga.torda@gmail.com

Table. 1. The four datasets of the values of fluorescence induction measurements. Co dataset contains all measurements of *Corylus avellana* seedlings. The measurements of *Quercus robur* seedlings sorted into three dataset. QT dataset contains seedlings of *Quercus* with only *Tuber aestivum* mycorrhiza. QTC dataset contains seedlings of *Quercus* with *Tuber aestivum* and also contaminant fungi. QA dataset contains all oak seedlings, which is the sum of QT and QTC datasets.

	Hazel	Oak		
dataset abbreviation	Co	QT	QTC	QA
Tuber aestivum mycorrhiza	x	x	x	x
contaminant mycorrhiza			x	x
population size	27	33	48	81

is barely studied compared to other commercially valuable fungal taxa (e.g. *T. melanosporum, Agaricus bisporus*). Summer truffle was shown to increase the vitality of older sessile oak (*Quercus petraea*) plants on a chlorophyll *a* fluorescence induction based technique, the development of this relationship has been hardly known yet (Solti et al. 2011). Thus, we studied the effect of *T. aestivum* mycorrhizal colonization on the vitality of young oak and hazel seedlings.

Materials and Methods

Plant material

Certificated seedlings (Bach et al. 2010) were produced and nursed by Pannon Szarvasgomba Ltd. Co. Pedunculate oak (*Quercus robur*) and common hazel (*Corylus avellana*) seeds were germinated and grown in plastic pots containing sterile peat-perlit mixture. One month old seedlings were planted to other plastic pots filled with the same medium but compounded summer truffle (*Tuber aestivum*) propagules (spores and mycelium fragments) into it. Plants were kept in greenhouse under controlled humidity conditions. Measurements were performed five month after inoculation. The company provided us nine hazel seedlings (in average height of 32±6.8 cm and stem diameter of 5±0.7 mm) and thirty-one oak seedlings (average height of 61±6.3 cm and stem diameter of 7.8±0.8 mm) for the measurements. Among the oak seedlings, contamination by other mycorrhizal fungi was found, but in every cases *T. aestivum* mycorrhiza was present as well.

Chlorophyll a fluorescence induction

Depend on the number of leaves, two or three (in one case only one) healthy, well developed leaves per seedlings were chosen and measured. Fluorescence induction measurements were carried out with intact leaves using a PAM 101-102-103 Chlorophyll *a* Fluorometer (Walz, Effeltrich, Germany). Leaves were dark-adapted for 15 min. The F_o level of fluorescence was determined by switching on the measuring light (modulation frequency of 1.6 kHz and photosynthetic photon flux density (PPFD) less than 1 μmol m^{-2} s^{-1}) after 3 s illumination with far-red light in order to eliminate reduced electron carriers (Belkhodja et al. 1998). The maximum fluorescence yield, F_m, was measured by applying a 0.7 s pulse of white light (PPFD of 3500 μmol m^{-2} s^{-1}, light source: KL 1500 electronic, Schott, Mainz, Germany). The maximal efficiency of PSII centres were determined as $F_v/F_m = (F_m - F_o)/F_m$.

Measurement of fungus colonisation

After the chlorophyll *a* fluorescence induction measurements, roots were gently washed, and the root tips were visually examined under a stereomicroscope. The percentage of the colonization was estimated by a visual investigation on the whole root system of the individual seedlings. In the case of hazel seedlings the estimation was less precise than that of oak seedlings because of the more dense root branching system.

Statistical analysis

For statistical analysis we used separately the independent chlorophyll *a* fluorescence induction values and analyzed four dataset (Table 1): (1) hazel seedlings (*Coryllus*; Co dataset with 27 data); (2) all oak seedlings, (*Quercus* All; QA dataset with 81 data); (3) a subset of QA dataset where only *Tuber aestivum* mycorrhizae were presented (*Quercus Tuber*; QT dataset with 33 data); (4) a subset of QA dataset which contains only those trees that has contaminant fungi together with *Tuber aestivum* mycorrhiza (*Quercus Tuber* and *Contaminant*; QTC dataset with 48 data). We also checked the relationship between the height of the trees and vitality / rate of colonization. Because the water status of the trees strongly affects the stem diameter (Kanalas et al. 2009) it was found not accurate enough to involve into the analyses.

Relation between the vitality and the rate of colonization were analyzed applying single linear regression using ordinary least squares (OLS) method. In the case of QTC and QA datasets, multiple linear regressions were applied, where two explanatory variables were presented: percentage of *Tuber aestivum* colonization and percentage of contaminant fungi colonization. Significance level of $p = 0.05$ was used in all cases. The normality of variables / residuals and the variance homogeneity of residuals were checked on quantile-quantile plot and scale-location plot respectively. The influential points, detected according Cook's distance, were deleted and also the regression outliers were deleted at 99% confidence interval using externally studentized residuals. The analyses were performed with the statistical software R version 3.0.2. (R Core Team 2014).

Results

On hazel seedlings, the average *Tuber aestivum* colonization percentage was 12±7.5%, while that of on oak seedlings was

the double (24±13%). In the case of QTC dataset (Table 1.), the average percentage of contamination was 11±9.8%. Most of the contaminants were *Scleroderma* spp. morphotypes, but on three seedlings, *Tuber brumale* mycorrhiza and on four seedlings, *Tomentella* spp. morphotypes were also occurred. In both hazel and oak, the PSII maximum quantum efficiency was between 0.78 and 0.83. There was no correlation between the height of the trees and the vitality or the rate of the colonization.

All datasets were normally distributed and no tendencies were found in the variances of residuals. None of the datasets (Table 1.) contains influential points, while in the case of QA dataset four, and in the case of Co dataset one regression outliers were deleted. According the multiple linear regression of QA dataset, no significant common effect of *Tuber aestivum* and contaminant fungi was found, while *T. aestivum* explanatory variable had significant negative effect (p=0.027). The two subset of QA dataset also confirm this result. In the case of QT, *T. aestivum* has significant negative effect (p=0.034) (Fig. 1), while in the case of QTC, no significant common or single effect of *T. aestivum* and contaminant fungi were detected. In the case of hazel seedlings (Co dataset) a significant negative effect of mycorrhization was also found (p=0.005) (Fig. 2).

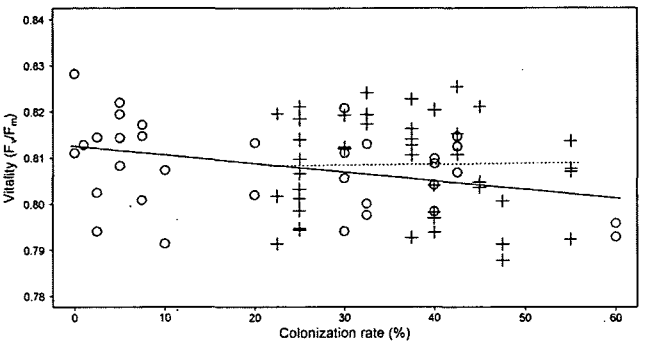

Figure 1. Relationship between the vitality of *Quercus robur* seedlings and rate of colonization of summer truffle. Crosses represent the QTC dataset and open circles represent the QT dataset (see Table 1.). Blank line is fitted to QT dataset, and dotted line is fitted to QTC dataset. In the case of QT dataset the summer truffle has a significant negative effect (p=0.034) on vitality of seedling. In the case of QTC dataset no common or single effects of summer truffle and contaminant mycorrhizal fungi were shown.

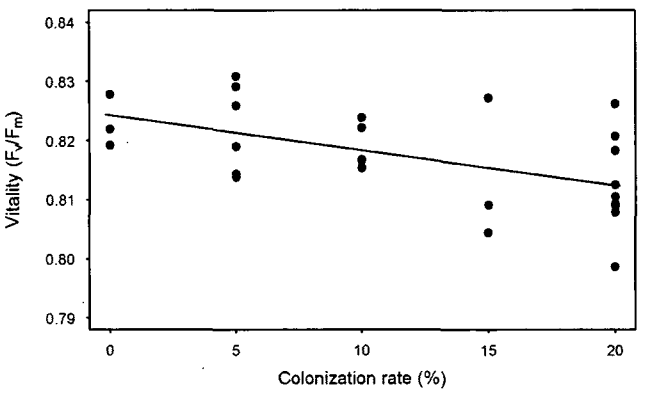

Figure 2. Relationship between the vitality of hazel seedlings and rate of colonization of summer truffle. Mycorrhizal colonization of summer truffle has a significant effect (p=0.005) on the vitality of seedlings.

Discussion

The *Tuber aestivum* mycorrhizal colonization had a significant negative effect on the vitality of seedlings, while the presence of other mycorrhizal fungi seems to fade this effect of summer truffle. Similar results were also shown under the colonization phase of mycorrhiza by other authors. Kraj and Grad (2013) found that mycorrhizal colonization had a negative effect on pigment content of *Pinus sylvestris*. Nevertheless, in a later stage, the pigment accumulation of inoculated plants was enhanced compared to non-inoculated plants. They also showed differences between the effects of different mycorrhizal fungi in respect to the beginning of their beneficial stadium. Colpaert et al. (1992) showed decrease of plant biomass and lower nitrogen content of mycorrhizal plants contrast to control. There is also an example for positive effect of colonized roots on plant dry weight, but no positive relation between the growth rate and the rate of colonization (Lu et al. 1998).

Previous studies have already showed the effect of ECM on green plants. However only just a few article deal with the fluorescence induction parameters of the photosystems. Corrêa et al. (2006) applied chlorophyll *a* fluorescence induction based methods to monitor the effect of *Pisolithus tinctorius* on *Pinus pinaster* vitality through the colonization process. They generally found that mycorrhizal colonization has negative effect on the vitality of plants, but the strength of this effect depends on the availability of the nitrogen source and the age of the plant at the time of inoculation. Solti et al. (2011) found a positive correlation (under 10% of colonization) or no correlation (above 10% of colonization) between the maximal quantum efficiency of PSII centers and summer truffle rate of colonization on *Quercus petraea*. They could observe this positive or no effect because they measured older seedlings.

In the present study, a balancing effect of *Scleroderma* mycorrhization was observed. This could be explained by the differentiation between the physiology of *Scleroderma* sp. and *Tuber aestivum*. *Scleroderma* spp. mycelium is a fast growing one in contrast to *T. aestivum*. The mycorrhiza of *Scleroderma* spp. is a long distance exploration type in contrast to the short distance exploration type that of *T. aestivum* (Agerer 2001, www.deemy.de). Additionally, mycorrhiza of the two species has evolved in two different ways. According the genome of *Tuber melanosporum* (Martin et al. 2010)

and *Laccaria bicolor* (Martin et al. 2008), ascomycetes and basidiomycetes have different 'symbiosis toolbox'. Ragnelli et al. (2013) showed programmed cell death in plant roots caused by ECM of *Tuber* spp., which could ascribe to their degrading enzymes. On one hand, the faster grow of mycelia of *Scleroderma* sp. can cause a faster colonization of the host plant, thus if *Scleroderma* sp. colonization has a negative effect this process could have elapsed and the mycorrhizal relationship may turns to beneficial. Because of the slower mycelia growth of summer truffle it may develop mycorrhiza only when *Scleroderma* sp. is already in its beneficial stage, so the negative effect of summer truffle could be faded by *Scleroderma* spp. On the other hand, exploration types can utilize different nitrogen sources (Hobbie and Agerer 2009), therefore different effects of the colonization rates and nitrogen metabolism may also affect the vitality of the host plant. The common occurrence of *T. aestivum* and *Scleroderma* spp. on Hungarian natural sites have been observed by truffle collectors, that is in dried years *Scleroderma* spp. produces fruit bodies, while in wet years *T. aestivum* has a bigger amount of yield. Furthermore, in the case of *T. melanosporum*, *Scleroderma verrucosum* seems to have neutral effect on truffle orchards (Sourzat 2011). Despite the negative effect of *T. aestivum*, the values of maximal quantum efficiency of PSII centres ranged between 0.78 and 0.83 which can be qualified as a non-stressed condition (Baker 2008).

In conclusion, colonization of *Tuber aestivum* ECM has a little, however measureable negative effect on young host trees. The negative effect might depend on the nutrition demand and acquisition of fungi, and the physiological condition of the plant.

Acknowledgements

This research has been supported by the MIKOQUAL project under the Ányos Jedlik Program and by the QUTAOMEL project under the National Technology Program of Hungary. We are grateful for the Pannon Szarvasgomba Ltd. Co. who provided the seedlings of this study.

References

Agerer R (2001) Exploration types of ectomycorrhizae. Mycorrhiza 11:107–114.

Baker NR (2008) Chlorophyll fluorescence: a probe of photosynthesis *in vivo*. Annu Rev Plant Biol 59:89–113.

Belkhodja R, Morales F, Quílez R, López-Millán AF, Abadía A, Abadía J (1998) Iron deficiency causes changes in chlorophyll fluorescence due to the reduction in the dark of the photosystem II acceptor side. Photosynth Res 56:265–276.

Benucci GMN, Raggi L, Albertini E, Grebenc T, Bencivenga M, Falcinelli M, Di Massimo G (2011) Ectomycorrhizal communities in a productive *Tuber aestivum* Vittad. orchard: composition, host influence and species replacement. FEMS Microbiol Ecol 76:170–84.

Benucci GMN, Bonito G, Baciarelli Falini L, Bencivenga M (2012) Mycorrhization of pecan trees (*Carya illinoinensis*) with commercial truffle species: *Tuber aestivum* Vittad. and *Tuber borchii* Vittad. Mycorrhiza 22:383–92.

Berger S, Benediktyová Z, Matou K, Bonfig K, Mueller MJ, Nedbal L, Roitsch T (2007) Visualization of dynamics of plant pathogen interaction by novel combination of chlorophyll fluorescence imaging and statistical analysis: differential effects of virulent and avirulent strains of *P. syringae* and of oxylipins on *A. thaliana*. J Exp Bot 58:797-806.

Bougher NL, Grove TS, Malajczuk N (1990) Growth and phosphorus acquisition of karri (*Eucalyptus diversicolor* F. Muell.) seedlings inoculated with ectomycorrhizal fungi in relation to phosphorus supply. New Phytol 114:77–85.

Brundrett M (2004) Diversity and classification of mycorrhizal associations. Biol Rev 79:473–495.

Chen H-X, Li W-J, An S-Z, Gao H-X (2004) Characterization of PSII photochemistry and thermostability in salt-treated *Rumex* leaves. J Plant Physiol 161:257–264.

Chevalier G, Frochot H (1997) La truffe de Bourgogne. Pétrarque, Levallois-Perret, France. ISBN: 2-911730-13-5.

Colom MR, Vazzana C (2003) Photosynthesis and PSII functionality of drought-resistant and drought-sensitive weeping lovegrass plants. Environ Exp Bot 49:135-144.

Colpaert JV, Assche JA, Luijtens K (1992) The growth of the extramatrical mycelium of ectomycorrhizal fungi and the growth response of *Pinus sylvestris* L. New Phytol 120:127–135.

Corrêa A, Strasser, RJ, Martins-Loução, MA (2006). Are mycorrhiza always beneficial? Plant Soil 279:65–73.

Danielsen L, Polle A (2014) Poplar nutrition under drought as affected by ectomycorrhizal colonization. *Environ Exp Bot* doi:10.1016/j.envexpbot.2014.01.006

Downes GM, Alexander IJ, Cairney JWG(1992) A study of ageing of spruce [*Picea sitchensis* (Bong.) Carr.] ectomycorrhizas. I. Morphological and cellular changes in mycorrhizas formed by *Tylospora fibrillosa* (Burt.) Donk and *Paxillus involutus* (Batsch. ex Fr.) Fr. New Phytol 122:141–152.

Hall IR, Yun W, Amicucci A (2003) Cultivation of edible ectomycorrhizal mushrooms. Trends Biotechnol 21:433–438.

Hall IR, Brown G, Zambonelli A (2007) Taming the truffle: The history, lore, and science of the ultimate mushroom. Timber Press, Portland, Or., USA, pp. 1–304.

Hobbie EA, Agerer R (2009) Nitrogen isotopes in ectomycorrhizal sporocarps correspond to belowground exploration types. Plant Soil 327:71–83.

Kanalas P, Oláh V, Szöll si E, Mészáros I, Ander I, Fenyvesi A (2009) Study of the sap-flow and related quantities of oak trees in field experiments. ATOMKI Annual Report 24, ISSN 0231-3596, CODEN AREAE9, p. 73.

Kirk PM, Cannon PF, Minter DW, Stalpers JA (2008) Dictionary of the fungi. CAB International, Wallingford, UK, 10th Edition, pp. 451-452.

Koide RT, Fernandez CW, Peoples MS (2011) Can ectomycorrhizal colonization of Pinus resinosa roots affect their decomposition? New Phytol 191:508–514.

Kraj W, Grad B (2013) Seasonal dynamics of photosynthetic pigment, protein and carbohydrate contents in *Pinus sylvestris* L. seedlings inoculated with *Hebeloma crustuliniforme* and *Laccaria bicolor*. J Plant Nutr 36:633–650.

Lippemeier S, Hintze R, Vanselow k, Hartig P, Colijn F (2001) In-line recording of PAM fluorescence of phytoplankton cultures as a new tool for studying effects of fluctuating nutrient supply on photosynthesis. Eur J Phycol 36:89-100.

Lu X, Malajczuk N, Dell B (1998) Mycorrhiza formation and growth of *Eucalyptus globulus* seedlings inoculated with spores of various ectomycorrhizal fungi. Mycorrhiza 8:81–86.

Martin, F, Aerts A, Ahrén D, Brun A, Danchin EGJ Duchaussoy F, Gibon J, Kohler A, Lindquist E, Pereda V, Salamov A, Shapiro HJ, Wuyts J, Blaudez D, Buée M, Brokstein P, Canbäck B, Cohen D, Courty PE, Coutinho PM, Delaruelle C, Detter JC, Deveau A, DiFazio S, Duplessis S, Fraissinet-Tachet L, Lucic E, Frey-Klett P, Fourrey C, Feussner I, Gay G, Grimwood J, Hoegger PJ, Jain P, Kilaru S, Labbé J, Lin YC, Legué V, Le Tacon F, Marmeisse R, Melayah D, Montanini B, Muratet M, Nehls

U, Niculita-Hirzel H, Oudot-Le Secq MP, Peter M, Quesneville H, Rajashekar B, Reich M, Rouhier N, Schmutz J, Yin T, Chalot M, Henrissat B, Kües U, Lucas S, Van de Peer Y, Podila GK, Polle A, Pukkila PJ, Richardson PM, Rouzé P, Sanders IR, Stajich JE, Tunlid A, Tuskan G, Grigoriev IV(2008) The genome of *Laccaria bicolor* provides insights into mycorrhizal symbiosis. Nature, 452:88–92.

Martin F, Kohler A, Murat C, Balestrini R, Coutinho PM, Jaillon O, Montanini B, Morin E, Noel B, Percudani R, Porcel B, Rubini A, Amicucci A, Amselem J, Anthouard V, Arcioni S, Artiguenave F, Aury JM, Ballario P, Bolchi A, Brenna A, Brun A, Buée M, Cantarel B, Chevalier G, Couloux A, Da Silva C, Denoeud F, Duplessis S, Ghignone S, Hilselberger B, Iotti M, Marçais B, Mello A, Miranda M, Pacioni G, Quesneville H, Riccioni C, Ruotolo R, Splivallo R, Stocchi V, Tisserant E, Viscomi AR, Zambonelli A, Zampieri E, Henrissat B, Lebrun MH, Paolocci F, Bonfante P, Ottonello S, Wincker P (2010) Périgord black truffle genome uncovers evolutionary origins and mechanisms of symbiosis. Nature, 464:1033–1038.

Muhsin TM, Zwiazek JJ (2002) Ectomycorrhizas increase apoplastic water transport and root hydraulic conductivity in *Ulmus americana* seedlings. New Phytol 153:153–158.

Nylund JE, Kasimir A, Arveby AS (1982) Cell wall penetration and papilla formation in senescent cortical cells during ectomycorrhiza synthesis *in vitro*. Physiol Plant Pathol 21:71-73.

Peterson RL, Massicotte HB, Melville LH (2004) Mycorrhizas: Anatomy and Cell Biology. NRC Research Press, Ottawa, Canada, pp. 1-173.

Ragnelli AM., Aimola P, Maione M, Zarivi O, Leonardi M, Pacioni G (2013) The cell death phenomenon during *Tuber* ectomycorrhiza morphogenesis. Plant Biosyst148:473–482.

R Core Team (2014) R: A language and environment for statistical computing. In: R Foundation for statistical computing. Vienna, Austria. http://www.R-project.org

Smith, SE, Read DJ (2008) Mycorrhizal symbiosis. Academic Press, London, UK, pp. 1–787.

Sen R, Hietala AM, Zelmer CD (1999). Common anastomosis and internal transcribed spacer RFLP groupings in binucleate *Rhizoctonia* isolates representing root endophytes of *Pinus sylvestris*, *Ceratorhiza* spp. from orchid mycorrhizas and a phytopathogenic anastomosis group. New Phytol 144:331–341.

Šetlík I, Allakhverdiev SI, Nedbal L, Šetlíková E, Klimov VV (1990) Three types of Photosystem II photoinactivation. Photosynth Res 23:39-48.

Solti Á, Tamaskó G, Lenk S, Barócsi A, Bratek Z (2011) Detection of the vitalization effect of *Tuber* mycorrhiza on sessile oak by the recently-innovated FMM chlorophyll fluorometer. Acta Biol Szeged 55:147–149.

Sourzat P (2011) Black truffe cultivation and competing fungi. In Savoie JM, Foulongne-Oriol M, Largeteau M, Barroso G eds, Proceedings of the 7th International Conference on Mushroom Biology and Mushroom Products. Arcachon, France, pp. 516–528.

Takahashi S, Murata N (2005) Interruption of the Calvin cycle inhibits the repair of Photosystem II from photodamage. Biochim Biophys Acta 1708:352–361.

Tsimilli-Michael M, Strasser RJ (2008) In vivo assessment of stress impact on plants' vitality: applications in detecting and evaluating the beneficial role of mycorrhization on host plants. In Varma A (ed.) Mycorrhiza: State of the Art, Genetics and Molecular Biology, Eco-Function, Biotechnology, Eco-Physiology, Structure and Systematics, 3rd ed. Springer, Berlin, Germany, pp. 679–703.

Vaario L-M, Heinonsalo J, Spetz P, Pennanen T, Heinonen J, Tervahauta A, Fritze H (2012) The ectomycorrhizal fungus *Tricholoma matsutake* is a facultative saprotroph in vitro. *Mycorrhiza 22*:409–418.

Vodnik D, Gogala N. (1994) Seasonal fluctuations of photosynthesis and its pigments in 1-year mycorrhized spruce seedlings. Mycorrhiza 4:277–281.

Wedén C, Pettersson L, Danell E (2009) Truffle cultivation in Sweden: Results from *Quercus robur* and *Corylus avellana* field trials on the island of Gotland. Scand J Forest Res 24: 37–53.

Volume 58(1):55-59, 2014
Acta Biologica Szegediensis
http://www.sci.u-szeged.hu/ABS

ARTICLE

Investigation of arbuscular mycorrhizal status and functionality by electrical impedance and capacitance measurement

Tünde Takács*, Anna Füzy, Kálmán Rajkai, Imre Cseresnyés

Institute for Soil Sciences and Agricultural Chemistry, Centre for Agricultural Research, Hungarian Academy of Sciences, Budapest, Hungary

ABSTRACT Applicability of electrical impedance (EI) and electrical capacitance (EC) measurement for the investigation of root colonization of mixed arbuscular mycorrhizal fungi (AMF) and functional diversity of separated AMF strains were studied in two pot experiments. In the first experiment, mycorrhizal and non-mycorrhizal maize cultivars were compared for testing the sensitivity of EI and EC measurement in relation to mycorrhizal status of host plants. In the second one, root colonization, biomass production, EI and EC of *Rhizophagus intraradices* or *Funneliformis mosseae,* inoculated and non-inoculated cucumber and bean hosts were monitored. The mycorrhizal plants showed lower EI and higher EC than control plants for each species. Since fungal colonization did not produce an increase in root surface area of maize, the higher root-soil interface showed by EI and EC values was undeniably due to the increased absorption surface area caused by the growth of AMF hyphae. As for cucumber and bean, the two selected AMF strains differed significantly in infectivity and effectivity, and the measured values also vary with host plants. Measuring EI and EC proved to be well applicable for *in situ* investigation of functional aspects of mycorrhizae. **Acta Biol Szeged 58(1):55-59 (2014)**

KEY WORDS

arbuscular mycorrhiza
functional diversity
electrical capacitance
electrical impedance
root-soil interface

Conventional root investigation methods are unsuitable for *in situ* monitoring of root growth and function (Čermák et al. 2006; Cao et al. 2010). Measurement of electrical impedance (EI – basically the resistance against alternating current) and electrical capacitance (EC – charge-storing ability of root membranes) in a plant–soil system can provide a rapid *in situ* assessment about root status without plant damaging. This method was developed by Chloupek (1972). By inserting an electrode at the plant stem and the other one into the soil, and connecting them by a capacitance meter (LCR-bridge), root EI and EC proved to be negatively and positively correlated, respectively, with root fresh or dry weight and root surface area. Since the theoretical background was described (Dalton 1995), the EI and EC method has been modified and optimized for the practice (Rajkai et al. 2005; Čermák et al. 2006; Cseresnyés et al. 2013).

The arbuscular mycorrhizal fungi (AMF) form important symbiotic associations with the roots of nearly all native and crop plants (Brundrett 2009). The plant provides the fungus with carbon compounds, and the fungus, in turn, is beneficial to the host plant by enhancing its capability for extracting water, macro- and micronutrients from the soil (Marschner 1997). The AMF colonization often induces root morphological changes in host plants: fungal infection can affect root mass, root length or root architecture (Kothari et al. 1990). It has been suggested that extraradical hyphae may enhance the total surface area of roots and fungus, conducing to an increase in the soil–plant interface (Augé 2004). AM fungi show different degrees of host compatibility, in terms of infectivity of isolates and effectivity of inoculation both.

Standard methods to assess AMF presence are based on investigation of fungal colonization in roots. In most cases, these techniques are destructive, time-consuming and information about AMF functionality is not provided. As root conductivity and permeability are reliable indicators for water uptake activity and absorptive root surface area (Aubrecht et al. 2006), we supposed that differences in root functionality induced by AMF colonization could be monitored by EI and EC measurement. In the present work, the applicability of EI and EC measurement for the investigation of root colonization of mixed arbuscular mycorrhizal fungi (AMF) and functional diversity of separated AMF strains were studied in two pot experiments. We investigated the relationships between the mycorrhizal and non-mycorrhizal root properties (root mass, length and surface area) and the measured EI and EC values. It was assumed that the application of the EI and EC method could contribute to confirming several former observations about AMF presence in host roots and moreover mycorrhizal function.

Accepted Aug 25, 2014
*Corresponding author. E-mail: takacs@rissac.hu

Materials and Methods

In the first experiment, mycorrhizal and non-mycorrhizal maize (*Zea mays* L., DK-440 Hybrid) cultivars were compared for testing the sensitivity of EI and EC measurement in relation to mycorrhizal status of host plants. In the second one, root colonization, biomass production, EI and EC of *Rhizophagus intraradices* (R) or *Funneliformis mosseae* (F), inoculated and non-inoculated cucumber (*Cucumis sativus* L. cv. 'Perez-F1') and bean (*Phaseolus vulgaris* L. cv. 'Goldrush') hosts were monitored. Plant cultivation, AMF inoculation, as well as EI and EC measurements were carried out in the same manner in both experiments.

At experiment day 1, germinated seeds were planted into 1.25 l pots containing 1.1 kg of sterile (free of infective AMF propagules) pumice medium with 0.6–1 mm particle size, pH of 6.5, 0.94 kg/l bulk density and 0.26 cm^3/cm^3 water content at field capacity.

15 replicates of maize [M(RF)] in the first experiment and same number of cucumber [C(R) or C(F)] and bean [B(R) or B(F)] in the second one were treated with 10 g of AMF inoculum that contained pumice medium, and dried root cuttings of white clover (*Trifolium repens* L.) colonized by AM fungi. 15 non-inoculated plants for each species [M(Ø), C(Ø) and B(Ø)] were used as controls.

In the first experiment, a mixed inoculum [(RF); 1:1 %w/w] of *Funneliformis mosseae* (Schüssler and Walker; syn. *Glomus mosseae* Nicholson and Gerdeman) and *Rhizophagus intraradices* (Schüssler and Walker; syn. *Glomus intraradices* Schenck and Smith) strains were used for inoculation, while in the second one, the same amounts of these strains were separately put in the mycorrhizal fungi treated pots. The inoculum was applied as a thin layer in 5 cm depth below seedlings in pots. Plants were maintained randomly in growth chamber (26/18 °C and 16/8 h for day/night and 300 µmol/m^2/s photon flux density) with changing their places daily to avoid position effect. Planting medium was daily irrigated to field capacity. Optimal plant nutritional status was kept up by weekly irrigation with modified Hoagland's solution (with only 10% KH_2PO_4).

Root EI and EC were measured weekly during plant development with a GW-8101G precision LCR instrument (GW Instek, Taiwan) at 1 kHz frequency with 1 V terminal voltage. One terminal of the instrument was connected to the plant stem with a spring tension clamp fixed at 15 mm above the substrate level and a second one earthed by a stainless steel rod (6 mm ID, 15 cm long) inserted to the substrate. Electrocardiograph paste was smeared around stem to keep up electrical contact (Rajkai et al. 2005; Cseresnyés et al. 2013).

The parameters of the AMF colonization were measured every second day in the early phase of symbiotic associations and weekly after the 14th or 21st day of the experiments. On each occasion, 2–2 pots were destructively sampled in order to follow the temporal development of AMF colonization. Roots were stained with cotton-blue (Phillips and Hayman 1970), and frequency (F%) and intensity (M%) of AMF colonization were determined by the method of Trouvelot et al. (1986).

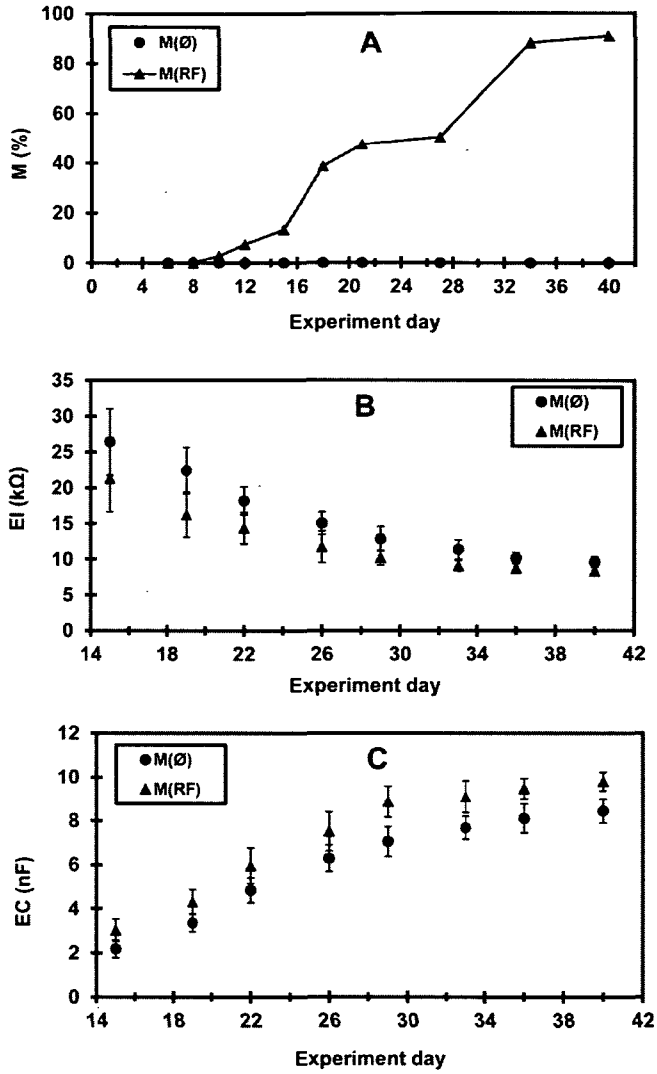

Figure 1A-C. Intensity of fungal root colonization (M%) in AMF-treated maize [M(RF)] (Fig. 1A) and signal intensity of root electrical impedance (EI; Fig. 1B) and electrical capacitance (EC; Fig. 1C) related to time in control (MØ) and mycorrhizal maize [M(RF)]. AM fungi treatments: R – Rhizophagus intraradices, F – Funneliformis mosseae; RF – mixed inoculum of the two strains

Standard regression analysis was carried out in order to relate root EI and EC to root dry mass and root surface area in case of mycorrhizal and non-mycorrhizal plants. A non-parametric Welch test was applied if the standard deviations of the compared groups (*F* test) were not identical. Statistical significance was assessed at $p<0.05$ in each case. Computations were performed by using Statistica software (ver. 9., StatSoft Inc., OK, USA).

Table 1. Biomass production of maize (M), cucumber (C) and bean (B) non-treated (control - Ø) or treated with AM fungal inoculum (R – *Rhizophagus intraradices*, F – *Funneliformis mosseae*; RF – mixed inoculum of the two strains).

Plants and treatments	Root dry weight (g)	Shoot dry weight (g)	Root surface area (cm^2)
MØ	1.756 (±0.262)	3.935 (±0.515)	1704 (±215)
M(RF)	1.795 (±0.281) NS	4.115 (±0.604) NS	1406 (±186) NS
CØ	0.505 (±0.071)	3.159 (±0.323)	665 (±93.5)
C(F)	0.539 (±0.053) NS	4.067 (±0.473) ***	708 (±69.6) NS
C(R)	0.556 (±0.076) NS	4.204 (±0.386) ***	729 (±99.6) NS
BØ	0.702 (±0.088)	1.723 (±0.125)	357 (±44.7)
B(F)	0.956 (±0.115) ***	2.912 (±0.045) ***	487 (±58.6) ***
B(R)	0.924 (±0.110) ***	2.458 (±0.057) **	470 (±55.9) ***

*, **, ***: significantly different from the control plants, at the $p < 0.05$, 0.01 and 0.001 levels respectively; NS: not significant.

Results

In the first experiment, the electrical measurement proved to be adequate to discriminate the AMF-infected and non-AM maize plants. AMF infection was not detected in control plants (MØ). AMF root presence (F= 8.3%; M= 1.3%) was first detected in 10 days old maize plants, and AMF colonization parameters (F and M) increased with age of maize. Microscopic examination of harvested roots showed 100% frequency and 90.9% intensity of fungal colonization in mycorrhizal plants (Fig. 1A). Mycorrhizal status of maize had no effect on shoot dry weight, root dry weight, but AMF colonization altered the root morphology: significantly increased the average root diameter (by 22.8%), and decreased the root length (by 33.0%; data not shown) and the root surface area (by 17.4 %) (Table 1).

In relation to plant root expansion through the experiment time, the amplitude of EI and EC showed a continuous decrease and increase, respectively (Fig. 1B–C; EI is basically inversely proportional to EC). The effect of AMF colonization on root electrical properties was clearly reflected by the EI and EC monitoring. Decrease of EI and increase of EC by time correlated strongly with mycorrhizal status of maize during plant development. At inoculated maize plants [M(RF)], root EI and EC were significantly lower and higher, respectively, over the non-inoculated control (MØ), indicating

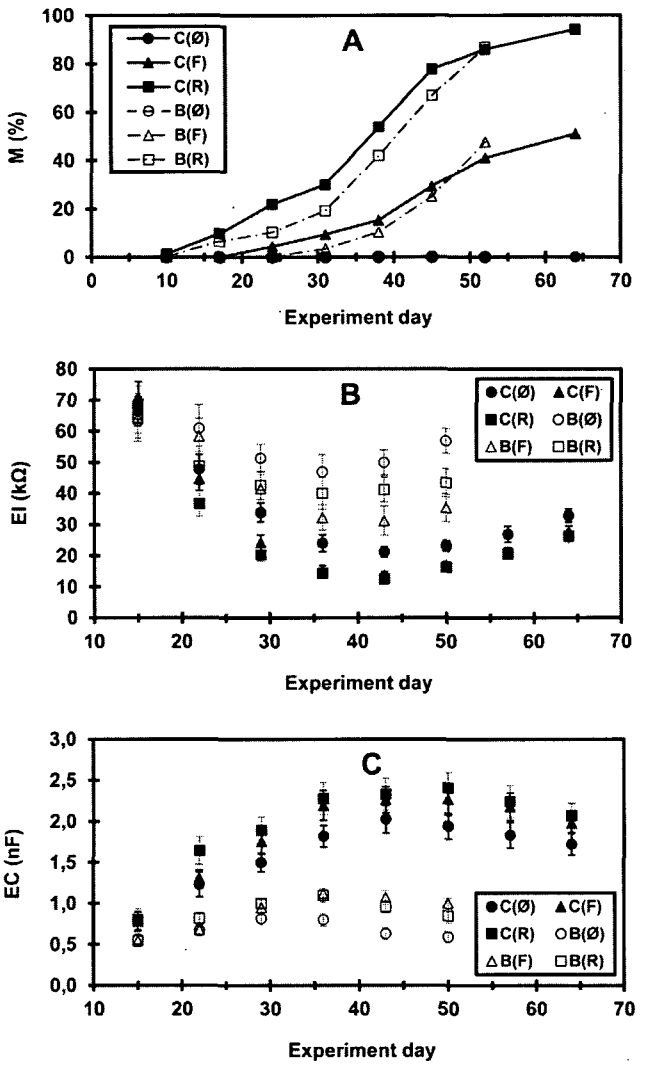

Figure 2A-C. Intensity of fungal root colonization (M%) in cucumber (C) and bean (B) inoculated with *Rhizophagus intraradices* (R) or *Funneliformis mosseae* (F) AMF strain (Fig. 2A) and signal intensity of root electrical impedance (EI; Fig. 2B) and electrical capacitance (EC; Fig. 2C) related to time in control (Ø) and mycorrhizal plants [C(R); C(F); B(R); B(F)].

the expansion of the absorbing root–soil interface caused by AMF colonization.

In the second experiment, root EI and EC measurement were used for *in situ* monitoring of functional differences that appears due to the specific colonization strategy of AMF strains in cucumber and bean hosts.

R. intraradices strain colonized both plants more effectively than *F. mosseae* (Fig. 2A). In the root of 10 days old plants, the presence of *R. intraradices* was detected in each host. In contrary, the structures of *F. mosseae* were found in host roots not earlier than the 24th experimental day. The colonization parameters (F and M) increased with the age

of plants. The maximal colonizations were similar at the two host plants, but early colonization was higher in case of cucumber. Mycorrhizal colonization exerted a significant influence on biomass production of both crop species. Post-harvest biomass measurement showed higher shoot dry weight and root dry weight at AMF-plants compared with the non-infected ones (Table 1). The effect of the AMF strains differed more significantly on host response in case of the high mycorrhizal-dependent bean. 29-33% and 43-69% relative shoot dry weight increments caused by AMF colonization were calculated for cucumbers and beans, respectively. Considering root growth, the effect of AMF colonization proved to be significant only for beans, in which 32-37% difference in root dry weight or root surface area was observed, as opposed to cucumbers, where AMF infection had just an insignificant effect on root development (Table 1).

EI decreased continuously with growing of both mycorrhizal and non-mycorrhizal plants (Fig. 2B). EC values had an upward trend during the vegetative stage of plant development, culminated at the flowering stage then reduced continuously through the fruit setting (Fig. 2C). Cucumbers expressed 1.5 to 3 fold higher EC than was detected for beans. The values of EI and EC are very similar at control (CØ; BØ) and colonized plants [C(R), C(F); B(R), B(F)] in early stage, when colonization has not occurred, yet. After the first mycorrhizal structures appeared, EI and EC values of colonized plants became significantly lower and higher, respectively, than those of control plants (Fig. 2B–C). At late colonization, higher M% values are not in relation to higher capacitance values. The differences in the root colonization of the two AMF strains were well expressed by root EI and EC. The infectivity of *R. intraradices,* that was higher than that of *F. mosseae*, caused higher decrease in EI and higher increase in EC values compared to control plants..

Discussion

AMF fungi are one of the key components of soil organisms; therefore, it is important to understand the physiological and ecological role of AMF in host plant community. Methods to detect and estimate AM fungi colonization and structures in roots are essential tools in mycorrhizal research. The basic techniques to detect the AMF infection and colonization degree are stainings and light-microscopic observations. Numerous destructive – both vital and non-vital – staining methods for observation of intraradical structures of AMF has been reported by the detailed overview of Vierheilig et al. (2005). In most cases they do not provide information about AMF functionality. The challenge of methodological developments is to establish routine and cost-effective techniques to measure the quantitative and qualitative AMF properties simultaneously to providing information about the AMF functionality.

In the presented work, significant effect of AMF colonization on root EI and EC values, as a consequence of the increased root–soil interface, was shown in maize, cucumber or bean cultivars. AMF colonization caused significant decrease in the root EI and increase in the root EC, respectively. The degree of host growth responses to AMF colonization is expressed as mycorrhizal dependency (MD). The AMF-induced relative increment not only in total plant biomass but also in root EC proved to be higher in bean than in cucumber (respectively for the last EC measurement), in relation to the higher degree of MD generally observed in legumes (Muleta 2010). The root surface area of slightly mycorrhiza-dependent hosts (maize or cucumber) was similar to that of control plants, indicating the expansion of the absorbing root–soil interface. Changes in electrical properties could be due either to the increased area of plant root surface or to the enhanced absorption surface area by extraradical fungal hyphae (possibly to the complex interaction of the two phenomena). AMF external mycelial network is mostly dynamically developing and functioning component of plant–AMF symbiosis. The rate of intraradical AMF colonization is correlated with the extent of extraradical hyphae which promotes host supply (Luciano et al. 2006). Symbiotic efficiency can be assessed through host biomass production due to the ability of AMF isolates or species to promote stress tolerance and to improve mineral nutrition.

In the second experiment, the functionality of infective and absorptive AMF hyphae were visualized with EI and EC measurements, concurrently monitoring the stage of root colonization. The AMF isolates were characterized by the EI, EC and biomass production of host plants. In our case, the effectivity of inoculation depended strongly on AMF species, especially in the highly mycorrhiza-dependent bean host. The EI and EC measurement is a suitable method to detect little differences among various plant–fungi symbiosis, such as variations in the beginning of symbiotic phase or the spreading of intra- or extraradical hyphae.

We can concluded, that the introduced non-destructive and simple electrical impedance and capacitance measurement is an adequate technique for *in situ* monitoring of AMF colonization and function. Synthesizing the methods and knowledge of plant physiology, soil physics or soil microbiology sciences (in our case the EI and EC applications in detection of AMF colonization or stress diagnostic of terrestrial plants) could be contribute to understanding of functions and relationships in soil–plant–symbiont systems.

References

Aubrecht L, Staněk Z, Koller J (2006) Electrical measurement of the absorption surfaces of tree roots by the earth impedance methods: 1. Theory. Tree Physiology 26:1105-1112.

Augé RM (2004) Arbuscular mycorrhizae and soil/plant water relations. Can J Soil Sci 84:373-381.

Brundrett M (2009) Mycorrhizal associations and other means of nutrition of vascular plants: understanding the global diversity of host plants by resolving conflicting information and developing reliable means of diagnosis. Plant Soil 320:37-77.

Cao Y, Repo T, Silvennionen R, Lehto T, Pelkonen P (2010) An appraisal of the electrical resistance method for assessing root surface area. J Exp Bot 61:2491-2497.

Čermák J, Ulrich R, Staněk Z, Koller J, Aubrecht L (2006) Electrical measurement of tree root absorbing surfaces by the earth impedance method: 2. Verification based on allometric relationships and root severing experiments. Tree Physiol 26:1113-1121.

Chloupek O (1972) The relationship between electric capacitance and some other parameters of plant roots. Biol Plantarum 14:227-230.

Cseresnyés I, Takács T, Végh RK, Anton A, Rajkai K (2013) Electrical impedance and capacitance method: A new approach for detection of functional aspects of arbuscular mycorrhizal colonization in maize. Eur J Soil Biol 54:25-31.

Dalton FN (1995) In-situ root extent measurements by electrical capacitance methods. Plant Soil 173:157-165.

Kothari SK, Marschner H, George E (1990) Effect of VA mycorrhizal fungi and rhizosphere microorganism on root and shoot morphology, growth and water relations in maize. New Phytol 116:303-311.

Luciano A., Pellegrino E, Bonari E, Giovanetti M (2006) Functional diversity of arbuscular mycorrhizal fungal isolates in relation to extraradical mycelial networks. New Phytol 172:347-357.

Marschner H (1997) The soil-root interface (Rhizosphere) in relation to mineral nutrition. In Marschner H, ed., Mineral nutrition of higher plants. Academic Press, London, pp. 537-594.

Muleta D. (2010): Legume responses to arbuscular mycorrhizal fungi inoculation in sustainable agriculture. In Khan MS, Zaidi A, Musarrat J.eds., Inoculation microbes for legume improvement. Springer, Wien, pp. 293-323.

Phillips JM, Hayman DS (1970) Improved procedures for clearing roots and staining parasitic and vesicular-arbuscular mycorrhizal fungi for rapid assessment of infection. T Brit Mycol Soc 55:157-160.

Rajkai K, Végh KR, Nacsa T (2005) Electrical capacitance of roots in relation to plant electrodes, measuring frequency and root media. Acta Agron Hung 53:197-210.

Trouvelot A, Kough JL, Gianinazzi-Pearson V (1986) Mesure du taux de mycorhization VA d'un système radiculaire. Recherches et methods d'estimation ayant une signification fonctionnelle. In Gianinazzi-Pearson V, Gianinazzi S eds., Physiological and genetical aspects of mycorrhizae. INRA, Paris, pp. 217-221.

Vierheilig H, Schweiger P, Brundrett M (2005) An overview of methods for the detection and observation of arbuscular mycorrhizal fungi in roots. Physiol Plantarum 125:393-404.

Volume 58(1):61-64, 2014
Acta Biologica Szegediensis
http://www.sci.u-szeged.hu/ABS

ARTICLE

Antifungal effect of selected European herbs against *Candida albicans* and emerging pathogenic non-albicans *Candida* species

Elvira Nacsa-Farkas[1], Eliza Kerekes[2], Erika Beáta Kerekes[1], Judit Krisch[2]*, Popescu Roxana[3], Daliborca Cristina Vlad[3], Pauliuc Ivan[4], Csaba Vágvölgyi[1]

[1]Department of Microbiology, Faculty of Science and Informatics, University of Szeged, Szeged, Hungary, [2]Institute of Food Engineering, University of Szeged, Szeged, Hungary, [3]Faculty of Medicine, University of Medicine and Pharmacy Timisoara, Romania, [4]Faculty of Horticulture and Forestry, University of Agricultural Sciences and Veterinary Medicine of Banat, Timisoara, Romania

ABSTRACT The anti-candidal effect of some European medicinal plants *Allium ursinum* (wild garlic or ramson); *Aristolochia clematitis* (birthwort), *Melilotus officinalis* (sweet clover), *Salvia officinalis* (garden sage) and *Viscum album* (mistletoe) was investigated. In general, *C. inconspicua*, *C. zeylanoides* and *C. norvegica* were among the most sensitive species, while *C. albicans* together with *C. orthopsilosis* showed much lower sensitivity. Best results were achieved with wild garlic showing a broad spectrum anti-yeast activity in some cases with fungicidal MIC (3.52 mg/ml). The other plant extracts showed moderate, mainly fungistatic action.
Acta Biol Szeged 58(1):61-64 (2014)

KEY WORDS

Candida species
medicinal plants
Allium ursinum

Candida species are opportunistic pathogens causing candidiasis. Invasive candidiasis is a life-threatening infection in immunocompromised hosts such as bone marrow and organ transplant recipients, in patients receiving intensive chemotherapy regimens and in AIDS patients (Lyles et al. 1999). Development of resistance is common among HIV-positive patients receiving fluconazole for long-term therapy. In some cases, resistance to fluconazole triggers cross-resistance to other azoles or pathogen shift from *Candida albicans* to less sensitive species such as *Candida glabrata* and *Candida krusei* (Bastert 2001). Moreover, systemic *Candida* infections are observed in patients with extensive surgery or burns, intensive antibiotic therapy, indwelling catheters, patients with diabetes mellitus, and in elderly patients (Dean et al. 1996; Wenzel 1995). Nowadays, *Candida* species are important agents of nosocomial bloodstream infections (BSIs) (Pfaller et. al. 2011; Diekema et al. 2012). The incidence of BSIs caused by *Candida* spp. has risen in the past 20 years (Pfaller et al. 1998; Seifert et al. 2007; Diekema et al. 2012). Although *C. albicans* remains the most frequently isolated agent of candidiasis, non-albicans *Candida* (NAC) species now account for a substantial part of clinical isolates collected worldwide in hospitals. In a survey covering 52 hospitals in the USA between 1998 and 2006, *C. albicans* was the most prevalent species, accounting for 50.7% of all isolates, followed by *C. parapsilosis* (17.4%), *Candida glabrata* (16.7%) and *Candida tropicalis* (10.2%); 5.1% BSIs were caused by other *Candida* spp. (Wisplinghoff et al. 2014). NAC species of particular importance include the prominent species *Candida guilliermondii*, *Candida lusitaniae*, *Candida kefyr*, *Candida famata* (synonym: *Debaryomyces hansenii*), *Candida inconspicua*, *Candida rugosa*, *Candida dubliniensis* and *Candida norvegensis*.

There is a growing interest to find new, natural compounds with anti-candidal activity because most *Candida* species show reduced sensitivity towards traditional antifungal compounds (Papon et al. 2013). Plant derived antimicrobials are, among others, in the focus of research because of their easy accessibility and wide antimicrobial spectrum. Usually several ingredients with different target sites are responsible for the antimicrobial properties which decreases the possibility of development of microbial resistance. In this study, the anti-candidal effect of European medicinal plants: *Allium ursinum* (wild garlic or ramson); *Aristolochia clematitis* (birthwort), *Melilotus officinalis* (sweet clover), *Salvia officinalis* (garden sage) and *Viscum album* (mistletoe) was investigated.

Allium ursinum is a perennial herbaceous plant, distributed in Europe and Asia. It has been used for centuries in traditional medicine to prevent cardiovascular diseases, to detoxify the body, and to stimulate digestion (Sobolewska et al. 2013). Although bulbs are also edible, leaves are preferred and are consumed mainly fresh. Nowadays, there is a renaissance of wild garlic consumption because of its supposed

Accepted Sept 5, 2014
*Corresponding author. E-mail: krisch@mk.u-szeged.hu

Table 1. Minimum inhibitory concentration (MIC) in mg/ml of the investigated herbs' ethanol (30%v/v) extracts against *Candida* species.

Candida species	*Allium ursinum*	*Aristolochia clematitis*	*Melilotus officinalis*	*Salvia officinalis*	*Viscum album*
C. albicans	3.52	>32.8	19.3	13.2	11.3
C. guillermondii	0.88	32.8	19.3	6.6	11.3
C. glabrata	1.76	>32.8	19.3	13.2	11.3
C. inconspicua	1.76	32.8	9.65	13.2	5.65
C. krusei	1.76	>32.8	19.3	13.2	11.3
C. lusitaniae	0.88	>32.8	19.3	13.2	11.3
C. metapsilosis	1.76	32.8	19.3	6.6	11.3
C. norvegica	0.88	32.8	19.3	6.6	11.3
C. orthopsilosis	3.52	32.8	19.3	13.2	>11.3
C. parapsilosis	1.76	32.8	19.3	6.6	11.3
C. pulcherrima	3.52	32.8	19.3	6.6	11.3
C. zeylanoides	0.88	32.8	9.65	6.6	11.3

health benefits. The main ingredients are sulfur containing compounds: the odorless and non-volatile S-alk(en)yl-L-cysteine-sulfoxides (methiin and alliin) which in crushed leaves hydrolyze to a range of volatile compounds such as thiosulfinates and allicin (Bagiu et al. 2012; Sobolewska et al. 2013). The volatile compounds are thought to be responsible for the wide antimicrobial effect of *A. ursinum* (Bagiu et al. 2012).

Aristolochia species are also used in traditional medicine although aristolochic acid with its cytotoxic effect can cause chronic renal failure. Aristolochic acid is supposed to have also antimicrobial properties (Pozdzik 2010; Benzakour 2011).

Melilotus officinalis (L.) Pallas is traditionally used to treat inflammation and infection in the throat and gastrointestinal system. The plant contains melilotin and other coumarin glycosides, and an essential oil, making sweet clover aromatic (Anwer 2008).

Salvia officinalis L. is an aromatic plant and has been used since ancient times in folk medicine. Biologically active compounds are phenol acids, like rosmarinic, caffeic, ferulic acids, and tannins (Then et al. 2004).

Viscum album L. grows as an obligate hemiparasitic plant on the branches of deciduous trees. Mistletoes have been used in traditional medicine in the treatment of many diseases such as diabetes mellitus, stroke, chronic cramps, stomach problems, heart palpitations (Ochocka and Piotrowski 2002). The bioactive compounds are mistletoe lectins and viscotoxins (Urech et al. 2006).

Materials and Methods

Plants

Aristolochia clematitis L., *Melilotus officinalis* (L.) Pallas, *Salvia officinalis* L., *Viscum album* L., were collected in Romania (near Timisoara), and were identified in the University Botanical Garden of Szeged. Leaves of *A. ursinum* were of Hungarian origin and purchased from a local market in Szeged.

Microorganisms

C. norvegica CBS 4239, *C. inconspicua* CBS 180, *C. zeylanoides* CBS 619, *C. pulcherrima* CBS 5833, *C. guilliermondii* CBS 566, *C. albicans* ATCC 10231, *C. krusei* CBS 573, *C. lusitaniae* CBS 6936, *C. glabrata* CBS 138, C. *parapsilosis* CBS 604, *C. metapsilosis* SZMC 8092 and *C. orthopsilosis* SZMC 8116 strains were obtained form the American Type Culture Collection (ATCC, Manassas, VA, USA), from the Centraalbureau voor Schimmelcultures (CBS, Utrecht, The Netherlands), and from the Szeged Microbial Collection (SZMC, Szeged, Hungary). Yeasts were maintained and cultured on YEPD medium (1% (w/v) yeast extract, 2% peptone, 2% glucose, 2% agar) at 30 °C.

Preparation of herbs extracts

The aerial parts of *A. clematitis, M. officinalis, S. officinalis,* and *V. album* were naturally air dried in shade for 14 days. Once dried, they were milled into a fine powder with an electric grinder. To 10 g powdered plant material, 100 ml 96% (v/v) ethanol was added, and the solution was agitated at room temperature in the dark for 24 hours. The extracts were filtered and concentrated by vacuum drying at 50 °C. After the dehydration process, dry plant extracts were dissolved in 30% (v/v) ethanol to a final concentration of 50 mg ml^{-1} and were sterilized by filtration through a 0.45 μm membrane filter (Millipore). *Allium ursinum* extract was prepared from fresh material; crushed leaves were macerated in ethanol:water (30:70) solution for 24 h. Thereafter, the crude extract was filtered and the liquid was evaporated at 50 °C. The solid residue was dissolved in 30% (v/v) ethanol and the concentration was adjusted to 50 mg/ml. The solution was sterile filtered in the

Table 2. Minimum fungicidal concentration (MFC) in mg/ml of the investigated herbs' ethanol (30%v/v) extracts against *Candida* species. ND - not detected.

Candida species	*Allium ursinum*	*Aristolochia clematitis*	*Melilotus officinalis*	*Salvia officinalis*	*Viscum album*
C. albicans	3.52	ND	-	ND	ND
C. guillermondii	1.76	ND	19.3	ND	ND
C. glabrata	ND	ND	-	ND	ND
C. inconspicua	0.88	ND	-	ND	ND
C. krusei	1.76	ND	-	ND	ND
C. lusitaniae	0.88	ND	-	ND	ND
C. metapsilosis	14.06	ND	-	ND	ND
C. norvegica	0.88	ND	19.3	ND	ND
C. orthopsilosis	14.06	ND	-	ND	ND
C. parapsilosis	ND	ND	-	ND	ND
C. pulcherrima	1.76	ND	19.3	ND	ND
C. zeylanoides	0.88	ND	9.65	6.6	ND

Table 3. Anti-*Candida* MIC values of the antifungal amphotericin B and different herbs and fruits extracts from the literature. R - resistant; nd - no data.

Candida species	Amphotericin B (µg/ml)	*Rosmarinus officinalis* methanol extract (mg/ml)	*Punica granatum* methanol extract (mg/ml)	*Ribes nigrum* methanol extract (mg/ml)	Xanthorizzol from *Curcuma xanthorriza* (mg/ml)
Reference	Galgóczy et al. 200	Höfling et al. 2010	Höfling et al. 2010	Krisch et al. 2009	Rukayadi et al. 2006
C. albicans	2.0	0.001	0.003	nd	2.5 - 15
C. guillermondii	nd	0.003	0.001	6.13	2.0 – 8.0
C. glabrata	nd	R	0.003	nd	4.0 - 10
C. inconspicua	2.0	nd	nd	4.22	nd
C. krusei	2.0	0.001	0.001	nd	2.5 – 7.5
C. lusitaniae	1.0	0.001	0.001	nd	nd
C. norvegica	0.5	nd	nd	nd	nd
C. parapsilosis	nd	0.003	0.003	4.41	10 - 25
C. zeylanoides	1.0	nd	nd	nd	nd

above mentioned way and the concentration was determined again. All extracts were kept at -20 °C until use.

Investigation of anti-candidal effect

In vitro anti-candidal activities were evaluated by microtiter plate assay in RPMI 1640 medium (Sigma-Aldrich, St. Louis, MO, USA), according to National Committee for Clinical Laboratory Standards (CLSI) recommendations. In each well, 100 µl sterile-filtered (0.45 µm, Millipore, USA) plant extract diluted up to 1/32 of the stock solution was mixed with 100 µl yeast cell suspension (10^5 cells/ml). Each test plate contained an uninoculated control, a positive growth control, a medium-free control and a drug sterile control. Absorbance was measured after 24 h cultivation at 37 °C. MIC values were determined as the concentration of extracts where the absorbance of the treated culture was ≤10% of the non-treated culture (positive growth control). To determine MFC values, tracking plate method (Jett at al. 1997) was used. MFC was defined as the concentration where no colony growth was observed.

Results and Discussion

The lowest MIC values for *Candida* species were obtained by wild garlic extracts followed by salvia and mistletoe (Table 1). The sensitivity of *Candida* species to the extracts varied substantially. In general, *C. inconspicua*, *C. zeylanoides* and *C. norvegica* were among the most sensitive species, while *C. albicans* together with *C. orthopsilosis* showed much lower sensitivity. In most cases MFC values could not be determined in the investigated concentration ranges, showing that MIC values were mainly fungistatic (Table 2). Best results were achieved with wild garlic showing in some cases fungicidal MICs even at low concentrations (3.52 mg/ml). Lemar and coworkers (2002) have found that fresh garlic and garlic powder extracts had fungicidal effect on *C. albicans* above 10 and 20 mg/ml thus our wild garlic extract showed stronger antifungal activity than garlic. Garlic and wild garlic have common main compounds (alliin, methiin and their deriva-

tives) and these compounds are responsible for the antimicrobial effect. According to literature, these compounds inhibit microorganisms by reacting with the sulfhydryl (SH) groups of cellular proteins (Kyung 2012). It seems that plants with volatile ingredients like allicin or essential oils have good antifungal activity. In our experiments MIC values for *Salvia* were in the range of 6.6-13.2 mg/ml while rosemary extracts investigated by Höfling et al. (2010) showed MIC values close to amphotericin B (Table 3). Extracts rich in flavonoids and anthocyanins as black currant pomace extracts in our previous experiments or a pure phenolic compound, xanthorrizol showed MIC values in the range of 2 - 20 mg/ml (Table 3). Based on MIC values, the effect of most natural antifungals is weaker than that of the usual synthetic agents. Natural antimicrobials may be of importance, however, because they are less likely to induce resistance, and may act synergistically with the synthetic ones.

Acknowledgement

This work was supported by the Hungarian-Romanian Intergovernmental Cooperation Program TÉT_10-1-2013-0019.

References

Anwer M, Suhail M, Mohtasheem IA, Ahmed SW, Bano H (2008) Chemical constituents from *Melilotus officinalis*. J Basic Appl Sci 4(2):89-94.

Bagiu RV, Vlaicu B, Butnariu M (2012) Chemical composition and in vitro antifungal activity screening of the *Allium ursinum* L. (Liliaceae). Int J Mol Sci 13:1426-1436.

Bastert J (2001) Current and future approaches to antimycotic treatment in the era of resistant fungi and immunocompromised hosts. Int J Antimicrob Agents 17:81-91.

Benzakour G, Benkirane N, Amrani M, Oudghiri M (2011) Immunostimulatory potential of *Aristolochia longa* L. induced toxicity on liver, intestine and kidney in mice. J Toxicol Environ Health Sci 3(8):214-222.

Clinical and Laboratory Standards Institute (CLSI), Reference method for broth dilution antifungal susceptibility testing of yeasts; Approved Standard Second Edition (M27-A2), 2002

Dean DA, Burchard KW (1996) Fungal infection in surgical patients. Am J Surg 171:374-382.

Diekema D, Arbefeville S, Boyken L, Kroeger J, Pfaller M (2012) The changing epidemiology of healthcare-associated candidemia over three decades. Diagn Microbiol Infect Dis 73:45-48.

Galgóczy L, Bácsi A, Homa M, Virágh M, Papp T, Vágvölgyi Cs (2011) In vitro antifungal activity of phenothiazines and their combination with amphotericin B against different *Candida* species. Mycoses 54:737-743.

Höfling JF, Anibal PC, Obando-Pereda GA, Peixoto IAT, Furletti VF, Foglio MA, Gonçalves RB (2010) Antimicrobial potential of some plant extracts against *Candida* species. Braz J Biol 70(4):1065-1068.

Jett BD, Hatter, KL, Huycke MM, Gilmore MS (1997) Simplified agar plate method for quantifying viable bacteria. BioTechniques 23:648-650.

Krisch J, Ördögh L, Galgóczy L, Papp T, Vágvölgyi Cs (2009) Anticandidal effect of berry juices and extracts from *Ribes* species. Cent Eur J Biol 4:86-89.

Kyung KH, Lee YC (2001) Antimicrobial activities of sulfur compounds derived from S-alk(en)yl-L-cysteine sulfoxides in *Allium* and *Brassica*. Food Rev Int 17(2):183-198.

Lemar KM, Turner MP, Lloyd D (2002) Garlic (*Allium sativum*) as an anti-*Candida* agent: a comparison of the efficacy of fresh garlic and freeze-dried extracts. J Appl Microbiol 93: 398–405.

Lyles RH, Chu C, Mellors JW, Margolick JB, Detels R, Giorgi JV, Al-Shboull Q, Phair JP (1999) Prognostic value of plasma HIV RNA in the natural history of *Pneumocystis cariniipneumonia*, cytomegalovirus and *Mycobacterium avium* complex. Multicenter AIDS cohort study. AIDS 13:341-349.

Ochocka JR, Piotrowski A (2002) Biologically active compounds from European mistletoe (*Viscum album* L.). Can J Plant Pathol 24:21-28.

Papon N, Courdavault V, Clastre l M, Bennett RJ (2013) Emerging and emerged pathogenic *Candida* species: beyond the *Candida albicans* paradigm. PLOS Pathogens 9(9):1003550. doi:10.1371/journal.ppat.1003550.

Pfaller MA, Jones RN, Messer SA, Edmond MB, Wenzel RP (1998) National surveillance of nosocomial blood stream infection due to species of *Candida* other than *Candida albicans*: frequency of occurrence and antifungal susceptibility in the SCOPE Program. Diagn Microbiol Infect Dis 30:121-129.

Pfaller MA, Moet GJ, Messer SA, Jones RN, Castanheira M (2011) *Candida* bloodstream infections: comparison of species distributions and antifungal resistance patterns in community-onset and nosocomial isolates in the SENTRY Antimicrobial Surveillance Program, 2008-2009. Antimicrob Agents Chemother 55:561-566.

Pozdzik AA, Berton A, Schmeiser HH, Missoum W, Decaestecker C, Salmon IJ, Vanherweghem JL, Nortier JL (2010) Aristolochic acid nephropathy revisited: A place for innate and adaptive immunity? Histopathol 56(4):449-463.

Rukayadi1Y, Yong D, Hwang J-K (2006) In vitro anticandidal activity of xanthorrhizol isolated from *Curcuma xanthorrhiza* Roxb. J Antimicrob Chemother 57:1231-1234.

Seifert H, Aurbach U, Stefanik D, Cornely O (2007) In vitro activities of isavuconazole and other antifungal agents against *Candida* bloodstream isolates. Antimicrob Agents Chemother 51:1818-1821.

Sobolewska D, Podolak I, Makowska-Was J (2013) *Allium ursinum*: botanical, phytochemical and pharmacological overview. Phytochem Rev. DOI 10.1007/s11101-013-9334-0.

Stajner D, Milic N, Canadanovic-Brunet J, Kapor A, Stajner M, Popovic BM (2006) Exploring *Allium* species as a source of potential medicinal agents. Phytother Res 20:581-584.

Then M, Vásárhelyi-Perédi K, Szöllősy R, Szentmihályi K (2004) Polyphenol-, mineral element content and total antioxidant power of sage (*Salvia officinalis* L.) extracts. Acta Hort 629:123-129.

Urech K, Schaller G, Jäggy C (2006) Viscotoxins, mistletoe lectins and their isoforms in mistletoe (*Viscum album* L.) extracts in vitro. Drug Res 56(6):428-434.

Wisplinghoff H, Ebbers J, Geurtz L, Stefanik D, Major Y, Edmond MB, Wenzel RP, Seifert H (2014) Nosocomial bloodstream infections due to *Candida* spp. in the USA: species distribution, clinical features and antifungal susceptibilities. Int J Antimicrob Ag 43:78- 81.

Volume 58(1):65-68, 2014
Acta Biologica Szegediensis
http://www.sci.u-szeged.hu/ABS

ARTICLE

Detection of self-complementary inverted repeats by single forward primer driven PCR

Tünde Kupi[1], Tamás Deák[1], György D. Bisztray[1], Ernő Szegedi[2]*

[1]Corvinus University of Budapest, Department of Viticulture, Budapest, Hungary, [2]National Agricultural Research and Innovation Centre, Research Institute for Viticulture and Enology, Research Station of Kecskemét, Kecskemét-Katonatelep, Hungary

ABSTRACT Inverted repeat gene structures designed for silencing functional genes have been widely used both in academic and applied research. The correct orientations of such structures are usually validated with restriction analysis and/or sequencing. We speculated that the inverted repeat nature of such constructs can be shown by a simple PCR reaction with a single forward primer. To test this hypothesis five different constructs were established from grapevine sequences in a hairpin-intron style silencing system. We were able to amplify the appropriate products in each case. Thus a forward-primed PCR alone may be sufficient to prove the inverted repeat nature of the desired constructs. **Acta Biol Szeged 58(1):65-68 (2014)**

KEY WORDS

Agrobacterium tumefaciens
crown gall
Phire Taq polymerase
plant diseases
RNA interference

Gene silencing plays an increasing role both in plant and animal biology to study physiological processes of living cells. It has also become a popular strategy to establish disease resistance in plants (Doran and Helliwell 2009). RNA-silencing or RNA interference (RNAi) is based on the sequence-specific recognition and subsequent degradation of target mRNA through RNA-induced silencing complexes (RISCs). RISCs contain short 21 bp RNA sequences that recognize the complementary RNA sequences resulting in its complete degradation by the RISC complex (Rana 2007; Pratt and MacRae 2009). RNAi-based strategies have been extensively studied in agriculture, e.g., to elaborate new strategies for controlling viral diseases of plants (Bonfim et al. 2007; Nahid et al. 2011; Wang et al. 2012; Shimizu et al. 2013), for silencing *Agrobacterium tumefaciens* oncogenes to prevent crown gall disease (Alburquerque et al. 2012) as well as for nematode (Gheysen and Vanholme 2007; Huang et al. 2014) and insect pest control (Gu and Knipple 2013).

From the technical aspect, gene constructs producing hairpin-structures of self complementary RNA in which the inverted repeats are separated by an intron sequence proved to be a highly efficient tool for gene silencing. To establish such structures several improved applications of the Gateway technology based on site specific DNA-recombination and related pHellsgate vectors have been constructed and widely used (Wesley et al. 2001; Helliwell et al. 2002; Helliwell and Waterhouse 2003; Earley et al. 2006; Traore and Zhao 2011). An improved technology, 'Golden Gate' (Engler et al. 2008) uses the type II restriction enzyme *BsaI*. A special characteristic of this enzyme is that it cleaves DNA adjacent to the recognition site. This feature of the enzyme has two important impacts on cloning strategy. On one hand, after cleavage and subsequent ligation the recognition site is not included in the DNA fragment anymore, such cleavage and ligation of both vector and insert can be carried out in one tube and one step, making the cloning process very simple. The second important feature of the enzyme is that different sticky ends can be created by the digestion with the same enzyme, which means that directional cloning of the PCR product in two copies and opposite orientation can be also achieved in the same digestion/ligation step. Thus cloning of genes of interest in opposite orientation becomes possible in a single restriction digestion-ligation step into the pRNAi-GG binary vector (Yan et al. 2012). The vector is specifically designed for the fast and effective creation of inverted repeat constructs. pRNAi-GG is introducing a complex selection system for clones including both copies of the insert and a copy of a pyruvate dehydrogenase kinase (Pdk) intron between the two copies (Fig. 1.). The opposite oriented insert PCR products are replacing two copies of the bacterial toxin CcdB, thus selecting for clones carrying both arms of the hairpin structure. The inclusion of the Pdk intron is ensured by a chloramphenicol resistance gene included in the intron sequence (for more detailed description of the cloning system see Yan et al. 2012).

Figure 1. The schematic representation of the self-complementary inverted repeat clones established during this study.

Accepted June 8, 2014
*Corresponding author. E-mail: szegedi.erno@naik.hu

Although the use of the 'Golden Gate' cloning system highly simplified cloning of genes coding for self-complementary hairpin RNAs, the identification of the correct orientation of clones needs detailed PCR analysis, restriction analysis and/or sequencing (Nahid et al. 2011; Alburquerque et al. 2012; Yan et al. 2012). Here we show that a single forward primer designed for the gene of interest (cloned in inverted orientation surrounding an intron sequence) reliably detects self-complementary RNAi structures in one PCR reaction.

Materials and Methods

Homologous genes were selected from the published grapevine genome sequence (Jaillon et al. 2007). Five genes of interest, each contributing to *Agrobacterium*-transformation in tobacco or *Arabidopsis* were chosen for this study: RTNL2 and Rab8a (Hwang and Gelvin 2004), Hta2 and Hta10 (Zhu et al. 2003) and Vip1a (Li et al. 2005). Partial sequences of these genes were amplified by PCR with specific primers (Table 1.) using the cDNA from the grapevine variety *Vitis berlandieri* x *Vitis rupestris* cv. 'Richter 110' as template. RNA was extracted from *in vitro* plants using PureLink Plant RNA Reagent (Life Technologies) following the manufacturer's instructions. cDNA was synthesized using High Capacity cDNA Reverse Transcription Kit (Life Technologies) in 20 µl reaction volume from 600 ng total RNA. PCR products were cloned into pJet vector using the CloneJET PCR Cloning Kit (Thermo Scientific). The sequence accuracy of the cloned PCR products was confirmed by sequence analysis.

Chosen sequences were cloned into pRNAi-GG in inverted orientation into the left and right side of a Pdk intron containing a chloramphenicol resistance gene using a single *Bsa*I digestion-ligation step as described by Yan et al. (2012).

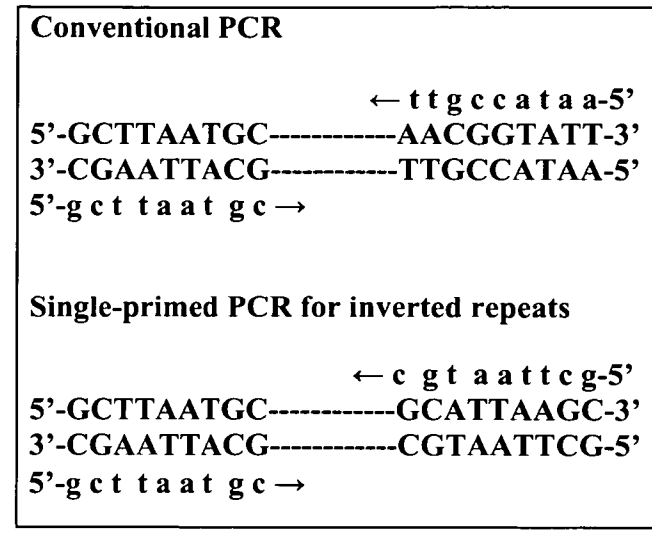

Figure 2. Schematic presentation of amplification of inverted repeats with a single forward primer. In conventional PCR (above) two different primers, called forward (red) and reverse (blue) primers are used that are designed to the two DNA strands in opposite orientation. In the case of inverted repats (below) the forward primer alone directs the synthesis of DNA in both strands in opposite orientation yielding well-defined amplification products.

The schematic structure of these clones is shown on Figure 1. The cloned genes were transformed into *Escherichia coli* DH5α for further work using kanamycin/chloramphenicol selection.

Restriction analysis

The pRNAi-GG plasmids containing the silencing constructs were isolated from *E. coli* DH5α cell suspensions using the

Table 1. Primers used for cloning (forward and reverse for each sequence, see Fig. 1) and PCR analysis of inverted repeat constructs (forward only) designed on the basis of grapevine sequence data (Jaillon et al. 2007). The 5' end of the primers includes 15 base pair long (*underlined italics*) flanking sequences used for the cloning procedure but they are not essential for the amplification. Further details on the grapevine genes involved in this study have been described earlier (Deák et al. 2013).

Primer name (specificity)		Primer sequence (5'→3')	Size of the cloned fragment (bp)	Size of the product amplified by the forward primer (bp)
VvHta2	Forward	*ACCAGGTCTCAGGAG*ACGGGATCTCAGTGGCTTCT	165	1,995
	Reverse	*ACCAGGTCTCATCGT*TTCCACAATTGGTCTGTTAGGA		
VvHta10	Forward	*ACCAGGTCTCAGGAG*CGATTCTCATGAAGTACAAAACG	268	2,201
	Reverse	*ACCAGGTCTCATCGT*GGAAACCAAACATCCCAGTC		
VvVip1a	Forward	*ACCAGGTCTCAGGAG*CTAATTGGCAGGAAGGCAGA	214	2,093
	Reverse	*ACCAGGTCTCATCGT*TCCATCCATTAAATGCTCCA		
VvRab8a	Forward	*ACCAGGTCTCAGGAG*CCAGGGGAAGGTTCTTCAAG	124	1,913
	Reverse	*ACCAGGTCTCATCGT*TGCCAAAGCCAGTAGTTGAA		
VvRTNL2	Forward	*ACCAGGTCTCAGGAG*TTCCAAGTGGTAGGGCAATC	289	2,243
	Reverse	*ACCAGGTCTCATCGT*CTGGGCAGAAGGAACAATGC		

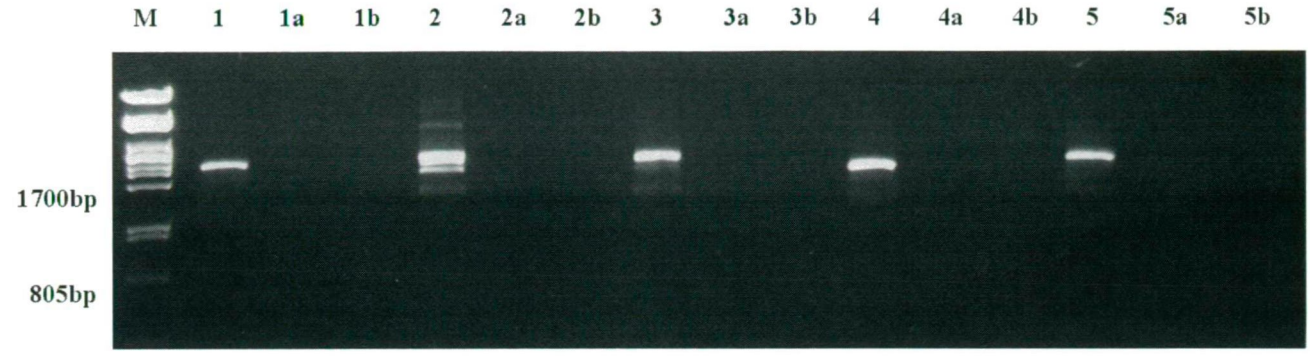

Figure 3. Detection of inverted repeats with single forward primed PCR. M: size marker (*Pst*I-digested λ-Phage DNA), followed by reactions with forward primers specific for VvHta2 (1-1b), VvHta10 (2-2b), VvVip1a (3-3b), VvRab8a (4-4b) and VvRTNL2 (5-5b). Single numbers indicate the inverted repeat constructs, „a" lanes contain DNA samples of the empty pRNAi-GG vector, and „b" samples are DNA-free controls.

alkaline lysis method (Sambrook et al. 2001). The extracted plasmid DNA was digested with *Bgl*II and *Pst*I Fast Digest restriction enzymes (Fermentas) at 37 °C for 20 min. The digested DNA fragments were separated on agarose gels and stained with ethydium bromide dye.

PCR conditions

PCR reactions were performed using an Applied Biosystems 9700 thermal cycler in 20 µl final volume with 0.4 µl of Phire Hot Start II Polymerase (Thermo Scientific) in 1x buffer supplemented with 0.5 µM of forward primer (Table 1) and 0.2 mM of each dNTP. One single colony of *E. coli* DH5α cells containing the pRNAi-GG vector with the corresponding silencing construction was used as template of the PCRs. Bacterial colonies containing blank pRNAiGG vectors were used as negative control samples with all of the applied primers. Template DNA from *E. coli* was isolated by lysing the cells in hot Triton X-100/sodium-azide buffer (Abolmaaty et al. 2000). The cycling parameters were: 98 °C for 3 min, 98 °C for 10 s, 66 °C for 5 s, 72 °C for 20 s, for 35 cycles, and then 72 °C for 3 min.

Results and Discussion

In this work we used the Golden Gate cloning system according to Yan et al. (2012) to set up silencing constructions harbouring self complementary hairpin structures in pRNAi-GG vectors. Short (124-289 bp) sequences of five different grapevine genes (Table 1.) were cloned into the pRNAi-GG vector on both sides of the 1599 bp long Pdk intron in opposite orientation, resulting in five constructions: pRNAiGG-VvVip1si, pRNAiGG-VvRtnl2si, pRNAiGG-VvRab8si, pRNAiGG-VvHta2si and pRNAiGG-VvHta10si. The results of the one step digestion-ligation process were checked by restriction analysis using *Bgl*II and *Pst*I enzymes. Digestion by the *Pst*I enzyme proves the incorporation of the inverted repeats surrounding the Pdk intron, while the *Bgl*II digestion provides information about the direction and incorporation of the Pds intron.

Due to the structure of inverted gene repeats yielding self-complementary RNAs we speculated that a single forward primer should amplify the full length of „gene of interest→intron←gene of interest" sequence since the forward primer designed corresponding to the 5'-3' strand will behave as a reverse primer and direct an 5'-3' DNA synthesis at the 3' of this strand (Fig. 2). To prove if this works, we tested various conventional PCR with *Taq* polymerases, but the expected relatively long DNA sequences were not properly amplified.

When PCRs were challenged by Phire Hot Start II polymerase (Thermo Scientific) specifically designed for the synthesis of long or difficult DNA templates, we obtained the expected DNA fragments. Figure 3. shows the products of colony PCR synthesized by using only the forward primers of the five constructs. The templates were *E. coli* DH5α colonies containing the pRNAi-GG vectors with the inserted silencing constructions. Colonies with pRNAi-GG vectors did not yield any PCR products (Fig. 3).

The identification of the inverted repeat constructions requires multiple PCR analysis, or restriction analysis of purified plasmid DNA, and/or DNA sequencing (Nahid et al. 2011; Alburquerque et al. 2012; Yan et al. 2012). The strategy described here offers a fast and cost-effective method to directly screen inverted repeat constructions from bacterial colonies after cell lysis by a simple PCR reaction using only the forward primer. Moreover, the same PCR primers which were applied during the cloning process can also be used for the detection. Thus these results show that the structure of hairpin constructs containing self complementary inverted repeats can be confirmed by a single primer driven PCR.

Acknowledgements

This work was supported by Hungarian National Science

Found (OTKA) grant no. K83121. We thank Professor Léon Otten (CNRS, Institut de Moléculaire des Plantes, Strasbourg, France) for critical reading of the manuscript prior to submission.

References

Abolmaaty A, Vu C, Oliver J and Levin RE (2000) Development of a new lysis solution for releasing genomic DNA from bacterial cells for DNA amplification by polymerase chain reaction. Microbios 101:181-189.

Alburquerque N, Petri C, Faize L, Burgos L (2012) A short-length single chimeric transgene induces simultaneous silencing of *Agrobacterium tumefaciens* oncogenes and resistance to crown gall. Plant Pathol 61:1073-1081.

Bonfim K, Faria JC, Nogueira EOPL, Mendes ÉA, Aragão FJL (2007) RNAi-mediated resistance to *Bean golden mosaic virus* in genetically engineered common bean (*Phaseolus vulgaris*). Mol Plant-Microbe Interact 20:717-726.

Deák T, Kupi T, Oláh R, Lakatos L, Kemény L, Bisztray GyD, Szegedi E (2013) Candidate plant gene homologues in grapevine involved in *Agrobacterium* transformation. Centr Eur J Biol 8:1001-1009.

Doran T, Helliwell C, eds. (2009) RNA interference: methods for plant and animals. CAB International.

Earley KW, Haag JR, Pontes O, Opper K, Juehne T, Song K, Pikaard CS (2006) Gateway compatible vectors for plant functional genomics and proteomics. Plant J 45:616-629.

Engler C, Kandzia R, Marillonnet S (2008) A one pot, one step, precision cloning method with high throughput capability. PLOS ONE 3:e3647.

Gheysen G, Vanholme B (2007) RNAi from plants to nematodes. Trends Biotechnol 25:89-92.

Gu L, Knipple DC (2013) Recent advances in RNA interference research in insects: implications for future insect pest management strategies. Crop Prot 45:36-40.

Helliwell C, Waterhouse P (2003) Constructs and methods for high-throughput gene silencing in plants. Methods 30:289-295.

Helliwell CA, Wesley SV, Wielopolska AJ, Waterhouse PM (2002) High-throughput vectors for efficient gene silencing in plants. Funct Plant Biol 29:1217-1225.

Huang Y, Mei M, Mao Z, Lv S, Zhou J, Chen S, Xie B (2014) Molecular cloning and virus-induced gene silencing of *MiASB* in the Southern root-knot nematode, *Meloidogyne incognita*. Eur J Plant Pathol 138:181-193.

Hwang H-H, Gelvin SB (2004) Plant proteins that interact with VirB2, the *Agrobacterium tumefaciens* pilin protein, mediate plant transformation. Plant Cell 16:3148-3167.

Jaillon O, Aury J-M, Noel B, Policriti A, Clepet C, Casagrande A et al. (2007) The grapevine genome sequence suggests ancestral hexaploidization in major angiosperm phyla. Nature 449:463-468.

Li J, Krichevsky A, Vaidya M, Tzfira T, Citovsky V (2005) Uncoupling of the functions of the *Arabidopsis* VIP1 protein in transient and stable plant genetic transformation by *Agrobacterium*. Proc Natl Acad Sci USA 102:5733-5738.

Nahid N, Amin I, Briddon RW, Mansoor S (2011) RNA-interference based resistance against a legume mastrevirus. Virol J 8:499.

Pratt AJ, MacRae IJ (2009) The RNA-induced silencing complex: a versatile gene-silencing machine. J Biol Chem 284:17897-17901.

Rana TM (2007) Illuminating the silence: understanding the structure and function of small RNAs. Nat Rev Mol Cell Biol 8:23-36.

Sambrook J, Fritsch EF, Maniatis T (2001) Molecular Cloning: Vol. 1: A Laboratory Manual, CSH Laboratory Press.

Shimizu T, Ogamino T, Hiraguri A, Nakazono-Nagaoka E, Uehara-Ichiki T, Nakajima M, Akutsu K, Omura T, Sasaya T (2013) Strong resistance against *Rice grassy stunt virus* is induced in transgenic rice plants expressing double-stranded RNA of the viral genes for nucleocapsid or movement proteins as targets for RNA interference. Phytopathology 103:513-519.

Traore SM, Zhao B (2011) A novel Gateway®-compatible binary vector allows direct selection of recombinant clones in *Agrobacterium tumefaciens*. Plant Methods 7:42.

Wang M-B, Masuta C, Smith NA, Shimura H (2012) RNA silencing and plant viral diseases. Mol Plant-Microbe Interact 25:1275-1285.

Wesley SV, Helliwell C, Smith NA, Wang MB, Rouse DT et al. (2001) Construct design for efficient, effective and high-throughput gene silencing in plants. Plant J 27:581-590.

Yan P, Shen W, Gao XZ, Li X, Zhou P, Duan J (2012) High-throughput construction of intron-containing hairpin RNA vectors for RNAi in plants. PLOS ONE 7(5):e38186.

Zhu Y, Nam J, Humara JM, Mysore KS, Lee L-Y, Cao H. et al. (2003) Identification of *Arabidopsis rat* mutants. Plant Physiol 132:494-505.

Volume 58(1):69-72, 2014
Acta Biologica Szegediensis
http://www.sci.u-szeged.hu/ABS

ARTICLE

The effect of the antioxidant drug U-74389G on endometrial edema during ischemia reperfusion injury in rats

C. Tsompos[1]*, C. Panoulis[2], K Toutouzas[3], G. Zografos[3], A. Papalois[4]

[1]Department of Obstetrics and Gynecology, Mesologi County Hospital, Etoloakarnania, Greece, [2]Department of Obstetrics and Gynecology, Aretaieion Hospital, Athens University, Attiki, Greece, [3]Department of Surgery, Ippokrateion General Hospital, Athens University, Attiki, Greece, [4]Exprerimental Research Center ELPEN Pharmaceuticals, S.A. Inc., Co., Pikermi, Attiki, Greece

ABSTRACT The aim of this experiment was to study the effects of the antioxidant drug U-74389G on rat model, particularly in ischemia reperfusion (IR) protocol. The beneficial or other effects of that molecule were studied pathologically using endometrial edema (EE) lesions. Forty rats were used of mean weight 231.875 gr. EE lesions were evaluated 60 min after reperfusion (groups A and C) and 120 min after reperfusion (groups B and D), with administration of the drug U-74389G in groups C and D. Results were that U-74389G administration non-significantly decreased without lesions the EE scores by 0.41 [-1.00 - 0.17] (p= 0.1607). This finding was in accordance with the results of Wilcoxon signed-rank test (p= 0.5229). Reperfusion time non-significantly increased without lesions the EE scores by 0.21 [-0.38 - 0.81] (p= 0.4701), also in accordance with Wilcoxon signed-rank test (p= 0.1022). However, U-74389G administration and reperfusion time together non-significantly decreased without lesions the EE scores by 0.17 [-0.53 - 0.18] (p= 0.3383). Results of this study indicate that U-74389G administration hardly non-significantly decreases without lesions the EE within short-term time context of 2 hours.
Acta Biol Szeged 58(1):69-72 (2014)

KEY WORDS

antioxidant drug
endometrial edema
reperfusion
U-74389G

Tissue ischemia and reperfusion (IR) remain one of the main causes of permanent or transient damage with serious implications on adjacent organs and certainly on patients' health. The use of antioxidant substances has been a research subject for many years. However, even if important progress has been made, satisfactory answers have not been given yet to fundamental questions, such as, how much powerful should an antioxidant be, when should it be administered, and in which dosage. The particularly satisfactory action of the antioxidant U-74389G in tissue protection has been noted in several performed experiments. Since a careful literature search (PubMed - Medline) was conducted, it was realized that this certain antioxidant has been tried in IR experiments. However, just few relative reports were found, not covering completely this particular matter. Also, a lot of publications addressed trials of other similar molecules of aminosteroids (lazaroids) to which the studied molecule also belongs to. U-74389G or better 21-[4-(2,6-di-1-pyrrolidinyl-4-pyrimidinyl)-1-piperazinyl]-pregna-1,4,9(11)-triene-3,20-dione maleate salt (Cayman Chemical Product Catalog) is an antioxidant which prevents both arachidonic acid-induced and iron-dependent lipid peroxidation. It protects against IR injury in animal heart, liver, and kidney models. These membrane-associating antioxidants (Shi et al. 1995) are particularly effective in preventing permeability changes in brain microvascular endothelial cells monolayers. The same authors (Tsompos et al. 2014) found a light non-significant decline in chloride serum levels in related IR injury experiments in rats by 0.58%±0.77% (p=0.4533) 1h after reperfusion, by 0.97%±0.53% (p=0.0879) 1.5h after reperfusion, by 0.75%±0.38% (p=0.0159) after time and drug interaction and by 1.36%±0.76% (p=0.1113) 2h after reperfusion.

The aim of this experimental study was to examine the effect of the antioxidant drug U-74389G on rat model and particularly in a uterus IR protocol. The beneficial effect or non-effectiveness of that molecule was studied by evaluating mean endometrial edema (EE) lesions.

Materials and Methods

Animal preparation

This experimental study was approved by Scientific Committee of Ippokrateion General Hospital, Athens University and by Veterinary Address of East Attiki Prefecture under 3693/12-11-2010 & 14/10-1-2012 decisions. Institutional and national guide for the care and use of laboratory animals

Accepted July 31, 2014
*Corresponding author. E-mail: constantinostsopos@yahoo.com

was followed. This experimental study was carried out at the Experimental Research Center of ELPEN Pharmaceuticals Co. Inc. S.A. at Pikermi, Attiki. All settings needed for the study including consumables, equipment and substances used, were provided by them. Albino female Wistar rats were used in accordance with accepted standards of humane animal care. They spent 7 days in laboratory before experimentation with an easy access to water and food. The experiment was acute, that is, the animal usage was completed by following experimental set of times without awakening and preservation of the rodents. They were randomly assigned to four experimental groups (10 animals in each group). Group A: Ischemia for 45 min followed by reperfusion for 60 min. Group B: Ischemia for 45 min followed by reperfusion for 120 min. Group C: Ischemia for 45 min followed immediately by U-74389G intravenous (IV) administration and reperfusion for 60 min. Group D: Ischemia for 45 min followed immediately by U-74389G IV administration and reperfusion for 120 min. The molecule U-74389G was administered in a dose of: 10 mg/kg body weight of the animal. The experiment was beginning by prenarcosis and general anesthesia administration to the animals. Their electrocardiogram and acidometry were continuously monitored. The inferior aorta was prepared so as its blood flow, it could be excluded by forceps. After exclusion, the protocol of IR was applied, exactly as is described in experimental groups. The molecules were administered at the time of reperfusion, through inferior vena cava catheterization, which had been carried out after general anesthesia. The EE evaluation was performed at 60 min after reperfusion for groups A and C and at 120 min after reperfusion for groups B and D.

Protocol of the experiment

The experimental rats were given general anesthesia by initial intramuscular (IM) administration of 0.5 cc of a compound, constituting 0.25 cc xylazine, [25 cc, 20mg/cc] and 0.25 cc ketamine hydrochloride [1000, 100mg/cc, 10cc]. 0.03 cc butorphanol [10mg/cc, 10cc] anesthetic agent was administered subcutaneously (SC) before laparotomy. Continuous oxygen supply was administered during the whole experiment. Ischemia was caused by clamping inferior aorta over renal arteries for 45 min after laparotomic access. Reperfusion was achieved by removing the clamp and inferior aorta patency re-establishment. Forty (40) female Wistar albino rats were used with a mean weight of 231.875 gr [Std. Dev: 36.59703 gr], with min weight $\geq$ 165 gr and max weight $\leq$ 320 gr. Rats weight could be potentially a confusing factor, e.g. fatter rats to have greater EE thickness. This suspicion will be investigated. Also, detailed histopathological (Osmanağaoğlu et al. 2012) study (pathology) and grading of edema findings was performed by scores, this is: 0 when lesions were not found, 1 when mild lesions were found, 2 when moderate lesions were found and 3 when serious lesions were found. The previous grading is transformed as follows: (0-0.499) without lesions, (0.5-1.499) the mild lesions, (1.5 -2.499) the moderate lesions and (2.5-3) the serious lesions damage, because the study concerns score ranges rather than point scores.

Table 1. Weight and endometrial edema (EE) score mean levels and Std. Dev. of groups.

Groups	Variable	Mean	Std. Dev
A	Weigh	243 gr	45.77 gr
	EE	mild 1.2	0.78
B	Weigh	262 gr	31.10 gr
	EE	mild 1.3	1.15
C	Weigh	212.5 gr	17.83 gr
	EE	mild 0.7	0.67
D	Weigh	210 gr	18.10 gr
	EE	mild 1	1.05

Std. Dev: standard deviation

Model of ischemia-reperfusion injury

Control groups: 20 control rats of mean weight 252.5 gr [Std. Dev: 39.31988 gr] were subjected to ischemia for 45 min followed by reperfusion.

Group A: 10 controls rats of mean weight 243 gr [Std. Dev: 45.77724 gr], mean mild EE score 1.2 [Std. Dev: 0.78] were subjected to 60 min reperfusion (Table 1).

Group B: 10 controls rats of mean weight 262 gr [Std. Dev: 31.10913 gr], mean mild EE score 1.3 [Std. Dev: 1.15] (Table 1) were subjected to 120 min reperfusion (Table 1).

Lazaroid (L) group: 20 rats of mean weight 211.25 gr [Std. Dev: 17.53755 gr] were subjected to ischemia for 45 min followed by reperfusion in the beginning of which 10 mg U-74389G/kg body weight were IV administered.

Group C: 10 L rats of mean weight 212.5 gr [Std. Dev: 17.83411 gr], mean mild EE score 0.7 [Std. Dev: 0.67] (Table 1) were subjected to 60 min reperfusion (Table 1).

Group D: 10 L rats of mean weight 210 gr [Std. Dev: 18.10463 gr], mean mild EE score 1 [Std. Dev: 1.05] (Table 1) were subjected to 120 min reperfusion (Table 1).

Results

Every weight group of rats was compared initially with another one from 3 remained groups applying statistical paired t-test (Table 1). Any emerging significant difference among EE scores will be investigated whether owed in the above mentioned significant weight correlations. Every EE scores rats groups initially were compared with other one from 3 remained groups applying Wilcoxon signed-rank test (Table 2). Applying generalized linear models (glm) with dependant variables of the EE scores and with independent variables of the U-74389G administration or without that, the reperfusion time and their interaction, resulted in: U-74389G administra-

Table 2. Statistical significance of mean values difference for groups (DG) after statistical paired t test application for weight and Wilcoxon signed-rank test for scores.

DG	Variable	Difference	p-value
A-B	Weight	-19 gr	0.2423
	EE	without lesions -0.1	0.8728
A-C	Weight	30.5 gr	0.0674
	EE	mild 0.5	0.2212
A-D	Weight	33 gr	0.0574
	EE	without lesions 0.2	0.5164
B-C	Weight	49.5 gr	0.0019
	EE	mild 0.6	0.1573
B-D	Weight	52 gr	0.0004
	EE	without lesions 0.3	0.4935
C-D	Weight	2.5 gr	0.7043
	EE	without lesions -0.3	0.4818

DG: difference for groups

Table 3. The decreasing influence of U-74389G in connection with reperfusion time.

Decrease	95% c. in		p-values	
		Reper-fusion time	Wil-coxon	glm
mild 0.5	-1.18 - 0.18	1 h	0.2212	0.1451
without lesions 0.4	-0.99 - 0.19	1.5 h	0.1816	0.1781
without lesions 0.3	-1.34 - 0.74	2 h	0.4935	0.5525

c. in: confidence interval

tion non-significantly decreased without lesions the EE scores by 0.4 [-0.99 - 0.19] (p= 0.1781). This finding was also in accordance with the result of Wilcoxon signed-rank test (p= 0.1816). Reperfusion time non-significantly increased without lesions the EE scores by 0.2 [-0.40 - 0.80] (p= 0.5046), approximately in accordance with Wilcoxon signed-rank test also increased without lesions by 0.3 [-0.87 - 0.27] (p= 0.3330). However, U-74389G administration and reperfusion time together non-significantly decreased without lesions the EE scores by 0.16 [-0.52 - 0.19] (p= 0.3641). Reviewing above and Table 2, Table 3 sums up concerning the decreasing influence of U-74389G in connection with reperfusion time. Inserting the weight of the rats also as an independent variable at glm analysis, a non-significant relation results in (p=0.4934), so further investigation is not needed.

Discussion

The following clinical situations show the association between ischemia and EE. Canisso et al (2013) detected a reduction in endometrial edema during progestagen treatment, which returned to normal after cessation of treatment similarly with effectively abolished estrous behavior response to the stallion within 24h which returned to the control level after cessation of treatment, in mares, being received progestagen treatment when confirmed in estrus. Ludwig (1982) considered difficult to describe the morphology of the endometrial reaction, thus, he evaluated the endometria of women with respect to stromal edema. Sridhar et al. (2000) considered amniotic membrane transplantation in chemical injury with severe limbal ischemia and in severe thermal injury in acute phase, as in an eye with opaque cornea, stromal edema, and scarring within the first few weeks of injury. Batra et al. (1995) observed prominent hypoplasia of the syncytium, stromal edema, ischemia findings, increased basement membrane thickening and high villous edema scores statistically significant in numerous representative samples taken from premature placentas immediately after delivery as compared to controls.

EE is involved in endometrial cancer and infertility. Gaete et al (2012) have previously shown that an estradiol-like hypertrophy of uterine cells may not be associated with cell proliferation, uterine eosinophilia, or endometrial edema. However, estrogen-induced cell proliferation in the uterus increases the risk of cancer development. Gaete et al (2011) found that complete inhibition of estradiol-induced mitoses in uterine luminal epithelium, endometrial stroma, myometrium and RNA content are followed by partial inhibition estradiol-induced uterine eosinophilia and endometrial edema in prepubertal rats. Protection against estrogen-induced cell proliferation in uterus suggests the decrease of the risk for uterine cancer after hormone replacement therapy in climacteric women. Canisso et al. (2013) detected a reduction in endometrial edema during progestagen treatment, which returned to normal after cessation of treatment in cyclic mares. Witte et al. (2012) induced endometritis associated with increased amounts of intrauterine (i.u.) fluid or viscous mucus in estrus detected by ovarian follicle >3.0 cm and endometrial edema, which may contribute to low fertility in mares. Integrity of epithelium was not affected.

Conclusion

U-74389G administration hardly non-significantly decreases the EE within short-term time context of 2 hours. Perhaps, a longer study time may reveal clearer and more significant results. Also, a more detailed study of molecular pathway of antioxidant capacity involvement of U-74389G in edema is required.

Acknowledgment

This study was funded by Scholarship by the Experimental Research Center ELPEN Pharmaceuticals (E.R.C.E), Athens, Greece. The research facilities for this project were provided by the aforementioned institution.

References

Batra S, Sen R, Jain K, Gulati N (1995) Phase contrast microscopic evaluation of placental pathology in premature gestation. Indian J Pathol Microbiol 38(4):407-411.

Canisso IF, Gallacher K, Gilbert MA, Korn A, Schweizer CM, Bedford-Guaus SJ, Gilbert RO (2013) Preovulatory progestagen treatment in mares fails to delay ovulation. Vet J 197(2):324-328.

Canisso IF, Gallacher K, Gilbert MA, Korn A, Schweizer CM, Bedford-Guaus SJ, Gilbert RO (2013) Preovulatory progestagen treatment in mares fails to delay ovulation. Vet J 197(2):324-328.

Cayman Chem Prod Cat https://www.caymanchem.com/app/template/Product.vm/catalog/75860.

Gaete L, Tchernitchin AN, Bustamante R, Villena J, Lemus I, Gidekel M, Cabrera G, Astorga P (2012) Daidzein-estrogen interaction in the rat uterus and its effect on human breast cancer cell growth. J Med Food 15(12):1081-1090.

Gaete L, Tchernitchin AN, Bustamante R, Villena J, Lemus I, Gidekel M, Cabrera G, Carrillo O (2011) Genistein selectively inhibits estrogen-induced cell proliferation and other responses to hormone stimulation in the prepubertal rat uterus. J Med Food 14(12):1597-1603.

Ludwig H (1982) The morphologic response of the human endometrium to long-term treatment with progestational agents. Am J Obstet Gynecol 142(6 Pt 2):796-808.

Osmanağaoğlu MA, Kesim M, Yuluğ E, Menteşe A, Karahan SC (2012) Ovarian-protective effects of clotrimazole on ovarian ischemia/reperfusion injury in a rat ovarian-torsion model. Gynecol Obstet Invest 74(2):125-130.

Shi F, Cavitt J, Audus KL (1995) 21-aminosteroid and 2-(aminomethyl) chromans inhibition of arachidonic acid-induced lipid peroxidation and permeability enhancement in bovine brain microvessel endothelial cell monolayers. Free Rad Biol Med 19(3):349-357.

Sridhar MS, Bansal AK, Sangwan VS, Rao GN (2000) Amniotic membrane transplantation in acute chemical and thermal injury. Am J Ophthalmol 130(1):134-137.

Witte TS, Melkus E, Walter I, Senge B, Schwab S, Aurich C, Heuwieser W (2012) Effects of oral treatment with N-acetylcysteine on the viscosity of intrauterine mucus and endometrial function in estrous mares. Theriogenology 78(6):1199-1208.

Tsompos C, Panoulis C, Toutouzas K, Zografos G, Papalois A (2014) The effect of the antioxidant drug "U-74389G" on chloride during ischemia reperfusion injury in rats. Med Rev 50(2):40-44.

Volume 58(1):73-94, 2014
Acta Biologica Szegediensis
http://www.sci.u-szeged.hu/ABS

DISSERTATION SUMMARIES

Evaluation of the effect of unsaturated fatty acids and irradiation on U87 glioma cell line

Otilia Antal

Laboratory of Functional Genomics, Laboratories of Core Facilities, Biological Research Centre, Hungarian Academy of Sciences, Szeged, Hungary

Glioma is an invasive, aggressive form of brain tumors, with high rate of recurrence and resistance to radio and chemotherapy. Patients usually survive less than two years after diagnosis. The common treatment consists of surgical resection, followed with radiotherapy and/or chemotherapy. There is a great necessity for development of new therapeutic methods. Strategies are under development or clinical phase.

UFAs (unsaturated fatty acids) are one of the adjuvants that are applied as therapeutic agents for the treatment or alleviation of the symptoms of several diseases, like diabetic retinopathy, insulin resistance, inflammatory Bowel disease, cardiovascular diseases and several types of cancer. Numerous *in vitro* and *in vivo* studies prove the benefic effect of application of PUFAs (polyunsaturated fatty acids) as agents (solely or combined with chemo- or radiotherapy) in glioma therapy. Application of γ-linolenic acid on human glioma in clinical phase inhibited recurrence.

In order to determine the ideal type and concentration of UFAs as adjuvants in radiotherapy, we performed *in vitro* evaluation on U87 MG glioma cell line. We evaluated the effect of the following UFAs: arachidonic acid (AA, 20:4n-6), docosahexaenoic acid (DHA, 22:6n-3), gamma-linolenic acid (GLA, 18:3n-6), eicosapentanoic acid (EPA, 20:5n-3) and oleic acid (OA, 18:1n-9). Cells were treated with each fatty acid solely and in combination with 5 or 10 Gy.

We performed biochemical (LDH and MTS) and biophysical (RT-CES) assay to evaluate the effect of these fatty acids. We found that AA, DHA and GLA was more effective in sensitizing U87 cells to radiotherapy, so further experiments were performed with these three compounds, namely morphological, gene and miRNA expression analysis.

Statistical analysis of more than forty parameters based on holographic images was performed. Cell number and confluence was significantly diminished when they were treated with AA or when they were exposed to 10 Gy combined with AA, DHA or GLA. Application of PUFAs as adjuvants to 10 Gy caused significant alteration in cell thickness and irregularity, which indicate that cells have rounded and detached from the surface.

The molecular pathways that influence and determine the course of glioma when it is treated with UFAs (solely or in combination with radiotherapy) are not entirely deciphered yet. Thus, we decided to investigate the effect of AA, DHA and GLA at gene and miRNA expression level. Based on the scientific literature we have chosen to investigate gene expression on U87 cells that were solely PUFA treated or irradiated or co-exposed to PUFA and 10 Gy. We noticed significant alteration for at least one of these parameters in expression of endoplasmatic reticulum stress related genes (Grp78, DDIT3); genes which respond to oxidative stress (HMOX1, AKR1C1, NQO1), oncogenes (p53, c-Myc); early response genes (Egr1, TNF- , FOSL1, c-Fos); Gadd45a - a validated target in cancer treatment - and Notch1, a potential therapeutic target in glioblastoma. Out of the oxidative stress responsive genes that responded significantly to co-exposure to PUFA and 10 Gy HMOX1 is a potential target in glioma treatment, and NQO1 is a priority one.

Due to their small size and stability the study of the effect of miRNA on glioma therapy is an intensively investigated field (Low et al., 2014). We investigated the effect of AA, DHA, GLA and/or 10 Gy on U87 cells for the following miRNAs: miR34a, miR96, miR146, miR181a, miR148a, miR148b and miR152. Significant effect was noticed in case of miR146 and miR181a.

Our gene expression studies indicate that GLA and irradiation alter the expression of the therapeutic target Notch1 significantly. When 10 Gy is combined with AA, but not with DHA or GLA, changed the expression of several genes in a significant manner (p53, c-Myc, TNF-α and c-Fos). Our results confirm that UFAs are potent agents which enhance the effectiveness of radiotherapy.

Supervisor: László Puskás
E-mail: antalotilia@gmail.com

Synaptic changes in depression disorders

Judith Baka

Neuronal Plasticity Research Group, Institute of Biophysics, Biological Research Center of the Hungarian Academy of Sciences, Szeged, Hungary

Major depressive disorder (MDD) is predicted to become the leading cause of disability worldwide by the year 2030, representing an enormous financial and social burden. Clinical management of MDD is quite limited due mostly to the fact that the neurobiology of depression and the mechanisms of antidepressant therapy are still largely unknown.

Depression and stress are associated with the loss of hippocampal dendritic spines of principal cells, contributing to hippocampal dysfunction. Hippocampal neuroplasticity mechanisms have the potential to mediate rapid mood change. Because pyramidal cell spine synapse remodelling vitally influences hippocampal activity, we hypothesize that major depression are associated with loss of hippocampal spine synapses. Recently, we have confirmed the validity of the new "synaptogenic hypothesis" of depression by demonstrating an inverse correlation between the number of synapses in limbic brain areas and the severity of depressive symptoms, both in animal models and in human beings. It is hypothesized that loss of synapses in depression is, at least partly, caused by prolonged stress and the resultant glutamate excitotoxicity, which could be prevented by antagonizing glutamate release in response to stress. In addition to their anxiolytic, anticonvulsant, muscle-relaxant, and sedative/hypnotic effects, benzodiazepines, such as diazepam, strongly inhibit glutamate release at high, pharmacological doses.

Postpartum depression is a serious clinical problem that affects approximately 10-15% of postpartum women during the six-month period following childbirth. Symptoms of postpartum depression are similar to those of a major depressive episode, exerting a severe impact on family functioning and mother-infant relations in this critical period of life.

To test our theory that remodeling of hippocampal spine synapses also occurs in postpartum depression, we utilized a rat pseudopregnancy model. Ovariectomized CD(SD) rats were subcutaneously implanted with continuous release pellets, providing pregnancy levels of estradiol and progesterone. After 21 days, the hormones were withdrawn and the ensuing week was considered as the postpartum period. "Pregnant" and "postpartum" rats were tested in the learned helplessness paradigm and the number of their hippocampal spine synapses estimated using electron microscopic stereology. Inescapable stress caused a severe loss of spine synapses in "postpartum" animals, while there were no synaptic changes in "pregnant" females. In line with synaptic alterations, performance of "pregnant" rats was significantly better in the active escape test compared to "postpartum" animals.

We can conclude that maintaining pregnancy levels of estradiol and progesterone prevents the synaptic and behavioral effects of inescapable stress, suggesting that the sudden decrease in ovarian hormone levels after childbirth plays a major role in predisposing to postpartum depression.

Our result presents a series of experiments, investigating whether diazepam is able to prevent helplessness and to protect synapses in the learned helplessness (LH) model of depression. Diazepam, when administered intraperitoneally to ovariectomized female CD(SD) rats dose-dependently decreased depressive symptoms in LH and demonstrated synaptoprotective effects in electrophysiological and morphological measurements.

These findings further support the synaptogenic hypothesis of depression and suggest that synaptoprotective treatment is able to antagonize the negative effect of stress on mood, which may be useful in the clinical management of patients with recurrent and/or treatment-resistant depression.

Supervisor: Tibor Hajszán
E-mail: baka.judith@brc.mta.hu

Occurrence and importance of Aspergilli in agricultural products and clinical sources

Nikolett Baranyi

Department of Microbiology, Faculty of Science and Informatics, University of Szeged

Aspergillus species are filamentous fungi which are widespread on agricultural products in subtropical and tropical areas of the world. Aspergilli are able to produce a range of mycotoxins, which can be harmful to animals or humans, including aflatoxins, ochratoxins, fumonisins and patulin. *Aspergillus flavus* is also an important pathogen of various cultivated plants including maize, cotton and peanut, and cause serious yield losses throughout the world. Since aflatoxin production is favoured by moisture and high temperature, *A. flavus* is able to produce aflatoxins in warmer, tropical and subtropical climates. According to recent studies, climate change accompanied by global warming affects the occurrence of fungi and their mycotoxins in our foods and feeds. A shift has recently been observed in the occurrence of aflatoxin producers in Europe, with consequent aflatoxin contamination in agricultural commodities in several European countries not facing with this problem before (Italy, Serbia, Slovenia, Croatia, Romania, Ukraine). Although aflatoxin contamination of agricultural products is not treated as a serious threat to Hungarian agriculture due to climatic conditions, these observations led us to examine the mycobiota and mycotoxin content of different agricultural products (wheat, maize, chili pepper, nut, etc.) collected from different locations in Hungary and Vojvodina. The surface-sterilized products were placed on selective media, and the isolated fungal strains were identified using morphological and sequence-based methods.

Aspergillus strains are among the most common organisms causing fungal keratitis in tropical and subtropical areas. The main risk factor for the infection is trauma by vegetable matter during agricultural activities. Among *Aspergillus* species, mainly *A. flavus*, *A. terreus*, *A. fumigatus* and *A. niger* have been isolated from fungal keratitis cases. During our study, 52 *Aspergillus* strains isolated from keratitis cases in South India were examined. Based on morphological studies, all isolates were classified to the *A. flavus* species. For the molecular identification, part of the calmodulin gene was amplified and sequenced. As a result, 46 isolates were identified as *A. flavus*, while four as *A. tamarii*, one as *A. terreus* and one was found to belong to the *A. pseudotamarii* species. That was the first case that *A. pseudotamarii*

was identified from a human infection. Antifungal susceptibility tests of clinical isolates were carried out using disc diffusion and E-test methods. The detected antifungal susceptibility values were mostly within the value ranges determined previously for *A. flavus* isolates, although the *A. pseudotamarii* isolate proved to be more susceptible to amphotericin B than either *A. flavus* or *A. tamarii*. Aflatoxin producing abilities of the isolates were tested in YES culture media, and determined by HPLC analysis. Most of the examined *A. flavus* isolates carry the MAT1 mating-type gene.

Further investigations of the genetic variability of the *A. flavus* isolates by UP-PCR, microsatellite analysis and mating-type locus gene (MAT) analysis, and aflatoxin producing ability testing using an ELISA method are in progress.

Supervisor: János Varga
E-mail: nikolett.baranyi@gmail.com

The role of glutathione transferases in the stress tolerance of different plant species

Dániel Benyó

Plant Molecular Biology Group, Department of Plant Biology, University of Szeged, Szeged, Hungary

Physiological processes involved in detoxification have important role in agriculture (and so in plant biology), because plants are exposed to disadvantageous environmental conditions. Abiotic stressors, e.g. xenobiotics, heavy metals presented in the soil, and drought are able to launch the production of toxic by-products of metabolic processes (such as lipid peroxides) and harmful amount of reactive oxygen species in stress-exposed plants, which can cause reduced growth and decreased yields.

Glutathione transferases (GSTs) are a divergent enzyme family with two major *in vivo* detoxification functions in plants: conjugating toxic compounds with a glutathione molecule, thereby making them less harmful and promoting their compartmentalisation to the vacuole, and the glutathione-dependent peroxidase activity, which plays a role in maintaining membrane integrity under stress conditions. To examine the role of GSTs in the abiotic stress tolerance of different plant species, we used two experimental set-up.

First, two inbred lines of the cereal model organism *Brachypodium distachyon,* Bd21 and Bd21-3 were grown hydroponically, and were exposed to osmotic stress treatment for modelling drought stress. We observed the effects of osmotic stress to growth parameters, water status, enzymatic responses, and gene expression pattern of the plants. As results, we concluded that root growth of the *Brachypodium* lines differed (Bd21 had increased root growth, while it was reduced in Bd21-3). The water homeostasis of the two line were similar: both showed isohydric strategy during our experiments. We observed higher guaiacol peroxidase and glutathione transferase activities in line Bd21, and all examined enzymes showed induced activities during the osmotic treatment. For quantitative real-time PCR, six GST genes were selected based on our previous studies on wheat cultivars, expression data published in literature, and promoter sequence analysis. In line Bd21 we observed the induction of a wider range of genes under the osmotic stress, which indicates the importance of the selected genes in the detoxification process, and also suggests (according to the other parameters) that line Bd21 may be more tolerant to the applied osmotic treatment. In addition, we may conclude that both lines are highly resistant, compared to cereals previously studied in our research, so using *Brachypodium* lines for experimental purposes may give important results for cereal breeding.

Our other experimental system was equipped to examine the detoxification processes of bred poplar clones. Poplars (*Populus spp.*) are widely cultivated plants for their rapid growth and high biomass, and are increasingly used in scientific research as model organism of trees, and for phytoremediation purposes. Stress adaptation processes against heavy metals and osmotic stress were examined on three outstanding biomass producer poplar lines. Cuttings were grown hydroponically, and treated by copper, zinc, and polyethylene-glycol. We described the water potential of plants, the malondialdehyde content of shoots and roots, enzyme activities (guaiacol peroxidase, glutathione peroxidase, and glutathione transferase activities), amount of reactive oxygen (total intracellular ROS, superoxid radical) and nitrogen species (nitrogen oxide, peroxynitrite). Furthermore, we quantified the induction of ten transcripts, which probable are fundamental parts of the poplars stress adaptation processes. Among these were four glutathione transferases, two ABC transporters, three metallothioneins, and a phytochelatine synthase. Our results shows, that all three poplar clones are efficient in stress adaptation, but this properties have different molecular backgrounds. *P. deltoides* clones B-229 and PE 19/66 showed slightly lower water potential during zinc and hyperosmotic treatment, and in all treatments, they have significantly lower glutathione transferase activities, than *P. x canadensis* clone M-1. By contrast, B-229 and PE 19/66 clones are more effective to induce the gene expression of various components of the detoxification process, such as the GSTs. Based on our research, *P. deltoides* clones may be well utilized for phytoremediation purposes on heavy metal contaminated sites with good water supply, but under osmotically inappropriate circumstances further research needed to understand acclimatization processes.

During our work, evidence was found for the important role of GSTs in the stress responses of *Brachypodium* and *Populus*.

Supervisor: Ágnes Gallé
E-mail: benyo.daniel@gmail.com

Volume 58(1):73-94, 2014
Acta Biologica Szegediensis
http://www.sci.u-szeged.hu/ABS

Ecophysiological characterisation of a biocontrol *Bacillus subtilis* strain

Bettina Bóka

Department of Microbiology, University of Szeged, Szeged, Hungary

As conventional chemical pesticides considerably increase the environmental load of agricultural areas, serious efforts are made to find and develop effective biocontrol agents with no ecotoxicological risks. Good extracellular enzyme and antibiotic producing microorganisms could be excellent antagonists of phytopathogenic fungi and bacteria. *Bacillus subtilis* is a Gram positive, aerobic, endospore-forming, soil bacterium, which is able to produce various antibiotics and a broad spectrum of extracellular enzymes. This bacterium may produce various non-ribosomal oligopeptides, such as iturin, surfactin and fengycin. These cyclic lipopeptides have both antifungal and antibacterial effects. Previously, elevated protease and -amylase secretion was reported by Kurosawa et al. (2006) from streptomycin resistant *B. subtilis*. This phenomenon appeared in connection with spontaneous mutations in the *rpsL* gene encoding the ribosomal protein S12. The aims of our study were *(1)* to make an ecophysiological characterization of the isolated *B. subtilis* strain and *(2)* to prove the effectiveness of the simple approach of Kurosawa (2006) for generating a series of biocontrol strains without the need for induced genetic modification of the original bacterium.

After isolating several bacteria from soil samples and rhizosphere of tomato, the isolates were identified based on the partial sequencing of the *gyrA* gene. Sequence of the whole genome of one strain (B23), which showed the best biocontrol abilities, was determined and compared with the that of the *B. subtilis* type strain (DSM-10). Antibiotic production of the two strains was also compared by TLC analysis. By sequence analysis, several single-nucleotide polymorphisms were found in various genes involved in the antibiotic production. These changes are suggested to be responsible for the enhanced antibiotic production of the newly isolated strain.

From the B23 isolate, spontaneous streptomycin resistant colonies were selected. Chymotrypsin-type protease activity in the ferment broths of the streptomycin resistant strains were determined and compared with the B23 strain. From the 20 tested mutants the K2 strain was outstanding with its fourfold chymotrypsin producing activity. Among the spontaneous streptomycin resistant mutants, six showed significantly enhanced tyrosine-containing antibiotic production. *In vitro* antagonism of the B23 strain and its streptomycin resistant mutants against phytopathogenic microorganisms and some mycotoxin producing fungi were characterized. Elevated inhibition zones were detected in case of some important pathogens. Effect of metal ions (*i.e.* cadmium, copper, manganese, nickel and iron) and pesticides (*i.e.* 2,4-dichlorophenoxyacetic acid, carbendazim, chlortoluron and linuron) to the enzyme production and activity were also examined. Manganese had positive effect on the enzyme production, while the presence of pesticides had no inhibitory effect. Analysis of the antibiotic profiles in the presence of metal ions and pesticides produced very similar results. Effect of the carbon and nitrogen sources on the production of antibiotics was tested. Saccharose, glycerol, cellobiose, starch, Na-nitrate and proline elevated the production rate of the tyrosine containing antibiotics.

Kurosawa K, Hosaka T, Tamehiro N et al. (2006) Appl Environ Microbiol 72:71-77.

Supervisor: László Manczinger
manczing@bio.u-szeged.hu

Investigation of redox homeostasis and elements of abiotic stress responses in *Arabidopsis* model plant

Szilvia Brunner

Department of Plant Biology, University of Szeged, Szeged, Hungary

The growth and yield of plants are highly dependent on environmental factors. The extremes of these conditions act as stressors leading to the formation of reactive compounds in the cells and to the imbalance of redox homeostasis. Adequate stress responses may restore the redox balance. Growing evidence suggests a model for redox homeostasis in which the reactive oxygen species (ROS)-antioxidant interaction acts as a metabolic interface for signals derived from metabolism and from the environment during stress.

The aim of my research was to explore the elements of defence mechanism, with focus on the redox re-establishment of redox homeostasis. In this work, the effect of salicylic acid (SA) and salt stress were investigated using *Arabidopsis thaliana* L. Columbia ecotype (wild type), glutathione reductase (*gr*) and dehydroascorbate reductase (*dhar*) mutant lines which grown in hydroponics. In order to increase salinity tolerance, as a priming effect, plants were pretreated with 10^{-9}-10^{-4} M SA followed by 100 mM NaCl in long-term experiments.

The stress induces serious metabolic perturbations in plants, as it generates ROS which disturb the cellular redox system. In this study we examined the viability of cells and ROS level and its derivatives by fluorescent dyes. We determined the levels of antioxidants and the activities of some antioxidant enzyme such as total ascorbate (Asc) and reduced (GSH) and oxidized (GSSG) glutathione, glutathion reductase (GR) and dehydroascorbate reductase (DHAR), which are protecting plants against ROS damages. The amounts of Asc and GSH increased under stress conditions mainly at 10^{-7}-10^{-5} M SA concentrations also at mutants lines. In addition, maintaining a high ratio of GSH/GSSG showed to play an important role in SA and salt tolerance of *Arabidopsis* wild type and mutants. The activities of GR and

DHAR enzymes also contributed and helped to maintain the cell balance under stress conditions.

Most importantly, antioxidants provide essential information on cellular redox state and they influence gene expression associated with abiotic stress responses to maximize defense. We analyzed also the expression levels of GR and DHAR genes by real-time-PCR with focus on the role of GR and DHAR izoenzymes and our data also showed changes in their transcript levels under stress conditions and in the acclimatization process.

Redox reactions are the fundamental metabolic processes through which cells convert and distribute the energy that necessary for growth and maintenance. *Arabidopsis* plants transformed with a redox-sensitive GFP (roGFP) targeted to the cytosol (c-roGFP1) were used for monitoring the real-time redox status of the cytosol in SA and salt stressed plants. Utilization a flourometer to detect redox-related changes of roGFP has been demonstrated. The utilization of a fluorimeter enables the processing of many samples and it averages the whole tissue rather than only few cells within a tissue, as in the case of confocal imaging.

It is concluded that constitutively high level of reduced GSH are advantageous to act as a strong buffer against ROS but would make the system less responsive to changes in redox potential that may be needed to upregulate the inducible defence components. In this study we have adapted fluorometer reading and compared this assay with confocal imaging. Nevertheless, the data showed that roGFP is redox sensitive in plant cells and that sensor makes it possible to monitor, in real time, dynamic changes in redox homeostasis *in vivo*. During long-term experiments, we were able to apply this technology in combination with many aspects of the antioxidant defence system measurements to the analysis of redox changes in response to stresses or to various mutants.

Supervisor: Jolán Csiszár
E-mail: brunner.szilu@gmail.com

Protecting roles of 27 kDa heat shock protein Hsp27

Balázs Csibrány

Laboratory of Animal Genetics and Molecular Neurobiology, Institute of Biochemistry, Biological Research Center of the Hungarian Academy of Sciences, Szeged, Hungary

Hsp27 belongs to the small heat shock protein family, which are ATP-independent chaperones. The most important function of Hsp27 is based on its ability to bind non-native proteins and inhibit the aggregation of incorrectly folded proteins maintaining them in a refolding-competent state. Additionally, it has anti-apoptotic and antioxidant activities.

Several studies have shown cytoprotective effects of Hsp27 against reactive oxygen species. Doxorubicin is a widely used chemotherapeutic agent against several types of cancer. Beside it's cytostatic properties, doxorubicin has a severe cardiotoxic side effect. To study the cardioprotective effect of Hsp27 *in vivo*, a transgenic FVB mouse strain overexpressing the human Hsp27 protein was established. Transgenic mice and their wild type littermates were injected with a single dose of doxorubicin, control animals were treated with saline. We detected significant level of apoptosis in cardiac tissues of doxorubicin treated wild-type mice using caspase-3 immunhistochemistry and TUNEL (terminal deoxynucleotidyl dUTP nick end labelling) assay. However, the number of apoptotic cells were substantially reduced in Hsp27 overexpressing transgenic hearts. Caspase-3 western blot analysis also confirmed the cardioprotective effect of Hsp27 against doxorubicin. Using qPCR analysis, we found significant increase in the expression of proteasomal genes in wild-type hearts after doxorubicin treatment. mRNAs of proteasome subunit 3, Psmc3 interacting subunit and ubiquitin conjugase 4 showed the most remarkable increases. However, overexpression of Hsp27 did not repressed the expression of these genes, suggesting that cytoprotective effect of Hsp27 is not directly linked to proteasome function.

Hsp27 has well known neuroprotective effect as well. Previously, using APPxPSe1xHsp27 triple transgenic mice we have shown that overexpression of Hsp27 protein ameliorates certain symptoms of Alzheimer's disease. Alzheimer's disease (AD) model mice overexpressing Hsp27 showed reduced number of amyloid plaques and improved presynaptic and cognitive functions. In order to clarify the molecular role of Hsp27 in amyloid plaque number reduction, we monitored the gene expression of several genes potentially involved in ß-amyloid metabolism such as APP, ApoA1, ApoD, ApoE, LDLr, Lrp1, Lrp2, Hsp90, and neurodegeneration (NOS1 and NOS2) in the cortex of Hsp27 transgenic mice using qPCR. Expression levels of ApoD and Lrp2 were slightly increased (128% and 128%, respectively), in the brain of Hsp27 transgenic mice compared to wild type controls (100%), whereas there was no change in the mRNA level of APP, ApoE, LDLr, Lrp1, Hsp90, NOS1, and NOS3. Rather surprisingly, cortical expression of ApoA1 was reduced by half in Hsp27 transgenics versus wild type mice. Decreased ApoA1 expression in Hsp27 transgenic mice was further confirmed using western blotting. ApoA1 protein level was reduced in Hsp27 transgenic mice (61.1%), but slightly elevated in AD model mice (126.7%) compared to wild types (100%). However, AD mice overexpressing human Hsp27 protein possessed similar ApoA1 protein level than wild type mice, indicating that Hsp27 influenced ApoA1 expression .

A less studied aspect of Hsp27 mediated cell protection is its possible role in DNA repair mechanisms. Heat shock protein 27 have been reported to be overexpressed in various cancers and to associated with poor prognosis for survival in patients with cancer. Association of Hsp27 with UV light- and radiosensitivity in cancer cells was also shown by several studies. Phosphorylated Hsp27 can stimulate pentose phosphate pathway (PPP) via binding and activating glucose-6-phosphate dehydrogenase (G6PD). PPP is responsible for producing nucleotide precursors for DNA repair, and G6PD-deficient cells are impaired for DNA double strand break (DSB) repair. To study the possible

role of Hsp27 in DSB repair mechanisms, qPCR analysis of non-homologous end-joining (NHEJ) and homologous recombination (HR) associated genes was performed. Total RNA was isolated and reverse transcribed from Hsp27 overexpressing B16 mouse melanoma cells as well as wild type B16 cells, then primer pairs for 32 different genes were used in qPCR analysis. We detected increased expression of breast cancer protein 2 (BRCA2) (222%), replication protein A3 (RPA3) (241%) and aprataxin (APTX) (192%) in Hsp27 overexpressing B16 cells compared with wild type B16 cells. Further analyses of protein expression of these genes are necessary in Hsp27 overexpressed and silenced B16 cells, in order to understand better the multiple role of Hsp27 in cancer.

Supervisor: Miklós Sántha
E-mail: santha.miklos@brc.mta.hu

Regulation of protective proline synthesis during reactive carbonyl stress

Aleksza Dávid

Laboratory of Molecular Regulators of Plant Growth, Department of Plant Biology, Hungarian Academy of Sciences, Biological Research Centre, Szeged, Hungary

Enviromental stresses impact on all aspects of plant architecture and represent a serious challenge for developing sustainable agriculture at a time of significant growth in the global population. To cope with these stresses, plants have evolved a wide spectrum of molecular programs to sense change rapidly and adapt accordingly. Understanding, and - if it is possible – improving these reprogramming events under constantly changing environmental conditions has been a subject of great interest.

Plants have evolved diverse strategies of acclimatization and avoidance to cope with adverse environmental conditions. Proline, as free amino acid is common among stress-induced metabolites and has been shown to accumulate during different environmental stresses including drought, salinity, and oxidative stress; moreover proline level responses to certain biotic stresses. Several protective functions were attributed to proline, such as scavenging ROS, acting as osmoprotectant and maintenance of redox equilibrium. Due to its action as singlet-oxygen quencher and scavenger of OH• radicals, proline is able to stabilize proteins, DNA and membrans. The in vitro use of reactive carbonyls, like methylglyoxal or glycolaldehyde is a straightforward method to imitate the ROS mediated in vivo damages. To comfirm this theory, we examined the protective effects of proline on glycolaldehyde treated lactate-dehydrogenase. In these experiments, we used protein oxidation assay and *in vitro* activity measurements. We can conclude that proline can not directly protect this enzyme from oxidation in *in vitro* assays. Several *in vitro* enzyme activity measurements showed, that proline can protect that enzyme activity and may be it interact directly with the reactive carbonyl. The *in vivo* experiments were carried on *Arabidopsis thaliana* (Columbia ecotype). In *A. th*aliana the synthesis of prolin is perfomed by two enzymes, the P5CS2 acts as a housekeeping enzyme and the P5CS1 is the stress-induced one which is int he centre of our interest. Earlier in silico analyses showed that in the *P5CS1* promoter, transcription factor binding sites from G-Box and MYB families can be found. The yeast one-hybrid system is a powerful method to identify heterologous transcription factors that can interact with a specific regulatory DNA sequence of interest. In the course of the experiments on this gene we focused on its methylation pattern too, because these posttranscriptional modifications can cause significant alterations in gene expression. In the promoter fragment of P5CS1 next to the potential transcriptional factor binding sites, a theoratical small RNA binding site and a potential methylation site were identified. By the McrBc digestion of isolated plant DNA followed by PCR, we can make the methylation profile of the promoter and the gene body. Therethrough we can conclude that the abovementioned DNA fragment is the mostly methylated region of the promoter, may be it has an important role in the regulation of gene expression. We can alternate the methylation pattern by treating the plants with 5-azacitidine in vivo. This way we can have a more focused point on the relation between the methylation set(status) of the gene and its expression level. These results suggests that the methylation pattern of *A. thaliana* P5CS1 shows a dinamic phenomenon upon development and stress response.

Supervisor: Gábor V. Horváth
Email: aldoaat@gmail.com

Sulfide oxidizing enzymes in a purple sulfur photosynthetic bacterium

Ágnes Duzs

Department of Biotechnology, University of Szeged, Szeged, Hungary

Phototrophic purple sulfur bacteria can utilize various reduced inorganic sulfur compounds (e.g. sulfide) as electron donor during anoxygenic chemoautotrophic photosynthetic growth. In these bacteria, flavocytochrome c and sulfide quinone oxidoreductase proteins oxidize sulfide to sulfur and supply the electrons into the photosynthetic electron transport chain. These ancient enzymes belong to the disulfide oxidoreductase protein family. Flavocytochrome c (Fcc) is a periplasmic enzyme consisting of a large sulfide-binding flavoprotein (FccB)

and a smaller, heme c binding cytochrome c subunit (FccA). Sulfide quinone oxidoreductases are monomeric membrane-bound flavoproteins which present in all domains of life. Sqr can transfer electrons from sulfide directly into the membrane quinone pool while Fcc reduces periplasmic c-type cytochrome proteins.

Thiocapsa roseopersicina is a photosynthetic purple sulfur bacterium. Three genes encoding sulfide oxidizing disulfide oxidoreductases were identified in the genome sequence: *fcc*, *sqr* and *sqn*. The Sqr and Sqn belong to group IV and group VI of the Sqr-type proteins, respectively. A detailed comparative biochemical, structural and functional analysis of these proteins is in the focus of this study.

The FccAB complex, the FccB, the Sqr and the Sqn proteins fused to Strep II affinity tag were expressed in *T. roseopersicina* strains. The recombinant flavocytochrome c variants and the Sqn enzyme could be purified to homogenity by affinity chromatography. In the absorption spectra of the oxidized and reduced forms of FccB, FccAB and Sqn, characteristic peaks of redox active flavin prosthetic group were identified. The flavin moiety apparently bound covalently to the proteins. The flavocytochrome c had also a redox active heme cofactor non-covalently bound to the FccA subunit. The Fcc variants were subjected to ultrafast fluorescence kinetic measurements in order to determine the interaction between the FAD cofactor and the protein. The affinity purified recombinant FccAB could oxidize sulfide and was able to reduce bovine heart cytochrome c at low sulfide concentrations. The temperature and pH dependences of the activity of the recombinant Fcc complex were determined: the optimal temperature was 45 °C while the optimal pH was 8.0. The FccAB was a moderately thermostable enzyme which had remarkable activity up to 60 °C. The recombinant Sqn and Sqr catalyzed the sulfur-dependent quinone reduction. The temperature and pH optima of quinone reductase activity of the Sqn were the same as determined for FccAB. Kinetic analysis of the Sqn activity at various pH revealed a lag phase preceding the reaction at high pH. This might mean that the enzyme needed activation for being able to reduce quinones at alkaline conditions. Additionally, the macromolecule structure of the Sqn was analyzed to explore the connections between the quaternary structure and the catalytic properties of the protein. Enzyme kinetic parameters of the Sqn disclosed that the enzyme affinity for sulfide was low as compared to other well-known sulfide quinone oxidoreductases. Consequently, Sqn might play role in the sulfide oxidation at high sulfide concentration. In contrast, the FccAB could have important function at low sulfide concentration in the sulfur metabolism in *T. roseopersicina*. The structural and functional analyses of the wild and mutant flavocytochrome c might lead to better understanding of the structure/function relationships of the disulfide oxidoreductase protein family. On the other hand, the biochemical and biophysical characterization of the Sqn should disclose specific properties of the group VI. of the Sqr-type proteins.

Supervisor: Gábor Rákhely, András Tóth
E-mail: duzs.agnes@gmail.com

Heavy metal induced nitro-oxidative stress in *Brassica* species

Gábor Feigl

NO-signalling group, Department of Plant Biology, University of Szeged, Szeged, Hungary

Copper (Cu) and zinc (Zn) are essential micronutrients, which can be present in soils naturally or can be accumulated in the environment due to anthropogenic activities. Cu is a redox-active element, directly inducing the formation of reactive oxygen species (ROS) leading to oxidative stress. Zn, on the other hand, is a non-redox-active element, causing oxidative stress indirectly by the modulation of antioxidant capacity. Moreover, in excess, both metal trigger changes in the metabolism of reactive nitrogen species (RNS), such as nitric oxide (NO) and peroxynitrite ($ONOO^-$) leading to nitrosative stress. The oxidative and nitrosative signalling interact with each other resulting nitro-oxidative stress during which the cellular functions damage by lipid peroxidation and nitration, protein carbonylation, tyrosine nitration and S-nitrosylation.

The primary goal of my study was to determine the degree of nitro-oxidative stress in two metal tolerant *Brassica* species exposed to Cu or Zn. Furthermore, I wanted to draw conclusions about the Cu- and Zn tolerance and phytoremediation usability of the species.

Nine-days-old hydroponically grown *Brassica juncea* and *Brassica napus* were treated with 0 (control), 10, 25 and 50 μM $CuSO_4$ or 0 (control), 50, 150 and 300 μM $ZnSO_4$ in nutrient solution for 7 or 14 days. Changes in microelement contents, formation of different ROS and RNS, cell viability, lipid peroxidation, cell wall alterations and enzymatic- and non-enzymatic antioxidants were examined in the root system.

Most of the Cu and Zn taken up by the plants were retained in the roots; however, the increment of Cu and Zn content within the *Brassica* shoots indicated an efficient translocation. Both metals in excess markedly modified the microelement homeostasis of *Brassica* plants. Both Cu and Zn treatment caused significant morphological alterations in the root system of *Brassica* species, e.g Cu and Zn were able to increase the lateral root number, especially in *B. juncea*, which may be part of a morphological adaptation process. A Cu concentration-dependent decrease of cell viability was also found after both 7 and 14 days of treatment; however in short term *B. juncea* root meristem did not show Zn-induced viability loss. Also, cell wall alterations were notable, since intensified lignification and callose formation were detected in the root system of Cu-stressed plants; however excess Zn caused only increased callose deposition.

Exposure to Cu induced nitric oxide generation in the root tips and this event proved to be dependent on the duration of the exposure and on the plant species. In short-and long-term treatments, *B. juncea* showed more significant activation of superoxide dismutase (SOD), inhibition of ascorbate peroxidase (APX) and oxidation of ascorbate (AsA) than *B. napus*. Moreover, hydrogen peroxide (H_2O_2)-dependent lignification was also observed in the Cu-exposed plants. In longer term, significant AsA accumulation and callose deposition were observed,

reflecting serious oxidative stress in *B. juncea*.

Due to the short-term Zn stress, SOD and APX showed higher activities in the roots of *B. juncea* keeping the amount of superoxide anion ($O_2^{\cdot-}$) and H_2O_2 at a control-like or lower level. Contrary, NO and $ONOO^-$ showed significant accumulation as the effect of Zn exposure. Despite the elevation of $ONOO^-$ levels, there was no detectable lipid peroxidation, which may indicate that it has a role in stress tolerance in *B. juncea* roots.

In the background of the serious growth inhibition and the viability loss of *B. napus* roots severe oxidative stress was observed: despite the elevated SOD activity $O_2^{\cdot-}$ accumulated, while the cells failed to eliminate the formed H_2O_2 because of the reduced APX activity. Moreover, a remarkable lipid peroxidation was visualized in the roots.

Long-term Zn excess caused oxidative and nitrosative stress in both species and despite their higher level in *B. juncea* root tips, it proved to be more tolerant according to the growth parameters.

Based on the morphological and physiological results, I conclude that *B. napus* tolerates Cu excess better than *B. juncea*. In contrast, *B. juncea* possesses elevated Zn tolerance compared to the other species. My results support the species-specificity of metal tolerance.

Supervisors: László Erdei, Zsuzsanna Kolbert
E-mail: fglgbr@gmail.com

Study of cuckoo-host relationships on a great reed warbler population in Hungary

Nikoletta Geltsch

Department of Ecology, University of Szeged, Szeged, Hungary

The brood parasitic common cuckoo (*Cuculus canorus*) lays its eggs to nests of other bird species, where the foster parents incubate, hatch and feed the cuckoo. A typical host species is the great reed warbler (*Acrocephalus arundinaceus*), breeds in wetland areas in Hungary, and builds open nest in reed beds. The modal clutch size of great reed warblers is 5 eggs and incubation time is about 11-12 days. We investigated several aspects of ecological relationships between common cuckoos and great reed warblers, including behavioural and evolutionary adaptations. However, we also applied microbiological and molecular methods.

In our first study, we examined bacterial loads on the eggshells of common cuckoos and great reed warblers. During our field work we collected samples from the eggshell surface of both cuckoo and great reed warbler eggs, either from parasitized and non-parazitized clutches to compare bacteria of the eggshells. We hypothesize that cuckoos, as nest visitors, may influence on the hygiene of nests of great reed warblers by changing bacteria loads. Previous studies showed that environmental factors, such as temperature and humidity, may affect bacterial loads on the eggshells in cavity nesting birds. We hypothesized that these environmental factors also affected the hygiene of open nests of great reed warblers. From these factors we measured ambient light conditions, both in the visible and UV spectra.

Keeping eggs dry in avian nests during the incubation period may reduce bacteria load on the eggshells, so it may protect the eggs from bacterial infections. A few previous studies have already showed the antimicrobial effects of incubation in cavity nesting birds, but, in the first time, we studied these effects under more variable environmental conditions, on an open-nesting bird species.

During the co-evolution arms race between common cuckoos and great reed warblers both the brood parasites and hosts developed ecological adaptations. The adaptations developed by the brood parasite help successful parasitism (e.g. "mimetic eggs"), but the adaptations by the hosts are against the brood parasites ("antiparasite adaptations", e.g. egg discrimination). We evaluated the changes of eggshell spottiness of common cuckoos and great reed warblers in time. Previously, we photographed parasitized clutches of host eggs held in museum collections (Natural History Museum, Tring, Mátra Museum, Gyöngyös, and Hungarian Natural History Museum, Budapest), and we also took digital photos during our field work. All eggs were collected from Hungary. We had four treatments from the years of 1900s, 1930s, 1960s, and 2000s. For analysing images we used ImageJ and Matlab programs. We wanted to reveal how spottiness changed in common cuckoos and great reed warblers. We analysed these changes by statistical pattern analysis on eggs from the last hundred years, focusing on cuckoo egg mimicry to host eggs.

The study was supported by the European Union and the State of Hungary, co-financed by the European Social Fund in the framework of TÁMOP-4.2.4.A/ 2-11/1-2012-0001 'National Excellence Program'.

Supervisor: Csaba Moskát
E-mail: moskat@nhmus.hu

Volume 58(1):73-94, 2014
Acta Biologica Szegediensis
http://www.sci.u-szeged.hu/ABS

Investigation of South-Indian *Fusarium* isolates from human keratitis

Mónika Homa

Department of Microbiology, University of Szeged, Szeged, Hungary

The genus *Fusarium* is a large group of hyaline filamentous fungi. They are widely distributed in soil as harmless, saprophytic organisms. However, some members of this genus are capable of causing infection in plants, animals and humans. *Fusarium* spp. are the most frequently isolated causative agents of human keratomycosis in South India. Antifungal susceptibilities of different *Fusarium* species complexes (SCs) vary, and members of the *F. solani* SC (FSSC) show remarkable resistance to most clinically applied antifungal drugs. Thus the misidentification of the causative agent and the subsequent application of an inappropriate antifungal therapy could result in the loss of vision. Using molecular techniques in laboratory practice instead of conventional morphological methods can make the identification process more accurate and faster. New antifungals and alternative treatments would also be appropriate to prevent or treat the infection.

For these reasons, first we identified *Fusarium* strains isolated from human keratomycosis at the Aravind Eye Hospital and Postgraduate Institute of Ophthalmology (Coimbatore, India) in the years 2004-2005 and 2010-2011 using different molecular methods. We also examined the SC diversity between the two sampling periods. Our results indicate that the members of the FSSC are the most frequently isolated species from keratomycosis in South India, and the incidence of the less frequent human pathogenic *Fusarium* species seems to be increasing.

We also determined and compared the antifungal susceptibilities of the previously mentioned strains. Natamycin (NTM) proved to be the most effective drug against the tested isolates, followed by amphotericin B and terbinafine (TRB). Changes in the minimal inhibitory concentration (MIC) values of NTM and TRB were not observed between the isolates derived from the two sampling periods, but the *in vitro* susceptibility to azoles decreased up to 2011. NTM and TRB were also applied in antifungal combination susceptibility tests because of their high *in vitro* efficacy and their differing antifungal mechanisms. These compounds together showed a similar or a better antifungal activity on Fusaria than each of the compounds alone, as they could interact synergistically.

As a potential alternative cure for the infection, we examined the *in vitro* inhibitory effect of 9 different essential oils on 18 *Fusarium* strains isolated from keratitis. The lowest MICs were observed in the case of *Cinnamomum zeylanicum* oil; and its component, trans-cinnamaldehyde (tCA) was also tested and showed the same activity against the investigated isolates. The *in vitro* interaction between tCA and NTM was also determined. Furthermore, we investigated the antifungal mechanism of cinnamon oil and tCA by microscopic observations. Based on these observations both the oil and its component caused delayed or inhibited germination of conidia and reduced cellular metabolism. Thus, they can be potentially used in the treatment of *Fusarium* keratitis. However, the preliminary *in vitro* studies suggest that their simultaneous application with antifungal drugs, such as NTM, will not increase the efficacy of the therapy.

The investigation of phylogenetic relationships among clinical and environmental isolates and the production of extracellular enzymes, as potential virulence factors, are in progress.

The research of M.H. was supported by the European Union and the State of Hungary, co-financed by the European Social Fund in the framework of TÁMOP 4.2.4.A/2-11-1-2012-0001 'National Excellence Program'. The relating research groups were also supported by the INSA-HAS interacademic bilateral project (SNK-49/2013) providing infrastructure and research equipment.

Supervisors: László Galgóczi, László Kredics
E-mail: homamoni@gmail.com

Up-regulation of defense genes in pepper leaves inoculated with tobamoviruses

Csilla Juhász

Plant Protection Institute, Centre for Agricultural Research, Hungarian Academy of Sciences, Budapest, Hungary

Virus infections result in substantial alterations of gene expression patterns in infected plant tissues including the up-regulation of a wide variety of defense-related genes. These defense reactions are controlled by a complex, multilayered regulatory network in which various transcription factors and defense-related plant hormones play critical roles. In addition, host intracellular membrane lipids also substantially influence virus replication. Upon infection, tobamoviruses induce substantial modifications in intracellular host membranes in order to create protected viral replication compartments. During this process the structure of membrane lipid bilayers is substantially modified. Viral RNA synthesis is highly sensitive to lipid composition and particularly to the level of unsaturated fatty acids.

In recent years our research has been focused on the defense reactions of pepper (*Capsicum annuum* L.) plants following virus inoculations. We have used two different viruses in order to compare compatible and incompatible pepper-virus interactions. Inoculation with *Obuda pepper virus* (ObPV) led to the appearance of hypersensitive necrotic lesions on the inoculated leaves. In contrast, very mild symptoms appeared on the leaves inoculated with *Pepper mild mottle virus* (PMMoV). Although these plants seem to be healthy, the virus is spreading from the infection site into the whole plant causing very serious stunting and the pepper fruits will be very strongly distorted.

Volume 58(1):73-94, 2014
Acta Biologica Szegediensis
http://www.sci.u-szeged.hu/ABS

ObPV-inoculation resulted in the marked up-regulation of genes encoding PR-proteins, a patatin-like lipase (lipid acil hydrolase), a defensin, a 1-aminocyclopropane-1-carboxylic acid (ACC) oxidase and a dioxygenase participating in carotenoid degradation. In addition, ObPV-inoculation led to a rapid and massive up-regulation of several individual 9-lipoxygenase (*9-LOX*) genes. In contrast, *13-LOX* genes were only moderately induced by ObPV. The expression of several genes encoding WRKY transcription factors were also induced by ObPV. In contrast, the expression of defense genes increased in most cases to a lesser extent in PMMoV-inoculated, susceptible leaves or in mock-inoculated leaves. Plant hormones and an ethylene precursor (salicylic acid, methyl-jasmonate, and ACC) induced very differently the expression of individual *LOX* and *WRKY* genes.

In summary, our results showed that the rapid and massive up-regulation of defense genes encoding PR-proteins, LOXs and WRKY transcription factors in the incompatible pepper-ObPV interaction contributes to antiviral resistance. We suppose that by the rapid up-regulation of *9-LOX* genes pepper plants are able to alter the structure of intracellular membranes in order to inhibit the replication of invading tobamoviruses.

Supervisor: Gábor Gullner
E-mail: juhasz.csilla@agrar.mta.hu

Investigation of the different mechanisms of the innate immune response of *Drosophila melanogaster*

Beáta Kari

Immunology Unit, Institute of Genetics, Biological Research Centre of the Hungarian Academy of Sciences, Szeged, Hungary

Drosophila melanogaster has been widely used model organism to study host response to microbial and parasitic infections. The chitin cuticle of the adult *Drosophila* is the first barrier against microbial invasion. Injury of the cuticle activates hemolymph clotting, which blocks the loss of body fluids and the spreading of the microorganisms into the hemocoel by immobilizing bacteria at the wound site. Pathogens entering the hemocoel activate both cell-mediated and humoral immune responses. The cell-mediated arm of the immune response is carried out by the hemocytes, the production of antimicrobial peptides are regulated by the Toll and the immune deficiency (Imd) pathways.

We developed and validated a new method to identify novel factors involved in the hemolymph coagulation and in the host-pathogen interactions after septic injury.

The method, based on inducing lesion by removing the tarsal segments of the first pair of legs of *Drosophila* adults and exposing them to different bacteria, imitates injury that often occurs in the natural habitat. The technique was validated by using mutant variations of different components of the immune response; blood clotting as well as the involvement of a number of genes known to be instrumental in the humoral and cell-mediated immune responses of *Drosophila* was confirmed. We used the slightly pathogenic *E. coli*, the semi-pathogenic *B. cereus* and the highly pathogenic *S. marcescens* and monitored the viability of the flies. First, we tested the survival of the control w^{1118} and mutant flies after sterile injury and the survival of the non-injured w^{1118} and mutant lines (spz^2/spz^4, $Dredd^{EP1412}$, Rel^{20} and Hml^{f03374}) treated with *E. coli, B. cereus* and *S. marcescens*. We found that the survival of non-injured mutant flies treated with *E. coli, B. cereus* and *S. marcescens* were similar. The injury itself do not affect the survival of the animals, except for the Hml^{f03374} homozygotes, which lose more hemolymph after wounding and showed decreased survival rate following both sterile and septic injury compared to the control. We found that the Imd pathway mutants $Dredd^{EP1412}$ and Rel^{E20} and the hemolymph clotting factor *Hemolectin* (Hml^{f03374}) mutant flies showed reduced viability after either *B. cereus* or *E. coli* infection, while the *spätzle* (spz^2/spz^4), involved in the Toll pathway, was significantly sensitive to *B. cereus* infection. By using this novel method, we have found that the *raspberry* gene is involved in the survival of the fly after septic injury, since the mutants have decreased survival rate after *B. cereus* infection. This gene encodes the *Drosophila* inosine monophosphate dehydrogenase, and is a key enzyme of the *de novo* synthesis of guanine nucleotides. In mammals, *de novo* GMP synthesis is required for lymphocyte proliferation and in the immune response. We will study the function of the *raspberry* in the immune response of the *Drosophila*.

Our new method is suitable for high-scale screening of key factors involved in host-pathogen interactions following a septic injury. It also offers an alternative to previous experiments, where microinjection needle were used to administer microbes into the body cavity. A major advantage of this method is that the wound by itself is insignificant, the effect on survival can be attributed entirely to the infection and the defensive capabilities of the host organism.

Furthermore, we identified a new marker molecule 3A5 in the cytoplasm of a subset of plasmatocytes in all hematopoietic compartments, in the circulation, in the lymph gland and in the sessile tissue and in the hemolymph. We study the function of 3A5 molecule in the *Drosophila* immune response and in the coagulation reaction.

Supervisor: Éva Kurucz
E-mail: kari.beata@brc.mta.hu

Volume 58(1):73-94, 2014
Acta Biologica Szegediensis
http://www.sci.u-szeged.hu/ABS

Analysis of fungal fatty acids and prostaglandin-like compounds

Anita Kecskeméti

Department of Microbiology, University of Szeged, Szeged, Hungary

Candida parapsilosis is the third most frequently isolated *Candida* species in candidiases, especially in special patients groups such as low birth weight neonates, where *C. parapsilosis* even outmarks *C. albicans*. A number of biochemical parameters could influence the virulence of these fungal species, whose research is important to understand the mechanisms of whole infection process. According the previous results of our research group based on the transcriptome analysis of the *in vitro* host-pathogen interactions process, the prostaglandin- and the fatty acid pathways of *C. parapsilosis* could play an important role in the pathogenesis. Therefore, we aimed to develop a reliable measurement method for the analysis of metabolites, which are originated from the pathogenicity-linked biochemical pathways and are involved through the interactions as the final chemical effectors including prostaglandins and fatty acids.

In the first part of our work, we developed a liquid chromatographic method using fluorescence detector to analyse prostaglandins from the ferment broths of the wild type and UGA3 (a putative transcription factor, that can play a crucial role in fungal prostaglandin biosynthesis) mutant *C. parapsilosis* strains. After the optimization of sample preparation on solid phase, the evaporated extracts were derivatized to create fluorescence-active derivatives of prostaglandins. In this reaction the fluorescence molecule (Br-DMEQ) was linked to the carboxyl group of prostaglandins in the presence of aprotic solvent and catalyzer. The amounts and the ratios of the reaction components were optimized for the amount of the reaction products leading to the opportunity of the more sensitive measurement. The separation after the testing of several stationary- and mobile phases was carried out on the Phenomenex XB-C18 column with water/acetonitrile supplemented both with 0.1% acetic acid resulting the determination of seven prostaglandins. For the enlargement of the number of the detectable prostaglandins a mass spectrometric analysis was also developed in negative ESI ionization mode, which was able to determine 18 prostaglandin components. Furthermore, the fatty acid content of the wild type and a fatty acid desaturase deficient strain (OLE2) were analyzed with GC-FID technique developed for the analysis of 37 both of saturated and desaturated fatty acid methyl esters.

In the second part of our study, we dealed with the development of a rapid, high-throughput analytical method for the monitoring of the economically important fungal products, fatty acids, from the biomass of the *Mortierella* species to collect information about the effect of abiotic parameters of cultivation media to the production and the composition. In the method, the carboxyl groups of the extracted fatty acids were also tagged with Br-DMEQ and a short HPLC run was applied on core-shell chromatographic column to separate eleven fatty acids, which were in the scope of the study.

This research was realized in the frames of TÁMOP 4.2.4. A/2-11-1-2012-0001 „National Excellence Program" – Elaborating and operating an inland student and researcher personal support system convergence program. The project was subsidized by the European Union and co-financed by the European Social Fund.

Supervisor: Attila Gácser, András Szekeres
E-mail: kecskemeti.anita@gmail.com

Application of various imaging techniques for plant stress diagnostics

Paul, Kenny

Molecular stress and photobiology group, Institute of Plant Biology, Biological Research Center, Szeged, Hungary

Plant growth is affected by various factors. The resistance of the plant to withstand various biotic and abiotic stress factors plays a vital role for its growth and development. Our objectives were to combine various non-invasive imaging techniques (Digital imaging, Near- infrared (NIR) imaging, thermal imaging and chlorophyll fluorescence imaging) for studying stress responses induced by drought, chemical treatment and fungal pathogens in wheat seedlings (*Triticum* spp). Severe drought stress was induced by growing drought tolerant and drought-sensitive wheat genotypes subjected to decreased soil water content (10% field capacity as compared to 60% in the well watered control), while chemical stress induced by silica nanoparticles (10-20 nm particle size, 1000 mg/L) was studied in hydroponically grown wheat seedlings. Two week old near-isogenic wheat lines possessing various tan spot resistance genes were infected with pyrenophora tritici-repentis (PTR) fungal pathogen and characterized. OJIP fluorescence induction kinetics showed characteristic differences between cultivars in response to drought stress as there was an increase in variable fluorescence in response to SiO_2 NPs treatment. Gas exchange measurements showed lower net photosynthetic CO_2 uptake during drought stress, while CO_2 uptake was enhanced in response to SiO_2 NPs treatment. Thermal imaging indicated stomatal closure based on lower transpiration rate under drought stress, while increased evaporative cooling through the stomata was seen in response to SiO_2 NPs. Increasing drought stress activates photosynthetic electron transport rates in water stressed drought sensitive cv. However, we observed higher quantum yields of PSI and PSII photochemistry in SiO_2 NPs treated wheat seedlings. Chlorophyll fluorescence imaging has proven to be a promising tool for characterization and early detection of tan spot disease in wheat *in vivo*. NIR images were able to detect the loss of water content in the area of tan spot infection on various wheat cultivars.

Supervisor: Imre Vass
Email: kpaul@brc.hu

Volume 58(1):73-94, 2014
Acta Biologica Szegediensis
http://www.sci.u-szeged.hu/ABS

Genetic analysis of the cooperation between the *bxd* PRE and the neighboring embryonic enhancers

Viktória Kiss

Drosophila Developmental Biology Group, Institute of Genetics, Biológical Research Center of the Hungarian Academy of Sciences, Szeged, Hungary

During embryonic development, proliferating cells are getting committed to different cell fates to create different tissues. This process is regulated by epigenetic factors generating tissue specific gene expression profiles maintained during the life of a cell and transmitted to its descendants by modifications of higher order chromatin structure.

To study the process of epigenetic gene regulation, the homeotic bithorax-complex (BX-C) of Drosophila proved to be an excellent model-system. Subtle alterations of the chromatin structure of BX-C results in easily detectable segmental transformation. The three genes of BX-C are regulated by nine large, segment-specific *cis*-regulatory regions. The appropriate active or inactive conformation of these regulatory regions is maintained by the TRITHORAX or POLYCOMB group of proteins, binding to specific elements in the regulatory regions, called Trithorax- or Polycomb-Response-Elements (TRE or PRE), respectively.

Previously, we have analyzed a chromatin silencer, called PRE, in the *bithoraxoid* (*bxd*) *cis*-regulatory region of the *Ultrabithorax* (*Ubx*) homeotic gene. In the recent work we studied two embryonic enhancers, S1 and S2, straddling the *bxd* PRE. These enhancers have been identified in transgenic assays, but we wanted to reveal their role and the functioning in their natural chromosomal environment. For this purpose, the S1 and S2 enhancers were deleted using an advanced form of gene conversion developed by our group. We analyzed the mutant phenotypes in adults, as well as changes in gene expression patterns using immuno-histochemistry and native GFP fluorescence combined with high resolution confocal microscopy. In addition, we generated several other deletions, which removed additional regulatory elements in the *bxd* region. We found that S1 and S2 have significant roles in the initiation of the *bxd cis*-regulatory region. Our results also suggest that the S2 embryonic enhancer cooperates with the *bxd* PRE, but the mechanism of this cooperation is not fully understood yet. We try to explain the mechanism of this cooperation, hereby to answer how early initiators can affect chromatin structure and functioning of regulatory regions. We hope our experiments will contribute to the understanding of the general and the specific role of enhancer function.

Supervisor: László Sipos
E-mail: vikikiss@brc.hu

The role of an anionic lipid, the phosphatidylglycerol, in the cyanobacterial cellular processes

Tímea Ottilia Kóbori

Laboratory of Plant Lipid Function and Structure, Institute of Plant biology, Biological Research Centre of Hungarian Academy of Sciences, Szeged, Hungary

Cyanobacteria are Gram negative photosynthetic bacteria.

Phospholipids play important role in the structure of cell membranes and actively participate in different membrane related cellular processes.

Cyanobacterial membranes contain four types of lipids, two neutral and two negatively charged lipid. The phosphatidylglycerol (PG) is the only phospholipid present in the cyanobacteria. It has been demonstrated that the PG plays important role in the structure formation and function of the photosynthetic complexes.

In case of PG deprivation, the *Synechocystis* sp. PCC6803 cells show enlarged cell volume and *Synechococcus* sp. PCC7942 elongated cell size. If the PG is re-added to the cultures, the normal cell morphology is recovered. This might suggest that the lack of PG affects the normal division process of the cyanobacterial cells.

Many cell division proteins have been identified mainly in *Escherichia coli* bacteria. The homologues of these proteins were found in cyanobacteria.

A determining step of bacterial cell division is the polymerization of the tubuline-like FtsZ protein in a ring like structure in the mid-cell region. The localization of the Z-ring is a highly regulated process. The regulation differs in Gram negative and Gram positive bacteria. The cyanobacteria possess proteins characteristic to Gram negative and Gram positive division along with cell division proteins unique to cyanobacteria or higher plant plastids. During the division process, a number of division proteins get in contact with the plasma membrane. Changes in the membrane composition might affect the cell division. Many studies suggest the importance of phospholipids in the division processes. In our studies, we follow the changes in cell division in a phospholipid-lacking live cyanobacterial system.

Supervisors: Bettina Ughy, Zoltán Gombos
E-mail: koboriotti@yahoo.com

Volume 58(1):73-94, 2014
Acta Biologica Szegediensis
http://www.sci.u-szeged.hu/ABS

Examination of *Trichoderma* strains isolated from the rhizosphere of vegetables for the purposes of developing environment-friendly in field technologies

Péter Körmöczi

Department of Microbiology, University of Szeged, Szeged, Hungary

Organic farming is becoming nowadays more and more important in the agriculture. Organic farmlands are exposed to dangerous xenobiotics through distinct pollution drift effects such as wind-driven, pesticide-containing dusts and xenobiotic-containing rains. In order to achieve organic farming, there is a need for the development of new techniques which allow the bioremediation of lands previously used in common, intensive agricultural practice. Organic agriculture also faces the problem of pests including the damage caused by plant pathogenic fungi, therefore the implementation of biological control as a possible, environment-friendly solution is also of increasing importance.

Trichoderma strains were isolated from vegetable rhizosphere samples on dichloran-Rose Bengal medium. After purification of genomic DNA, the PCR amplification of the internal transcribed spacer (ITS1-5.8S rDNA-ITS2) region and its sequence analysis were used for the identification of the isolates at the species level. Altogether, 45 *Trichoderma* isolates were identified from the examined samples. The detected *Trichoderma* species were *T. asperellum*, *T. atroviride*, *T. citrinoviride*, *T. gamsii*, *T. hamatum*, *T. harzianum*, *T. koningiopsis/T. ovalisporum*, *T. longibrachiatum/H. orientalis*, *T. pleuroticola* and *T. virens*.

In vitro antagonism of selected isolates was examined in dual culture tests and the Biocontrol Index (BCI) values were determined for the particular isolates. Certain *T. asperellum*, *T. virens* and *T. atroviride* isolates proved to possess good *in vitro* antagonistic activities against plant pathogenic *Fusarium solani*, *F. oxysporum*, *Phoma cucurbitacearum*, *Alternaria alternata*, *Botrytis cinerea*, *B. pseudocinerea* and *Rhizoctonia solani* strains.

Fungicide susceptibilities were measured by the microdilution method and the Minimum Inhibitory Concentration (MIC) values were recorded. Ten fungicides were tested in the concentration range of 512 µg/ml to 1 µg/ml. Strain *T. asperellum* SZMC 20866 showed resistance to 9 fungicides and was sensitive only to Maneb (MIC: 256 µg/ml). The *T. atroviride* strain SZMC 20781 showed similar fungicide resistance properties to those of *T. asperellum* SZMC 20866. MIC values of *T. harzianum* SZMC 20770 were 256, 512, 32, 64, 512 and 128 µg/ml for Cyproconazole, Fenarimol, Imazalil, Maneb, Penconazole and Thiram, respectively. The strain most sensitive to the tested fungicides was *T. virens* SZMC 20779.

The effect of temperature on growth in a range of 5 – 40 °C was also examined, and the water activity (a_w 0.997 – 0.922) and pH (2.2 – 8.0) dependence determined in the case of the isolated *Trichoderma* strains. Temperature values of 20-30 °C were optimal for the growth of *Trichoderma* strains, while none of the strains were able to grow at 5 °C. The examined strains were able to grow in a wide range of pH from 2.2 to 8.0, the maximal growth was observed under acidic conditions at pH 4.0. The highest tested a_w value (0.997) seemed to be optimal for the growth of all strains. Only limited growth was observed at 0.945 in the case of only three examined strains.

The results of the recent study suggest that the rhizosphere of vegetables may be a rich source of potential biocontrol agents for environment-friendly, organic agricultural production. We identified 3 *Trichoderma* strains which seem to be very promising for the development of microbial products with multiple beneficial effects for the purposes of organic farming.

Supervisor: László Kredics
E-mail: kormoczipeti@gmail.com

Physiological and molecular analysis of salt stress-induced PCD in tomato

Judit Kovács

Stress Physiology Research Group, Department of Plant Biology, University of Szeged, Szeged, Hungary

As saline soils and waters are common around the world, salinity is one of the major abiotic stress which largely limits plant growth and productivity. The ability of plants to tolerate salt stress is determined by multiple biochemical pathways; the most important is that the plant facilitates retention and/or acquisition of water, protects chloroplast functions, and maintains ion homeostasis. Severe salinity induces programmed cell death (PCD) in plants takes place in eukaryotic cells of different origin. One typical hallmark of PCD in plants is an increase in the process of protein degradation which is initiated by reactive oxygen species (ROS) and nitric oxid (NO) and involves the action of proteolytic enzymes. ROS and NO generation is one of the earliest response of plant cells under abiotic stresses. Protein degradation is probably the most important degradation process that occurs during PCD. The total protein content of tomato leaf gradually decreased with increasing concentration of NaCl. This decrease in protein content might be due to the increasing activity of cysteine- and serine proteases. For this reason, many of the genes up-regulated during PCD are proteases. The four major classes of proteases: cysteine, serine, aspartic acid and metalloproteases, exist in plant cells. Genes that encode proteases are activated by different ways. Expression of these genes that encode cysteine proteases has been shown to induced by environmental stress such as salinity. We studied different genes, for instance *MCA1*, *CYP*, *CP*, which encode various types of proteases participating in plant PCD. In addition, inhibitors encoding genes (*PI2* and *LTC*)

and BAX inhibitor-1 homolog gene (*BI1*) were also tested. According to our results in addition to the cysteine proteases their inhibitors also have fundamental role in the regulation of protein degradation. It is very important to see the connection between the processes of salt induced PCD and different stress hormones from which one of the most important is abscisic acid (ABA) which might have a role in this regulatory pathway. ABA is commonly recognized as naturally occurring plant hormone. ABA plays a key role in many developmental processes, from the promotion of seed desiccation tolerance to the synthesis of storage proteins and organ senescence. In addition, ABA acts as an endogenous messenger in the regulation of plant-water status and regulates some aspects of the plant's physiological responses to environmental stresses, such as osmotic stress-induced stomatal closure and salt, drought and cold tolerance. Our first results show that ABA might induce protease activity during PCD.

To gain a better understanding of the salinity stress responses at physiological and molecular level in cultivated tomato we carried out a comparative physiological analysis. Tomato has a medium tolerance to salinity and it can acclimate to high salinity at morphological and physiological level. In addition to the wild-type, an ABA deficient-tomato mutant, *flacca* was studied, too. Plants were treated with sublethal and lethal concentrations of NaCl. The growth of this plant is not inhibited by medium NaCl stress but it is affected by strong one. The salt stress-induced changes in ROS content and in the gene expression level were shown at the beginning of the treatment. Protein content and protease activity were also studied as a function of time. There was a nice correlation between decreased protein content and increased protease activity in the first 24 hours. Finally, we suggest that cysteine proteases might participate in salt-induced PCD in tomato as a function of time depending on intensity of the stress.

Supervisor: Irma Tari
E-mail: juditkovacsbio@gmail.com

Nuclear function for the actin binding cytoskeletal protein, moesin

Ildikó Kristó

Laboratory of Drosophila Nuclear Actin Research, Institute of Genetics, Biological Research Center of the Hungarian Academy of Sciences, Szeged, Hungary

The most dynamic component of the cytoskeleton in every eukaryotic cell is the microfilament network of linear polymers of actin subunits. Extensive research in the past decade has significantly broadened our view about the role actin plays in the life of the cell and added novel aspects to actin research. The discovery of the existence of nuclear actin became evident only recently. Nuclear activities, including transcriptional activation in the case of all three RNA polymerases, export of certain mRNAs and proteins, chromatin remodeling, and nuclear assembly after mitosis, all depend on actin.

Moesin, the well-known cytoplasmic actin binding protein is the only member of the evolutionary conserved mammalian ezrin-radixin-moesin (ERM) protein family in *Drosophila melanogaster*. ERM proteins are responsible for the organization of the cortical actin network and anchor membrane proteins to it. They all have an N-terminal FERM domain, which is a general protein binding domain, a mid-domain which is a flexible hinge region and a C-terminal actin-binding domain. Our laboratory demonstrated previously that moesin is present in the interphase nucleus but the biological significance of this localisation remained unknown.

We are studying currently the exact localisation and function of moesin in the interphase nucleus. Our experiments showed that moesin accumulates as a ring at the nuclear envelope; it is present in the nucleoplasm, in some chromosome regions and occasionally in the nucleolus. We found that the quantity of moesin in the nucleus increases upon heat stress, which suggests a function for moesin in the nucleus and that its transportation into the nucleus is an active process.

To further analyse the chromosomal localisation of moesin, we performed immunostaining experiments on larval polytene chromosomes. Moesin was detected in the euchromatic bands moreover, it also showed colocalisation with the active form of RNA Polymerase II, and the intensity of the accumulation of the two proteins on the chromosomes was identical. Moesin staining was found especially strong in the chromosome puffs which are special euchromatic regions of extremely active transcription sites in the polytene chromosomes. The transcription on a transgene regulated by an inducible promoter resulted in the formation of an extra moesin band in the corresponding chromosome region suggesting that moesin is required for transcription rather than the formation of the puff structure. This idea was confirmed by the finding that the disassembly of the RNA polymerase complex caused by the drug triptolide, resulted in the detachment of moesin from the chromosomes.

We have also performed a preliminary screen to identify the proteins that are responsible for the nuclear transport of moesin. Our results both with cultured cells and in the live animal revealed that the Nup98 protein is involved in the nuclear export of moesin.

In summary, our results demonstrate that besides its cytoplasmic functions, moesin also plays important roles in the nucleus. We have shown that moesin is actively transported to the nucleus where it participates in the process of RNA transcription.

Supervisor: Péter Vilmos
E-mail: kristoi@brc.hu

Volume 58(1):73-94, 2014
Acta Biologica Szegediensis
http://www.sci.u-szeged.hu/ABS

Discovery of novel fluorochromes for use in plant studies

Soujanya Kuntam

Cellular Imaging Laboratory, Institute of Plant Biology, Biological Research Centre of the Hungarian Academy of Sciences, Szeged, Hungary

Plant cells store neutral lipids such as triacylglycerols in distinct cytosolic organelles called oil bodies (OBs) (also referred to as lipid bodies/droplets, spherosomes or oleosomes) Although initially thought to be found only in oleogenic seeds and fruits, where they serve as fuel for the growth and development of seedlings prior to photosynthetic establishment, in recent years, studies have shown that OBs are quite ubiquitous. Their role extends from being static depots for carbon storage to stress response, lipid homeostasis, pathogen resistance, hormone metabolism and signaling and a specialized role in anther development. Plant OBs similar to their counterparts in yeast and mammals, are highly dynamic. Proteomic analyses have revealed that, there are a host of proteins which reside on the surface of these OBs and the exact content is changing under varying conditions. But a lot still remains to be uncovered in the area of OB protein and lipid composition as well as OB transport, mechanism of protein targeting, assembly and regulation. Live cell analysis is thus required to unravel the dynamic regulation of this important organelle.

Live-cell imaging offers a unique opportunity for investigating OB regulation. A large collection of imaging tools based on fluorescence is currently available. Varying colors of photostable genetically-encoded fluorescent proteins can be used in multiplexed tracking of protein remodeling on OBs. Photo-switchable fluorescent proteins as well as fluorescent timers allow quantitative assessment of OB protein dynamics. Fluorescent sensors, such as those based on fluorescence resonance energy transfer (FRET), can be applied to follow protein conformational changes or protein-protein interactions relevant to OBs. These tools, combined with the use of reliable OB markers, represent a versatile scheme for investigating OB biology. However, commercially available live cell dyes are limiting in their ability to penetrate cell walls and those that are permeable, in addition to other drawbacks such as photostability (BODIPY) and broad emission range (Nile Red), also restrict multicolor imaging, as most fluoresce in the green to red region of the visible spectrum.

In the present study, we report new fluorochromes as markers for OB in living plant cells. The fluorochromes, which are thalidomide analogs were in-house synthesized and were tested on live plant suspension cultured cells at various concentrations. The spectral emission range for the fluorochromes was identified and cell viability assays were also performed. We could also observe that the OBs remain highly mobile after staining with these fluorochromes, suggesting that the mobility dynamics were not affected significantly. We expect that these new chemicals will provide a novel approach for microscopy analyses of OBs in live plant cells.

Supervisor: Dr Ferhan Ayaydin
Email: ferhan@brc.hu

Bacterial symbionts enhance photo-fermentative hydrogen evolution of *Chlamydomonas* algae

Gergely Lakatos

Laboratory of Microbial Genomics, Institute of Biochemistry Biological Research Center of the Hungarian Academy of Sciences, Szeged, Hungary

Chlamydomonas reinhardtii represents a well-established algae model system for biohydrogen generation. Two major methods are known for sustained *Chlamydomonas*-based hydrogen evolution. Hydrogen production using sulfur-deprived photoheterotrophic cultures of *Ch. reinhardtii* is the most widespread approach. Sulfur deprivation leads to complete anoxia via the inactivation of the photosynthetic system, thus, the extremely oxygen-sensitive algal Fe-hydrogenase will be able to become functional. Another algal hydrogen evolution approach is possible through dark fermentation. In dark and anaerobic conditions algae can catabolize endogenous carbohydrates or secondary metabolites generating organic acids, ethanol, CO_2 and H_2. The vast majority of algal hydrogen evolution studies were conducted using pure algae cultures. Our knowledge on the exploitability of algal-bacterial consortia in biohydrogen production is fairly short. Biohydrogen production capacity and growth rate of *Ch. reinhardtii* cc849 or the transgenic strain Iba co-cultured with *Bradyrhizobium japonicum* has been investigated. The sulfur-deprivation method together with *B. japonicum* inoculation resulted in enhanced rate of the oxygen consumption in the cultures, increased growth rate of algae and significantly improved hydrogen evolution rate. Our investigations aimed the elucidation of the nature and dynamics of algal hydrogen evolution observed in various algal-bacterial interactions.

The green algae *Chlamydomonas* sp. strain 549 was investigated for its hydrogen-evolution capability in algal-bacterial mixed cultures. Stable bacterial contaminations were identified during algae cultivation, the symbionts belonged to various genera, mostly *Brevundimonas* sp., *Rhodococcus* sp. and *Leifstonia* sp. All natural symbiotic partners enhanced fermentative algal hydrogen production. This phenomenon was not limited for the natural associations, increased algal hydrogen evolution was achieved by simple artificial algae-bacterium communities as well. Designed algal-bacterial co-cultures were tested in hydrogen evolution experiments, the highest hydrogen yield was obtained

when hydrogenase-deficient *E. coli* was applied as symbiotic bacterium. The results showed that the oxygen elimination process is the most crucial factor for algal hydrogen production, efficient bacterial respiration is essential for the activation of algal Fe-hydrogenase.

Supervisor: Gergely Maróti
E-mail: lakger86@brc.hu

Identification of a novel effector cell type in the cell-mediated immunity of *Drosophila*, the multinucleated giant hemocyte

Zita Lerner

Immunology Unit, Institute of Genetics, Biological Research Centre of the Hungarian Academy of Sciences, Szeged, Hungary

Innate immunity is the first line immune defense against microbes, parasites and tumours which is composed of humoral and cell mediated events. In *Drosophila*, three main classes of blood cells, so called hemocytes, are the effector cells of cell mediated immunity. The plasmatocytes engulf microbes, produce extracellular matrix components, and provide systemic signals during microbial infections. Crystal cells contain crystallized prophenoloxidase enzyme, which is necessary for the melanization response. Lamellocytes arise upon immune induction, such as infestation by parasitoid wasps, and are required for the encapsulation reaction by forming a multilayered capsule around the parasitic wasp egg, which later melanizes. The effector hemocytes of the *Drosophila* larva originate from three hematopoietic compartments: the lymph gland which is a compact hematopoietic organ with multiple lobes, the sessile tissue where hemocytes are attached to the wall of the hemocoel, and the circulation. All three compartments contribute to differentiation of the effector hemocyte pool following immune induction.

The cell mediated immunity of *Drosophila melanogaster* is well studied; however, our knowledge on the immune response of other insects, in particular, other members of the *Drosophilidae* family is far from complete . The availability of various *Drosophila* species from different natural habitats allows to study the adaption of the cell mediated immune response to the different parasites. Recent studies show the diversity of the capsule forming cells of different Diptera species. According to these data the pseudopodocytes in *D. affinis* and *D. obscura* from the *obscura* group of *Drosophilidae* are capable of phagocytosis, similarly to plasmatocytes, however they are also involved in the capsule formation around foreign particles.

Our aim was to characterize the hemocyte subsets and the hematopoietic compartments in *Drosophila ananassae* from the *ananassae* subgroup. We identified a special giant hemocyte, which we named MGH (Multinuclear Giant Hemocyte) in *D. ananassae*, that appear after immune induction. To isolate different hemocyte subsets and to define their function, origin and formation, we produced monoclonal antibodies to subclasses of hemocytes and developed a transgenic reporter system which allows *in vivo* detection and manipulation of hemocytes and hematopoietic compartments in *D. ananassae.* As MGHs are similar to mammalian multinuclear giant cells, which play an important role in the formation of granulomas, we believe that *D. ananassae* could serve as a model for a better understanding of the development, structure and function of granulomas and of the multinucleated giant cells.

Supervisors: István Andó, Viktor Honti
E-mail: lerner.zita@brc.mta.hu

Methodology of ancient DNA, and results to date

Endre Neparáczki

Ancient DNA Group, Department of Genetics, University of Szeged, Szeged, Hungary

Our research group isolates and studies ancient DNA (aDNA) from excavated human remains in collaboration with the Department of Anthropology. Sequence data obtained from ancient bones can unravel genetic relatedness of individuals, and populations. From a representative data set one can surmise population movements, and population history. The aDNA research can complement anthropological and archaeological data. For kinship studies routinly matrilinearly inherited mitochondrial DNA sequences, or patrilinearly inherited Y-chromosomal sequences are used, but autosomal loci correlated with known phenotypes can also be examined, such as monogenic disease genes, hair and skin color genes, or FOX2P gene, associated with speech ability.

In addition, aDNA of ancient pathogenes can also be obtained from their deceased carriers, which makes it possible to determine the distribution of prehistoric infectious diseases, such TB caused by *Mycobacterium tuberculosis.*

The preservation of aDNA, largely depends on the environment, and even under best conditions, it is largely degraded and fragmented. Usually trace amounts of 50-200 bp long DNA fragments are left, so classical methods apply PCR amplification, and cloning. The risk of contamination with modern DNA is very high, therefore special sterile laboratories are required for aDNA work. In the last few years the

appearance of new generation sequencing techniques opened a new dimension of ancient DNA studies, since from traces of DNA, large amount of sequence data can be obtained with this method.

We heve recently created a special sterile aDNA laboratory at the Department of Genetics. This so called pre-PCR laboratory is supplemented with a post-PCR, standard molecular laboratory in a distant part of the building (a requirement to prevent contamination). Both laboratories are equipped, and we have optimized DNA extaraction and amplification. In the pre-PCR laboratory, a simple method was adapted for bone's milling. For DNA extraction we also adapted a cheap but reliable modified silica powder affinity purification method. For DNA amplification we are testing various enzyme brands and conditions recommended by the manufacturer.

Supervisor: Tibor Török, György Pálfi
E-mail: endre.neparaczki@gmail.com

Effect of hypoxia on MCF-7 cells' transcriptome and metabolic activities

Ferenc Pál

Balázs Papp's Lab, Synthetic and Systems Biology Unit, Institute of Biochemistry, Biological Research Centre of the Hungarian Academy of Sciences, Szeged, Hungary

The hypoxic condition is prevalent in solid tumours and it is often associated with poor prognosis. Metabolic alterations that make possible for the cancer cells to survive and thrive under hypoxic condition are subject to high interest, however a systems-level understanding is still missing.

In order to emulate the hypoxic state, cell of a well established breast cancer model cell line (MCF-7) were cultured under normal oxygen concentration and subsequently exposed to hypoxia. To detect the cells' response to hypoxia, RNA samples were collected and sequenced from both conditions and mRNA abundances were determined.

With the aim of inferring the metabolic routes that may play important roles in the cancer cells' response to hypoxia, we employed the iMAT method that integrates gene expression data and a human genome-scale metabolic network reconstruction to predict metabolic reactions that are specifically altered in hypoxic condition. Beside, to gain a more global view of the functional changes underlying the hypoxia-response, we carried out a Gene Ontology analysis on the RNASeq data. In addition, to generally assess the predictive capability of the human metabolic network model, we applied an essentiality analysis and compared predictions to available high-throughput data.

The analyses resulted in the identification of 33 metabolic reactions which are specifically activated under hypoxia. The the majority of the detected reactions is distributed across 4 modules of cellular metabolism, namely sphingolipid metabolism, pyruvate metabolism, nucleotides metabolism, inositol phosphate metabolism. In addition, C160 fatty acid activation, diacylglycerol phosphate kinase and the arginine/lysine transporter were predicted to be active.

The predicted arginine transported and the reactions of the pyruvate metabolism will be subject to further experimental investigations by our collaborators in order to assess their role in hypoxia.

Supervisor: Balázs Papp
E-mail: pal.ferenc@brc.mta.hu

Methane inhalation prevents from the quantitative changes in nitrergic myenteric neurons and intestinal motility disorders in a rat model of intestinal ischemic-reperfusion injury

Marietta Zita Poles

Department of Physiology, Anatomy and Neuroscience, University of Szeged, Szeged, Hungary

The gastrointestinal tract is highly susceptible to hypoxia, thus local or systemic circulatory disturbances are often associated with intestinal inflammation and enteric neuropathy. Inflammatory mediators influence the activity of enteric neurons, therefore, development of the intestinal inflammation is frequently associated with gut motility disturbances. Previously, we have demonstrated the anti-inflammatory effects of exogenous methane inhalation after IR. However, the effects of inhaled methane on the IR-related quantitative changes of enteric neurons or on the myoelectrical activity of the gastrointestinal tract were not investigated until now. Therefore, the main focus of this study was to investigate the consequences of intestinal IR and normoxic methane inhalation on the quantitative parameters of myenteric neurons and intestinal motility.

For the study 300-350 g male Sprague-Dawley rats were divided into three groups, these are: sham-operated, IR and methane-treated IR (n=8-8). Ischemia was induced by the occlusion of superior mesenteric artery. The inhalation of normoxic artificial air with 2.2% methane

was applied in the last five minutes of ischemia and first ten minutes during reperfusion. After anaesthesia the myoelectric activity of the gastrointestinal tract was monitored during ischemia (50 minutes) and reperfusion (120 minutes). Samples of the duodenum, ileum and colon were collected at the end of reperfusion phase. After an overnight fixation whole-mount preparations were prepared for immunhistochemical (HuC/HuD, nNOS and eNOS) staining. Biopsies from the small intestine were collected for biochemical studies. Tissue superoxide levels, xanthine oxidoreductase activity were determined to monitor the oxidative stress, and tissue nitrite/nitrate and nitrotyrosine levels were determined to study the levels of nitrosative stress.

At the beginning of ischemia the myoelectric activity sharply increased, then decreased gradually until the end of the reperfusion period. After methane inhalation a post-ischemic peak appeared in myoelectric activity at the beginning of the reperfusion period which then declined sharply and reached near the control level by the end of the reperfusion period.

After IR the total number of myenteric neurons did not change, but the density of nNOS and eNOS-positive myenteric neurons increased. Increase of the nNOS-immunreactive neurons in the duodenum were significant. After methane inhalation the density of the nitrergic myenteric neurons was similar to the neuronal density found in sham-operated rats. During IR the levels of tissue nitrite/nitrate, nitrotyrosine, and xanthine oxidoreductase activity increased significantly, while the methane inhalation prevented the intestinal tissues from the increase of oxidative and nitrosative stress markers.

Based on these results we hypothesize that due to the increased density of nitrergic myenteric neurons in IR the descending inhibition of intestinal peristalsis was enhanced. At the same time methane inhalation in the early stages of reperfusion prevented from the increase in the number of nitrergic myenteric neurons and the intestinal motility disorders.

Supported by OTKA K104656, TAMOP 4.2.2A-11/KONV-2012-0035 and co-financed by the European Social Fund in the framework of TÁMOP-4.2.4.A/2-11/1-2012-0001 'National Excellence Program'.

Supervisors: Éva Fekete Nikolett Bódi
e-mail: polesmarietta@gmail.com

Development of a novel, somatic gene transfer system in the mouse

David Pusztai

Laboratory of Cancer Genome Research, Institute of Genetics, Biological Research Center of the Hungarian Academy of Sciences, Szeged, Hungary

Cancer is the leading cause of death in the developed world. Tumorigenesis requires the acquisition of mutations in proto-oncogenes and tumor supressor genes. Such genetic changes can be caused by mutagenic agents, chromosomal translocations or the disruption of the balance in epigenetic networks. A class of mutations, called „driver" mutations, affect a relatively limited number of genes that are functionally related to the key attributes of cancer cells. Contrary to driver mutations, „mutator" mutations act as enhancers of the tumorigenic process. According to the mutator hypothesis, mutator mutations decrease genome stability and, hence, accelerate the accumulation of random mutations, including those in proto-oncogenes and tumor suppressor genes. Our aim is to create a novel, somatic genetransfer system for the identification of candidate genes involve in the enhancement of tumorigenesis through the over-expression of native/mutant coding sequences or gene silencing with artificial miRNAs.

Type 1 tyrosinemia is a liver-based *metabolic disorder* caused by a deficiency of the enzyme fumarylacetoacetate hydrolase (Fah). The mouse model of this disease (Fah knock-out strain [Fah -/-]) offers the possibility to develop the new transgenic system. The primary treatment for type 1 tyrosinemia is nitisinone (NTBC). This drug prevents the formation of fumarylacetoacetic acid, which has the potential to be converted to succinyl acetone, a toxin that damages hepatocytes. Consequently, liver degeneration occurs due to the withdrawal of NTBC. However, the high regenerative capacity of this organ can be utilized to establish a new, healthy liver: wild type hepatocytes (Fah +/+) can migrate to the diseased organ and repopulate that within a few months after cell transplantation into the spleen. Thus, a Fah +/+ transgenic liver can be obtained from a genetically engineered hepatocyte pool in a Fah -/- recipient mouse.

Liver repopulation can be monitorised with a fluoresence marker gene that also serves the expression of artificial miRNAs, in addition to its indicator role. Furthermore, this somatic gene transfer system is adaptable for library screens due to the large amount of hepatocytes potentially involved in repopulation, resulting in the possibility to express multiple transgenes. Considering the somatic nature of the system, the classical method for generating transgenic mice can be avoided, and the number of experimental animals reduced. These adventages make this new practice faster and more cost effective. We hope that our technique for producing transgenic liver will become a valuable tool for cancer genetics.

Supervisor: Lajos Mates
E-mail: pusztai.david@brc.hu

Volume 58(1):73-94, 2014
Acta Biologica Szegediensis
http://www.sci.u-szeged.hu/ABS

Anaerobic biodegradation of cellulose-rich substrates

Orsolya Strang

Department of Biotechnology, University of Szeged, Szeged, Hungary

Depletion of fossil fuels and increase of global climate changes demand the usage of renewable energy sources. Biogas forms anaerobically during the decomposition of different organic materials. In the process, three syntrophic groups of microbes work together. These are the polymer degraders, acetogens and methanogens. The main components of the produced biogas are methane (55-70%) and carbon-dioxide (30-45%). After upgrading, biogas could be injected into natural gas grid. For biogas production, many waste and raw material is suitable. Plant biomass is the largest amount of biomass on Earth. Plants can harvest solar energy during photosynthesis and convert it to plant tissues, therefore have vast energy potential. Plant tissues consist of lignocellulose as the major component. Lignocellulose is composed of cellulose, hemicellulose and lignin. Cellulose is a recalcitrant complex polymeric carbohydrate, cellulases are needed for its efficient decomposition. Cellulases are divided into three major groups: endoglucanases (EC 3.2.1.4), exoglucanases (3.2.1.91) and β-glucosidases (3.2.1.21). Endoglucanases cut at random internal sites into the cellulose polysaccharide chain, generating new chain ends. Exoglucanases act on the reducing or nonreducing ends of cellulose, liberating glucose or cellobiose units. β-glucosidases hydrolyze cellodextrins and cellobiose to glucose which can be used in metabolic pathways.

For the utilization of substrates having high cellulose content – without pretreatment - the biogas producing microbial community should contain a significant number of cellulose producing bacteria and they should break down cellulose to easily utilizable sugar monomers. An adaptation strategy to adapt the community to lignocellulosic substrate has been developed. The experiments were carried out under thermophilic conditions at 55 °C. α-cellulose was used as substrate for the adaptation and the control fermentors received glucose as carbon and energy source. The changes in the concentration of volatile fatty acids were followed by HPLC, the β-glucosidase enzyme activity was monitored regularly. From the adapted microbial community, cellulose degraders were isolated and were also used as inoculum in the next set of biogas experiments. The cellulose degrading microbes had positive effect, elevated the biogas and methane yield. DNA was purified from the cellulose degrading consortia and was undergone metagenome analysis. In the thermophilic cellulose degrading consortium, the main orders were Thermoanaerobacterales (70%) and Clostridiales (10%). *Thermoanaerobacterium thermosaccharolyticum*, *Caldanaerobacter subterraneus*, *Thermoanaerobacter pseudethanolicus* and *Clostridium cellulolyticum* were identified as dominant strains.

Supervisor: Kornél L. Kovács, Zoltán Bagi
E-mail: strangorsi@citromail.hu

Uniform or different? Heterogeneity of murine bone marrow mesenchymal stem cells in differentiation and immunosuppression

Enikő Szabó

Lymphocyte Signaling Group, Institute of Genetics, Biological Research Center of the Hungarian Academy of Sciences, Szeged, Hungary

Bone marrow mesenchymal stem (BMMSCs) are adherent, colony-forming cells and are defined as multipotent cells differentiating into several cell types (e.g. osteoblasts, chondrocytes and adipocytes). BMMSCs have been found therapeutically beneficent in models for numerous human diseases by multiple processes including enhancement of tissue regeneration, supporting angiogenesis, subduing inflammation and modulating the immune response at the site of tissue damage. Despite the incessantly increasing number of preclinical and clinical MSC studies, there are some basic issues about MSCs, which still remain unresolved. The heterogeneity in differentiation potential of MSCs was demonstrated decades ago. Up to this day, few and inconsistent data have been collected reporting uniform or different immunosuppressive properties of single MSC clones, even if it is highly relevant to the therapeutical effectivity of MSCs.

We aimed to examine the heterogeneity of murine BMMSC population through characterizing 6 single cell-derived MSC clones (MSC1-MSC6) in terms of differentiation potential, support of angiogenesis and immunmodulation.

To examine whether MSC clones maintain the multipotency of BMMSC population, MSC clones were induced to differentiate *in vitro* into adipocytes and osteoblasts. While MSC2-6 differentiated into both lineages, MSC1 differentiated only into adipocytes.

Analysis of the ability of the MSC clones to support angiogenesis has been carried out using an *in vitro* model, the capillary mimicry assay. MSC clones were co-cultured with H5V endothelial cells and the capillary-like structures were evaluated. Whereas neither MSCs nor H5V formed capillary-like structures alone, all MSC clones supported similarly the development of these structures when co-cultured with H5V.

The *in vitro* immunmodulatory properties of BMMSC clones were compared in ConA-stimulated T cell proliferation assay. MSCs were co-cultured with T cells isolated from mouse lymph nodes in the presence of ConA and cell division of CFSE (a fluorescent dye used for proliferation assays) labeled T cells was followed by flow cytometry. All MSC clones inhibited significantly but not uniformly the T cell proliferation in the following order: MSC2>MSC4=MSC5>MSC1>MSC3>MSC6. Differences in the inhibition of T cell proliferation

were reflected in expression level of *Nos2, Ptgs2*, the most important genes responsible for murine MSC-mediated immunosuppression. The strongest inhibitor MSCs expressed the most and the least inhibitor clones expressed the lowest level of these factors at mRNA level. Normally, MSCs exert immunosuppression at the site of inflammation, therefore the immunmodulation of MSC clones were tested in inflammation-mimicking milieu, treating MSC clones with pro-inflammatory cytokines, IFN-γ and TNF-α. Treatment of the cells with these cytokines resulted in upregulation of *Nos2* and *Ptgs2* gene expression in each MSC clone, and as a consequence, their inhibitory effect on T cell proliferation elevated. To find out whether MSC clones can exert immunmodulation *in vivo,* the effect of the most and the least immunosuppressive MSC2 and MSC6 clones, respectively, were tested in ovalbumin-induced delayed-type hypersensitivity response in mice. Intraperitoneal administration of MSC2 cells simultaneously with ovalbumin immunization significantly reduced, whereas MSC6 didn't change the ovalbumin-induced increase of footpad thickness, unless MSC6 cells were pretreated with IFN-γ and TNF-α prior to injection, in that case MSC6 also decreased footpad thickness increment vigorously.

Based on our results, we suggest that murine BMMSC population is homogenous in differentiation and angiogenesis support while heterogeneous in immunosuppression. Dissimilarity in the immunosuppressive function likely depends on the activation state of single MSC cells, since placing the cells into an inflammatory milieu, the immunomodulatory effect of different MSC clones becomes similar.

Supervisors: Monostori Éva, Czibula Ágnes
E-mail: szabo.eniko@brc.mta.hu

Genetic analysis of *Saccharomyces cerevisiae RAD5* gene

Róbert Tóth

Mutagenesis and Carcinogenesis Research Group, Institute of Genetics, Biological Research Center of the Hungarian Academy of Sciences, Szeged, Hungary

The sequence of DNA contains important information for the life of cells. Any damage of DNA leads to inaccurate function of the cell, or occasionally to its death. Therefore, proteins of DNA repair have a critical role in preserving the initial state of DNA.

At DNA damage, the replication polymerase stalls and the complex of Rad6 and Rad18 proteins ubiquitylates the Proliferating Cell Nuclear Antigen (PCNA), the processivity factor of replication polymerases, at its lysine 164 residue. Subsequently, the monoubiquitylated PCNA is polyubiquitylated by the protein complex of Rad5, Mms2 and Ubc13.

The Rad5 has three domains: RING, Helicase/ATPase and Hiran domain. While the RING domain has E3 ubiqutine ligase activity and the Helicase/ATPase domain has a replication fork reversal activity facilitating the formation of a chicken-foot DNA structure, the function of the Hiran domain is unknown despite of its predicted DNA binding capability.

To explore the particular functions of these Rad5 domains we tested the sensitivity of *ring* (CC914,917AA), *atpase* (DE681,682AA) and *ring-atpase* double point mutant strains with different mutagenic agents such as UV-light, methyl methanesulphonate and nitrogen-mustard.

We have found that the single mutant strains (*ring*, *atpase*) were sensitive to all tested mutagens and the double mutant strain (*ring-atpase*) had a higher sensitivity than the single mutants. We concluded that the ubiquitin ligase and the ATPase activities of Rad5 are not epistatic. This implies that these two activities have independent functions, but it is not exclude the existence of a common function. We also intended to investigate the relationship of these two activities of Rad5 with *RAD18* and *RAD51* DNA repair pathways. Although in our previous results epistatic relationship was not manifested among *RAD5*, *RAD18* and *RAD51* genes with none of the tested mutagens, one could not exclude the possibility that either the ligase or the ATPase activity of Rad5 could interact with one of these pathways. To explore this possibility the epistatic relationship of *ring* and *atpase* mutants was analyzed on *rad18Δ* and on *rad51Δ* background. On these deletion backgrounds point mutants represented the similar sensitivity like on wild type background. These results suggest that domains of Rad5 could function in the same DNA repair pathway with both of the proteins Rad18 and Rad51. Or probably none of the domains function with these two proteins, only they function with one or more other proteins out of Rad18 and Rad51. This hypothesis was confirmed by the higher sensitivity of *rad5Δ/rad18Δ/rad51Δ* triple mutant strain than *rad5Δ/rad18Δ*, *rad18Δ/rad51Δ* and *rad18Δ/rad51Δ* double mutants. Although this sensitivity could be caused by other functions of the Rad5 (e.g. function of Hiran domain). To prove this theory we intended to test the sensitivity of the point mutants on *rad18Δ/rad51Δ* background.

To explore the role of the Hiran domain, we generated mutations in its conserved regions. Five from the twelve mutant strains showed sensitivity to DNA damaging agents (nitrogen-mustard and hydroxyurea). Two mutant strains from the five showed the same growth curve like wild type on mutagenic treatment if over-expression of proteins were induced. It means the low expression level of these two mutant proteins caused their sensitivity in our previous experiments. The other three were overexpressed, purified and tested *in vitro* in biochemical assays. The LI265,266RR mutant protein exhibited wild type activity while the GA177,178RR and the G183R mutants showed no activity neither in helicase nor in ubiquitin ligase assays. We concluded that the GA177,178 and the G183 parts of Hiran domain are likely to have a basic role in both of the two functions of Rad5. Nevertheless it is possible that these mutations modify the whole structure of the protein and it loses all of its activities. To answer this question more structural studies are needed with both wild type and mutant proteins.

We concluded that the role of Rad5 out of the *RAD18* pathway is none or just partially related to *RAD51*. In addition, the ubiquitin ligase and the ATPase/helicase activities of Rad5 have independent function from each other, and these functions are not exclusively func-

tion with Rad18 or Rad51. Probably these independent functions act with one or more other proteins out of Rad18 and Rad51. Thus we expect that Rad5 has a more complex protein interaction network than it was previously known.

Supervisor: Lajos Haracska
E-mail: tothr@brc.hu

Heterologous protein expression and *in vitro* analysis of *Drosophila melanogaster* proteins involved in telomere maintenance

Balázs Vedelek

Department of Biochemistry and Molecular Biology, University of Szeged, Szeged, Hungary

Our laboratory is particularly interested in the maintenance of genome integrity and telomere structure in *Drosophila melanogaster*. In eukaryotic cells, telomere prevents the chromosome ends from being detected as DNA double strand breaks and protects the coding regions from degradation. Telomere "capping" by the multi-subunit complex Shelterin, expressed in higher eukaryotes, averts the triggering of the DNA damage signaling pathways. In *Drosophila* this capping process is performed by a putative complex called Terminin, which is believed to have HOAP, HipHop, Ver and DTL (or Moi) proteins as subunits and it binds to the DNA in a sequence-independent manner. HP1 is generally regarded as the fifth subunit of the putative complex, thought it is not a strictly terminin-specific protein. HP1 is evolutionary highly conserved and plays a role also at non-telomeric regions while Terminin proteins manifest an accelerated rate of evolution and localize only at chromosome ends. Deletion of any of these genes results in telomere fusions. The physical interactions among Terminin proteins have been demonstrated *in vitro*. All these data support the existence of the Terminin complex.

The aim of my research was to study in details the putative Terminin complex and its suggested components by bioinformatics and molecular biological methods.

In silico analysis on the proportion of synonym and non-synonym codon substitutions confirmed that the full length HOAP, HipHop, DTL and Ver molecules have accelerated evolution compared to HP1. Interestingly, specific protein domains showed different rates of evolution and some of the hyper-variable domains have a role in protein-protein interactions.

The cDNA of each protein was cloned and expressed both in bacterial and in baculoviral expression systems. Our results indicated that DTL and Ver proteins form inclusion bodies in bacteria. Co-expression with at least two interacting partners resulted in soluble DTL and Ver proteins. A polycistronic construct containing all the five cDNA was engineered, and the purification of the complex is in progress. Early data suggest the formation of several sub-complexes rather than the assembly of a holo-complex in bacteria. The DTL protein produced in baculovirus system was applied in far-western experiments and although we were unable to detect interactions with Terminin proteins by this method, an interaction with a nuclear protein has been revealed.

Supervisors: András Blastyák, Imre Miklós Boros
E-mail: balazsvedelek@gmail.com

Biological control of plant pathogenic fungi by use of a *Bacillus amyloliquefaciens* strain

Mónika Vörös

Department of Microbiology, University of Szeged, Szeged, Hungary

The damage in agricultural production and storage by phytopathogenic fungi is a serious problem in agriculture. Biological control is an alternative method against phytopathogenic microbes. An organism, which can interfere with pests or pathogen species, is referred to as a biological control agent. A biological control agent can compete for niche and nutrients in the rhizosphere, inhibit the growth of plant pathogens by the production of antibiotics and extracellular lytic enzymes and act indirectly, promoting plant growth and triggering defensive systems of plants against pathogens. It is beneficial if antagonistic strains used for protection against pathogenic microorganisms are resistant to metals present in the soil. The antagonistic microorganisms have to grow and reproduce as well as produce antibiotics and extracellular enzymes in the presence of different metals. The use of biological control may not always be sufficient against pathogenic species. In this case, we need to use combined methods such as use biological control agents with pesticides and appropriate cultivation methods. The biocontrol agent needs to tolerate against the pesticides used in combined treatments.

The *Bacillus* genus contains various species with potential biocontrol capabilities. *Bacillus amyloliquefaciens* SZMC 22206 has been isolated and studied as a potential biocontrol agent in our laboratory. Our aims were to investigate the effect of metals and pesticides on the growth, the extracellular chymotrypsin-like enzymes and the antibiotics produced by *B. amyloliquefaciens* SZMC 22206 strain and to

perform antagonisms test against plant pathogenic fungi.

Using chromogenic substrates we investigated the secretion of protease, chitinase, cellulase and lipase enzyme systems of the *B. amyloliquefaciens* SZMC 22206 strain. The chymotrypsin-like protease activity was significantly high, so in our further studies we analysed this enzyme activity. The effects of metals and pesticides on the growth and chymotrypsin-like protease activity were also investigated. The effects of metals were analyzed with 0,1 mM, 0,5 mM and 1 mM concentration of copper, manganese, nickel, iron and zinc. The manganese did not inhibit the growth and chymotrypsin-like protease activity in the analysed concentrations. The other metals inhibited the growth and enzyme activity at 0,5 mM concentration. We analysed the effects of four pesticides (2,4-dicholorophenoxyacetic acid, carbendazim, linuron and chlortoluron) on the growth and the extracellular chymotrypsin-like enzymes of *B. amyloliquefaciens* SZMC 22206. These results indicated that both bacterial growth and the tested exoenzyme activities were significantly reduced in the presence of these pesticides. These findings suggest that the presence of chemical pesticides (e.g. in agricultural soils) can strongly affect the behavior and effectiveness of the non-target biocontrol bacterial species. *B. amyloliquefaciens* SZMC 22206 strain can produce fengycin, that is a cyclic lipopeptide antibiotic. The production of fengycin is increased if glicerol was used as carbon source, and if aspartic acid, ornithin or alanine were used as nitrogen sources. During in vitro tests the strain inhibited the growth of plant pathogen fungi like *Fusarium solani*, *Phoma cucurbitacearum*, *Phytophtora infestans*, *Alternaria solani* and *Botrytis cinerea*. On the basis of our results *B. amyloliquefaciens* SZMC 22206 shows the potential of being a promising biological control agent against plant pathogenic fungi.

Supervisor: László Manczinger
E-mail: voros.monesz@gmail.com

Instructions to Authors

Submission of manuscripts

Submission of a manuscript to *Acta Biologica Szegediensis* automatically involves the assurance that it has not been published and will not be published elsewhere in the same form. Manuscripts should be written in English (consistent with either UK or US spelling). Since poorly-written material will not be considered for publication, authors are encouraged to have their manuscripts corrected for language and usage by a trusted expert. There are no explicit length limitations. However, a normal research article will occupy 4-8 printed pages; reviews might be considerably longer.

Manuscripts should be submitted to the Editor-in-Chief as an electronic attachment to **csaba@bio.u-szeged.hu**. All submitted manuscripts should be complete in themselves and firmly supported by properly detailed experimental data. *Instructions to Authors* is published in each issue and also available at **http://www2.sci.u-szeged.hu/ABS**. Correspondence relating to the status of the manuscripts, proofs, publication, reprints and advertising should be sent also to **abs@bio.u-szeged.hu**.

Manuscript format

The following file formats are acceptable for the main manuscript document: Microsoft word (doc, docx) and Rich text format (rtf). All pages should be printed with full double spacing, 2.5 cm margins, and a nonjustified right margin. A standard 12 point typeface (e.g. Times New Roman, Helvetica or Courier) should be used throughout the manuscript, with symbol font for Greek letters. Footnotes are not permitted. Each page should be numbered at the bottom as follows:

Page 1. Title page: Complete title, first name, middle initial, last name of each author; affiliations of the authors; mailing and e-mail addresses and phone and fax numbers of the corresponding author and a running title of no more than 48 characters.

Page 2. Abstract: no more than 200 words, followed by 4-6 key words. The abstract should not contain any undefined abbreviations and references.

Beginning on page 3: Introduction, Materials and Methods, Results, Discussion, Acknowledgments, References, Tables, Figures. Each section should be begun on a new page.

For reagents and instruments, the manufacturer's name should be given in parentheses. If microorganisms are used in the study, the collection or the strain number should be given; new isolates must be deposited in a publicly available culture collection. New nucleotide and amino acid sequences must be submitted in freely available databases (i.e. EMBL/GenBank) and the accession number should be provided. GenBank/EMBL accession number of the used amino acid or nucleic acid sequences also should be presented. Sources for all antibodies should be indicated. Customary abbreviations in common use need not be defined in the text (e.g. DNA, ATP or PCR). Other abbreviations should be defined at first mention and used consistently thereafter. Authors are required to use approved gene symbols and names; protein names should be in plain type. Quantitative results must be presented as graphs or tables and supported by appropriate experimental design and statistical tests. Only SI units may be used. For studies that involve animals or human subjects, the institutional, national or international guidelines that were followed should be indicated.

Acknowledgments

This section can include sources of the financial support received for the work and recognition for colleagues who assisted in the study or the manuscript preparation or provided unpublished data.

References

Only work that has been published or is in the press may be referred to. Personal communications should be acknowledged in the text and accompanied by written permission. In the text, references should be cited by name and year, e.g. Bloom (1983) or (Schwarz-Sommer et al. 1990) or (Maxam and Gilbert 1977) or (Schwarz-Sommer et al. 1990, Maxam and Gilbert 1977). In the References, references should be listed alphabetically by first authors (including all coauthors) and chronologically for a given author (beginning with the most recent date of publication). Where the same author has more than one publication in a year, lower case letters should be used (e.g. 1999a, 1999b, etc.). Periods should not be used after authors' initials or abbreviated journal titles (e.g. *Acta Biologica Szegediensis* should be cited as Acta Biol Szeged). Inclusive page numbers should be used. Examples:

Bloom FE (1983) The endorphins: a growing family of pharmacologically pertinent peptides. Annu Rev Pharmacol Toxicol 23:151-170.

Coons AH (1978) Fluorescent antibody methods. In Danielli JF, ed., General Cytochemical Methods. Academic Press, New York, 399-422.

Maxam AM, Gilbert WA (1977) A new method for sequencing DNA. Proc Natl Acad Sci USA 74:560-564.

Monod J, Changeux J-P, Jacob F (1963) Allosteric proteins and cellular control systems. J Mol Biol 6:306-329.

Schwarz-Sommer Z, Huijser P, Nacken W, Saedler H, Sommer H (1990) Genetic control of flower development by homeotic genes in *Antirrhinum majus*. Science 250:931-936.

Tables

Tables should be numbered consecutively with Arabic numerals. The first table in the text should be referred to as Table 1, and so on. A brief title should be included above the table. Each table should be double spaced, without vertical or horizontal lines, and on a separate sheet. Material in text should not be duplicated and methods should not be described.

Figure legends

Figures should be numbered consecutively with Arabic numerals. The first figure in the text should be referred to as Fig. 1, and so on. The following information should be provided in the figure legend: Figure number (using as Figure 1), short title of figure and the detailed legend. Material in the legend should not be duplicated and methods should not be described. The size of scale bars should be indicated when appropriate.

Figures

All figures should be submitted in separate files. Preferred file formats are TIFF or EPS. In some cases, MSOffice files are also acceptable. Adequate resolution (at least 300 dpi, preferably 600 dpi) should be used in making the original image. If figures are submitted with the main text, each of them should be presented in a separate page after the tables.